

CRANFIELD INSTITUTE OF TECHNOLOGY

COLLEGE OF AERONAUTICS

M.Phil. THESIS

Academic Years 1984-85 1985-86

E. MILONIDIS

The Development of the Mathematical Model of an RPV
and an
Investigation on the Use of an EKF for the
Identification of its Aerodynamic Derivatives

Supervisor:

P.G. Thomasson

May 1987

This thesis is submitted for the degree of Master of Philosophy.

ProQuest Number:10832191

All rights reserved

INFORMATION TO ALL USERS

The quality of this reproduction is dependent upon the quality of the copy submitted.

In the unlikely event that the author did not send a complete manuscript and there are missing pages, these will be noted. Also, if material had to be removed, a note will indicate the deletion.



ProQuest 10832191

Published by ProQuest LLC (2019). Copyright of the Dissertation is held by Cranfield University.

All rights reserved.

This work is protected against unauthorized copying under Title 17, United States Code
Microform Edition © ProQuest LLC.

ProQuest LLC.
789 East Eisenhower Parkway
P.O. Box 1346
Ann Arbor, MI 48106 – 1346

To my wife and son

ACKNOWLEDGEMENTS

I would like to express my gratitude to my parents, my mother in law and my relatives for their financial and moral support without which this work would not have been possible.

I am especially indebted to the College of Aeronautics for the two years grant I have received and to my supervisor Mr. P.G. Thomasson for his invaluable advice for the completion of this project.

Sincere appreciation is also due to my wife for her understanding and tolerance during this work.

Finally, I gratefully acknowledge my friends and colleagues for their moral support and encouragement during my study at the College of Aeronautics.

ABSTRACT

A six-degrees of freedom mathematical model of an experimental Remotely Piloted Vehicle (RPV) and the linearised longitudinal and lateral models at 30 m/sec are developed.

The longitudinal and lateral dynamics are analysed and the equivalent discrete systems are used to provide baseline data for the identification of the aerodynamic derivatives of the RPV.

An advanced aircraft parameter estimation method - the Extended Kalman Filter - is implemented for the estimation of the aerodynamic characteristics of the RPV. Conclusions are drawn about the identifiability of the stability and control derivatives from pitch, roll and yaw rate measurements.

CONTENTS

	<u>Page NO</u>
INTRODUCTION	1
Chapter 1, THE EQUATIONS OF MOTION OF A FLYING VEHICLE	3
1.1 Introduction	3
1.2 Assumptions Definitions and the Equations of Motion	3
1.2.1 Assumptions	3
1.2.2 Definitions	4
1.2.3 The Equations of Motion	6
1.3 External Forces and Moments	8
1.3.1 Gravity Forces and Moments	8
1.3.2 Aerodynamic Forces and Moments	9
1.3.3 Thrust Forces and Moments	10
1.4 The Complete Set of the Equations of Motion	11
Chapter 2 THE LINEARISATION OF THE EQUATIONS OF MOTION Longitudinal and Lateral Dynamics	12
2.1 Introduction	12
2.2 The Perturbed Equations of Motion	12
2.3 Aerodynamic Stability and Control Derivatives	14
2.3.1 Longitudinal Derivatives	15
2.3.1a Derivatives Due to Change in Forward Velocity	15
2.3.1b Derivatives Due to Change in Incidence	15
2.3.1c Derivatives Due to Downward Linear Acceleration	15
2.3.1d Derivatives Due to Rate of Pitch	16
2.3.1e Derivatives Due to Elevator Deflection	16
2.3.1f Derivatives Due to Change in Throttle Setting	17
2.3.2 Lateral Derivatives	17
2.3.2a Derivatives Due to Sideslip	17
2.3.2b Derivatives Due to Rate of Roll	18
2.3.2c Derivatives Due to Rate of Yaw	18
2.3.2d Derivatives Due to Control Deflections	19
2.3.2e Derivatives Due to Side Acceleration \dot{v}	19
2.4 Longitudinal Dynamics	20
2.5 Lateral Dynamics	21
Chapter 3 THE MATHEMATICAL MODELLING OF THE X-RAE1 RPV	23
3.1 Introduction	23
3.2 The Six Degrees of Freedom Mathematical Model of X-RAE1	23
3.2.1 Aerodynamic Forces	25
3.2.1a Lift	25
3.2.1b Drag	26
3.2.1c Side force	27
3.2.2 Aerodynamic Moments	28
3.2.2a Pitching Moment	28

CONTENTS (contd.)

	<u>Page NO</u>
3.2.2b Rolling Moment	28
3.2.2c Yawing Moment	28
3.2.3 Thrust Forces and Moments	30
3.2.4 The Equations of Motion of X-RAE1	31
3.2.5 Trim Conditions of X-RAE1	33
3.2.6 Moments and Products of Inertia	35
3.3 The Linearised Model of X-RAE1 at 30 m/sec	39
3.3.1 The Longitudinal Linear Model at 30 m/sec	39
3.3.2 The Lateral Linear Model at 30 m/sec	40
 Chapter 4 IDENTIFICATION OF THE STABILITY AND CONTROL DERIVATIVES OF X-RAE1	 51
4.1 Introduction	51
4.2 The General Problem of Identification and Its Application to Aircraft	51
4.3 The Extended Kalman Filter (EKF)	53
4.3.1 The EKF as State Estimator	53
4.3.2 The EKF as Parameter Estimator	55
4.4 The Estimation of the Longitudinal Aerodynamic Derivatives of X-RAE1	57
4.5 The Estimation of the Lateral Aerodynamic Derivatives of X-RAE1	62
 Chapter 5 THE SOFTWARE	 81
5.1 Introduction	81
5.2 Software for the Mathematical Modelling of X-RAE1	81
5.2.1 Aerodynamic Derivatives	81
5.2.2 Trim Conditions	85
5.2.3 Simulation Programmes	86
5.2.3a Nonlinear 6-DOF Simulation	86
5.2.3b Simulation for the Linear Longitudinal Model	86
5.2.3c Simulation for the Linear Lateral Model	88
5.3 Software for the Parameter Identification of X-RAE1	89
5.3.1 The EKF Algorithm	89
5.3.2 Supporting Subroutines	92
5.3.2a Subroutine SMTCS	92
5.3.2b Subroutine SYFN	92
5.3.2c Subroutine MTXPHI	93
5.3.2d Other Subroutines	93
 Chapter 6 CONCLUSIONS - RECOMMENDATIONS	 94
 REFERENCES	 96

CONTENTS (contd.)

	<u>Page NO</u>
APPENDIX A.1	98
APPENDIX A.2	107
APPENDIX A.3	112
APPENDIX A.4	118
APPENDIX A.5	123
APPENDIX A.6	125
APPENDIX A.7	126
APPENDIX A.8	129
APPENDIX A.9	131
APPENDIX MI	133
APPENDIX LA.1	135
APPENDIX LA.2	141
APPENDIX DE	144
APPENDIX PI.1	145
APPENDIX PI.2	158
APPENDIX S	159

LIST of FIGURES

	<u>Page NO</u>	
1.1	Body-fixed Axes	4
1.2	Euler angles and rates	5
1.3	Aircraft movement w.r.t. earth	7
1.4	Angles of attack and sideslip	9
1.5	Thrust configuration	11
3.1	X-RAE1 layout	24
3.2	Pitching moment reference point	32
3.3	General arrangement for the estimation of the moments and products of inertia	36
3.4 - 3.10	Response to elevator deflection	43 - 46
3.11 - 3.16	Response to aileron deflection	47 - 50
4.1	Basic identification procedure	52
4.2	The EKF state prediction and correction procedure	55
4.3	Bode plot of the Y-equation terms	66
4.4 - 4.11	Estimates of the longitudinal derivatives	68 - 75
4.12 - 4.21	Estimates of the lateral derivatives	76 - 80
5.1	Flowchart of the programme RPVDER.FOR	82
5.2	Flowchart of the programme TRIM.FOR	85
5.3	Simulation programme RPVPI.CSL	87
5.4	Simulation programme RPVLG.CSL	88
5.5	Simulation programme RPVLT.CSL	89
5.6	Flowchart of programme EXKAL.FOR	90
A.1-1	X-RAE1 longitudinal geometry	98
A.5-1	Aileron geometry of X-RAE1	123
A.7-1	C.G. nominal position	127
A.7-2	Maximum cross-sectional area	127
A.7-3	Equivalent elliptical area	127
A.7-4	Side elevation area	128
A.8-1	Geometry of X-RAE1 fin	129
MI.1	Assumed geometry for the estimation of the moments of inertia of X-RAE1	134
LA.1-1	Nominal and final C.G.	135
PI.1-1	Arrangement for the estimation of the diagonal elements of Q	148

LIST of FIGURES (contd.)

	<u>Page NO</u>
PI.1-2 to Estimates of the longitudinal derivatives PI.1-17	150 - 157

LIST of TABLES

	<u>Page NO</u>	
3.1	X-RAE1 specifications	25
3.2	Longitudinal aerodynamic derivatives	26
3.3	Side force aerodynamic derivatives	27
3.4	Rolling moment derivatives	29
3.5	Yawing moment derivatives	30
3.6	Normalised longitudinal derivatives at 30m/sec - Body Axes	39
3.7	Longitudinal modes of X-RAE1 at 30m/sec	40
3.8	Normalised lateral derivatives at 30m/sec	41
3.9	Lateral modes of X-RAE1 at 30m/sec	41
4.1	Nominal and estimated aerodynamic derivatives Longitudinal model	60
4.2	Nominal and estimated aerodynamic derivatives Lateral model	64
A.1-1	X-RAE1 longitudinal geometry	98
A.1-2	X-RAE1 parameters for the estimation of the longitudinal derivatives	99
A.7-1	X-RAE1 geometry	126
A.8-1	Fin characteristics	129
MI.1	Assumed mass and geometry for wing, tail fin and body of X-RAE1	133
MI.2	C.G positions of wing, tail, fin and body w.r.t. body axes	133
MI.3	Moments of inertia of X-RAE1	133

NOTATIONS

A	wing aspect ratio
\underline{a}	vector of unknown parameters
$\hat{\underline{a}}$	estimated vector of unknown parameters
b	wing span
C_D	drag coefficient
C_L	lift coefficient
C_l	rolling moment coefficient
C_m	pitching moment coefficient
C_n	yawing moment coefficient
C_y	side force coefficient
c	mean aerodynamic chord
D	drag
e	eccentricity
F	force
I_x, I_y, I_z I_{xy}, I_{yz}, I_{zx}	moments and products of inertia
L	lift, rolling moment
l_t	tail arm
M	pitching moment
m	aircraft mass
N	yawing moment
P, p	roll rate (body axes)
Q, q	pitch rate (body axes)
R, r	yaw rate (body axes)
S	wing area
S_t	tail area
T	thrust
U, u	forward velocity (body axes)
V, v	side velocity (body axes)
\underline{V}_T	total rectilinear velocity
W, w	downward velocity (body axes)
X	force (apart from gravitational) along x body-axis
$\overset{\circ}{X}_u, \dots, \overset{\circ}{N}_\zeta$	basic aerodynamic derivatives

X_u, \dots, N_ζ	normalised aerodynamic derivatives
\underline{x}	state vector
\underline{x}^*	augmented state vector
$\hat{\underline{x}}$	estimated state vector
Y	side force (apart from gravitational) in body axes
Z	force (apart from gravitational) along z body-axis

Greek Symbols

α	angle of attack
β	angle of sideslip
δ_T	throttle setting
ϵ	downwash angle thrust line orientation wing twist
ζ	rudder deflection
η	elevator deflection
θ, Θ	pitch angle
λ	taper ratio
ξ	aileron deflection
ρ	air density
ϕ, Φ	roll angle
ψ, Ψ	yaw angle
Ω	total angular velocity

SUBSCRIPTS

A	aerodynamic
B, b	body
F	fin
G	gravity
m	measured value
o	steady-state value
s	stability axes, sampling
T	total value, thrust
t	tail
W, w	wing
x	x-axis
y	y-axis
z	z-axis

ABBREVIATIONS

DOF	Degrees of Freedom
EKF	Extended Kalman Filter
RPV	Remotely Piloted Vehicle
w.r.t.	with respect to

MATHEMATICAL SYMBOLS

\equiv	equal by definition
\approx	almost equal
d	derivative operator
∂	partial derivative operator

INTRODUCTION

The determination of aircraft stability and control derivatives is of great importance in the design and testing of any aircraft. These derivatives are needed for the following reasons:

1. They define a given aircraft and can be used as quality criteria.
2. They provide model parameters for aircraft simulators.
3. They are used as a basis for the design of flight control systems.

Over the past few years, a great deal of effort has been placed in determining aerodynamic derivatives using parameter identification techniques. This new approach makes it possible to evaluate from one test run all the stability and control derivatives, their accuracy and their confidence intervals.

Aircraft parameter identification is particularly useful for Remotely Piloted Vehicles (RPVs), where the type of manoeuvre flown is not restricted by the human factor, an RPV having no pilot.

The purpose of this work is twofold:

1. Development of the six degrees of freedom mathematical model of an experimental RPV to provide simulation data for flight control system design and parameter identification.
2. Development of an Extended Kalman Filter (EKF) for the identification of the aerodynamic derivatives of the RPV.

The contents of this study are as follows:

In the first chapter, the equations of motion of a flying vehicle and the assumptions upon which they are based are presented.

The concepts of the aerodynamic stability and control derivatives and the linearisation of the equations of motion are given in Chapter 2. A brief discussion about the longitudinal and lateral dynamics is also presented in this chapter.

In Chapter 3, the mathematical model of an experimental RPV - the X-RAE1 - is derived based on static longitudinal wind-tunnel tests and on ESDU Data Sheets. Its purpose is to provide simulation data for six degrees of freedom motions of the RPV for flight regimes below stall.

The linearised longitudinal and lateral models at 30 m/sec are also given while their dynamics are analysed.

In Chapter 4, an EKF is implemented for the identification of the aerodynamic derivatives of the longitudinal and lateral models at 30 m/sec, assuming that measurements from the pitch, roll and yaw rates alone are available. Conclusions about the identifiability of the derivatives from these measurements are drawn.

The software developed to support the nonlinear and linear mathematical models of X-RAE1 and the computer implementation of the EKF algorithms is given in the fifth chapter, while the conclusions of this work and the recommendations for further research are presented in Chapter 6.

Chapter 1

THE EQUATIONS OF MOTION OF A FLYING VEHICLE

1.1 Introduction

The equations of motion of a rigid body and the assumptions upon which they are based are briefly presented in this chapter. Suitable systems of axes for the following analysis are defined and the process of converting from one system to another with different orientation is set forth using Euler angles.

Finally, the general origin of the forces and moments acting on a flying vehicle is discussed and they are incorporated within the equations of motion.

1.2 Assumptions Definitions and the Equations of Motion

In this section, the equations of motion of a flying vehicle are given with no attempt of any detailed proof. The interested reader is referred to the many texts available for this purpose (Refs 1,2,4,10).

1.2.1 Assumptions

Assumption 1. The aircraft is a rigid body and the mass and mass distribution of it are constant. Therefore, the motion of the aircraft can be described by a translation of its centre of gravity and a rotation about it. Any deformations of the structure are not taken into account nor the dynamics of any moving element with respect to the airframe apart from the static deflection characteristics of the control surfaces.

Assumption 2. The earth is flat and fixed in space. This assumption is particularly valid for an RPV where the flight time and the distances covered for each operation are generally small.

Assumption 3. The aircraft has a plane of symmetry.

Assumption 4. The atmosphere is assumed still and not moving with respect to earth.

1.2.2 Definitions

With the foregoing assumptions as a basis, suitable sets of axes can be defined where Newton's laws can be applied. All these systems are orthonormal and right-handed.

a. Earth-fixed Axes. They constitute an inertial frame fixed in earth with Oz axis directed towards geocentre.

b. Body-fixed Axes. They are fixed to the moving airframe with their origin at the centre of gravity of it.

b.1 Body Axes. Ox points "forward", Oz "downward" and Oy "to the right" (Fig. 1.1), so xz is the plane of symmetry of the air-craft.

b.2 Principal Axes. When Ox , Oy and Oz coincide with the principal axes of the airframe they are called principal axes.

b.3 Stability Axes. These are chosen so that Ox points in the direction of motion of the airframe in a condition of steady symmetric flight.

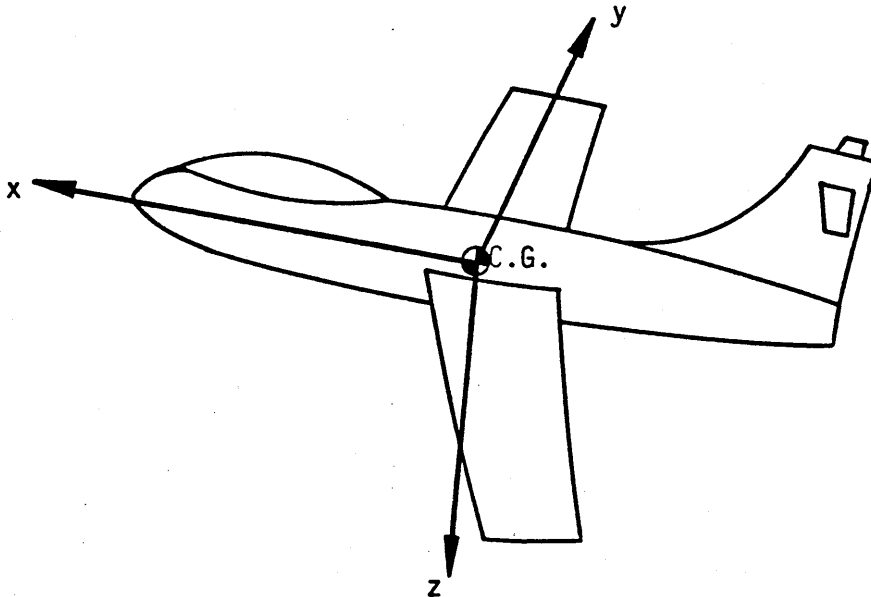


Fig. 1.1 Body-fixed Axes

The orientation of one system of axes with respect to another one needs to be defined. As most of the analysis is limited to perturbations about straight symmetric flight, the so-called Euler angles are considered as the most appropriate for this purpose. It can be proved that three angular displacements ϕ , θ , and ψ - and in that order - are necessary and sufficient (Ref. 13) to give the relative orientation of any two systems of axes (Fig. 1.2). In the flight mechanics literature, the Euler angles are usually referred as:

ϕ : yaw angle or azimuth or heading

θ : pitch angle or elevation

ψ : roll angle or bank

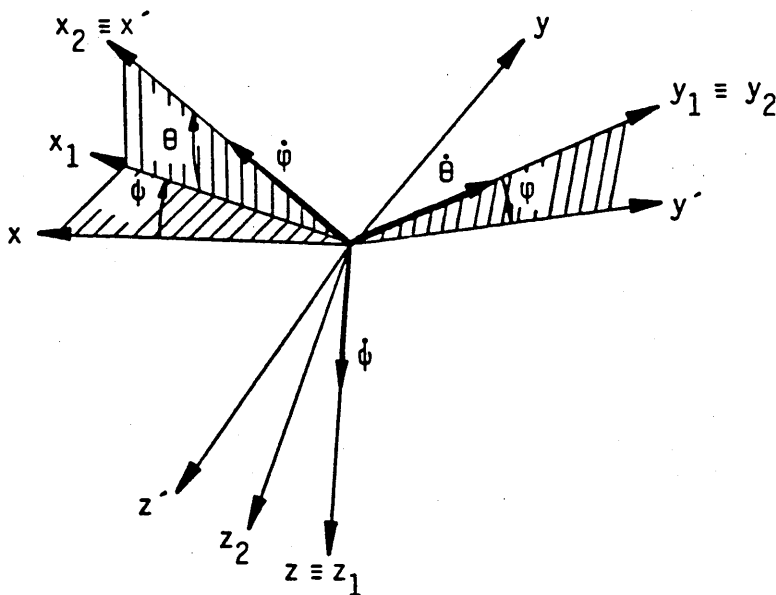


Fig. 1.2 Euler angles and rates.

The components of any vector along the axes of the displaced system can be determined if the Euler transformation R_{ELR} will be applied to its components with reference to the initial system, where

R_{ELR} is the orthogonal transformation given below:

$$R_{ELR} = \begin{bmatrix} \cos\phi\cos\theta & \sin\phi\cos\theta & -\sin\theta \\ \cos\phi\sin\theta\sin\varphi & \sin\phi\sin\theta\sin\varphi & \cos\theta\sin\varphi \\ -\sin\phi\cos\varphi & +\cos\phi\cos\varphi & \\ \cos\phi\sin\theta\cos\varphi & \sin\phi\sin\theta\cos\varphi & \cos\theta\cos\varphi \\ +\sin\phi\sin\varphi & -\cos\phi\sin\varphi & \end{bmatrix} \quad (1.1)$$

Then:

$$\begin{bmatrix} x' \\ y' \\ z' \end{bmatrix} = R_{ELR} \begin{bmatrix} x \\ y \\ z \end{bmatrix} \quad (1.2)$$

Because R_{ELR} is orthogonal, $R_{ELR}^{-1} = R_{ELR}^T$. Therefore:

$$\begin{bmatrix} x \\ y \\ z \end{bmatrix} = R_{ELR}^T \begin{bmatrix} x' \\ y' \\ z' \end{bmatrix} \quad (1.3)$$

Finally, the relation between the time derivative of a vector with respect to the inertial space and the time derivative of it as it is observed in a system rotating with angular velocity $\underline{\omega}$ is given (Refs 11, 13):

$$\left. \frac{d\underline{a}}{dt} \right|_{in} = \left. \frac{d\underline{a}}{dt} \right|_m + \underline{\omega} \times \underline{a} \quad (1.4)$$

where:

$\left. \frac{d\underline{a}}{dt} \right|_{in} \cong \frac{d\underline{a}}{dt}$ is the time derivative of the vector \underline{a} relative to the inertial space.

$\left. \frac{d\underline{a}}{dt} \right|_m \cong \dot{\underline{a}}$ is the time derivative of the vector \underline{a} observed in the rotating system.

1.2.3 The Equations of Motion

Suppose that the aircraft with mass m flies with rectilinear velocity \underline{v}_T and angular velocity $\underline{\Omega}$ with respect to the earth-fixed frame. The components of these vectors in body axes (Fig. 1.3) are:

$$\underline{v}_T = [U \ V \ W]^T$$

$$\underline{\Omega} = [P \ Q \ R]^T$$

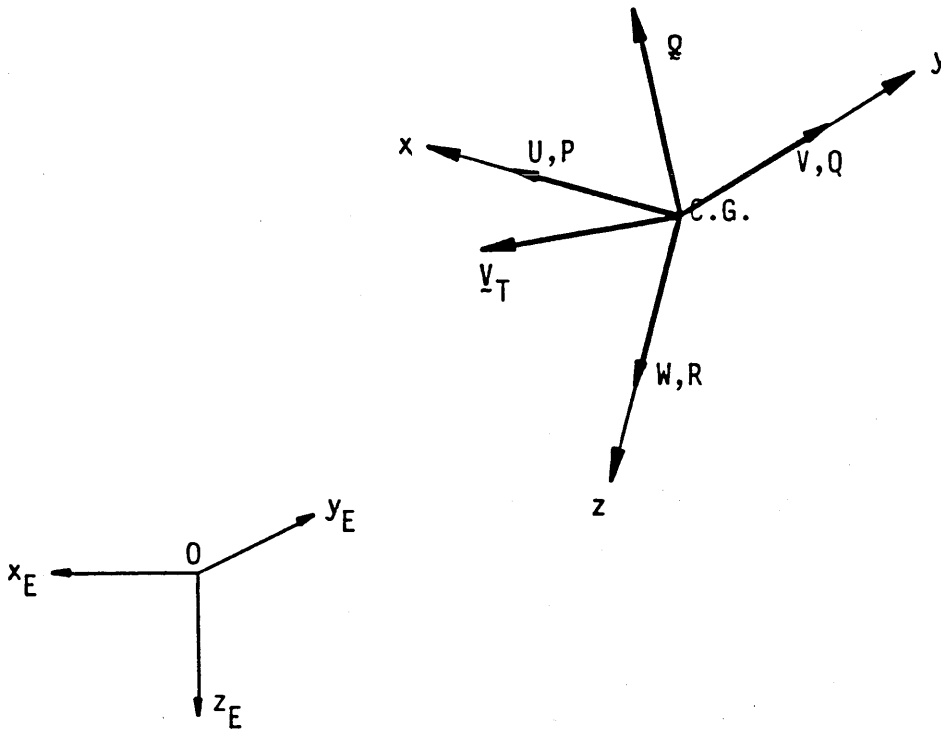


Fig. 1.3 Aircraft movement w.r.t. earth

Then according to Eqn 1.4 and the Newton's second law, the equations of motion of the flying vehicle become:

$$\frac{d\underline{V}_T}{dt} = \dot{\underline{V}}_T + \underline{Q} \times \underline{V}_T = \underline{F}/m$$

$$\frac{d\underline{H}}{dt} = \dot{\underline{H}} + \underline{Q} \times \underline{H} = \underline{M}$$

where \$\underline{F}\$ and \$\underline{M}\$ are all the external forces and moments applied to the aircraft and \$\underline{H}\$ is the angular momentum with the following components:

$$H_x = P I_x - Q I_{xy} - R I_{xz}$$

$$H_y = Q I_y - R I_{yz} - P I_{xy}$$

$$H_z = R I_z - P I_{xz} - Q I_{yz}$$

\$I_x\$, \$I_y\$ and \$I_z\$ are the moments of inertia about the corresponding body axes and \$I_{xy}\$, \$I_{yz}\$ and \$I_{xz}\$ are the products of inertia. Because the aircraft has the \$xz\$ plane as plane of symmetry \$I_{xy} = I_{yz} = 0\$.

Expanding the equations of motion in body coordinates we obtain the following set of equations:

$$\begin{aligned}
 F_x &= m(\dot{U} + QW - RV) \\
 F_y &= m(\dot{V} + RU - PW) \\
 F_z &= m(\dot{W} + PV - QU) \\
 L &= \dot{P}I_x - \dot{R}I_{xz} + QR(I_z - I_y) - PQI_{xz} \\
 M &= \dot{Q}I_y + PR(I_x - I_z) + (P^2 - R^2)I_{xz} \\
 N &= \dot{R}I_z - \dot{P}I_{xz} + PQ(I_y - I_x) + QR I_{xz}
 \end{aligned}
 \tag{1.5}$$

The external forces and moments are generally:

1. Gravity forces and moments.
2. Aerodynamic forces and moments.
3. Thrust forces and moments.

1.3 External Forces and Moments

1.3.1 Gravity Forces and Moments

The gravity forces can be evaluated by the projection of the gravitational acceleration g along the body axes, using Euler transformations (Eqns 1.1). Therefore:

$$\begin{aligned}
 F_{Gx} &= -mg\sin\Theta \\
 F_{Gy} &= mg\cos\Theta\sin\Phi \\
 F_{Gz} &= mg\cos\Theta\cos\Phi
 \end{aligned}
 \tag{1.6}$$

As the angles Φ and Θ are not generally the integrals of P and Q , we have to introduce new motion quantities. From Fig. 1.2, applying successive Euler transformations we have:

$$\begin{aligned}
 P &= \dot{\Phi} - \dot{\Psi}\sin\Theta \\
 Q &= \dot{\Theta}\cos\Phi + \dot{\Psi}\cos\Theta\sin\Phi
 \end{aligned}
 \tag{1.7}$$

$$\begin{aligned}
 R &= -\dot{\Theta}\sin\Phi + \dot{\Psi}\cos\Theta\cos\Phi \quad \text{or} \\
 \dot{\Phi} &= P + Q\tan\Theta\sin\Phi + R\tan\Theta\cos\Phi \\
 \dot{\Theta} &= Q\cos\Phi - R\sin\Phi \\
 \dot{\Psi} &= (R\cos\Phi + Q\sin\Phi)/\cos\Theta
 \end{aligned}
 \tag{1.8}$$

So, three more differential equations have to be added to the equations of motion 1.5.

The moments due to gravity are zero as the body-fixed axes are assumed to have their origin at the centre of gravity of the flying vehicle.

1.3.2 Aerodynamic Forces and Moments

The aerodynamic forces and moments are acted upon the vehicle by the surrounding airmass and they are generally due to the relative motion between the vehicle and the atmosphere. As the atmosphere is assumed to be still, the relative wind velocity is $-V_T$ (where V_T is the velocity of the vehicle w.r.t. earth). It can be proved that the aerodynamic forces can be expressed in the form:

$$F = \frac{1}{2} \rho V_T^2 S C_F \quad (1.9)$$

where:

ρ : is the air density

V_T : the relative velocity of the body w.r.t. air

S : a reference area of the body (wing area)

C_F : a dimensionless coefficient depending on the properties of the air and the airframe, the geometry of the airframe and the relative motion between the air and the airframe

The orientation of the air velocity vector with respect to body axes is usually given by two angles (Fig. 1.4):

angle of attack α and

angle of sideslip β where:

$$\alpha = \tan^{-1} \frac{W}{U} \quad (1.10)$$
$$\beta = \sin^{-1} \frac{V}{V_T}$$

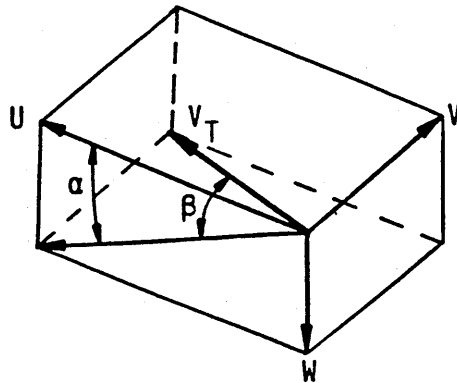


Fig. 1.4 Angles of attack and sideslip

The total steady aerodynamic force is conventionally given by two components: lift and drag (Ref. 10). The lift acts normal to the flight path and the drag parallel to the flight path. According to Eqn 1.9:

$$\begin{aligned} L &= \frac{1}{2}\rho V_T^2 S C_L \\ D &= \frac{1}{2}\rho V_T^2 S C_D \end{aligned} \quad (1.11)$$

Then:

$$\begin{aligned} F_{Ax} &= L \sin \alpha - D \cos \beta \cos \alpha \\ F_{Ay} &= D \sin \beta \\ F_{Az} &= -L \cos \alpha - D \cos \beta \sin \alpha \end{aligned} \quad (1.12)$$

Akin to Eqn 1.9 the aerodynamic moments can be expressed as follows:

$$\begin{aligned} \text{rolling} \quad L_A &= \frac{1}{2}\rho V_T^2 S b C_l \\ \text{pitching} \quad M_A &= \frac{1}{2}\rho V_T^2 S c C_m \\ \text{yawing} \quad N_A &= \frac{1}{2}\rho V_T^2 S b C_n \end{aligned} \quad (1.13)$$

where b is the wing span and c the mean aerodynamic chord of the wing.

The aerodynamic coefficients are generally functionals of the angle of attack and sideslip and their time rates, the angular velocities P, Q, R and their time rates, the control inputs and their time rates and so on. For example:

$$C_L(t) = C_L[\alpha(\lambda), \beta(\lambda), p(\lambda), \dots, \eta(\lambda), \dots, \dot{\alpha}(\lambda), \dots]$$

where it is understood that λ is a running variable in time over the interval $[0, t]$. This briefly means that generally the present behaviour of the aerodynamic coefficients does not depend only on the present values of their variables but on their time histories also (Ref. 16).

1.3.3 Thrust Forces and Moments

The thrust is assumed to act on the longitudinal plane xz along a thrust line with eccentricity e_T from the origin of the body axes (positive downwards) and all the gyroscopic effects are neglected. Then (Fig. 1.5):

$$\begin{aligned} F_{Tx} &= T \cos \epsilon_T \\ F_{Tz} &= T \sin \epsilon_T \\ M_T &= T e_T \end{aligned} \quad (1.14)$$

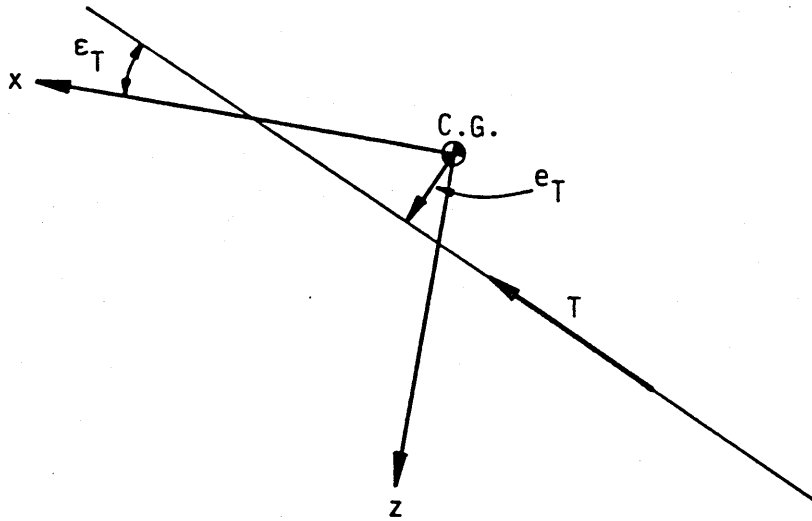


Fig. 1.5 Thrust configuration

1.4 The Complete Set of the Equations of Motion

As the gravitational forces are proportional to the mass of the vehicle it is convenient to combine them with the inertial ones. Then the equations of motion become:

$$\begin{aligned}
 m(\dot{U} + QW - RV + g\sin\Theta) &= F_{Ax} + F_{Tx} = X \\
 m(\dot{V} + RU - PW - g\cos\Theta\sin\Phi) &= F_{Ay} = Y \\
 m(\dot{W} + PV - QU - g\cos\Theta\cos\Phi) &= F_{Az} + F_{Tz} = Z \\
 \dot{P}I_x - \dot{R}I_{xz} + QR(I_z - I_y) - PQI_{xz} &= L_A = L \\
 \dot{Q}I_y + PR(I_x - I_z) + (P^2 - R^2)I_{xz} &= M_A + M_T = M \quad (1.15) \\
 \dot{R}I_z - \dot{P}I_{xz} + PQ(I_y - I_x) + QR I_{xz} &= N_A = N \\
 \dot{\Phi} &= P + Q\tan\Theta\sin\Phi + R\tan\Theta\cos\Phi \\
 \dot{\Theta} &= Q\cos\Phi - R\sin\Phi \\
 \dot{\Psi} &= (R\cos\Phi + Q\sin\Phi)/\cos\Theta
 \end{aligned}$$

These equations constitute the six degrees of freedom equations of motion of the flying vehicle on which all the following analysis is based.

Chapter 2

THE LINEARISATION OF THE EQUATIONS OF MOTION

Longitudinal and Lateral Dynamics

2.1 Introduction

The equations of motion as they have been presented in the first chapter, are in general dynamically and aerodynamically non-linear. In this chapter, they are linearised and also decomposed into two motions - longitudinal and lateral - by assuming small perturbations around the operating point or the trimmed conditions of the flying vehicle and certain aerodynamic properties.

The nature of the so-called aerodynamic stability and control derivatives is also briefly discussed.

2.2 The Perturbed Equations of Motion

The perturbed equations of motion can be obtained by performing the differentials on both sides of the six degrees of freedom equations of motion 1.15. If we designate the differential of each motion quantity by its lower case equivalent (ie $dU=u$, etc), the perturbed equations of motion become:

$$\begin{aligned}
 m[\dot{u} + W_0 q + Q_0 w - V_0 r - R_0 v + (g \cos \theta_0) \theta] &= dX \\
 m[\dot{v} + U_0 r + R_0 u - W_0 p - P_0 w \\
 &\quad - (g \cos \theta_0 \cos \phi_0) \psi + (g \sin \theta_0 \sin \phi_0) \theta] &= dY \\
 m[\dot{w} + V_0 p + P_0 v - U_0 q - Q_0 u \\
 &\quad + (g \cos \theta_0 \sin \phi_0) \psi + (g \sin \theta_0 \cos \phi_0) \theta] &= dZ \quad (2.1) \\
 \dot{p} I_x - \dot{r} I_{xz} + (Q_0 r + R_0 q)(I_z - I_y) - (P_0 q + Q_0 p) I_{xz} &= dL \\
 \dot{q} I_y + (P_0 r + R_0 p)(I_x - I_z) - (2R_0 r - 2P_0 p) I_{xz} &= dM \\
 \dot{r} I_z - \dot{p} I_{xz} + (P_0 q + Q_0 p)(I_y - I_x) + (Q_0 r + R_0 q) I_{xz} &= dN
 \end{aligned}$$

$$\begin{aligned}
 \dot{\psi} &= p + q \tan \theta_0 \sin \phi_0 + r \tan \theta_0 \cos \phi_0 \\
 &\quad + [(Q_0 \cos \phi_0 - R_0 \sin \phi_0) \tan \theta_0] \psi + [(Q_0 \sin \phi_0 + R_0 \cos \phi_0)(1 + \tan^2 \theta_0)] \theta \\
 \dot{\theta} &= q \cos \phi_0 - r \sin \phi_0 - (Q_0 \sin \phi_0 + R_0 \cos \phi_0) \psi \quad (2.1) \\
 \dot{\phi} &= r \cos \phi_0 / \cos \theta_0 + q \sin \phi_0 / \cos \theta_0 \\
 &\quad + [(Q_0 \cos \phi_0 - R_0 \sin \phi_0) / \cos \theta_0] \psi + [(Q_0 \sin \phi_0 + R_0 \cos \phi_0) \tan \theta_0 / \cos \theta_0] \theta
 \end{aligned}$$

where the zero subscripts denote steady state or trimmed conditions about which the small perturbations are performed.

If the functional representation of the aerodynamic coefficients is dropped and they are assumed to be depended on the present values of their variables and that symmetric reactions can be caused by symmetric disturbances (whereas asymmetric disturbances can cause only asymmetric reactions), the differentials of the aerodynamic forces and moments are the following:

$$\begin{aligned}
 dX &= \dot{X}_u u + \dot{X}_{\dot{u}} \dot{u} + \dot{X}_w w + \dot{X}_{\dot{w}} \dot{w} + \dot{X}_q q + \dot{X}_{\dot{q}} \dot{q} + \dot{X}_{\eta} \eta + \dot{X}_{\dot{\eta}} \dot{\eta} + \dot{X}_{\delta_T} \delta_T \\
 dY &= \dot{Y}_v v + \dot{Y}_{\dot{v}} \dot{v} + \dot{Y}_p p + \dot{Y}_{\dot{p}} \dot{p} + \dot{Y}_r r + \dot{Y}_{\dot{r}} \dot{r} + \dot{Y}_{\xi} \xi + \dot{Y}_{\dot{\xi}} \dot{\xi} + \dot{Y}_{\zeta} \zeta + \dot{Y}_{\dot{\zeta}} \dot{\zeta} \\
 dZ &= \dot{Z}_u u + \dot{Z}_{\dot{u}} \dot{u} + \dot{Z}_w w + \dot{Z}_{\dot{w}} \dot{w} + \dot{Z}_q q + \dot{Z}_{\dot{q}} \dot{q} + \dot{Z}_{\eta} \eta + \dot{Z}_{\dot{\eta}} \dot{\eta} + \dot{Z}_{\delta_T} \delta_T \quad (2.2) \\
 dL &= \dot{L}_v v + \dot{L}_{\dot{v}} \dot{v} + \dot{L}_p p + \dot{L}_{\dot{p}} \dot{p} + \dot{L}_r r + \dot{L}_{\dot{r}} \dot{r} + \dot{L}_{\xi} \xi + \dot{L}_{\dot{\xi}} \dot{\xi} + \dot{L}_{\zeta} \zeta + \dot{L}_{\dot{\zeta}} \dot{\zeta} \\
 dM &= \dot{M}_u u + \dot{M}_{\dot{u}} \dot{u} + \dot{M}_w w + \dot{M}_{\dot{w}} \dot{w} + \dot{M}_q q + \dot{M}_{\dot{q}} \dot{q} + \dot{M}_{\eta} \eta + \dot{M}_{\dot{\eta}} \dot{\eta} + \dot{M}_{\delta_T} \delta_T \\
 dN &= \dot{N}_v v + \dot{N}_{\dot{v}} \dot{v} + \dot{N}_p p + \dot{N}_{\dot{p}} \dot{p} + \dot{N}_r r + \dot{N}_{\dot{r}} \dot{r} + \dot{N}_{\xi} \xi + \dot{N}_{\dot{\xi}} \dot{\xi} + \dot{N}_{\zeta} \zeta + \dot{N}_{\dot{\zeta}} \dot{\zeta} \\
 &\quad \text{where } \dot{X}_u = \frac{\partial X}{\partial u}, \dot{X}_{\dot{u}} = \frac{\partial X}{\partial \dot{u}}, \dots, \dot{N}_{\zeta} = \frac{\partial N}{\partial \zeta}
 \end{aligned}$$

The partial derivatives of the aerodynamic forces and moments with respect to the motion quantities are called stability derivatives whereas the partial derivatives with respect to the control deflections and settings are called control derivatives.

The foregoing differentials do not really sound mathematically, as infinitesimal disturbance of any quantity does not necessarily imply infinitesimal disturbance of its time rate at the same instance.

If quasisteady flow is assumed all the derivatives with respect to the time rates of the variables can be neglected apart from those with respect to w and v rates. These derivatives are retained to model the downwash and sidewash effects, ie. the dependance of the flow at the tail on the time history of the motion of the wing.

When steady, straight, level and symmetric flight is assumed, ie:

$$\begin{aligned} V_0 &= 0 \\ P_0 &= Q_0 = R_0 = 0 \\ \phi_0 &= \psi_0 = 0 \end{aligned}$$

and with the quasisteady assumption, the perturbed equations of motion are decomposed into two sets of motion:

The Longitudinal Set (Symmetric Motion)

$$\begin{aligned} m[\dot{u} + W_0 q + (g \cos \Theta_0) \theta] &= \dot{X}_u u + \dot{X}_w w + \dot{X}_{\dot{w}} \dot{w} + \dot{X}_q q + \dot{X}_\eta \eta + \dot{X}_{\delta_T} \delta_T \\ m[\dot{w} - U_0 q + (g \sin \Theta_0) \theta] &= \dot{Z}_u u + \dot{Z}_w w + \dot{Z}_{\dot{w}} \dot{w} + \dot{Z}_q q + \dot{Z}_\eta \eta + \dot{Z}_{\delta_T} \delta_T \\ \dot{q} I_y &= \dot{M}_u u + \dot{M}_w w + \dot{M}_{\dot{w}} \dot{w} + \dot{M}_q q + \dot{M}_\eta \eta + \dot{M}_{\delta_T} \delta_T \\ \dot{\theta} &= q \end{aligned} \quad (2.3)$$

The Lateral Set (Asymmetric Motion)

$$\begin{aligned} m[\dot{v} + U_0 r - (g \cos \Theta_0) \varphi] &= \dot{Y}_v v + \dot{Y}_{\dot{v}} \dot{v} + \dot{Y}_p p + \dot{Y}_r r + \dot{Y}_\xi \xi + \dot{Y}_\zeta \zeta \\ \dot{p} I_x - \dot{r} I_{xz} &= \dot{L}_v v + \dot{L}_{\dot{v}} \dot{v} + \dot{L}_p p + \dot{L}_r r + \dot{L}_\xi \xi + \dot{L}_\zeta \zeta \\ \dot{r} I_z - \dot{p} I_{xz} &= \dot{N}_v v + \dot{N}_{\dot{v}} \dot{v} + \dot{N}_p p + \dot{N}_r r + \dot{N}_\xi \xi + \dot{N}_\zeta \zeta \\ \dot{\varphi} &= p + r \tan \Theta_0 \end{aligned} \quad (2.4)$$

Although the linearised equations of motion are absolutely valid only for infinitesimal disturbances, they have been proved very useful and widely applicable even when the disturbances are of much larger magnitude and their rates are kept in "reasonably" small values.

Before proceeding with the dynamics of the longitudinal and lateral motions a brief discussion about the origin of the aerodynamic stability and control derivatives follows.

2.3 Aerodynamic Stability and Control Derivatives

The definitions, the origin and the equations - when applicable - of the aerodynamic derivatives are given in this section. All the

derivatives are assumed to be expressed in stability axes and the compressibility and slipstream effects are neglected (Refs 1, 2, 3, 4, 10, 14, 15).

2.3.1 Longitudinal Derivatives

2.3.1a Derivatives Due to Change in Forward Velocity

<u>Definition</u>	<u>Origin</u>	<u>Equation</u>
$\dot{X}_u = \frac{\partial X}{\partial u}$	Variation of drag and thrust with u.	$-\rho V_T S C_D + \frac{\partial T}{\partial V_T}$
$\dot{Z}_u = \frac{\partial Z}{\partial u}$	Variation of normal force with u.	$-\rho V_T S C_L$
$\dot{M}_u = \frac{\partial M}{\partial u}$	Variation of pitch and thrust with u.	$\rho V_T S c c_m + e \frac{\partial T}{\partial V_T}$

2.3.1b Derivatives Due to Change in Incidence

<u>Definition</u>	<u>Origin</u>	<u>Equation</u>
$\dot{X}_w = \frac{\partial X}{\partial w}$	Lift and drag variations along the x-axis.	$\frac{1}{2} \rho V_T S (C_L - \frac{\partial C_D}{\partial \alpha})$
$\dot{Z}_w = \frac{\partial Z}{\partial w}$	Variation mainly of lift with incidence.	$-\frac{1}{2} \rho V_T S (C_D + \frac{\partial C_L}{\partial \alpha})$
$\dot{M}_w = \frac{\partial M}{\partial w}$	Static Longitudinal Stability.	$\frac{1}{2} \rho V_T S c \frac{\partial C_m}{\partial \alpha}$

2.1.3c Derivatives Due to Downward Linear Acceleration

<u>Definition</u>	<u>Origin</u>	<u>Equation</u>
$\dot{X}_w = \frac{\partial X}{\partial w}$	Downwash lag on drag (usually negligible).	$-\frac{1}{4} \rho S c \frac{\partial C_D}{\partial (\frac{\dot{\alpha}}{2V_T})}$

<u>Definition</u>	<u>Origin</u>	<u>Equation</u>
$\dot{z}_w = \frac{\theta Z}{\theta \dot{w}}$	Downwash lag mainly on lift of tail.	$-\frac{1}{4}\rho S c \frac{\theta C_L}{\theta \left(\frac{\dot{\alpha} c}{2V_T}\right)}$
$\dot{M}_w = \frac{\theta M}{\theta \dot{w}}$	Downwash lag on pitching moment.	$\frac{1}{4}\rho S c^2 \frac{\theta C_m}{\theta \left(\frac{\dot{\alpha} c}{2V_T}\right)}$

2.3.1d Derivatives Due to Rate of Pitch

<u>Definition</u>	<u>Origin</u>	<u>Equation</u>
$\dot{x}_q = \frac{\theta X}{\theta q}$	Effect of pitch rate on drag. Usually negligible.	$-\frac{1}{4}\rho V_T S c \frac{\theta C_D}{\theta \left(\frac{qc}{2V_T}\right)}$
$\dot{z}_q = \frac{\theta Z}{\theta q}$	Effect of pitch rate on lift (tail and wing contribution).	$-\frac{1}{4}\rho V_T S c \frac{\theta C_L}{\theta \left(\frac{qc}{2V_T}\right)}$
$\dot{M}_q = \frac{\theta M}{\theta q}$	Effect of pitch rate on pitching moment (damping in pitch).	$\frac{1}{4}\rho V_T S c^2 \frac{\theta C_m}{\theta \left(\frac{qc}{2V_T}\right)}$

2.3.1e Derivatives Due to Elevator Deflection

<u>Definition</u>	<u>Origin</u>	<u>Equation</u>
$\dot{x}_\eta = \frac{\theta X}{\theta \eta}$	Effect of elevator deflection on drag (usually negligible).	$-\frac{1}{2}\rho V_T^2 S \frac{\theta C_D}{\theta \eta}$
$\dot{z}_\eta = \frac{\theta Z}{\theta \eta}$	Effect of elevator deflection on lift.	$-\frac{1}{2}\rho V_T^2 S \frac{\theta C_L}{\theta \eta}$
$\dot{M}_\eta = \frac{\theta M}{\theta \eta}$	Effect of elevator deflection on pitching moment.	$\frac{1}{2}\rho V_T^2 S \frac{\theta C_m}{\theta \eta}$

2.3.1f Derivatives Due to Change in Throttle Setting

<u>Definition</u>	<u>Origin</u>	<u>Equation</u>
$\dot{X}_{\delta_T} = \frac{\theta X}{\theta \delta_T}$	Variation of thrust along x-axis with throttle.	$\frac{\theta T}{\theta \delta_T}$
$\dot{Z}_{\delta_T} = \frac{\theta Z}{\theta \delta_T}$	Variation of thrust with throttle along z-axis (usually neglected).	
$\dot{M}_{\delta_T} = \frac{\theta M}{\theta \delta_T}$	Variation of pitching moment with throttle.	$\frac{\theta T}{\theta \delta_T} e_T$

2.3.2 Lateral Derivatives

2.3.2a Derivatives Due to Sideslip

<u>Definition</u>	<u>Origin</u>	<u>Equation</u>
$\dot{Y}_v = \frac{\theta Y}{\theta v}$	Variation of side force with sideslip angle. Mainly from fin and body.	$\frac{1}{2} \rho V_T^2 S \frac{\theta C_y}{\theta \beta}$
$\dot{L}_v = \frac{\theta L}{\theta v}$	Rolling moment due to sideslip known as "effective dihedral derivative". Combination of wing dihedral effect and fin.	$\frac{1}{2} \rho V_T^2 S b \frac{\theta C_l}{\theta \beta}$
$\dot{N}_v = \frac{\theta N}{\theta v}$	"Weathercock" or static directional derivative. Main contribution from fin ; also wing-body.	$\frac{1}{2} \rho V_T^2 S b \frac{\theta C_n}{\theta \beta}$

2.3.2b Derivatives Due to Rate of Roll

<u>Definition</u>	<u>Origin</u>	<u>Equation</u>
$\dot{Y}_p = \frac{\partial Y}{\partial p}$	Change of side force due to rolling velocity. Fin is the main contributor although the wing may be significant for some configurations.	$\frac{1}{4}\rho V_T S b \frac{\partial C_y}{\partial \left(\frac{pb}{2V_T}\right)}$
$\dot{L}_p = \frac{\partial L}{\partial p}$	The roll damping derivative. Wing is the dominant factor when tail is of conventional size.	$\frac{1}{4}\rho V_T S b^2 \frac{\partial C_l}{\partial \left(\frac{pb}{2V_T}\right)}$
$\dot{N}_p = \frac{\partial N}{\partial p}$	Change in yawing moment from rolling velocity. Wing and fin the main contributors.	$\frac{1}{4}\rho V_T S b^2 \frac{\partial C_n}{\partial \left(\frac{pb}{2V_T}\right)}$

2.3.2c Derivatives Due to Rate of Yaw

<u>Definition</u>	<u>Origin</u>	<u>Equation</u>
$\dot{Y}_r = \frac{\partial Y}{\partial r}$	Variations in side force due to yawing velocity. Fin is the dominant contributor.	$\frac{1}{4}\rho V_T S b \frac{\partial C_y}{\partial \left(\frac{rb}{2V_T}\right)}$
$\dot{L}_r = \frac{\partial L}{\partial r}$	Rolling moment due to variations in yawing velocity. Quite important for spiral stability. Major contributors wing and fin.	$\frac{1}{4}\rho V_T S b^2 \frac{\partial C_l}{\partial \left(\frac{rb}{2V_T}\right)}$
$\dot{N}_r = \frac{\partial N}{\partial r}$	Yaw damping derivative. Contributions from wing fuselage and fin.	$\frac{1}{4}\rho V_T S b^2 \frac{\partial C_n}{\partial \left(\frac{rb}{2V_T}\right)}$

2.3.2d Derivatives Due to Control Deflections

<u>Definition</u>	<u>Origin</u>	<u>Equation</u>
$\dot{Y}_\xi = \frac{\partial Y}{\partial \xi}$	Side force due to aileron deflection. Usually negligible.	$\frac{1}{2}\rho V_T^2 S \frac{\partial C_Y}{\partial \xi}$
$\dot{L}_\xi = \frac{\partial L}{\partial \xi}$	Rolling moment due to aileron deflection known as aileron effectiveness.	$\frac{1}{2}\rho V_T^2 S b \frac{\partial C_l}{\partial \xi}$
$\dot{N}_\xi = \frac{\partial N}{\partial \xi}$	Yawing moment due to aileron deflection. It is caused from the difference between drag on up and down ailerons.	$\frac{1}{2}\rho V_T^2 S b \frac{\partial C_n}{\partial \xi}$
$\dot{Y}_\zeta = \frac{\partial Y}{\partial \zeta}$	Change in side force due to rudder deflection.	$\frac{1}{2}\rho V_T^2 S \frac{\partial C_Y}{\partial \zeta}$
$\dot{L}_\zeta = \frac{\partial L}{\partial \zeta}$	Rolling moment produced from rudder deflection (minor importance).	$\frac{1}{2}\rho V_T^2 S b \frac{\partial C_l}{\partial \zeta}$
$\dot{N}_\zeta = \frac{\partial N}{\partial \zeta}$	Variation in yawing moment with a change in rudder deflection known as rudder effectiveness.	$\frac{1}{2}\rho V_T^2 S b \frac{\partial C_n}{\partial \zeta}$

2.3.2e Derivatives Due to Side Acceleration \dot{v}

The derivatives due to \dot{v} usually arise from sidewash lags that produce angle of attack variations at the vertical tail. As only little is known for these aerodynamic derivatives, they are usually neglected in the usual formulation of the rigid body equations. However, there are cases where \dot{N}_v affects significantly the dutch roll damping and has to be accounted for, but the difficulty is that there is no good way of estimating \dot{N}_v or of knowing a priori for which configurations is important (Refs 10, 14).

Another reason for forces and moments to arise due to rate of change in side velocity is aeroelastic effects. These distortion effects are considered negligible for our analysis as the airframe is assumed to be rigid.

2.4 Longitudinal Dynamics

Rearranging Eqns 2.3 the state space model of the longitudinal equations of motion can be obtained:

$$\begin{bmatrix} \dot{u} \\ \dot{w} \\ \dot{q} \\ \dot{\theta} \end{bmatrix} = \begin{bmatrix} x_u & x_w & x_q & a_1 g \\ z_u & z_w & z_q & a_2 g \\ m_u & m_w & m_q & a_3 g \\ 0 & 0 & 1 & 0 \end{bmatrix} \begin{bmatrix} u \\ w \\ q \\ \theta \end{bmatrix} + \begin{bmatrix} x_\eta & x_{\delta_T} \\ z_\eta & z_{\delta_T} \\ m_\eta & m_{\delta_T} \\ 0 & 0 \end{bmatrix} \begin{bmatrix} \eta \\ \delta_T \end{bmatrix} \quad (2.5)$$

where:

$$\begin{aligned} x_u &= X_u + Z_u X_{\dot{w}} / (1 - Z_{\dot{w}}), & x_w &= X_w + Z_w X_{\dot{w}} / (1 - Z_{\dot{w}}) \\ x_q &= X_q - W_o + (Z_q + U_o) X_{\dot{w}} / (1 - Z_{\dot{w}}) \\ a_1 &= -\cos\theta_o - (\sin\theta_o) X_{\dot{w}} / (1 - Z_{\dot{w}}) \\ x_\eta &= X_\eta + Z_\eta X_{\dot{w}} / (1 - Z_{\dot{w}}), & x_{\delta_T} &= X_{\delta_T} + Z_{\delta_T} X_{\dot{w}} / (1 - Z_{\dot{w}}) \\ z_u &= Z_u / (1 - Z_{\dot{w}}), & z_w &= Z_w / (1 - Z_{\dot{w}}), & z_q &= (Z_q + U_o) / (1 - Z_{\dot{w}}) \\ a_2 &= -(\sin\theta_o) / (1 - Z_{\dot{w}}), & z_\eta &= Z_\eta / (1 - Z_{\dot{w}}), & z_{\delta_T} &= Z_{\delta_T} / (1 - Z_{\dot{w}}) \\ m_u &= M_u + Z_u M_{\dot{w}} / (1 - Z_{\dot{w}}), & m_w &= M_w + Z_w M_{\dot{w}} / (1 - Z_{\dot{w}}) \\ m_q &= M_q + (Z_q + U_o) M_{\dot{w}} / (1 - Z_{\dot{w}}) \\ a_3 &= -(\sin\theta_o) M_{\dot{w}} / (1 - Z_{\dot{w}}) \\ m_\eta &= M_\eta + Z_\eta M_{\dot{w}} / (1 - Z_{\dot{w}}), & m_{\delta_T} &= M_{\delta_T} + Z_{\delta_T} M_{\dot{w}} / (1 - Z_{\dot{w}}) \end{aligned} \quad (2.6)$$

The derivatives appearing on the right hand side of the Eqns 2.6 are the so-called normalised aerodynamic stability and control derivatives. They are obtained from the basic ones by dividing the force derivatives

by the mass of the aircraft and the moment derivatives by the corresponding moment of inertia, ie:

$$X_u \equiv \frac{\dot{X}_u}{m} = \frac{1}{m} \frac{\partial X}{\partial u}, \quad M_u \equiv \frac{\dot{M}_u}{I_y} = \frac{1}{I_y} \frac{\partial M}{\partial u}, \dots$$

The eigenvalues of the longitudinal system of equations for nearly all aircrafts in most flight conditions are two sets of complex numbers. Therefore the modes of the motion are two oscillations:

The Short Period. A relatively high frequency (ω_{sp}) oscillation with heavy damping (ζ_{sp}) primarily consisting of variations in α and θ with the forward velocity remaining almost constant and

The Phugoid. A relatively small frequency (ω_{ph}) oscillation with very light damping (ζ_{ph}) characterised by variations in u and θ with α about constant. It can be thought as an exchange of potential and kinetic energy as the aircraft tends to fly an oscillatory flight path on the longitudinal plane (Ref. 2).

2.5 Lateral Dynamics

The state space model of the lateral equations of motion (Eqns 2.4) becomes as follows:

$$\begin{bmatrix} \dot{v} \\ \dot{p} \\ \dot{r} \\ \dot{\phi} \end{bmatrix} = \begin{bmatrix} Y_v & Y_p + W_0 & Y_r - U_0 & g \cos \theta_0 \\ L_v & L_p & L_r & 0 \\ N_v & N_p & N_r & 0 \\ 0 & 1 & \tan \theta_0 & 0 \end{bmatrix} \begin{bmatrix} v \\ p \\ r \\ \phi \end{bmatrix} + \begin{bmatrix} Y_\xi & Y_\zeta \\ L_\xi & L_\zeta \\ N_\xi & N_\zeta \\ 0 & 0 \end{bmatrix} \begin{bmatrix} \xi \\ \zeta \end{bmatrix}$$

where all the derivatives are normalised.

The eigenvalues of the lateral system of motion are usually a set of two real and two complex numbers which constitute the three modes of the lateral motion:

The Dutch Roll. It primarily consists of sideslip and yaw. The damping and natural frequency of the dutch roll vary with aircraft and flight conditions where the damping may become very light.

The Roll Subsidence. It is the one degree of freedom rolling response to aileron deflection. Usually a small time constant is required.

The Spiral Divergence. It is a combination of an increase in yaw and roll angle and the aircraft eventually falls into a high-speed spiral dive. The spiral mode is not usually objectionable as the time constant is so large that it can be controlled by the pilot (Ref. 2).

Chapter 3

THE MATHEMATICAL MODELLING OF THE X-RAE1 RPV

3.1 Introduction

The concepts and principles presented and analysed in the first two chapters are applied in this chapter for the development of the six degrees of freedom model of an experimental RPV - the X-RAE1. A combination of static wind-tunnel tests and ESDU data sheets is used for the formulation of the aerodynamic characteristics of the RPV.

The linearised model for straight and level flight at forward velocity of 30 m/sec is derived and the longitudinal and lateral dynamics are analysed.

A new method also for the estimation of the moments and products of inertia of the airframe is proposed using an Extended Kalman Filter.

3.2 The Six Degrees of Freedom Mathematical Model of X-RAE1

X-RAE1 is a small low cost experimental RPV. The six degrees of freedom mathematical model of it is developed in this chapter. Its primary purpose is to provide baseline data for flight control system design and improvement and for the identification of the aerodynamic stability and control derivatives of X-RAE1. It can be considered as the necessary preliminary step for the assesment of the most appropriate identification algorithm before proceeding with the analysis of flight test data.

The model is dynamically nonlinear but as it is intended to provide simulation data for flight regimes well below stall, the aerodynamic characteristics of it are assumed linear.

The modelling work was preceded by static wind-tunnel testing of a full-scale unpowered model at RAE Farnborough. These data provided the basis for the derivation of the longitudinal aerodynamic characteristics of the RPV (static and rotational). The engine model and the lateral aerodynamics are based on ESDU data sheets and fundamental theoretical concepts as wind-tunnel or any other kind of data were not available.

A general arrangement of X-RAE1 and some of its specifications are shown in Fig. 3.1 and Table 3.1 respectively.

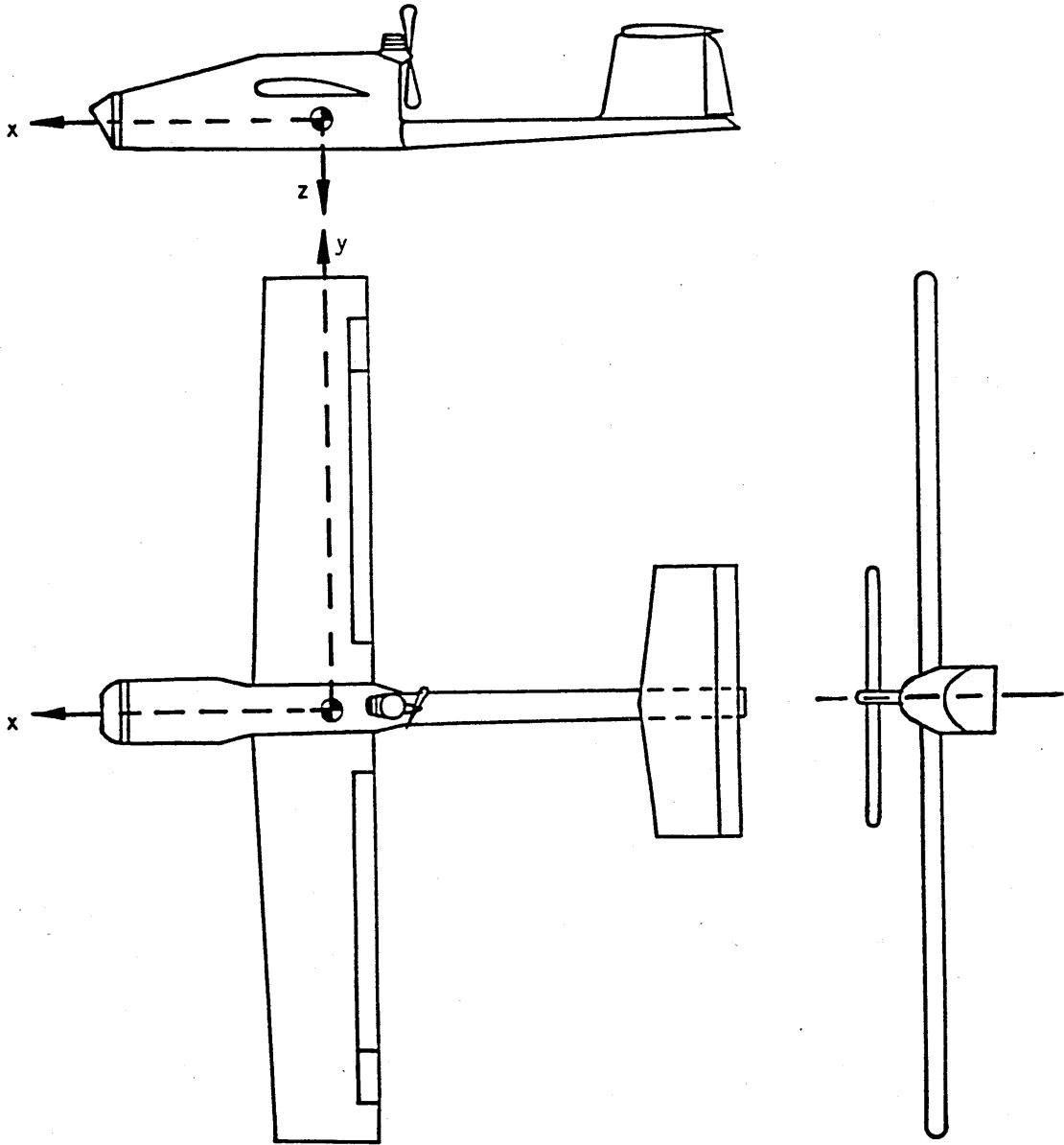


Fig. 3.1 X-RAE1 layout

Length (l_b)	2.1	m
Wing Area (S)	0.9307	m^2
Wing Span (b)	2.638	m^2
Mean Aerodynamic Chord (c)	0.353	m
Tail Area (S_t)	0.2576	m^2
Distance of the centre of gravity from the leading edge of the mean aerodynamic chord	0.34c = 0.121	m
Typical Weight (mg)	15	Kgr
Typical Payload	2	Kgr
Speed Range	40 to 68	Kts
<u>ENGINE:</u>	Webra '91' 1.5cc two stroke delivering approximately 1.9 Kw at 14000 RPM and driving a 14 inch dia. x 6 inch pitch propeller.	

Table 3.1 X-RAE1 specifications

3.2.1 Aerodynamic Forces

The aerodynamic forces are assumed to consist of three components: lift L , drag D and side force Y . Lift and drag act on the longitudinal plane normal and parallel respectively to the velocity vector in symmetric flight whereas side force acts along the Oy body axis.

Any aerodynamic quantity with subscript s is assumed to be expressed in stability axes.

3.2.1a Lift

Lift is mainly produced by the lifting surfaces - wing and tail - and by the deflection of the elevator. It is estimated from the formula:

$$L = \frac{1}{2} \rho v_T^2 S C_L \quad (3.1)$$

where $C_L = C_L(\alpha, \dot{\alpha}, q, \eta)$ is assumed a linear function of the angle of attack α , the time rate of the angle of attack $\dot{\alpha}$, the pitching

rate q and the elevator deflection η ie:

$$C_L = C_{L_0} + C_{L_\alpha} \alpha + C_{L_{\dot{\alpha}}} \left(\frac{\dot{\alpha}c}{2V_T}\right) + C_{L_q} \left(\frac{qc}{2V_T}\right) + C_{L_\eta} \eta \quad (3.2)$$

A full derivation of C_{L_α} , $C_{L_{\dot{\alpha}}}$, C_{L_q} and C_{L_η} from wind-tunnel data is given in Apx A.1 and for reasons of completeness their values are shown in Table 3.2 .

3.2.1b Drag

Drag is derived by a similar formula as lift, namely:

$$D = \frac{1}{2} \rho V_T^2 S C_D \quad (3.3)$$

Wing and body are the main contributors and C_D can be estimated from wind-tunnel data as:

$$C_D = C_{D_0} + k C_{L_w}^2 \quad (3.4)$$

where C_{D_0} is the zero-lift drag and $k C_{L_w}^2$ is the drag induced by the lift produced by the wing-body combination (Apx A.1 , Table 3.2).

$C_{L_\alpha} = 4.98 / \text{rad}$	$C_{D_0} = 0.0227$	$C_{m_\alpha} = -1.05 / \text{rad}$
$C_{L_{\dot{\alpha}}} = 2.78 / \text{rad}$	$k = 0.0514$	$C_{m_{\dot{\alpha}}} = -9.32 / \text{rad}$
$C_{L_q} = 4.83 / \text{rad}$		$C_{m_q} = -19.15 / \text{rad}$
$C_{L_\eta} = 0.49 / \text{rad}$		$C_{m_\eta} = -1.63 / \text{rad}$

Table 3.2 Longitudinal aerodynamic derivatives

3.2.1c Side Force

Akin to Eqn 1.9 the side force Y is expressed as follows:

$$Y = \frac{1}{2}\rho V_T^2 S C_y \quad (3.5)$$

where $C_y = C_y(V, P, R, \zeta)$ is a linear function of its variables ie:

$$C_y = \frac{1}{V_T} Y_v V + \frac{b}{V_T} Y_p P + \frac{b}{V_T} Y_r R + Y_\zeta \zeta \quad (3.6)$$

The main contribution to the side force arises from the rudder deflection with sideslip and yaw rate also having some effect. Side force due to roll rate is almost negligible.

The aerodynamic derivatives Y_v , Y_p , Y_r and Y_ζ are given in Table 3.3 . ESDU data sheets are mainly used for the estimation of the side force derivatives. Details can be found in Apcs A.2, A.3, A.4 and A.6 .

$Y_{v_s} \cong \frac{\partial Y}{\partial v} / \frac{1}{2}\rho V_T S$	- 0.3054
$Y_{p_s} \cong \frac{\partial Y}{\partial p} / \frac{1}{2}\rho V_T S b$	0.078C _L ⁽¹⁾ - 0.3133 [$\frac{11.32\cos\alpha - 110.19\sin\alpha}{263.8}$ - - 0.18 - $\frac{\theta \bar{\sigma}_\alpha}{\theta (\frac{pb}{V_T})}$ ⁽²⁾]
$Y_{r_s} \cong \frac{\partial Y}{\partial r} / \frac{1}{2}\rho V_T S b$	- 0.0109 + 0.2164 (109.51cos α + 8.87sin α) / 263.8
$Y_\zeta \cong \frac{\partial Y}{\partial \zeta} / \frac{1}{2}\rho V_T^2 S$	0.1184

Table 3.3 Side force aerodynamic derivatives

(1) Lift coefficient

(2) Sidewash term due to body

3.2.2 Aerodynamic Moments

3.2.2a Pitching Moment

The main contributors to the pitching moment are the wing and the tail. The equation for it is:

$$M_A = \frac{1}{2} \rho V_T^2 S c C_m \quad (3.7)$$

where:

$$C_m = C_{m_0} + C_{m_\alpha} \alpha + C_{m_{\dot{\alpha}}} \left(\frac{\dot{\alpha} c}{2V_T} \right) + C_{m_q} \left(\frac{qc}{2V_T} \right) + C_{m_\eta} \eta \quad (3.8)$$

C_{m_0} , C_{m_α} , $C_{m_{\dot{\alpha}}}$, C_{m_q} and C_{m_η} are derived from wind-tunnel data (Apx A.1) and their values are recalled in Table 3.2 .

3.2.2b Rolling Moment

The rolling moment is assumed that depends on the lateral motion quantities V, P, R and on the aileron deflection mainly, whereas rudder deflection contributes only a very small amount. The equation for the rolling moment is as follows:

$$L_A = \frac{1}{2} \rho V_T^2 S b C_l \quad (3.9)$$

where:

$$C_l = \frac{1}{V_T} L_V V + \frac{b}{V_T} L_P P + \frac{b}{V_T} L_R R + L_\xi \xi + L_\zeta \zeta \quad (3.10)$$

All the derivatives are estimated from ESDU data sheets (Apcs A.2, A.3, A.4, A.5 and A.6) and their values are given in Table 3.4 .

3.2.2c Yawing Moment

The yawing moment is derived by an analogous way to the rolling moment. The rudder deflection is now more important than the aileron deflection. The expression for the yawing moment is:

$$N_A = \frac{1}{2} \rho V_T^2 S b C_n \quad (3.11)$$

$L_{V_s} \cong \frac{\theta L}{\theta v} / \frac{1}{2} \rho V_T S b$	$- 0.0005 \alpha_b^{(1)} - 0.0119 - 0.0016 C_L^{(2)} - 0.1969 (8.87 \cos \alpha - 109.51 \sin \alpha) / 263.8$
$L_{P_s} \cong \frac{\theta L}{\theta p} / \frac{1}{2} \rho V_T S b^2$	$- 0.2457 + Y_{pF_s}^{(3)} (11.32 \cos \alpha - 110.91 \sin \alpha) / 263.8$
$L_{r_s} \cong \frac{\theta L}{\theta r} / \frac{1}{2} \rho V_T S b^2$	$- 0.00189 + 0.1243 C_L^{(2)} + Y_{rF_s}^{(4)} (8.87 \cos \alpha - 109.51 \sin \alpha) / 263.8$
$L_{\xi_s} \cong \frac{\theta L}{\theta \xi} / \frac{1}{2} \rho V_T^2 S b$	$- 0.2291$
$L_{\zeta} \cong \frac{\theta L}{\theta \zeta} / \frac{1}{2} \rho V_T^2 S b$	0.00398

Table 3.4 Rolling moment derivatives

- (1) Body incidence measured from its zero lift value.
- (2) Wing lift coefficient.
- (3) Contribution of fin to side force due to rate of roll.
- (4) Contribution of fin to side force due to rate of yaw.

where:

$$C_n = \frac{1}{V_T} N_V V + \frac{b}{V_T} N_P P + \frac{b}{V_T} N_R R + N_{\xi} \xi + N_{\zeta} \zeta \quad (3.12)$$

The values of the aerodynamic derivatives are recalled in Table 3.5 . Detailed analysis for their estimation is given in Apcs A.2, A3, A.4, A.5 and A.6 .

$N_{V_s} \cong \frac{\theta N}{\theta V} / \frac{1}{2} \rho V_T S b$	- 0.0363 + 0.1969 (109.51cos α + 8.87sin α) /263.8
$N_{P_s} \cong \frac{\theta N}{\theta P} / \frac{1}{2} \rho V_T S b^2$	- 0.034C _L ⁽¹⁾ + 1.23 $\frac{\theta C_D}{\theta \alpha}$ ⁽²⁾ - - Y _{PF_s} ⁽³⁾ (110.91cos α + 11.32sin α) /263.8
$N_{r_s} \cong \frac{\theta N}{\theta r} / \frac{1}{2} \rho V_T S b^2$	- 0.0022 - 0.1261C _{D_o} ⁽⁴⁾ - 0.009C _L ⁽⁵⁾ - - Y _{rF_s} ⁽⁶⁾ (109.51cos α + 8.87sin α) /263.8
$N_{\xi_s} \cong \frac{\theta N}{\theta \xi} / \frac{1}{2} \rho V_T^2 S b$	0.0195C _L ⁽⁵⁾
$N_{\zeta} \cong \frac{\theta N}{\theta \zeta} / \frac{1}{2} \rho V_T^2 S b$	- 0.0492

Table 3.5 Yawing moment derivatives

- (1) Lift coefficient.
- (2) Viscous drag derivative w.r.t. angle of attack (per degrees).
- (3) Contribution of fin to side force derivative due to rate of roll.
- (4) Wing drag at zero lift.
- (5) Wing lift coefficient.
- (6) Contribution of fin to side force derivative due to rate of yaw.

3.2.3 Thrust Forces and Moments

Thrust forces and moments are produced by one 12 inch diameter by 6 inch pitch two blade propeller. The propeller axis lies on the longitudinal plane of the RPV and is parallel to the body x-axis. As the only data available about the engine are those given in Table 3.1 ,

an analytical model has been developed based on a combination of the momentum and blade element theory and the use of power-required and power-available curves (Ref. 18) .

The resulting thrust force is given by the formula:

$$T = k_1 \delta_T - k_2 V_T^2 \quad (3.13)$$

where:

$$k_1 = 26.7154 \text{ Watts sec / m}$$

$$k_2 = 0.0055 \text{ Watts (m / sec)}^{-3}$$

δ_T : throttle setting (from zero to one)

A pitching moment is also produced due to the eccentricity e_T of the thrust line:

$$M_T = T e_T \quad (e_T = - 0.16 \text{ m}) \quad (3.14)$$

The rolling moment due to the torque moment M_{br} of the engine is assumed negligible and is not taken into account in the following analysis. A detailed development of the engine model is given in Apx A.1 .

3.2.4 The Equations of Motion of X-RAE1

After the evaluation of the aerodynamic and thrust forces and moments acting on the airframe the equations of motion of X-RAE1 can be developed. The following aspects are taken into account for their derivation:

1. All the derivatives given in stability axes have to be transformed to body axes.
2. The aerodynamic coefficients C_L , C_D and C_m are estimated with reference to the point O_A on the centre line chord of the wing at a distance $0.34c$ from the leading edge of the mean aerodynamic chord whereas the centre of gravity of the airframe is assumed to be the centroid of the equivalent cross-section at O_A (Fig. 3.2 and Apx B.1) .
3. The product of inertia I_{xz} is assumed to be zero.

An ACSL programme - the RPVPI.CSL - has been developed for the digital simulation of the six degrees of freedom motion of X-RAE1 (Ch. 5). The responses to small amplitude pulse deflections of the elevator and aileron, after the trimmed values have been subtracted, are shown in Figs 3.4 to 3.16 at the end of this chapter.

3.2.5 Trim Conditions of X-RAE1

X-RAE1 is assumed to be initially set to straight, horizontal and level flight with velocity V_{T0} . The deflections of the control surfaces, the throttle setting and the angle of attack required for sustained flight at V_{T0} m/sec are computed in this section.

The trimmed values of the motion quantities become:

$$U_0 = V_{T0} \cos \alpha_0, \quad W_0 = V_{T0} \sin \alpha_0, \quad Q_0 = 0, \quad \Theta_0 = \alpha_0$$

$$V_0 = P_0 = R_0 = 0, \quad \Phi_0 = \Psi_0 = 0$$

The lateral conditions can be easily obtained by setting the aileron and rudder at their zero value positions. Then, the longitudinal equations are the following:

$$F_x = m\dot{U} = -mg \sin \alpha + \bar{q}S(C_L \sin \alpha - C_D \cos \alpha) + T$$

$$F_z = m\dot{W} = mg \cos \alpha - \bar{q}S(C_L \cos \alpha + C_D \sin \alpha) \quad (3.16)$$

$$M = \dot{Q}I_y = \bar{q}S c C_m + T e_T + \bar{q}S(C_L \sin \alpha - C_D \cos \alpha) h_0$$

where:

$$C_L = C_{L0} + C_{L\alpha} \alpha + C_{L\eta} \eta$$

$$C_D = C_{D0} + k C_{Lw}^2$$

$$C_{Lw} = C_{L_{ow}} + C_{L_{\alpha w}} \alpha$$

$$C_m = C_{m0} + C_{m\alpha} \alpha + C_{m\eta} \eta$$

For equilibrium:

$$\dot{U} = \dot{W} = 0$$

$$M = 0$$

Eliminating thrust T from Eqns 3.16 we have:

$$T = - \frac{\bar{q}Sc}{e_T} C_m - \bar{q}S(C_L \sin\alpha - C_D \cos\alpha) \frac{h_0}{e_T} \quad (3.17)$$

$$F_x = - mg \sin\alpha + \bar{q}S \left(1 - \frac{h_0}{e_T}\right) (C_L \sin\alpha - C_D \cos\alpha) - \frac{\bar{q}Sc}{e_T} C_m \quad (3.18)$$

$$F_z = mg \cos\alpha - \bar{q}S(C_L \cos\alpha + C_D \sin\alpha)$$

The system of Eqns 3.18 is nonlinear and it is solved numerically for the unknown vector

$$\underline{x} = [\alpha \quad \eta]^T$$

using the Newton-Raphson method. Therefore (Ref. 5):

$$\underline{x}_{n+1} = \underline{x}_n - J^{-1} \begin{bmatrix} F_x \\ F_z \end{bmatrix}$$

where J is the Jacobian

$$J = \begin{bmatrix} \partial F_x / \partial \alpha & \partial F_x / \partial \eta \\ \partial F_z / \partial \alpha & \partial F_z / \partial \eta \end{bmatrix}$$

and

$$\frac{\partial F_x}{\partial \alpha} = \left(1 - \frac{h_0}{e_T}\right) \bar{q}S [(C_{L\alpha} + C_{D\alpha}) \sin\alpha + (C_L - C_{D\alpha}) \cos\alpha] - mg \cos\alpha - \frac{\bar{q}Sc}{e_T} C_{m\alpha}$$

$$\frac{\partial F_x}{\partial \eta} = \left(1 - \frac{h_0}{e_T}\right) \bar{q}S C_{L\eta} \sin\alpha - \frac{\bar{q}Sc}{e_T} C_{m\eta}$$

$$\frac{\partial F_z}{\partial \alpha} = \bar{q}S [(C_L - C_{D\alpha}) \sin\alpha - (C_{L\alpha} + C_D) \cos\alpha] - mg \sin\alpha$$

$$\frac{\partial F_z}{\partial \eta} = - \bar{q}S C_{L\eta} \cos\alpha$$

The solution for $V_{T0} = 30$ m/sec is

$$\underline{x} = \begin{bmatrix} \alpha_0 \\ \eta_0 \end{bmatrix} = \begin{bmatrix} -0.0245 \\ 0.0445 \end{bmatrix}$$

Then Eqns 3.13 and 3.17 give throttle setting $\delta_T = 0.7156$.
Summarising, the control deflections and the throttle setting for steady, straight, symmetric flight at 30 m/sec are as follows:

<u>elevator</u>	$\eta_0 = 0.0445$	rad
<u>aileron</u>	$\xi_0 = 0.0$	rad
<u>rudder</u>	$\zeta_0 = 0.0$	rad
<u>throttle</u>	$\delta_T = 0.7156$	or 71.56%

3.2.6 Moments and Products of Inertia

A method for the estimation of the moments and products of inertia of X-RAE1 is presented in this section. It is based on the use of an Extended Kalman Filter.

It is assumed that the position of the centre of gravity of the airframe is known and three accelerometers and three rate gyros are fitted on it along the body axes. The RPV is hung from a point on the longitudinal plane and is left to perform small amplitude oscillations. Therefore, the forces acting on the airframe are only the gravitational ones and the reaction at the hanging point (Fig. 3.3). The measurements are assumed to be corrupted by bias errors and white gaussian noise of zero mean (Ref. 9), ie:

$$y_m = y + b_y + n_y \quad (3.19)$$

where:

y_m : the measured value

y : the true value of the measured quantity

b_y : the bias error

n_y : the white noise, $E[n_y] = 0$, $E[n_y^2] = \sigma_y^2$

The equations of motion then become:

$$\begin{aligned} \dot{P}I_x - \dot{R}I_{xz} &= L \\ \dot{Q}I_y &= M \\ \dot{R}I_z - \dot{P}I_{xz} &= N \end{aligned} \quad (3.20)$$

where all the second order terms of the motion quantities have been ignored, and

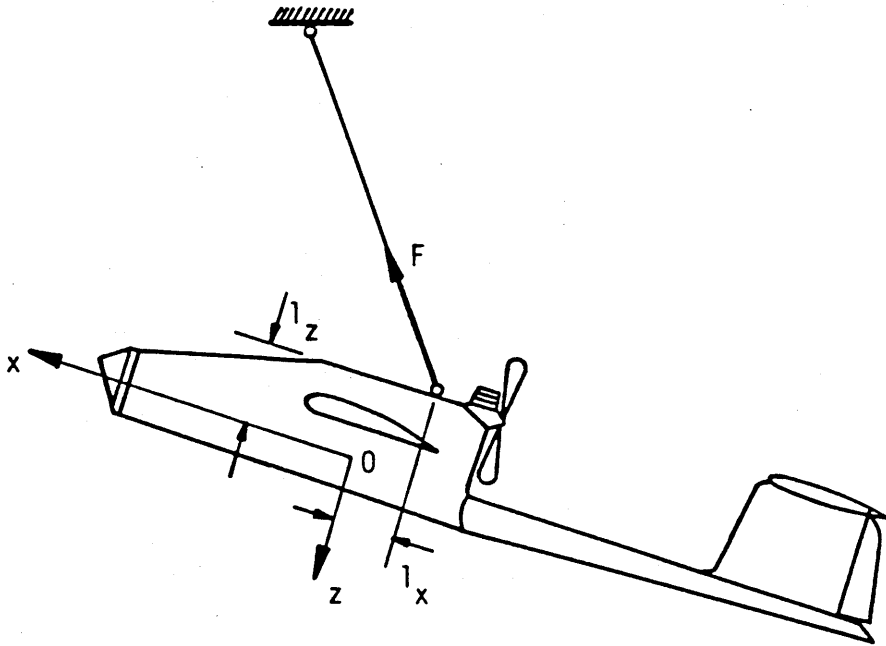


Fig. 3.3 General arrangement for the estimation of the moments and products of inertia

$$\begin{aligned}
 L &= - F_y l_z \\
 M &= F_x l_z - F_z l_x \\
 N &= F_y l_x
 \end{aligned}
 \tag{3.21}$$

F_x , F_y and F_z are the reactions at the hanging point and can be evaluated by the accelerometer readings according to Eqn 3.19, ie:

$$\begin{aligned}
 F_x &= ma_x = m(a_{xm} - b_{a_x} - n_{a_x}) \\
 F_y &= ma_y = m(a_{ym} - b_{a_y} - n_{a_y}) \\
 F_z &= ma_z = m(a_{zm} - b_{a_z} - n_{a_z})
 \end{aligned}
 \tag{3.22}$$

Incorporating Eqns 3.21 and 3.22 into Eqns 3.20, the equations of motion become as follows:

$$\begin{aligned} \dot{P} &= m(I_z l_z b_{a_y} - I_{xz} l_x b_{a_z} - I_z l_z a_{ym} + I_{xz} l_x a_{zm}) / (I_x I_z - I_{xz}^2) + \\ &\quad + m(I_z l_z n_{a_y} - I_{xz} l_x n_{a_z}) / (I_x I_z - I_{xz}^2) \\ \dot{Q} &= m(-l_z b_{a_x} + l_x b_{a_z} + l_z a_{xm} - l_x a_{zm} - l_z n_{a_x} + l_x n_{a_z}) / I_y \quad (3.23) \\ \dot{R} &= m(I_{xz} l_z b_{a_y} - I_x l_x b_{a_z} - I_{xz} l_z a_{ym} + I_x l_x a_{zm}) / (I_x I_z - I_{xz}^2) + \\ &\quad + m(I_{xz} l_z n_{a_y} - I_x l_x n_{a_z}) / (I_x I_z - I_{xz}^2) \end{aligned}$$

The system of equations 3.23 can be written in the form:

$$\dot{\underline{x}} = \underline{f}(\underline{x}, \underline{u}, t) + \Gamma(\underline{x})\underline{w}(t)$$

$$\dot{\underline{y}} = \underline{h}(\underline{x}, \underline{u}, t) + \underline{v}(t)$$

where:

$$\underline{x} = \left[p, q, r, b_{a_x}, b_{a_y}, b_{a_z}, b_p, b_q, b_r, I_x, I_y, I_z, I_{xz} \right]^T$$

is the state vector.

$$\underline{u} = \left[a_{xm}, a_{ym}, a_{zm} \right]^T$$

is the input vector.

$$\underline{y} = \left[p_m, q_m, r_m \right]^T$$

is the output vector.

$$\underline{w} = \left[n_{a_x}, n_{a_y}, n_{a_z} \right]^T$$

is the white process noise.

$$\underline{v} = \left[n_p, n_q, n_r \right]^T$$

is the white measurement noise.

$$\underline{f}(\underline{x}, \underline{u}, t) = \begin{bmatrix} m(I_z l_z b_{a_y} - \dots + I_{xz} l_x a_{zm}) / (I_x I_z - I_{xz}^2) \\ m(-l_z b_{a_x} + \dots - l_x a_{zm}) / I_y \\ m(I_{xz} l_z b_{a_y} - \dots + I_x l_x a_{zm}) / (I_x I_z - I_{xz}^2) \\ 0 \\ \cdot \\ \cdot \\ \cdot \\ 0 \end{bmatrix}$$

$$\underline{h}(\underline{x}, \underline{u}, t) = [p + b_p \quad q + b_q \quad r + b_r]^T$$

$$\Gamma(\underline{x}) = \begin{bmatrix} 0 & \frac{m I_z l_z}{I_x I_z - I_{xz}^2} & -\frac{m I_{xz} l_x}{I_x I_z - I_{xz}^2} \\ -\frac{m l_z}{I_y} & 0 & \frac{m l_x}{I_y} \\ 0 & \frac{m I_{xz} l_z}{I_x I_z - I_{xz}^2} & -\frac{m I_x l_x}{I_x I_z - I_{xz}^2} \\ 0 & 0 & 0 \\ \cdot & \cdot & \cdot \\ \cdot & \cdot & \cdot \\ \cdot & \cdot & \cdot \\ 0 & 0 & 0 \end{bmatrix}$$

The state vector \underline{x} and so the moments of inertia I_x , I_y , I_z and the product of inertia I_{xz} , can be estimated in principle using an Extended Kalman Filter. Their initial values are assumed to be:

$$\begin{aligned}
 I_x &= 2.1678 \text{ Kgr m}^2 \\
 I_y &= 1.6469 \text{ Kgr m}^2 \\
 I_z &= 3.6962 \text{ Kgr m}^2 \\
 I_{xz} &= 0.0 \text{ Kgr m}^2
 \end{aligned}$$

and they are evaluated in Apx MI. A brief discussion of the Kalman filter theory and its use as state and/or parameter estimator is given in the following Chapter 4.

3.3 The Linearised Model of X-RAE1 at 30 m/sec

The linear model of X-RAE1 about a steady, straight, symmetric and horizontal flight at a constant velocity of 30 m/sec is given in this section. The aerodynamic stability and control derivatives for this flight condition are computed and the dynamics of the longitudinal and lateral motions are analysed.

3.3.1 The Longitudinal Linear Model at 30 m/sec

The aerodynamic stability and control derivatives for a trimmed flight at 30 m/sec are evaluated for the linear longitudinal motion in Apx LA.1. Their normalised values in body axes are shown in Table 3.6.

$X_u = - 0.097$	$Z_u = - 0.789$	$M_u = 0.029$
$X_w = 0.037$	$Z_w = - 5.496$	$M_w = - 3.865$
$X_{\dot{w}} = - 0.00044$	$Z_{\dot{w}} = - 0.018$	$M_{\dot{w}} = - 12.381$
$X_q = - 0.019$	$Z_q = - 0.902$	$M_q = - 0.201$
$X_\eta = - 0.397$	$Z_\eta = - 16.172$	$M_\eta = - 179.079$
$X_{\delta_T} = 1.719$	$Z_{\delta_T} = 0.0$	$M_{\delta_T} = - 2.595$

Table 3.6 Normalised longitudinal derivatives
at 30 m/sec - Body Axes.

Then according to Eqns 2.5 and 2.6 the state space longitudinal model becomes:

$$\begin{bmatrix} \dot{u} \\ \dot{w} \\ \dot{q} \\ \dot{\theta} \end{bmatrix} = \begin{bmatrix} -0.097 & 0.039 & 0.704 & -9.804 \\ -0.775 & -5.399 & 28.575 & 0.236 \\ 0.185 & -2.782 & -18.117 & -0.047 \\ 0 & 0 & 1 & 0 \end{bmatrix} \begin{bmatrix} u \\ w \\ q \\ \theta \end{bmatrix} + \begin{bmatrix} -0.39 & 1.719 \\ -15.887 & 0 \\ -175.89 & -2.595 \\ 0 & 0 \end{bmatrix} \begin{bmatrix} \eta \\ \delta_T \end{bmatrix}$$

The characteristic equation of the longitudinal system is:

$$\rho(s) = s^4 + 23.613s^3 + 179.537s^2 + 18.048s + 31.018$$

and the eigenvalues of it (roots of the characteristic equation) are:

Short Period: $-11.767 \pm j6.249$

Phugoid: $-0.039 \pm j0.416$

The corresponding natural frequencies and damping ratios of the longitudinal dynamics are given in Table 3.7.

	natural frequency	damping
Short Period	$\omega_{n_{sp}} = 13.328 \text{ rad/sec}$	$\zeta_{sp} = 0.883$
Phugoid	$\omega_{n_{ph}} = 0.410 \text{ rad/sec}$	$\zeta_{ph} = 0.095$

Table 3.7 Longitudinal modes of X-RAE1 at 30 m/sec

It is apparent from the above table the need of controlling the phugoid mode to avoid low frequency oscillations due to the light damping ratio ζ_{ph} . Although the short period is heavily damped it is also a good control strategy to make it fast so the transient effects mainly on the pitching rate q will die out rapidly.

The programme RPVLG.CSL has been developed for the simulation of the linear longitudinal motion of X-RAE1. The response to a small amplitude pulse deflection of the elevator is shown in Figs 3.4 to 3.10 where the short period and phugoid characteristics can be observed.

3.3.2 The Lateral Linear Model at 30 m/sec

The normalised stability and control derivatives of the lateral motion at 30 m/sec are given in Table 3.8. Detailed determination of

their values can be found in Apx LA.2.

$Y_v = -0.336$	$L_v = -0.414$	$N_v = 0.558$
$Y_p = 0.175$	$L_p = 13.360$	$N_p = -0.622$
$Y_r = 0.224$	$L_r = 2.412$	$N_r = -1.426$
$Y_\xi = 0.0$	$L_\xi = -142.902$	$N_\xi = 4.182$
$Y_\zeta = 3.909$	$L_\zeta = 2.485$	$N_\zeta = -18.015$

Table 3.8 Normalised lateral derivatives
at 30 m/sec - Body Axes

Substituting the values of the derivatives to Eqns 2.7 the lateral equations of motion become as follows:

$$\begin{bmatrix} \dot{v} \\ \dot{p} \\ \dot{r} \\ \dot{\phi} \end{bmatrix} = \begin{bmatrix} -0.336 & -0.561 & -29.767 & 9.804 \\ -0.414 & -13.360 & 2.412 & 0 \\ 0.558 & -0.622 & -1.426 & 0 \\ 0 & 1 & -0.025 & 0 \end{bmatrix} \begin{bmatrix} v \\ p \\ r \\ \phi \end{bmatrix} + \begin{bmatrix} 0 & 3.909 \\ -142.902 & 2.485 \\ 4.182 & -18.015 \\ 0 & 0 \end{bmatrix} \begin{bmatrix} \xi \\ \zeta \end{bmatrix}$$

The characteristic polynomial of the lateral system matrix is:

$$\rho(s) = s^4 + 15.122s^3 + 41.897s^2 + 241.099s - 5.517$$

and the eigenvalues of it are the following:

Dutch Roll: $-0.903 \pm j4.163$

Roll Subsidence: -13.338

Spiral Divergence: 0.023

The corresponding natural frequency, damping ratio and time constants of the lateral modes are given in Table 3.9.

Dutch Roll	Roll Subsidence	Spiral Divergence
$\omega_{n_d} = 4.259 \text{ rad/sec}$	$T_r = 0.075 \text{ secs}$	$T_s = 43.478 \text{ secs}$
$\zeta_d = 0.212$		

Table 3.9 Lateral modes of X-RAE1 at 30 m/sec

The dutch roll mode is of reasonably short period and lightly damped so an attempt should be made to overcome its oscillations. The unstable spiral mode has a very large time constant ($T_s = 43.478$ secs) and can be easily tolerated by the pilot. As a stable spiral mode may be usually achieved at the expense of a less well damped dutch roll it does not seem advisable to be controlled by the flight control system.

An ACSL programme - the RPVLT.CSL - has been developed for the simulation of the lateral model of X-RAE1 (Ch. 5). The response to a small amplitude pulse deflection of the aileron is shown in Figs 3.11 to 3.16.

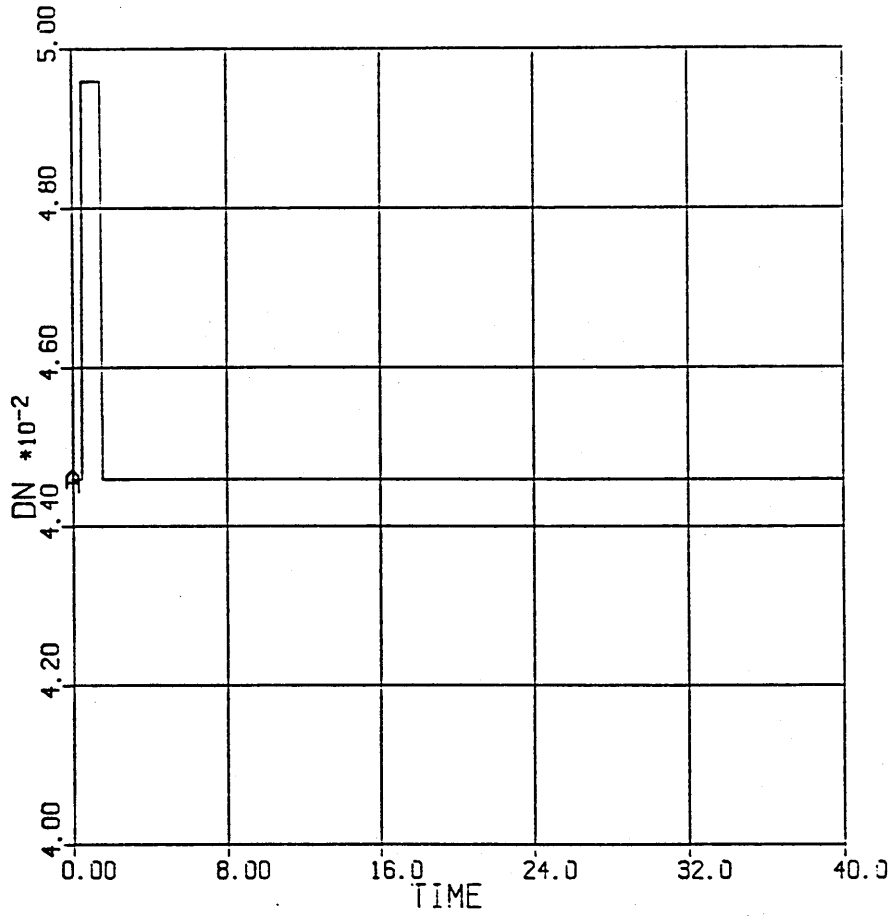


Fig. 3.4 Elevator deflection

Amplitude: 0.005 rad

Duration: 1.0 sec

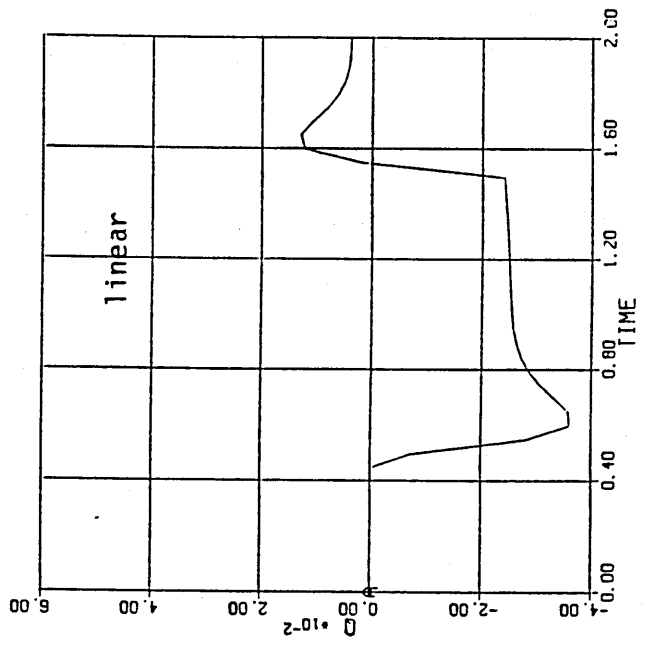
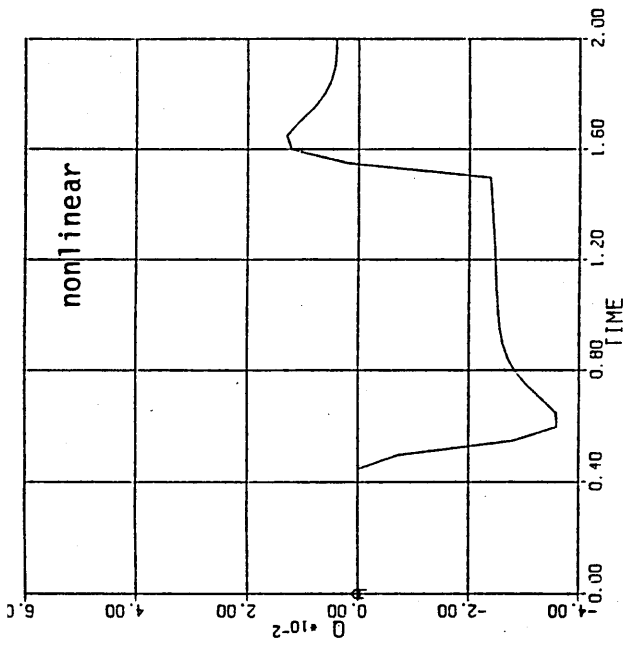


Fig. 3.5 q response to elevator deflection

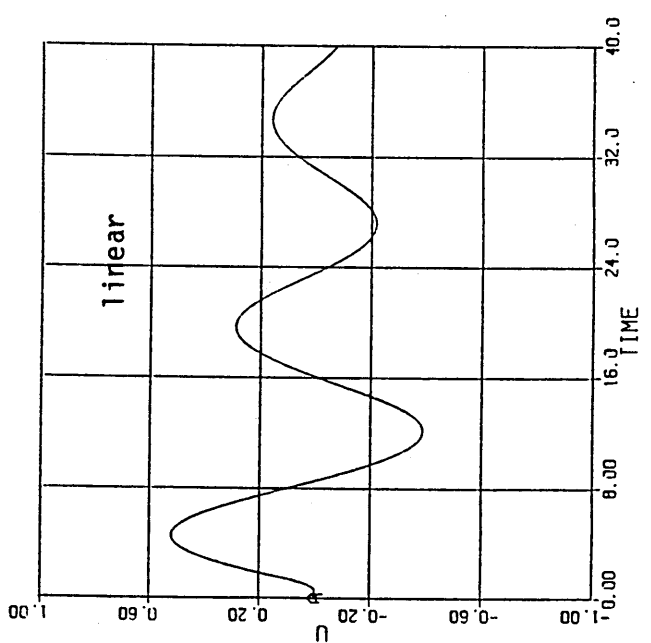
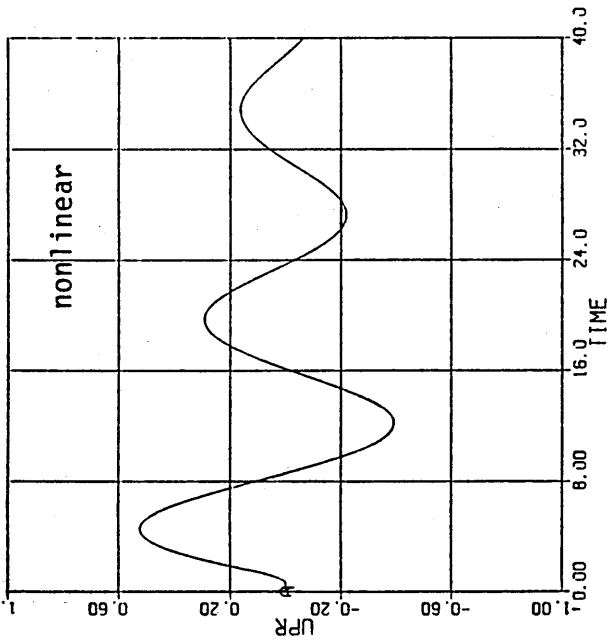


Fig. 3.6 u response to elevator deflection

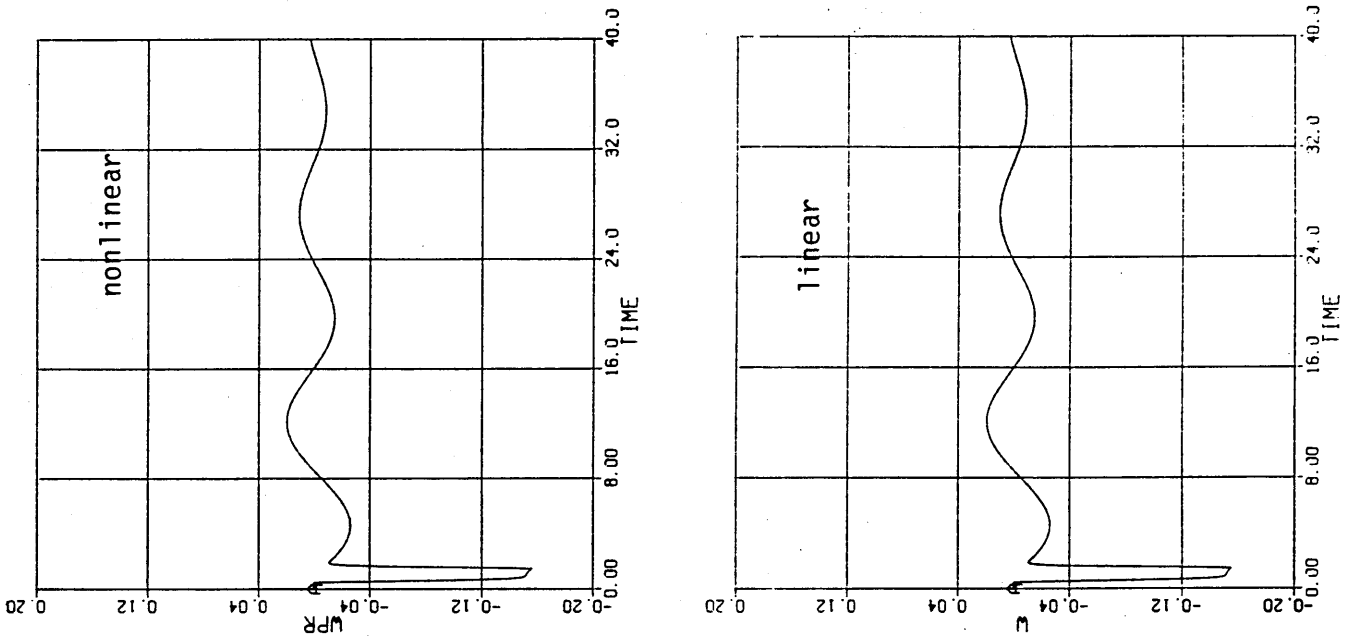


Fig. 3.7 w response to elevator deflection

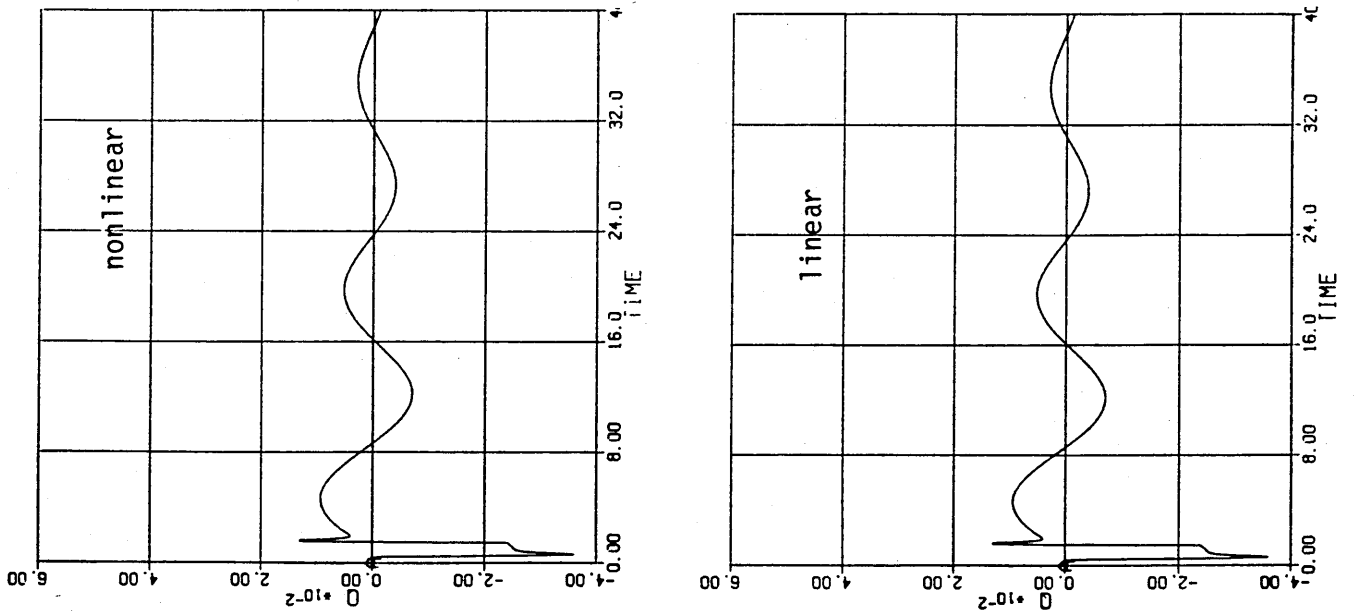


Fig 3.8 q response to elevator deflection

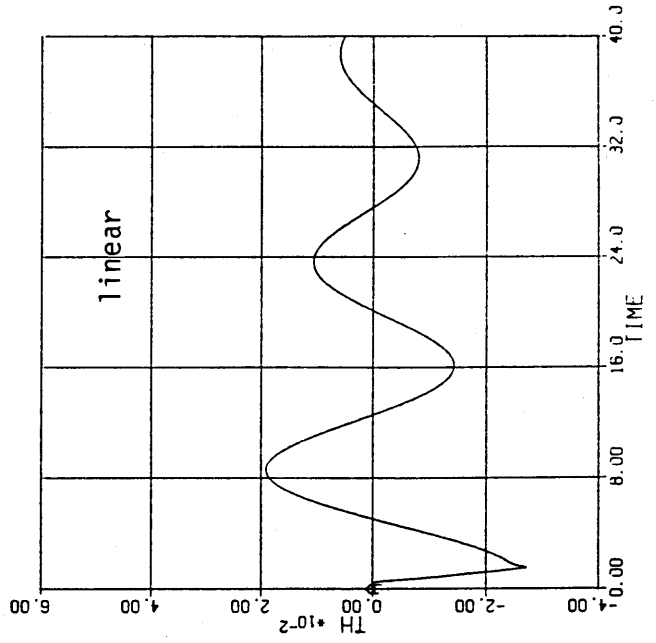
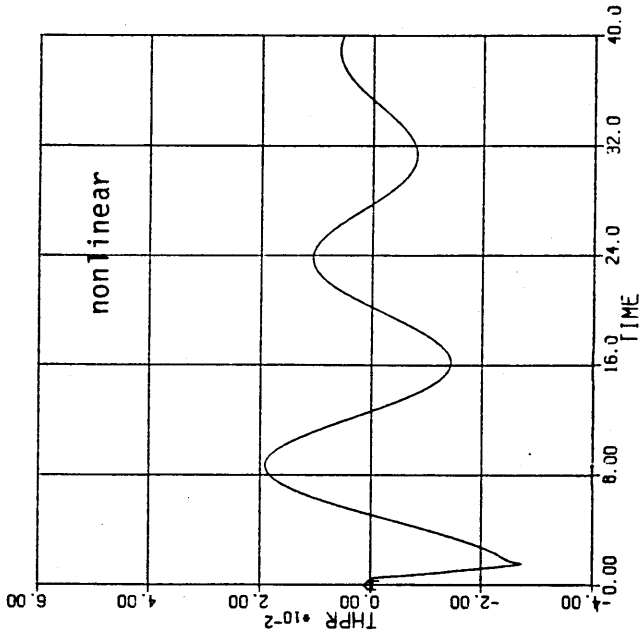


Fig 3.9 θ response to elevator deflection

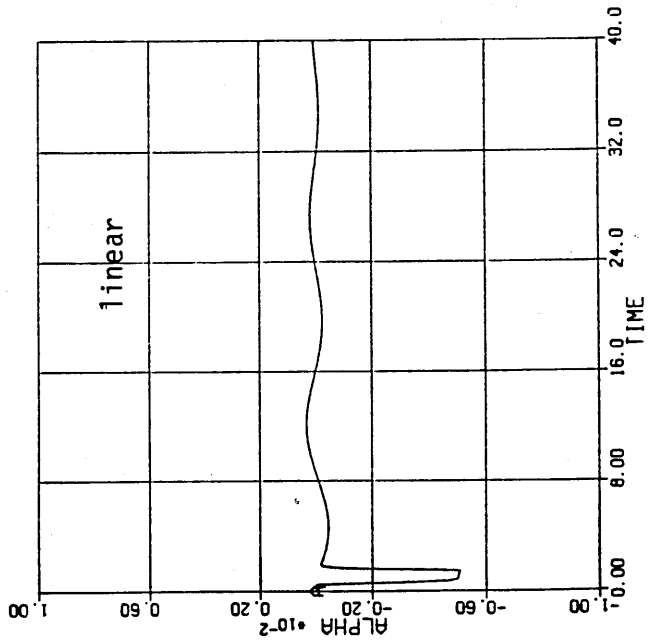
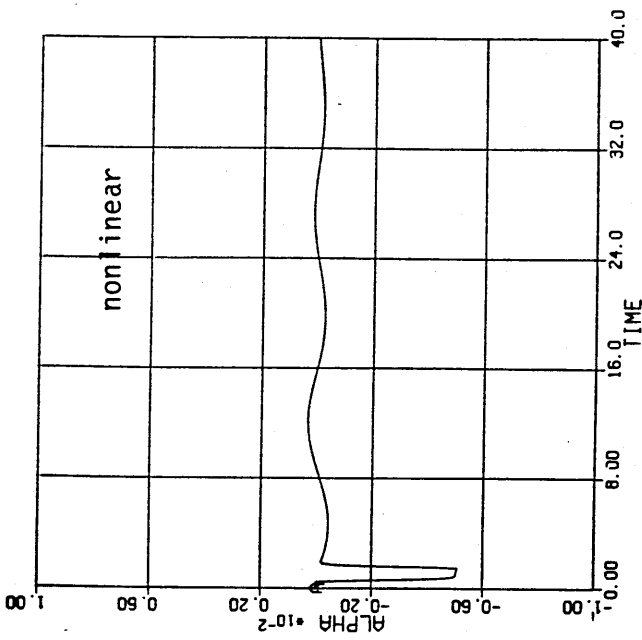


Fig.3.10 α response to elevator deflection

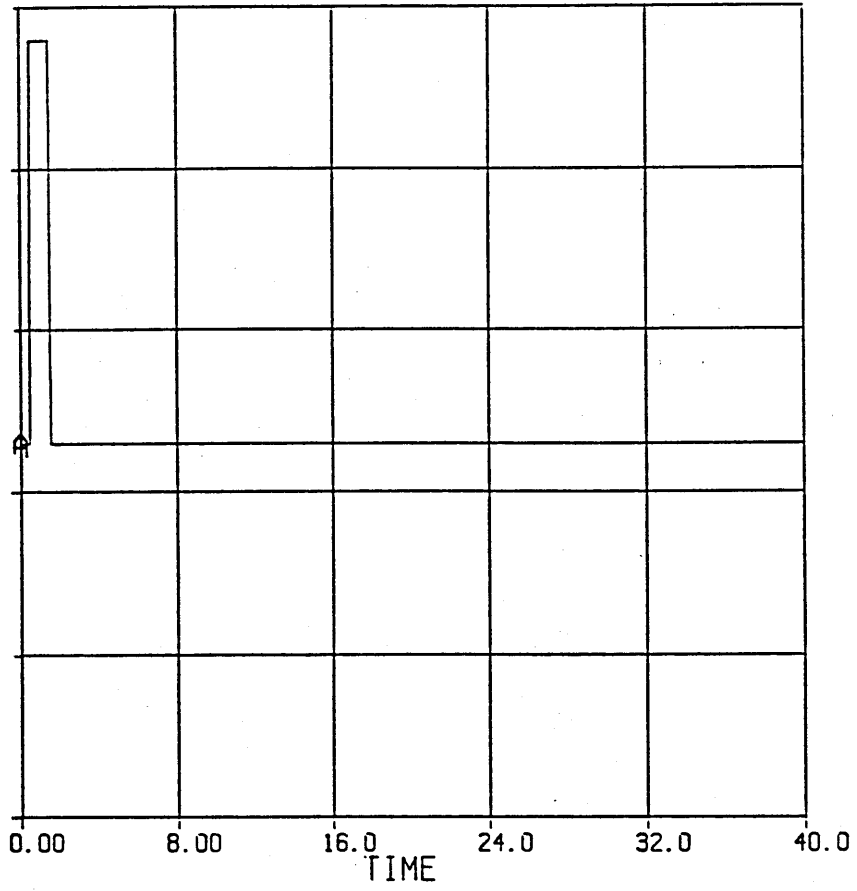


Fig. 3.11 Aileron deflection
Amplitude: 0.005 rad
Duration: 1.0 sec

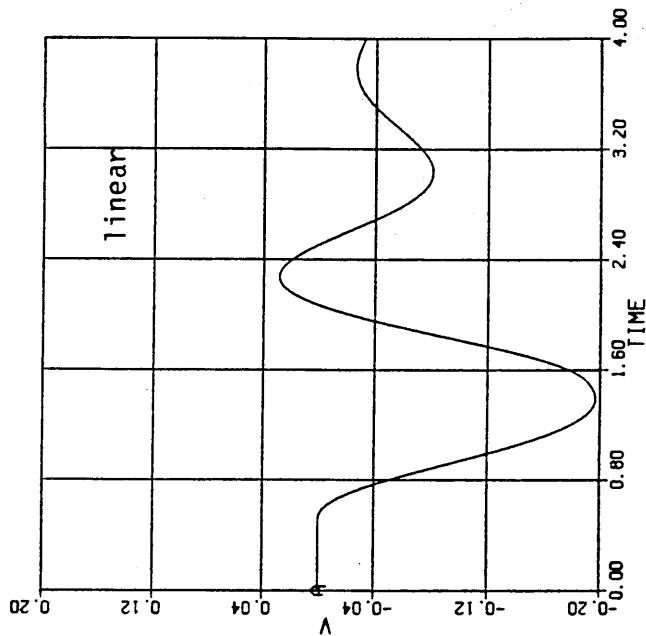
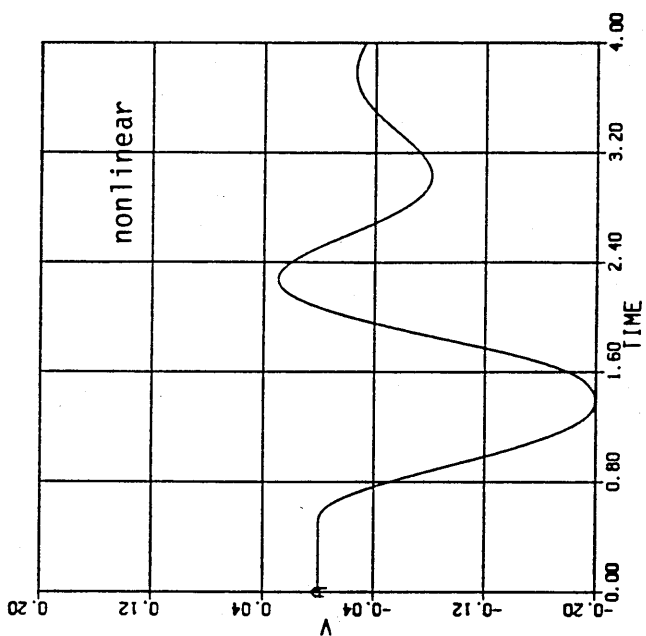


Fig. 3.12 v response to aileron deflection

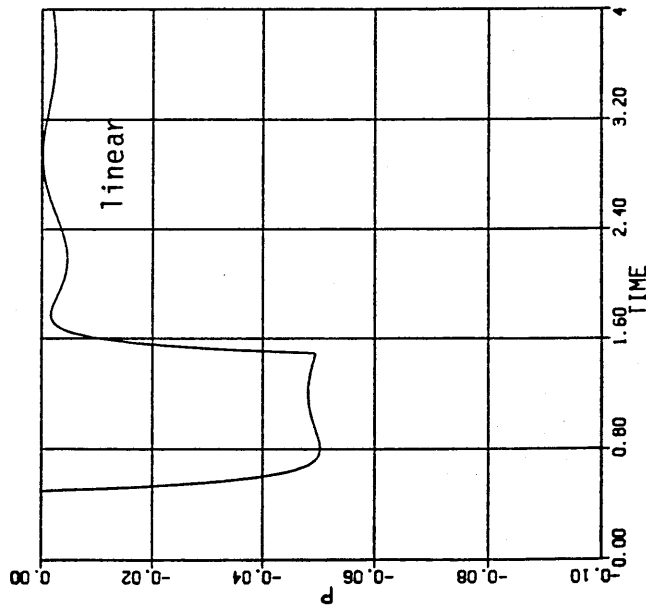
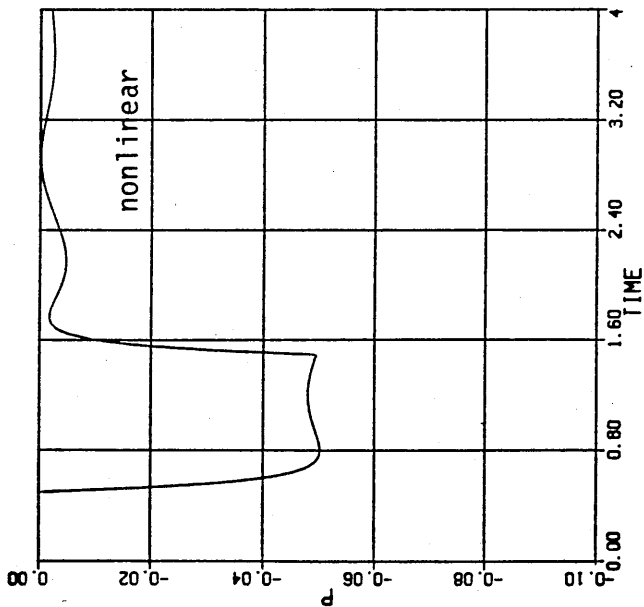


Fig. 3.13 p response to aileron deflection

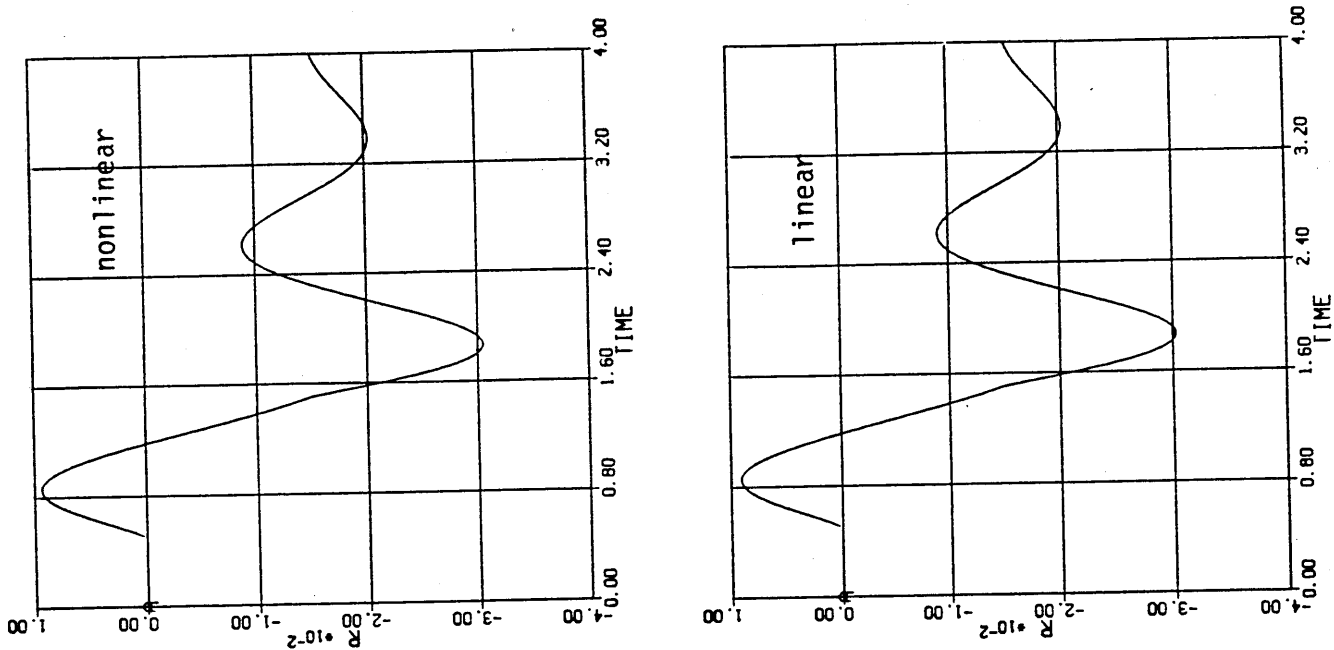


Fig. 3.14 r response to aileron deflection

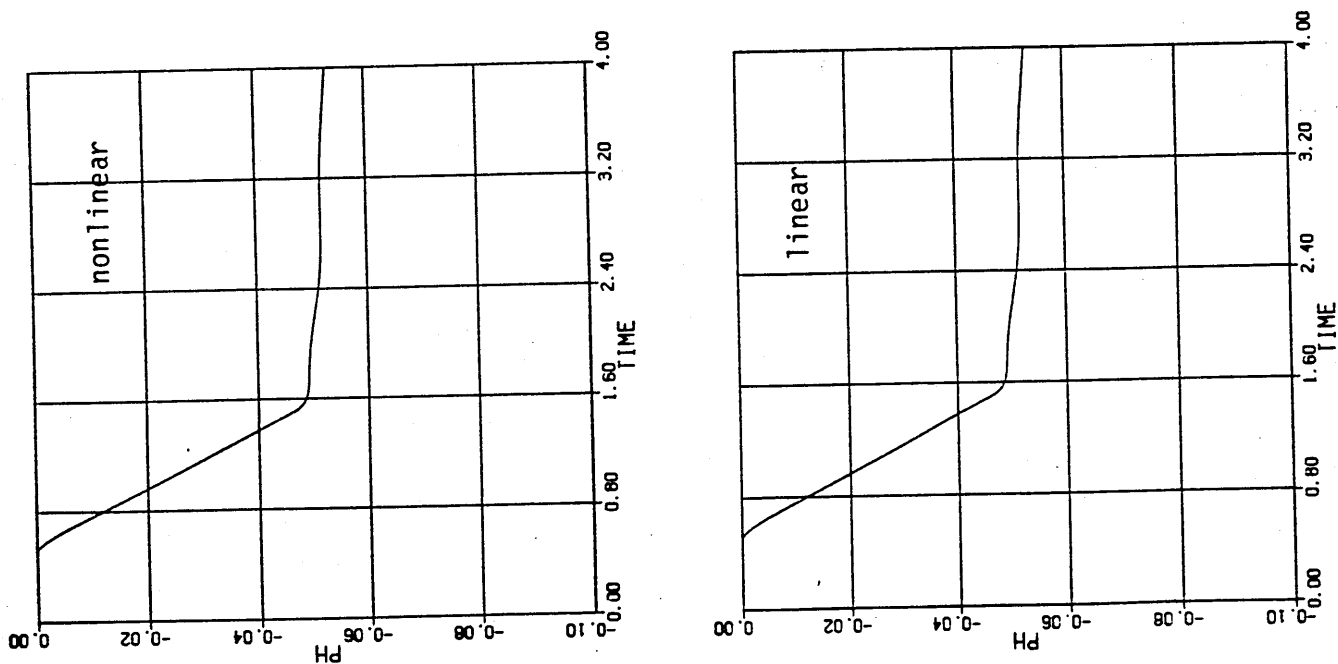


Fig. 3.15 ϕ response to aileron deflection

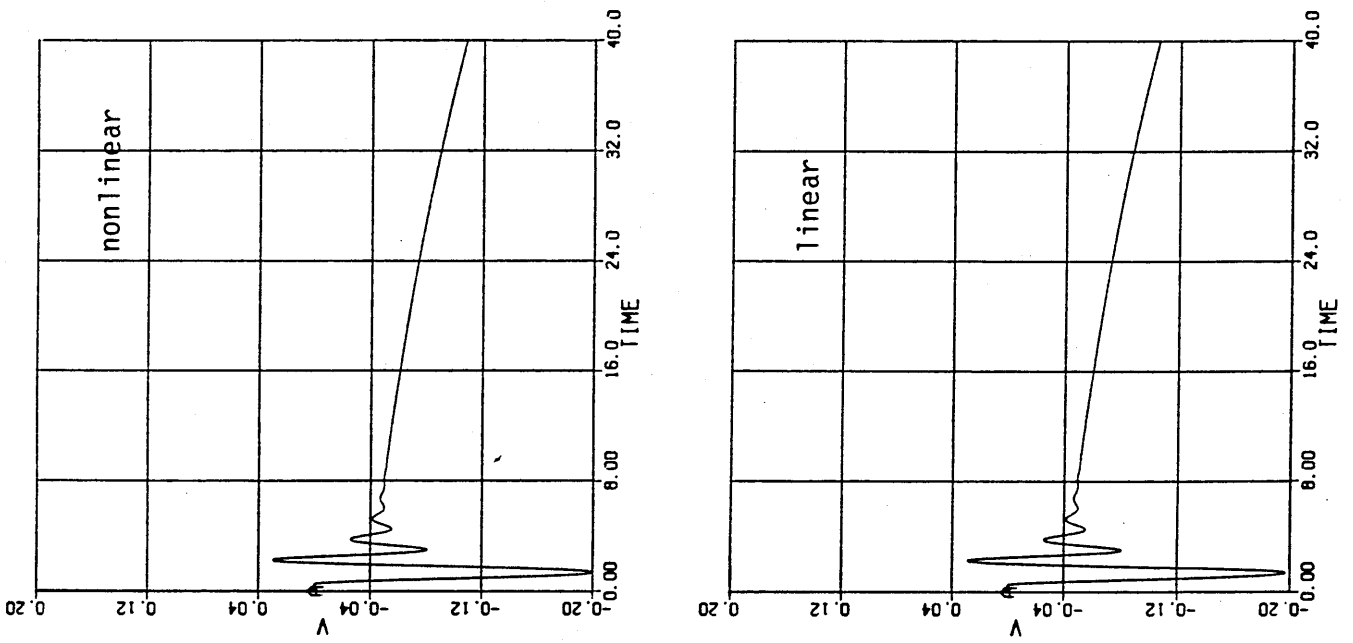


Fig. 3.16 v response to aileron deflection

Chapter 4

IDENTIFICATION OF THE STABILITY AND CONTROL DERIVATIVES OF X-RAE1

4.1 Introduction

An Extended Kalman Filter (EKF) is used in this chapter for the estimation of the aerodynamic derivatives of X-RAE1. It is based on simulated data (p , q and r measurements only) from the discretised longitudinal and lateral models of the RPV.

The general problem of identification and its application to aircraft is discussed in section 4.2 and the concepts of the EKF are presented and briefly analysed in section 4.3.

4.2 The General Problem of Identification and Its Application to Aircraft

System identification and parameter estimation can be considered as a technique for evaluating the properties of any system by the measurement of its input and output time histories (Ref. 8). As it appears from this definition the identification process is distinguished in the following two problems:

1. System Identification. The problem of determining the structure and the parameters of the system.
2. Parameter Estimation. The problem of determining the system parameters for a given or an assumed structure.

If the first problem has to deal with a "black" nontransparent box, then the second is related to a "grey" semi-transparent one (Ref. 17).

Both problems can arise in aircraft identification although parameter estimation is more common as any information about the possible aircraft structure or sufficiently general permissible structure can considerably accelerate the process of estimation.

Therefore, aircraft parameter estimation - as it has been developed over the past 25 years - is the process of extracting numerical values of the aerodynamic stability and control derivatives and other parameters (gusts, sensor errors etc) from the time history of the input and output

variables (Ref. 12). The basic identification procedure can be seen in Fig. 4.1.

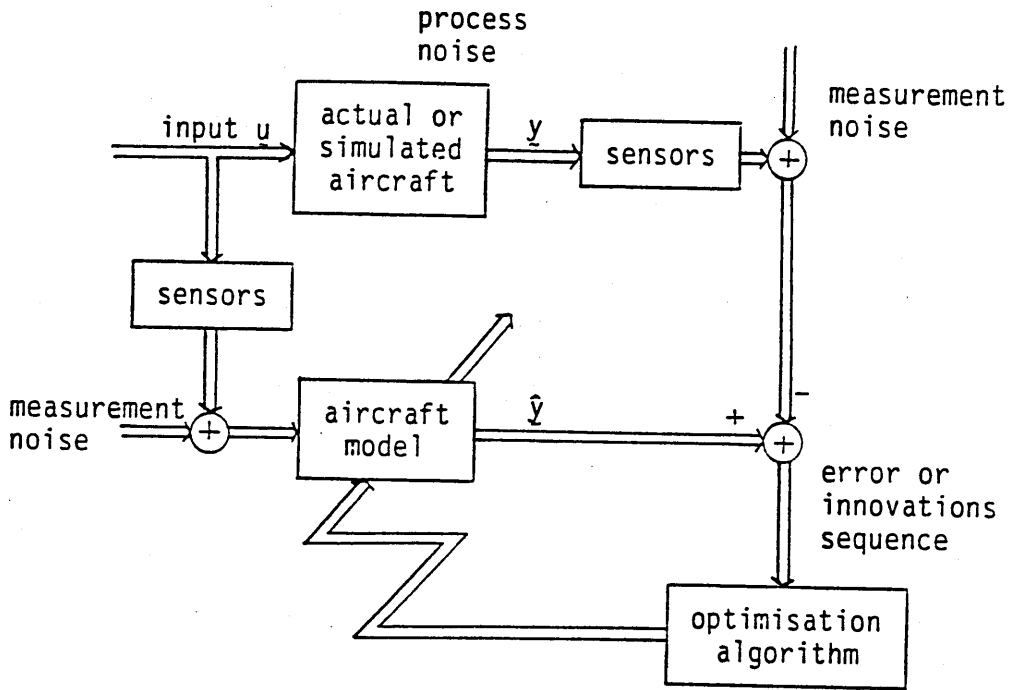


Fig. 4.1 Basic identification procedure

As the system is generally corrupted by process and measurement noise the problem of parameter estimation is that of stochastic approximation. The optimisation criterion can then be the evaluation of the extremum of a performance index $J(\hat{\alpha})$ given in the form of an expectation (Refs 17, 19):

$$J(\hat{\alpha}) = E_x[Q(x, \hat{\alpha})] \quad (4.1)$$

where:

$E_x[\cdot]$ is the expectation operator and

$Q(x, \hat{\alpha})$ is a function of the vector $\hat{\alpha} = (a_1, \dots, a_n)^T$ of

Consider the dynamical system:

$$\begin{aligned} \underline{x}(n+1) &= \underline{f}(\underline{x}(n), \underline{u}(n), n) + \Gamma(\underline{x}(n))\underline{w}(n) \\ \underline{y}(n) &= \underline{h}(\underline{x}(n), \underline{u}(n), n) + \underline{v}(n) \end{aligned} \quad (4.4)$$

where:

$\underline{x}(n)$: is the state vector

$\underline{u}(n)$: is the input vector

$\underline{y}(n)$: is the output vector

$\underline{w}(n)$: is zero mean white process noise, ie:

$$E[\underline{w}(n)] = \underline{0}, E[\underline{w}(n)\underline{w}^T(k)] = Q\delta_{nk}$$

$\underline{v}(n)$: is zero mean white measurement noise, ie:

$$E[\underline{v}(n)] = \underline{0}, E[\underline{v}(n)\underline{v}^T(k)] = R\delta_{nk}$$

and $\underline{w}(n)$, $\underline{v}(n)$ are not correlated each other and with the initial state vector, ie:

$$E[\underline{w}(n)\underline{v}^T(n)] = 0, E[\underline{w}(n)\underline{x}^T(n_0)] = 0, E[\underline{v}(n)\underline{x}^T(n_0)] = 0$$

Then the EKF algorithm for the estimation of the state vector is given by the following prediction and update equations:

Prediction

$$\begin{aligned} \hat{\underline{x}}_{n/n-1} &= \underline{f}(\hat{\underline{x}}_{n-1}, \underline{u}_{n-1}, n-1) \\ P_{n/n-1} &= F_n P_{n-1} F_n^T + \Gamma_{n-1} Q \Gamma_{n-1}^T \end{aligned}$$

Correction

$$\begin{aligned} \hat{\underline{x}}_n &= \hat{\underline{x}}_{n/n-1} + J_n [\underline{y}(n) - H_n \hat{\underline{x}}_{n/n-1}] \\ P_n &= P_{n/n-1} - P_{n/n-1} H_n^T [H_n P_{n/n-1} H_n^T + R]^{-1} H_n P_{n/n-1} \\ J_n &= P_{n/n-1} H_n^T [H_n P_{n/n-1} H_n^T + R]^{-1} \end{aligned} \quad (4.5)$$

where:

$\hat{\underline{x}}_{n/n-1}$ is the estimation of the state vector at the nth step based on information up to the previous step.

P_n is the error covariance matrix ie:

$$P_n = E[(\underline{x}(n) - \hat{\underline{x}}(n))(\underline{x}(n) - \hat{\underline{x}}(n))^T].$$

$$F_n = \left. \frac{\partial \underline{f}}{\partial \underline{x}} \right|_{\underline{x}=\hat{\underline{x}}_{n-1}}, \quad H_n = \left. \frac{\partial \underline{h}}{\partial \underline{x}} \right|_{\underline{x}=\hat{\underline{x}}_{n/n-1}}$$

Eqns 4.5 can be considered as a separation into update at the measurement times and prediction between measurement times as it is schematically shown in Fig. 4.2.

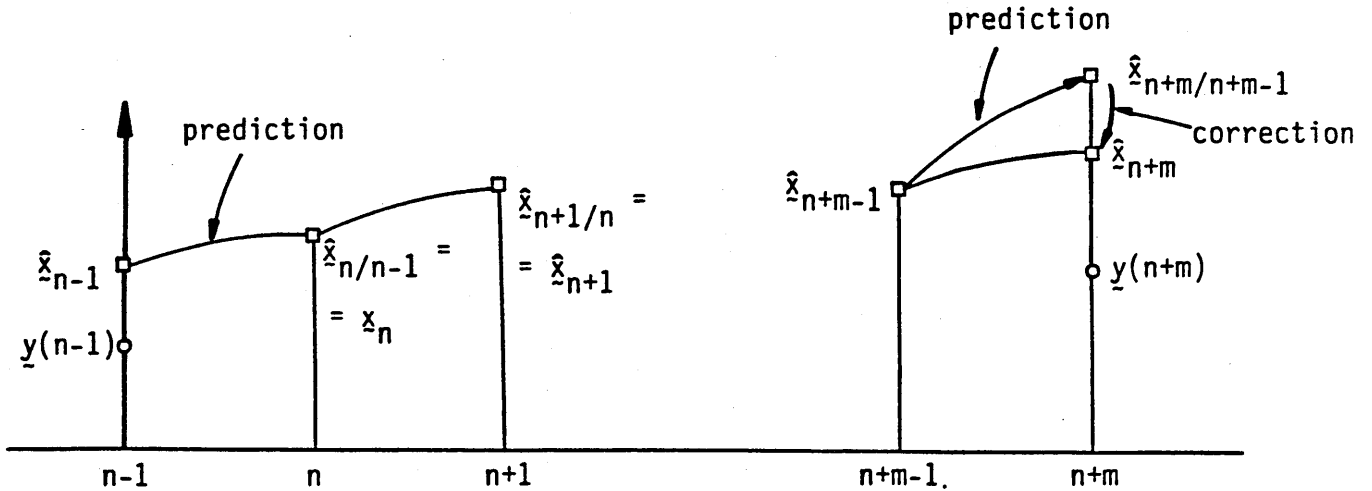


Fig. 4.2 The EKF state prediction and correction procedure

Notice that EKF linearises the equations around the latest best estimate of the state and it requires a priori knowledge of the statistics of the initial state $\hat{x}_{0/0}$ and $P_{0/0}$.

4.3.2 The EKF as Parameter Estimator

The EKF can also be used as parameter estimator if the problem of identification will be set up correctly and care will be taken for the utilisation of the algorithm. If the vector \underline{a} of the unknown parameters has to be estimated, the dynamical system can be rewritten as follows:

$$\begin{aligned} \underline{x}(n+1) &= \underline{f}(\underline{x}(n), \underline{a}, \underline{u}(n), n) + \Gamma(\underline{x}(n))\underline{w}(n) \\ \underline{y}(n) &= \underline{h}(\underline{x}(n), \underline{a}, \underline{u}(n), n) + \underline{v}(n) \end{aligned} \quad (4.7)$$

Including the unknown parameters in the state vector the system of Eqns 4.7 becomes:

$$\begin{aligned} \underline{x}^*(n+1) &= \underline{f}^*(\underline{x}^*(n), \underline{u}(n), n) + \Gamma^*(\underline{x}^*(n))\underline{w}^*(n) \\ \underline{y}(n) &= \underline{h}^*(\underline{x}^*(n), \underline{u}(n), n) + \underline{v}(n) \end{aligned} \quad (4.8)$$

where:

$$\underline{x}^*(n) = \begin{bmatrix} \underline{x}(n) \\ \underline{a}(n) \end{bmatrix} \text{ is the augmented state vector}$$

$$\underline{f}^*(\underline{x}^*(n), \underline{u}(n), n) = \begin{bmatrix} f(\underline{x}(n), \underline{a}, \underline{u}(n), n) \\ 0 \end{bmatrix}$$

$$\Gamma^* = \begin{bmatrix} \Gamma \\ 0 \end{bmatrix}$$

$$\underline{h}^*(\underline{x}^*(n), \underline{u}(n), n) = \underline{h}(\underline{x}(n), \underline{a}, \underline{u}(n), n)$$

$$\underline{w}^*(n) = \begin{bmatrix} w(n) \\ 0 \end{bmatrix}$$

An EKF can then be used for the estimation of the augmented states $\underline{x}^*(n)$ and therefore for the estimation of the states and the parameters of the initial system (Eqns 4.7).

As the EKF is a non-linear estimation procedure even if the system to be identified is linear, there is no guarantee of convergence nor is the P_n matrix necessarily any accurate estimate of the covariance of the estimation errors.

Because linearisation is applied to the normal stochastic state-space representation and not to the innovation representations ($y(n) - H_n^* \hat{x}_{n/n-1}^*$) the EKF is an approximate parameter estimator (Ref. 19). Problems of convergence and low statistical efficiency are often reported in the literature. Nevertheless if care is taken in its utilisation the algorithm appears to work well and has been very popular among users over the past fifteen years. The major disadvantage of the EKF method is that it requires knowledge of the a priori covariances which are unknown for the parameters but it is simpler and less computer-time demanding than the more advanced maximum likelihood estimation.

4.4 The Estimation of the Longitudinal Aerodynamic Derivatives of X-RAE1

The estimation of the aerodynamic derivatives of the longitudinal model of X-RAE1 is tried out in this section. Pitch rate q is assumed to be the only measurement available corrupted by small amounts of white noise with RMS level of 0.01 rad/sec. It is the response to small amplitude deflections of the elevator about its trim position. No attempt was made to model the sensors and the actuators of the system which is considered free of process noise.

The model to be identified is of the following form:

$$\begin{aligned} \dot{\underline{x}} &= A_{LG}\underline{x} + B_{LG}u \\ \underline{y} &= C_{LG}\underline{x} + \underline{v}(t) \end{aligned} \quad (4.9)$$

where:

$$A_{LG} = \begin{bmatrix} x_u & x_w & 0.704 & -9.804 \\ z_u & z_w & 28.575 & 0.236 \\ m_u & m_w & m_q & -0.047 \\ 0 & 0 & 1 & 0 \end{bmatrix}$$

$$B_{LG} = \begin{bmatrix} -0.390 \\ z_\eta \\ m_\eta \\ 0 \end{bmatrix}$$

$$C_{LG} = \begin{bmatrix} 0 & 0 & 1 & 0 \end{bmatrix}$$

$$\underline{x} = \begin{bmatrix} u & w & q & \theta \end{bmatrix}^T \quad \underline{u} = \eta$$

$\underline{v}(t) = v_q(t)$, white gaussian measurement noise with

$$\begin{aligned} E[v_q(t)] &= 0, \quad E[v_q(t)v_q(t-\tau)] = R\delta(t-\tau) \text{ and} \\ R &= (0.01)^2 \text{ (rad/sec)}^2 \end{aligned}$$

If the variation of the derivatives is modelled as a random walk accounting for the mismatch between the system and the model when the parameters are not known, the augmented system becomes:

$$\dot{\underline{x}}^* = \begin{bmatrix} A_{LG} \\ \underline{0} \end{bmatrix} \underline{x}^* + \begin{bmatrix} B_{LG} \\ \underline{0} \end{bmatrix} \eta + \begin{bmatrix} \underline{0} \\ \underline{w} \end{bmatrix}$$

$$\underline{y} = \begin{bmatrix} 0 & 0 & 1 & 0 & 0 & \dots & 0 \end{bmatrix} \underline{x}^* + \underline{y}$$

where:

$$\underline{x}^* = \begin{bmatrix} u & w & q & \theta & x_u & x_w & z_u & z_w & z_\eta & m_u & m_w & m_q & m_\eta \end{bmatrix}^T$$

$$= \begin{bmatrix} x_1 & x_2 & \dots & x_{13} \end{bmatrix}^T \quad \text{and}$$

$$\underline{w} = \begin{bmatrix} w_{x_u} & w_{x_w} & w_{z_u} & w_{z_w} & \dots & w_{m_\eta} \end{bmatrix}^T \quad \text{white gaussian noise}$$

with $E[\underline{w}(t)] = \underline{0}$, $E[\underline{w}(t)\underline{w}^T(t-\tau)] = Q_t \delta(t-\tau)$

The simulated pitch rate is derived from the equivalent discrete system of the continuous time Eqns 4.9 (Apx DE) as follows:

$$\begin{bmatrix} u(n+1) \\ w(n+1) \\ q(n+1) \\ \theta(n+1) \end{bmatrix} = \begin{bmatrix} 1+x_u T_s & x_w T_s & 0.704T_s & -9.804T_s \\ z_u T_s & 1+z_w T_s & 28.575T_s & 0.236T_s \\ m_u T_s & m_w T_s & 1+m_q T_s & -0.047T_s \\ 0 & 0 & T_s & 1 \end{bmatrix} \begin{bmatrix} u(n) \\ w(n) \\ q(n) \\ \theta(n) \end{bmatrix} + \begin{bmatrix} -0.390T_s \\ z_\eta T_s \\ m_\eta T_s \\ 0 \end{bmatrix} \eta(n)$$

$$\underline{y}(n) = \begin{bmatrix} 0 & 0 & 1 & 0 \end{bmatrix} \underline{x}(n) + \underline{y}(n)$$

where $T_s = 0.01$ secs is the sampling period (or the integration step for the EKF).

The augmented system to be identified by the EKF becomes:

$$\begin{aligned} \underline{x}^*(n+1) &= \underline{f}(\underline{x}^*(n), \eta(n)) + \Gamma(\underline{x}^*(n))\underline{w}(n) \\ \underline{y}(n) &= \underline{h}(\underline{x}^*(n), \eta(n)) + \underline{v}(n) \end{aligned}$$

where:

$$\underline{f}(\underline{x}^*(n), \eta(n)) = \begin{bmatrix} (1+T_s x_5)x_1 + T_s x_6 x_2 + 0.704T_s x_3 - 9.804T_s x_4 - 0.39T_s \eta \\ T_s x_7 x_1 + (1+T_s x_8)x_2 + 28.575T_s x_3 + 0.236T_s x_4 + x_9 T_s \eta \\ T_s x_{10} x_1 + T_s x_{11} x_2 + (1+T_s x_{12})x_3 - 0.047T_s x_4 + x_{13} T_s \eta \\ T_s x_3 + x_4 \\ 0 \\ \vdots \\ 0 \end{bmatrix}$$

$$\Gamma(\underline{x}^*(n)) = \begin{bmatrix} 0 & \cdot & \cdot & \cdot & 0 \\ \vdots & & & & \vdots \\ 0 & \cdot & \cdot & \cdot & 0 \\ T_s & & & & \bigcirc \\ & T_s & & & \\ \bigcirc & & \cdot & & \\ & & & & T_s \end{bmatrix}$$

$$\underline{h}(\underline{x}^*(n), \eta(n)) = \begin{bmatrix} 0 & 0 & 1 & 0 & 0 & \dots & 0 \end{bmatrix} \underline{x}^*(n)$$

The measurements are assumed to be obtained every 0.05 secs. Therefore, the equations for state prediction for the EKF are evaluated every $T_s = 0.01$ secs and they are corrected every measurement update ie. every 0.05 secs. Full derivation of the F and H matrices and of the noise covariances can be found in Apx PI.1.

The elevator deflections are assumed to be a pseudorandom gaussian sequence of zero mean and standard deviation $\sigma_\eta = 0.01$ rad. The trimmed conditions are assumed known whereas the derivatives are 50% in error initially, with the initial error covariance matrix set to the corresponding error values.

The nominal values of the derivatives and the estimated ones by the EKF after 50 secs are summarised in Table 4.1.

Nominal Derivatives		Estimated Derivatives	
		No measurement noise	Measurement noise of ± 0.01 rad/sec
x_u	-0.097	-0.0984	-0.0984
x_w	0.039	0.0374 (?)	0.0579 (?)
z_u	-0.775	-0.7879	-0.8936
z_w	-5.399	-5.3977	-5.4507
z_η	-15.887	—	—
m_u	0.185	0.1805	0.1517
m_w	-2.782	-2.7819	-2.7986
m_q	-18.117	-18.1170	-18.2888
m_η	-175.890	-175.8903	-175.3183

Table 4.1 Nominal and estimated aerodynamic derivatives Longitudinal model.

As it can be seen from the above Table and particularly from the recursive estimates of the derivatives (Figs 4.4 to 4.11), the estimates of x_u , x_w , z_u and m_u are relatively poor; especially x_w is dramatically affected by the measurement noise. The small deflections of the elevator about its trim position can explain the poor estimation of these derivatives.

As $\dot{u} = 0$ and $u = 0$, the model to be identified is eventually the following:

$$\begin{bmatrix} \dot{w} \\ \dot{q} \\ \dot{\theta} \end{bmatrix} = \begin{bmatrix} z_w & 28.575 & 0.236 \\ m_w & m_q & -0.047 \\ 0 & 1 & 0 \end{bmatrix} \begin{bmatrix} w \\ q \\ \theta \end{bmatrix} + \begin{bmatrix} z_\eta \\ m_\eta \\ 0 \end{bmatrix} \eta$$

Therefore, good estimates of z_w , z_η , m_w , m_q and m_η could be expected. Their values converge at about 20 secs but z_η is difficult to be identified. This can be explained by the transfer function of the complete longitudinal model (Eqns 4.9), between the elevator deflection η and the pitch rate q .

The transfer function between η and q is:

$$\frac{q(s)}{\eta(s)} = \frac{s(A_q s^2 + B_q s + C_q)}{A s^4 + B s^3 + C s^2 + D s + E}$$

where:

$$A_q = m_\eta$$

$$B_q = m_u x_\eta + m_w z_\eta - (z_w + x_u) m_\eta$$

$$C_q = (z_u m_w - m_u z_w) x_\eta - (x_u m_w - m_u x_w) z_\eta + (x_u z_w - x_w z_u) m_\eta$$

$$A = 1$$

$$B = -x_u - z_w - m_q$$

$$C = z_w m_q - 28.575 m_w - x_w z_u + x_u (m_q + z_w) - 0.704 m_u + 0.047$$

$$D = -x_u (z_w m_q - 28.575 m_w + 0.047) - 0.047 z_w - 0.236 m_w + \\ + z_u (x_w m_q - 0.704 m_w) - m_u (28.575 x_w - 9.804 + 0.704 z_w)$$

$$E = x_u (0.047 z_w + 0.236 m_w) - z_u (0.047 x_w - 9.804 m_w) - \\ - m_u (0.236 x_w + 9.804 z_w) + 9.804 (z_u m_w - m_u z_w)$$

As it can be seen from the above transfer function, z_η appears only in the B_q and C_q coefficients and all the terms involving z_η and x_η are negligible compared to the terms involving m_η ; in all frequencies:

$$B_q \text{ coefficient: } m_u x_\eta = -0.072 \\ m_w z_\eta = 44.198 \\ (z_w + x_u) m_\eta = 966.691$$

$$C_q \text{ coefficient: } (z_u m_w - m_u z_w) x_\eta = -1.230 \\ (x_u m_w - m_u x_w) z_\eta = -4.173 \\ (x_u z_w - x_w z_u) m_\eta = -97.430$$

Therefore, neither x_η nor z_η can be identified from q records as they little affect the pitch rate. Terms also involving x_w and m_u are very small compared to other terms in the q/η transfer function and this could be one more reason for the poor estimation of these derivatives and their dependance on the measurement noise.

Other inputs like square waves or trains of multisteps were also tried with similar results (Apx PI.1).

4.5 The Estimation of the Lateral Aerodynamic Derivatives of X-RAE1

The estimation of the lateral aerodynamic stability and control derivatives of the lateral model of X-RAE1 from roll and yaw rates only, is presented in this section. The model to be identified is of the form:

$$\begin{aligned}\dot{\underline{x}} &= A_{LT}\underline{x} + B_{LT}\underline{u} \\ \underline{y} &= C_{LT}\underline{x} + \underline{v}(t)\end{aligned}\tag{4.10}$$

where:

$$A_{LT} = \begin{bmatrix} Y_v & -0.561 & -29.767 & 9.804 \\ L_v & L_p & L_r & 0 \\ N_v & N_p & N_r & 0 \\ 0 & 1 & -0.025 & 0 \end{bmatrix}$$

$$B_{LT} = \begin{bmatrix} 0 & Y_\zeta \\ L_\xi & 2.485 \\ 4.182 & N_\zeta \\ 0 & 0 \end{bmatrix}$$

$$C_{LT} = \begin{bmatrix} 0 & 1 & 0 & 0 \\ 0 & 0 & 1 & 0 \end{bmatrix}$$

$$\underline{x} = [v \quad p \quad r \quad \varphi]^T \quad \underline{y} = [p \quad r]^T \quad \underline{u} = [\xi \quad \zeta]^T$$

$$\underline{v}(t) = \begin{bmatrix} v_p & v_r \end{bmatrix}^T, \text{ white gaussian measurement noise with}$$

$$E[\underline{v}(t)] = \underline{0}, \quad E[\underline{v}(t)\underline{v}^T(t-\tau)] = R\delta(t-\tau) \text{ and}$$

$$R = \begin{bmatrix} 0.0001 & 0 \\ 0 & 0.0001 \end{bmatrix}$$

The simulated data are derived from the equivalent discrete system with sampling period $T_s = 0.005$ secs:

$$\begin{bmatrix} v(n+1) \\ p(n+1) \\ r(n+1) \\ \varphi(n+1) \end{bmatrix} = \begin{bmatrix} 1+Y_v T_s & -0.561T_s & -29.767T_s & 9.804T_s \\ L_v T_s & 1+L_p T_s & L_r T_s & 0 \\ N_v T_s & N_p T_s & 1+N_r T_s & 0 \\ 0 & T_s & -0.025T_s & 1 \end{bmatrix} \begin{bmatrix} v(n) \\ p(n) \\ r(n) \\ \varphi(n) \end{bmatrix} +$$

$$+ \begin{bmatrix} 0 & Y_\zeta T_s \\ L_\xi T_s & 2.485T_s \\ 4.182T_s & N_\zeta T_s \\ 0 & 0 \end{bmatrix} \begin{bmatrix} \xi(n) \\ \zeta(n) \end{bmatrix}$$

and the augmented system is:

$$\underline{x}^*(n+1) = \underline{f}(\underline{x}^*(n), \underline{u}(n)) + \Gamma(\underline{x}^*(n))\underline{w}(n)$$

$$\underline{y}(n) = \underline{h}(\underline{x}^*(n), \underline{u}(n)) + \underline{v}(n)$$

where:

$$\underline{x}^*(n) = \begin{bmatrix} v & p & r & \varphi & Y_v & Y_\zeta & L_v & L_p & L_r & L_\xi & N_v & N_p & N_r & N_\zeta \end{bmatrix}^T$$

$$= \begin{bmatrix} x_1 & x_2 & \dots & x_{14} \end{bmatrix}^T$$

$$\underline{w}(n) = \begin{bmatrix} w_{Y_v} & w_{Y_\zeta} & w_{L_v} & \dots & w_{N_\zeta} \end{bmatrix}^T, \text{ gaussian white noise}$$

$$\text{with } E[\underline{w}(n)] = \underline{0}, \quad E[\underline{w}(n)\underline{w}^T(k)] = Q\delta_{nk}$$

$$f(\underline{x}^*(n), \underline{u}(n)) = \begin{bmatrix} (1+T_s x_5)x_1 - 0.561T_s x_2 - 29.767T_s x_3 + 9.804T_s x_4 + T_s x_6 u_2 \\ T_s x_7 x_1 + (1+T_s x_8)x_2 + T_s x_9 x_3 + T_s x_{10} u_1 + 2.485T_s u_2 \\ T_s x_{11} x_1 + T_s x_{12} x_2 + (1+T_s x_{13})x_3 + 4.182T_s u_1 + T_s x_{14} u_2 \\ T_s x_2 - 0.025T_s x_3 + x_4 \\ 0 \\ \vdots \\ \vdots \\ 0 \end{bmatrix}$$

$$h(\underline{x}^*(n), \underline{u}(n)) = \begin{bmatrix} 0 & 1 & 0 & 0 & 0 & \dots & 0 \\ 0 & 0 & 1 & 0 & 0 & \dots & 0 \end{bmatrix} \underline{x}^*(n)$$

and $\Gamma(\underline{x}^*(n))$ similar to that appearing in the longitudinal model.

The aileron and rudder deflections are pseudorandom gaussian sequences with zero mean and standard deviations $\sigma_\xi = \sigma_\zeta = 0.01$ rad. The EKF is started up with initial values of the derivatives 50% in error (more details can be found in Apx LA.2). The estimates of the derivatives after 50 secs and their nominal values are shown in Table 4.2 whereas their time histories can be found in Figs 4.12 to 4.21.

Nominal Derivatives		Estimated Derivatives
		Measurement noise of ± 0.01 rad/sec
Y_v	-0.336	-0.3215 (?)
Y_ζ	3.909	?
L_v	-0.414	-0.4582
L_p	-13.360	-13.2223
L_r	2.412	2.6635
L_ξ	-142.902	-140.6240
N_v	0.558	0.5557
N_p	-0.622	-0.6210
N_r	-1.426	-1.4099
N_ζ	-18.015	-18.2482

Table 4.2 Nominal and estimated aerodynamic derivatives Lateral model.

As it can be seen from Fig. 4.13 Y_{ζ} is not identifiable. Evaluating the transfer function between the rudder deflection ζ and the yaw rate r the following expression can be obtained:

$$\frac{r(s)}{\zeta(s)} = \frac{A_r s^3 + B_r s^2 + C_r s + D_r}{A s^4 + B s^3 + C s^2 + D s + E}$$

where:

$$A_r = N_{\zeta}$$

$$B_r = N_v Y_{\zeta} + N_p L_{\zeta} - (L_p + Y_v) N_{\zeta}$$

$$C_r = (L_v N_p - N_v L_p) Y_{\zeta} - (Y_v N_p + 0.561 N_v) L_{\zeta} + (Y_v L_p + 0.561 L_v) N_{\zeta}$$

$$D_r = 9.804(N_v L_{\zeta} - L_v N_{\zeta})$$

$$A = 1$$

$$B = -Y_v - L_p - N_r$$

$$C = L_p N_r - N_p L_r + Y_v (N_r + L_p) + 29.767 N_v + 0.561 L_v$$

$$D = Y_v (N_p L_r - L_p N_r) + 29.767 L_v N_p - 0.561 L_v N_r - N_v (29.767 L_p - 0.561 L_r) - 9.804 (L_v - 0.025 N_v)$$

$$E = 9.804 (L_v N_r - N_v L_r) + 0.245 (L_v N_p - N_v L_p)$$

Derivative Y_{ζ} appears only in coefficients B_r and C_r and its contribution to their values in all frequencies is small compared to contributions from terms involving N_{ζ} :

$$B_r \text{ coefficient: } N_v Y_{\zeta} = 2.181$$

$$N_p L_{\zeta} = -1.546$$

$$(L_p + Y_v) N_{\zeta} = 246.733$$

$$C_r \text{ coefficient: } (L_v N_p - N_v L_p) Y_{\zeta} = 30.148$$

$$(Y_v N_p + 0.561 N_v) L_{\zeta} = 1.297$$

$$(Y_v L_p + 0.561 L_v) N_{\zeta} = -76.685$$

Therefore, as N_{ζ} is the dominant factor in B_r and C_r coefficients Y_{ζ} is not expected to be identifiable from yaw measurements only.

Derivative Y_v also does not converge satisfactorily to its steady value but rather wavers about it (Fig. 4.12). This can be justified by the Bode plots of the terms

$$\dot{v}(s)/\zeta(s), Y_v v(s)/\zeta(s), Y_\zeta$$

of the Y-equation of motion and by the input that is used (pseudorandom sequence) for the identification of the lateral derivatives.

As it can be seen from Fig. 4.3, Y_v is identifiable at low frequencies only ($\omega < 15 \text{ rad/sec}$)⁽¹⁾. Therefore, a rudder input with a low frequency spectrum is more suitable than a pseudorandom sequence which theoretically contains almost all the frequency spectrum with uniformly distributed power.

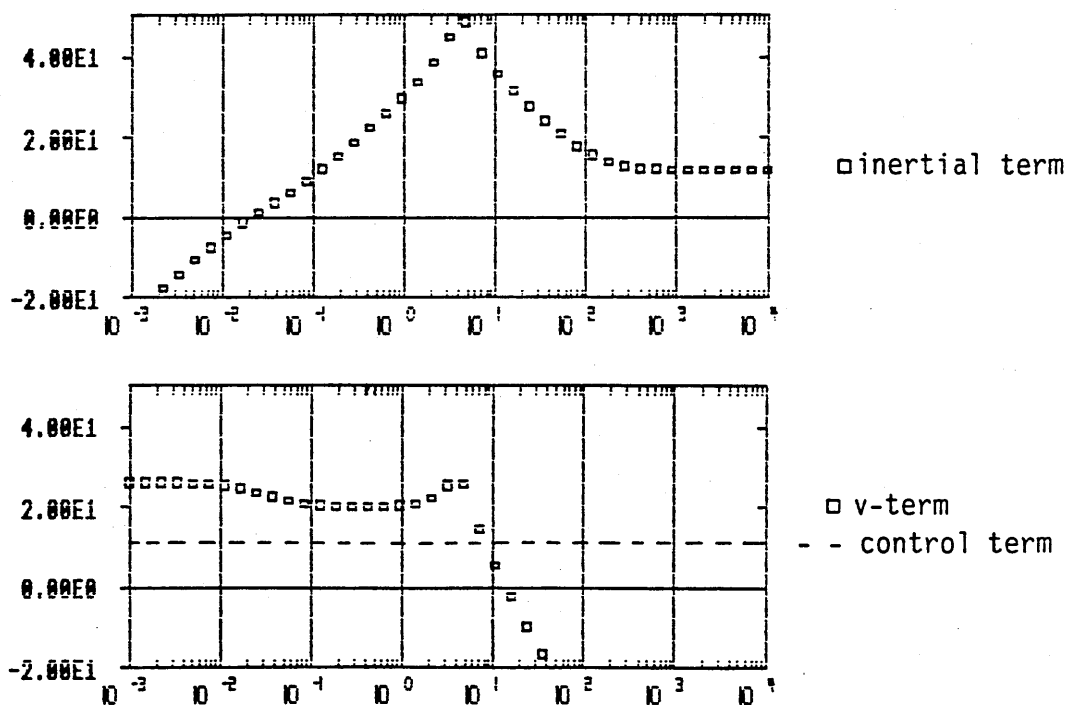


Fig. 4.3 Bode plot of the Y-equation terms

(1). "If at a given frequency the magnitude of a term is large compared with the other terms, it has a great influence within the equation of motion. Its derivative is well identifiable at this frequency. If a term has a small influence, its derivative can not be identified. As a rule of thumb, a derivative is considered to be identifiable when its term

has a magnitude of at least 10% of the largest term's magnitude. If the inertial term is small only ratios of the derivatives can be identified."

in "Practical Input Signal Design"

Plaetschke E. and Schulz G.

paper, AGARD LS-104 "Parameter Identification", Nov. 1979

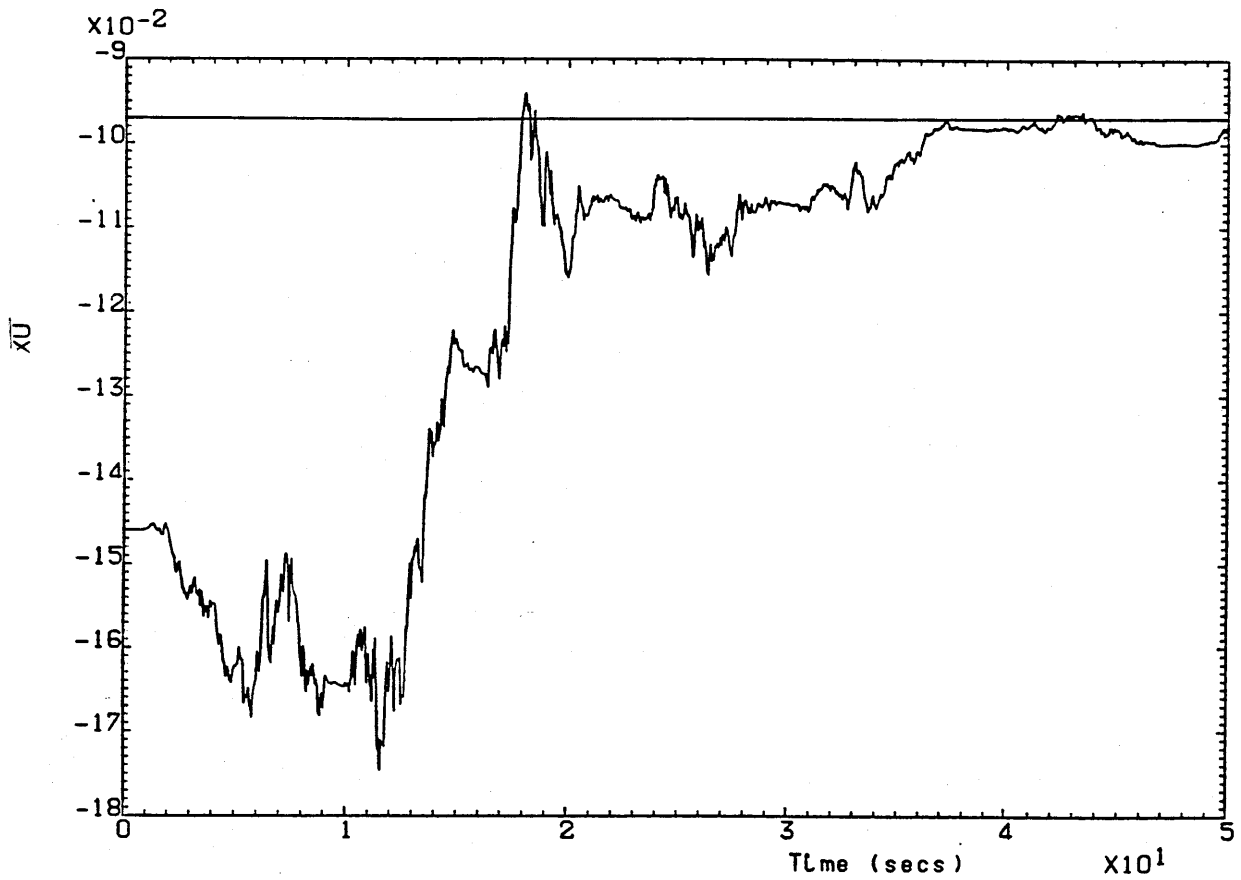
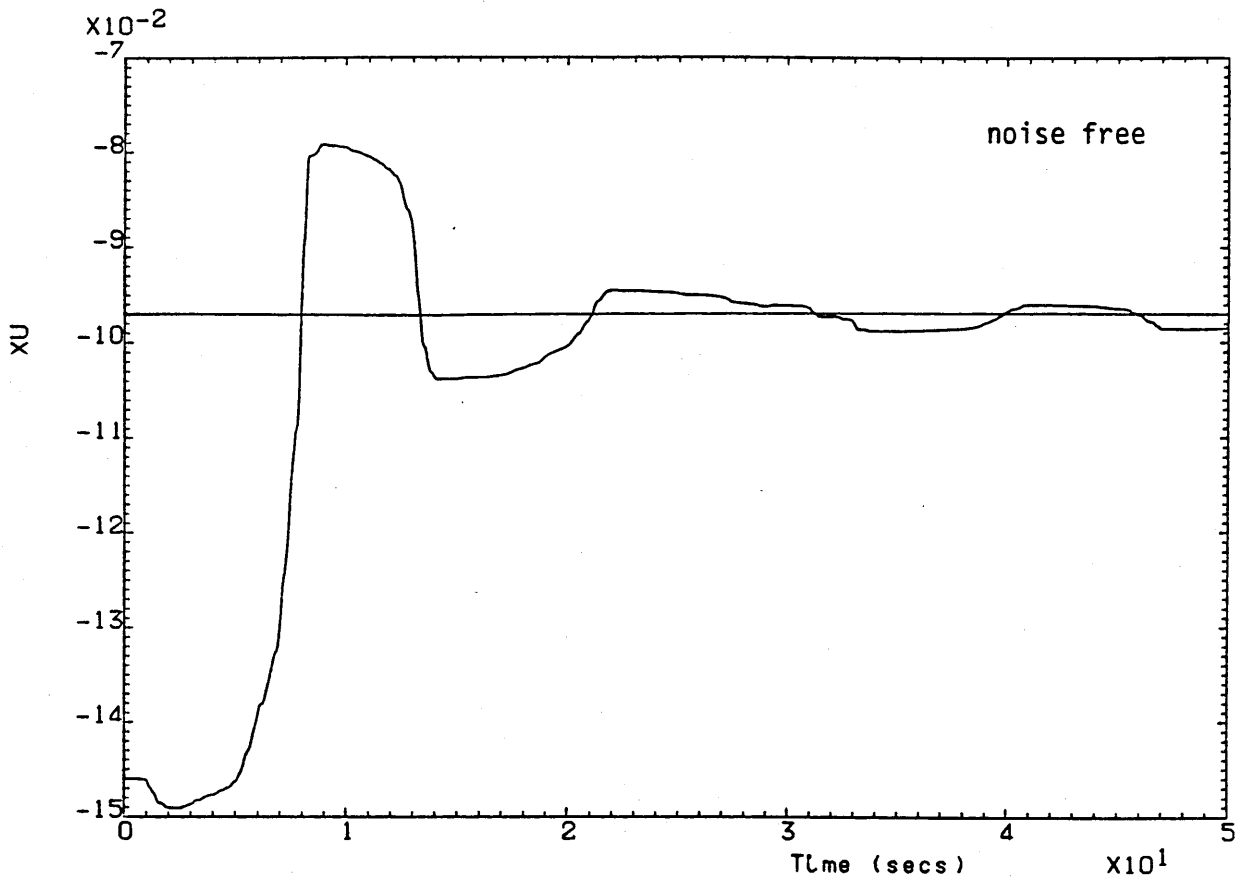


Fig. 4.4 x_u estimates

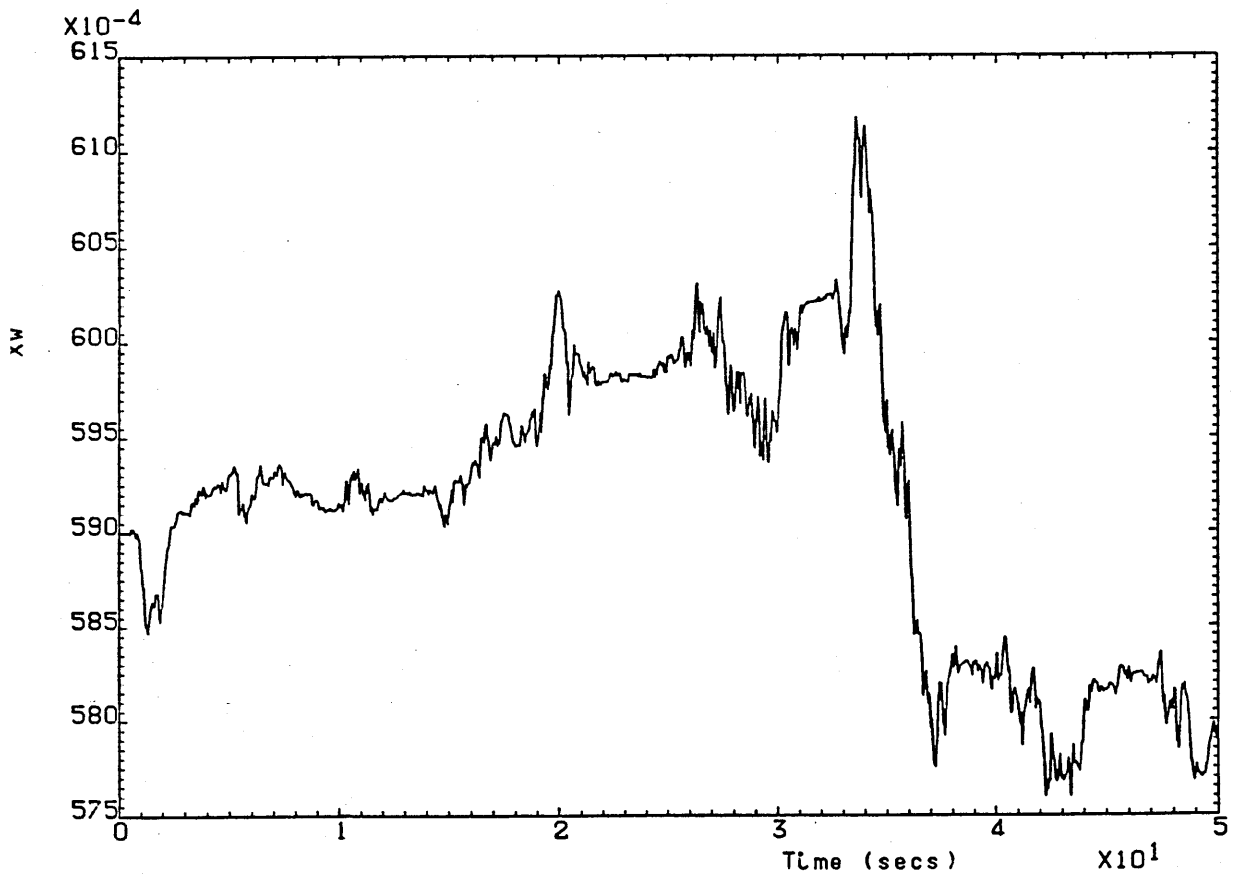
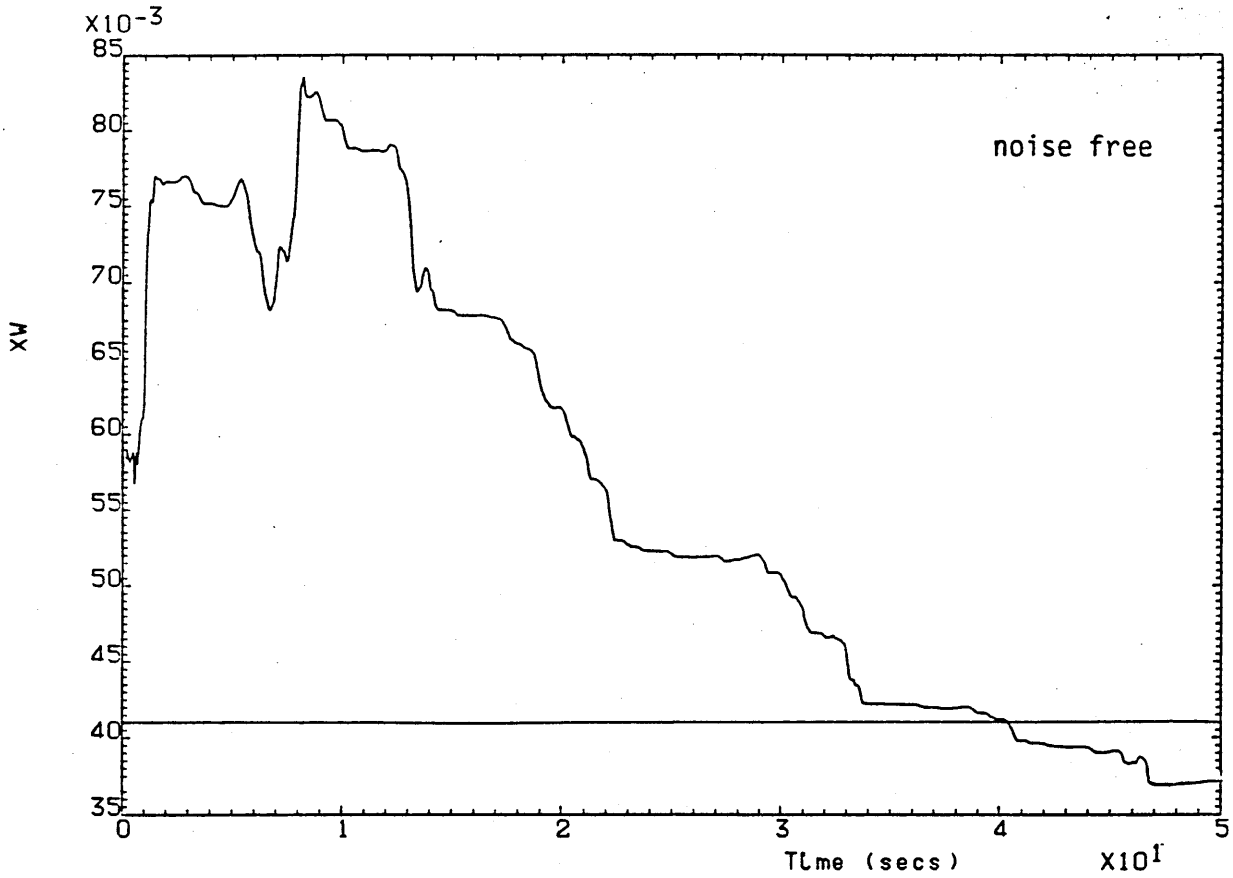


Fig. 4.5 x_w estimates

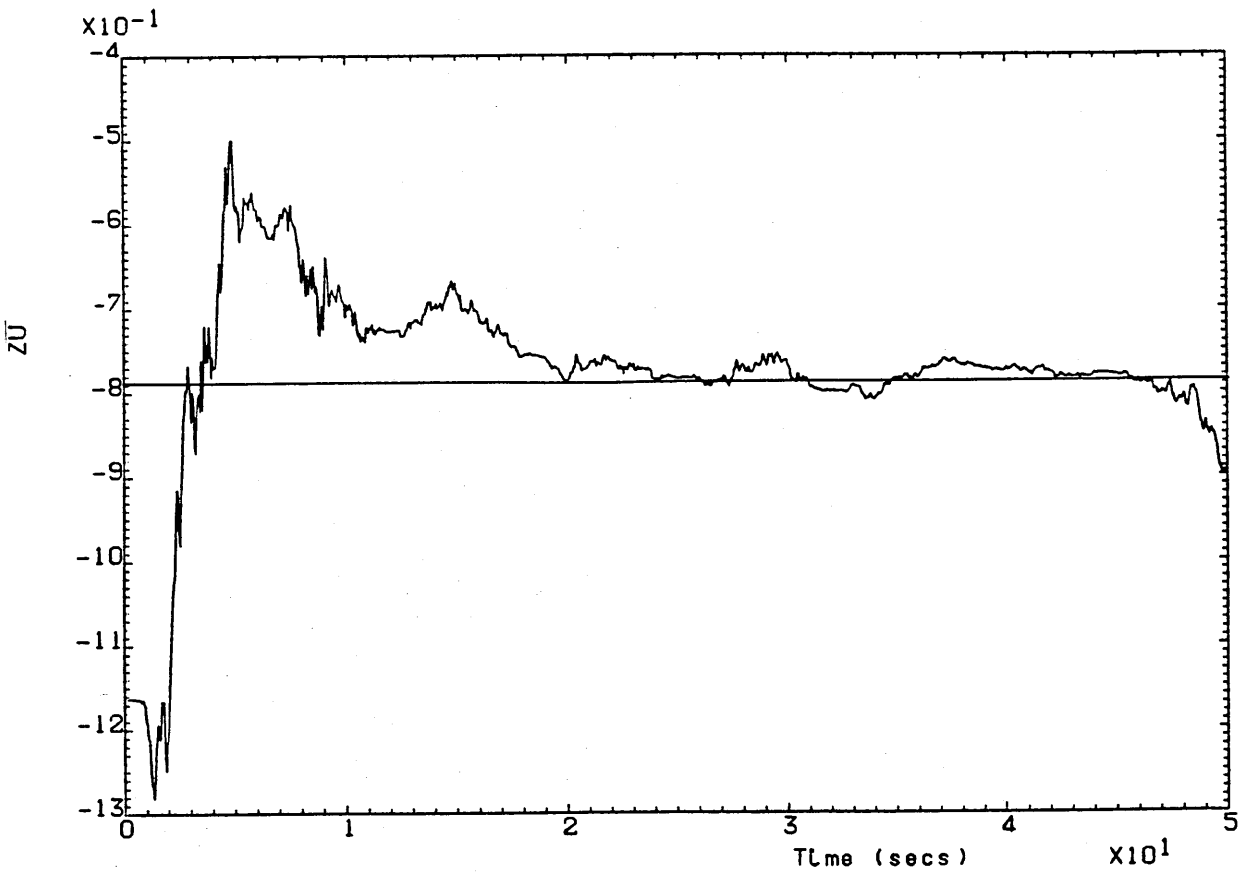
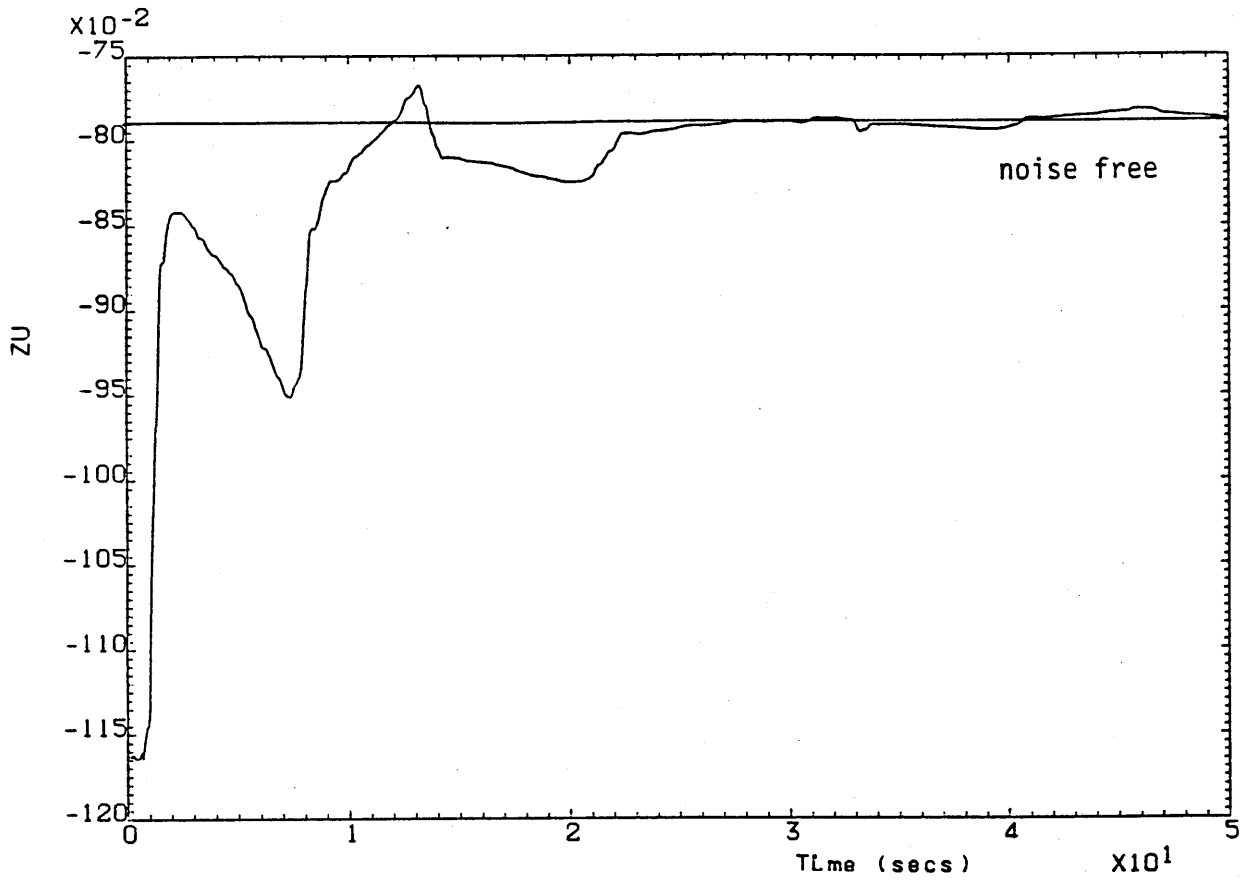


Fig. 4.6 z_u estimates

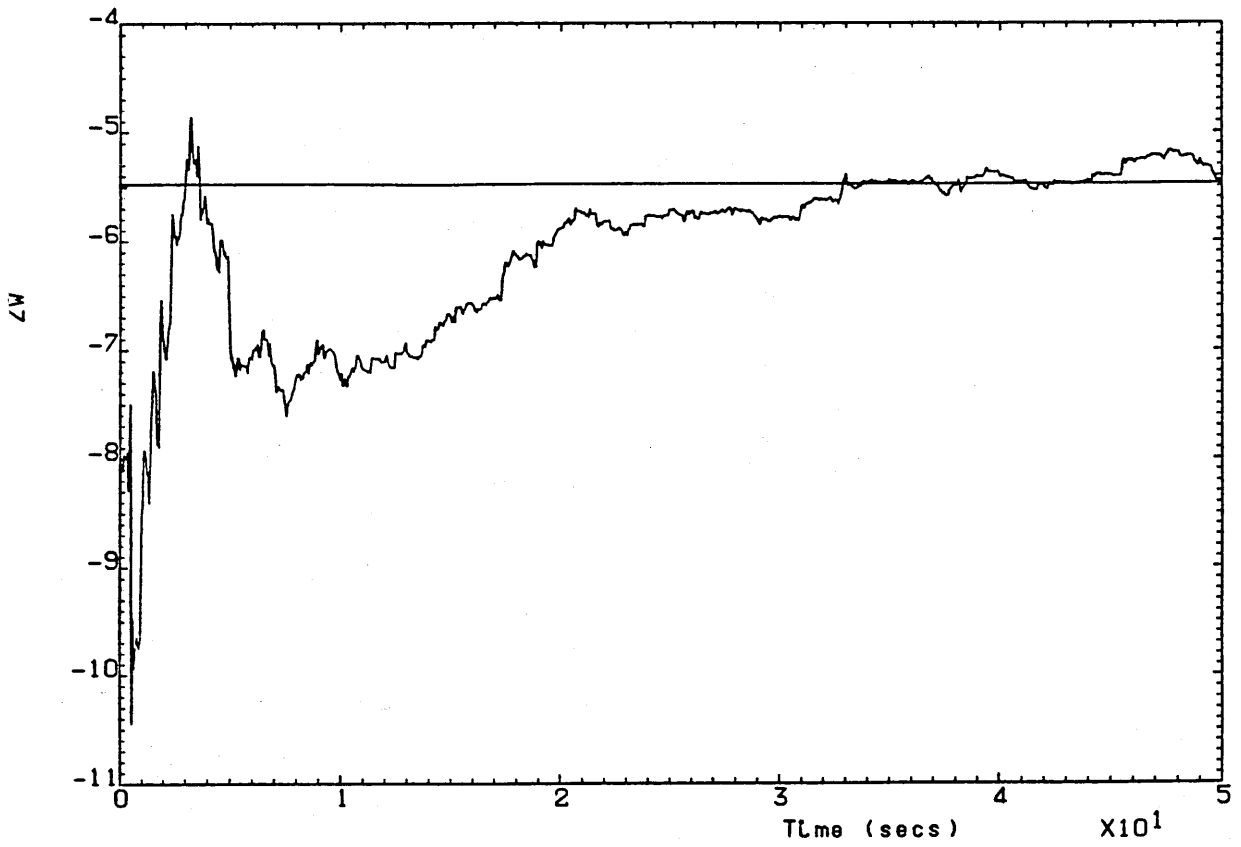
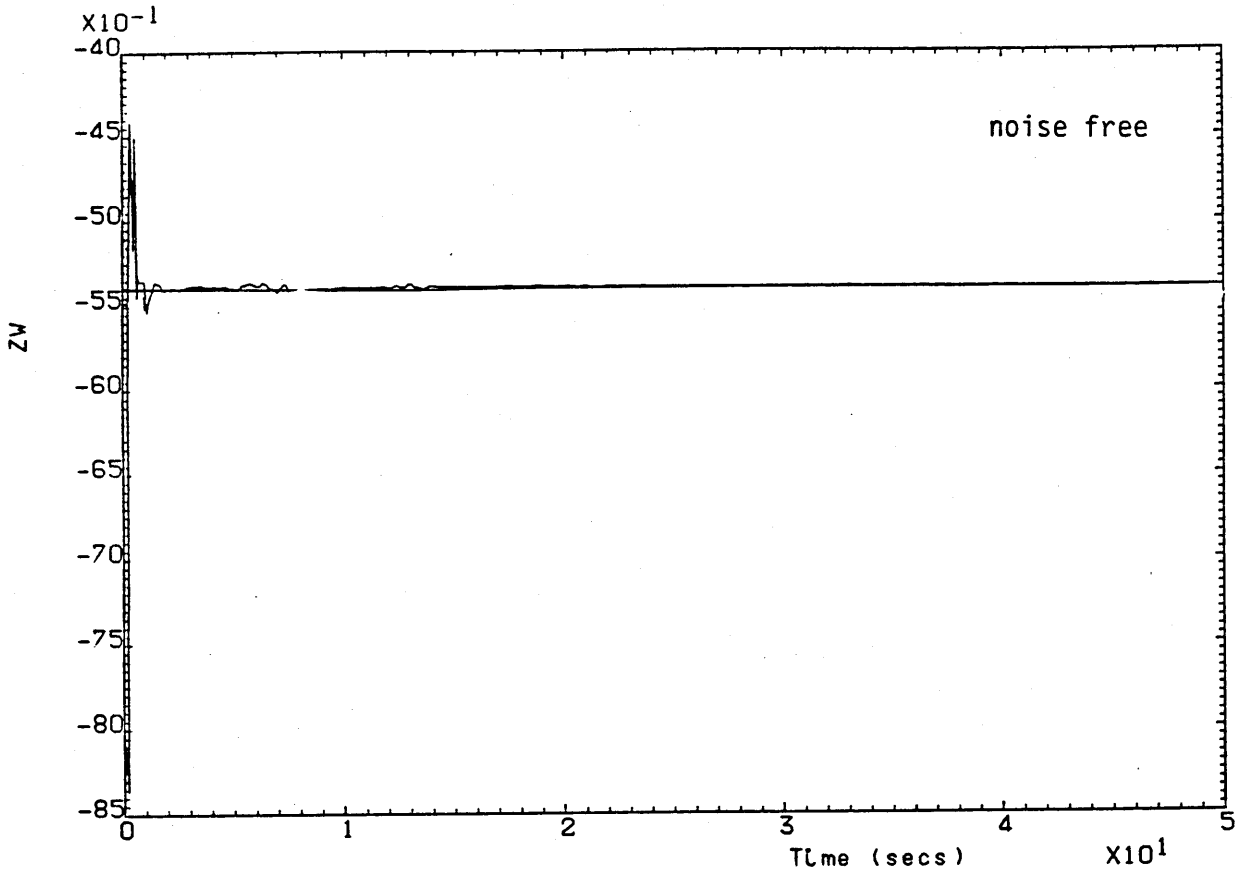


Fig. 4.7 z_w estimates

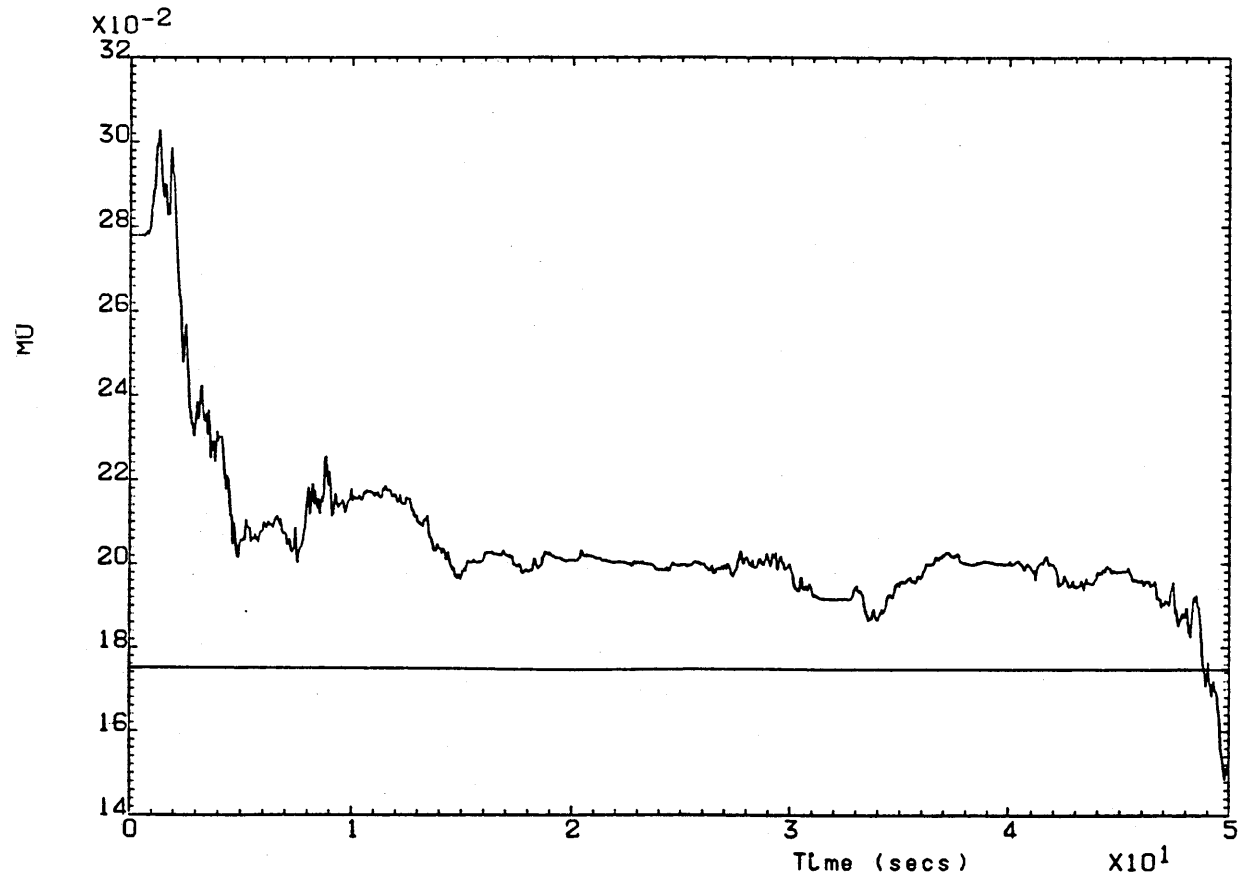
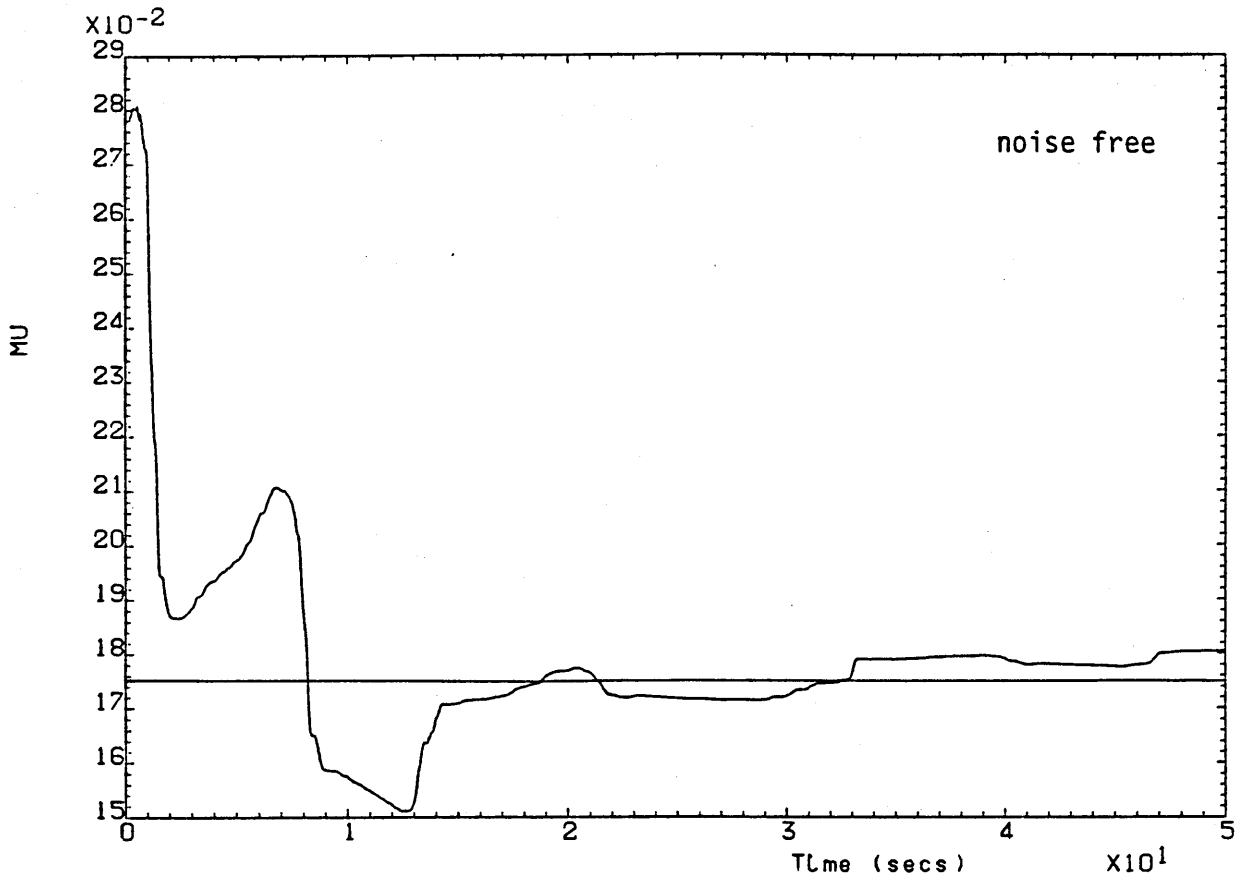


Fig. 4.8 m_u estimates

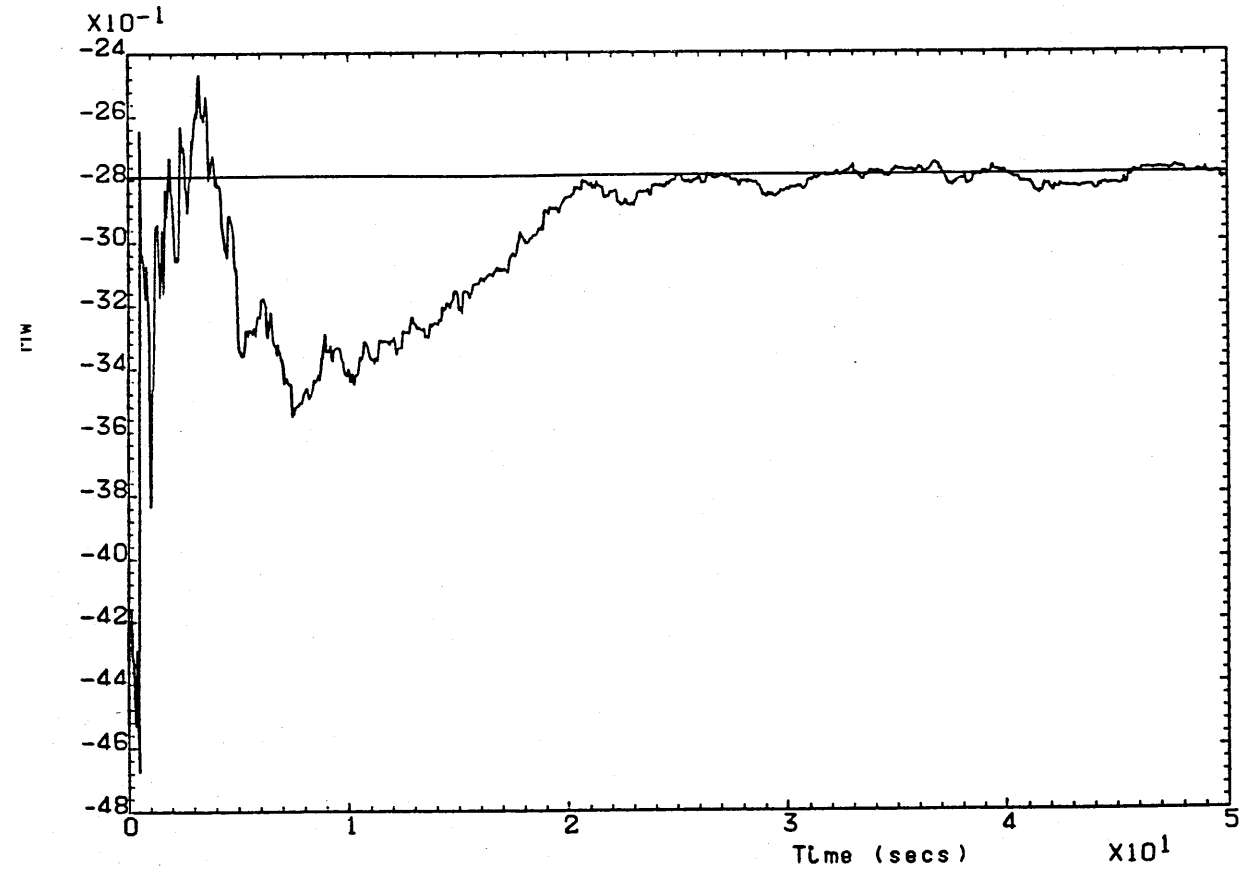
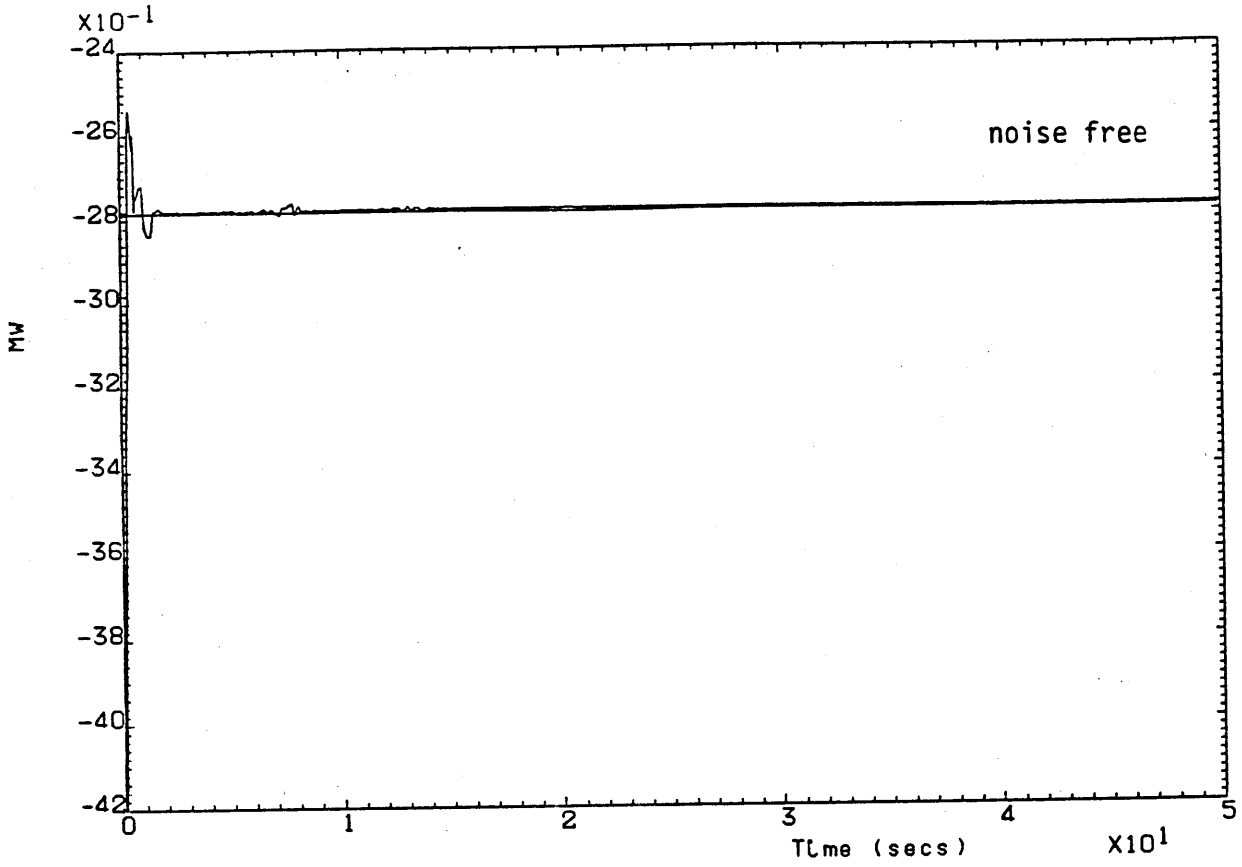


Fig. 4.9 m_w estimates

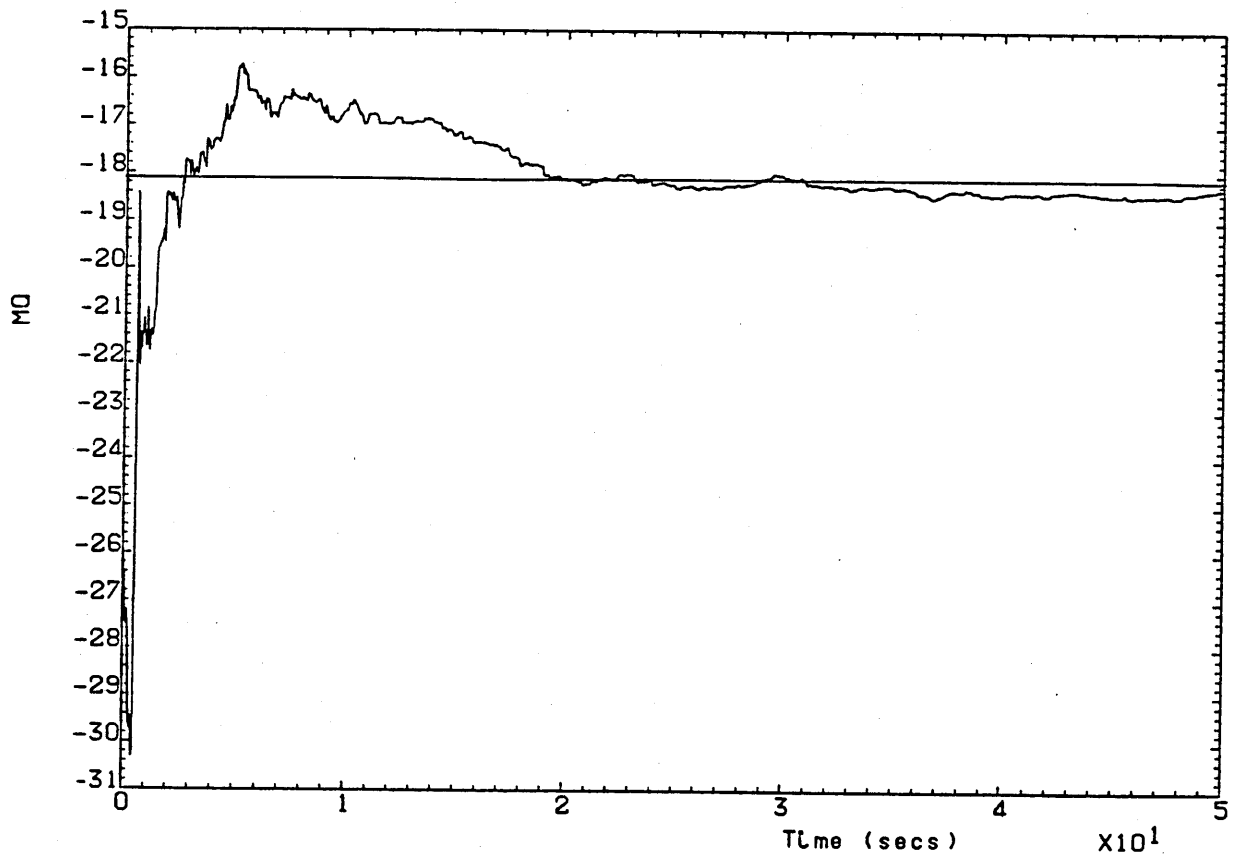
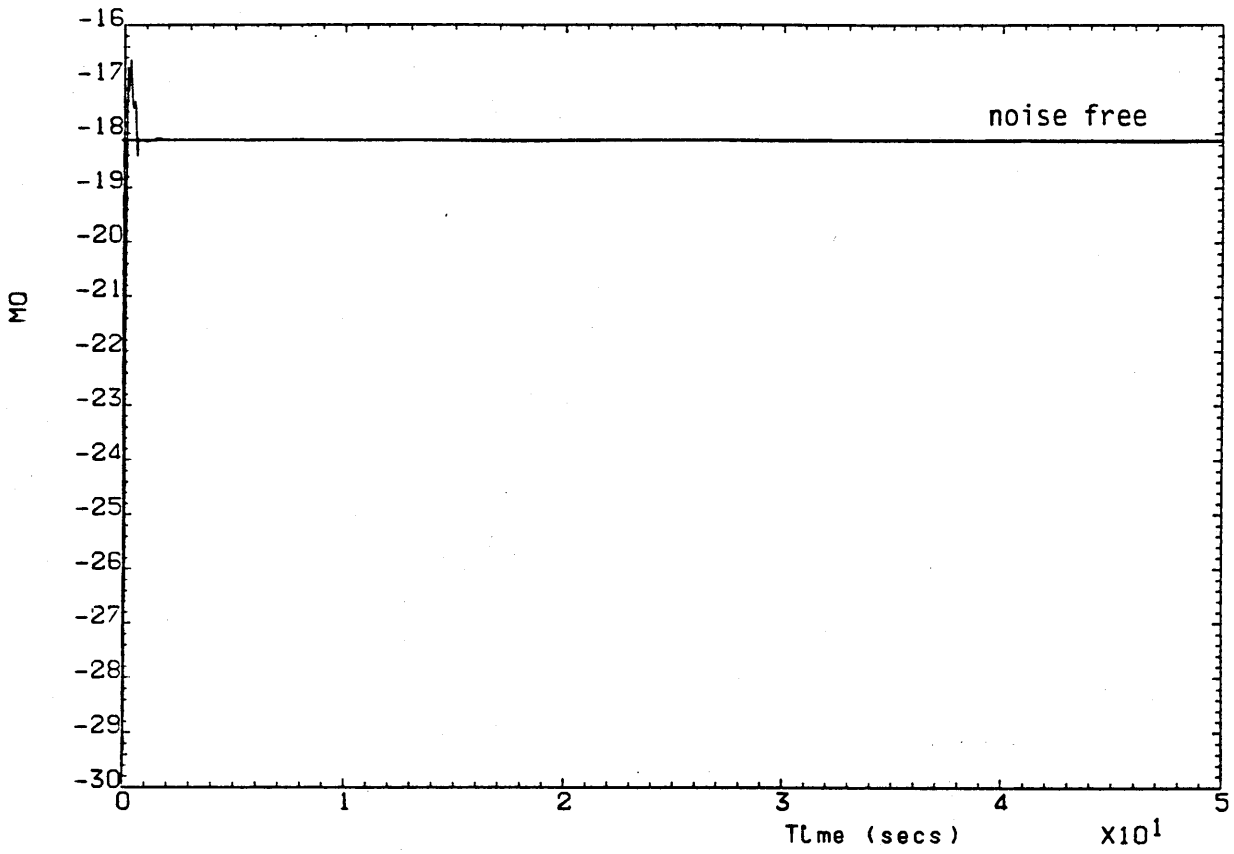


Fig. 4.10 m_q estimates

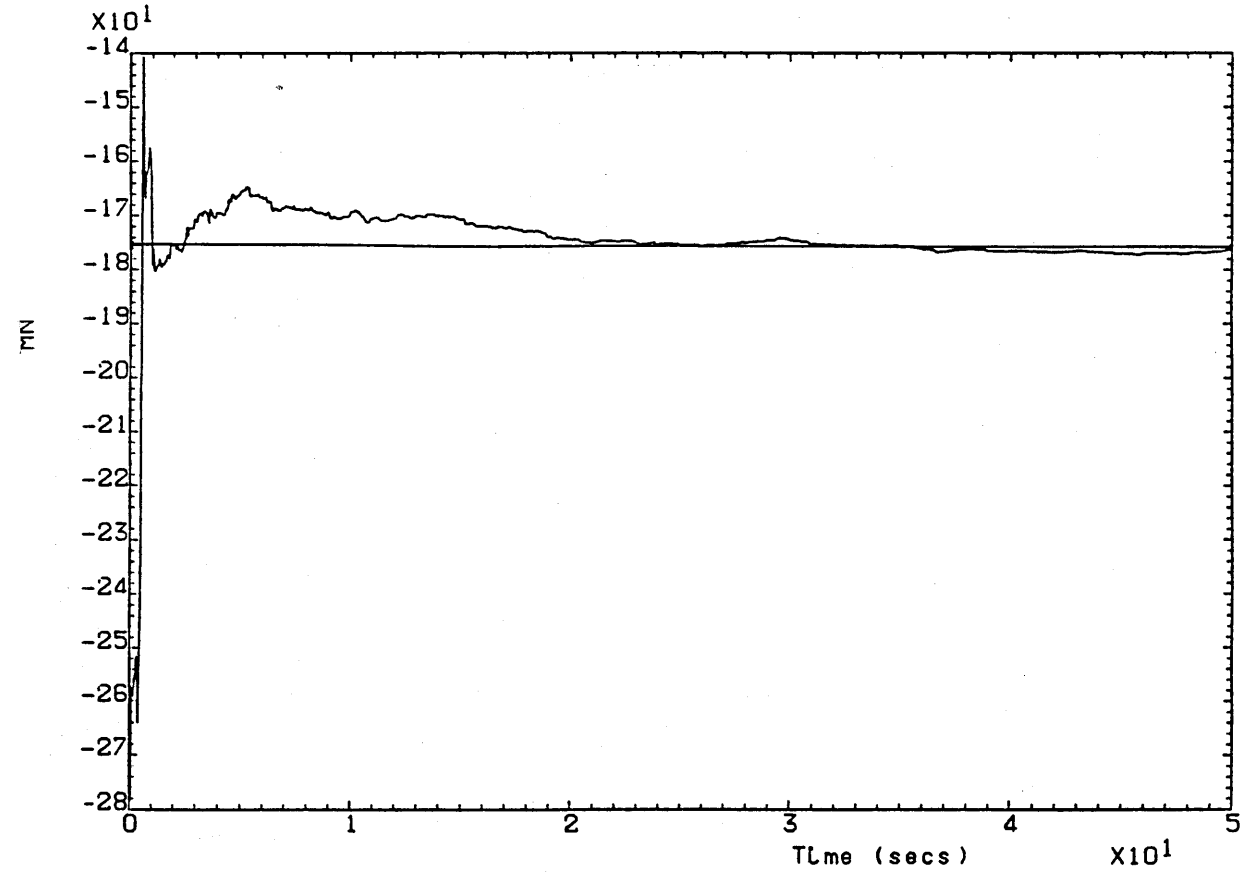
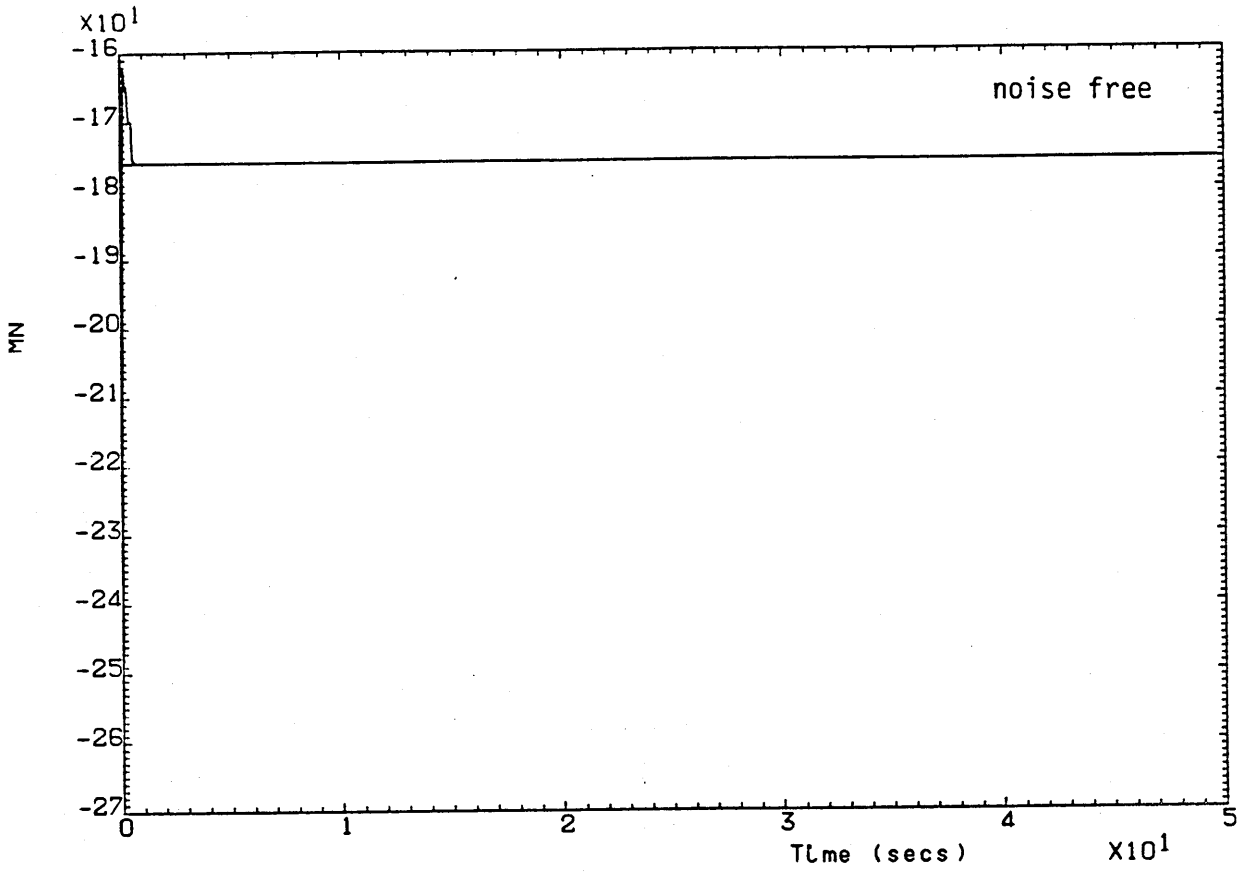


Fig 4.11 m_η estimates

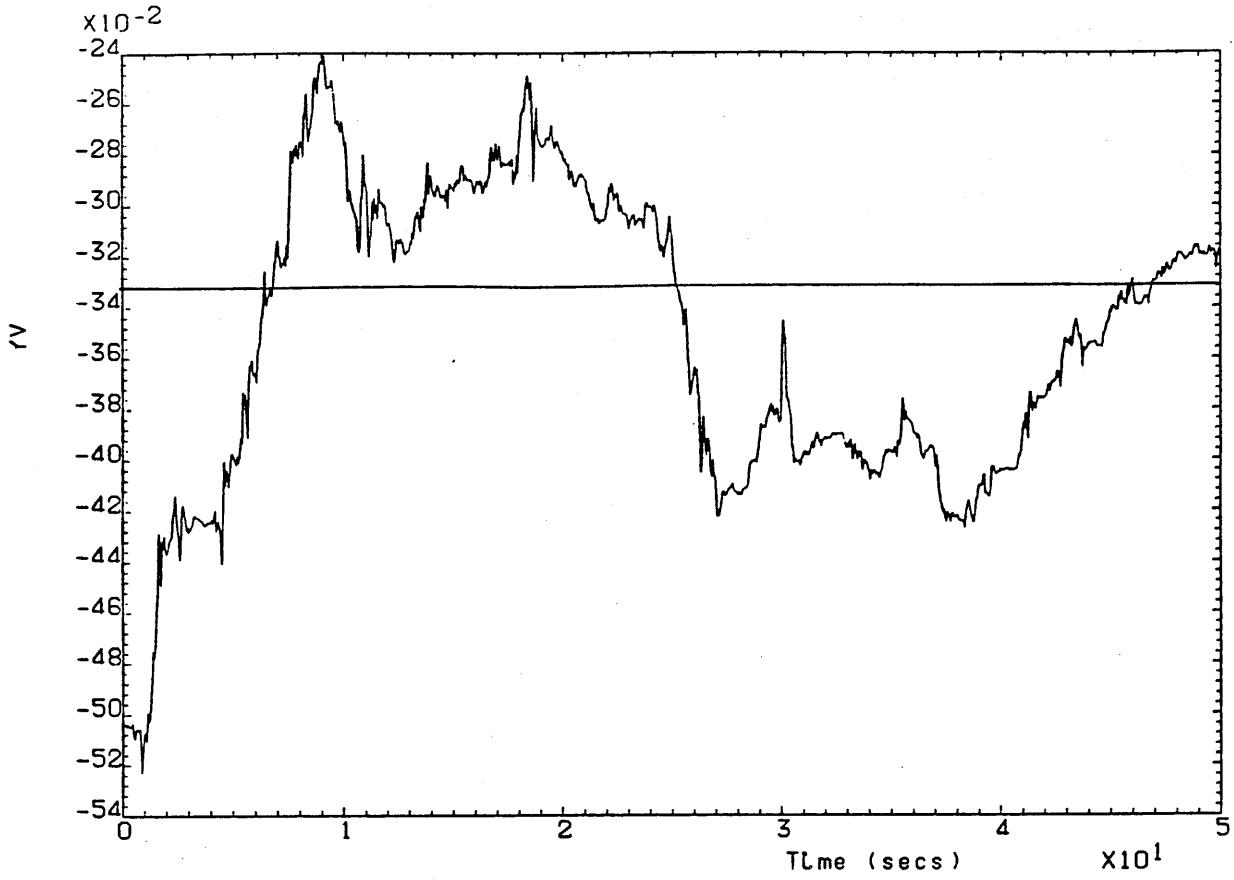


Fig. 4.12 Y_v estimates

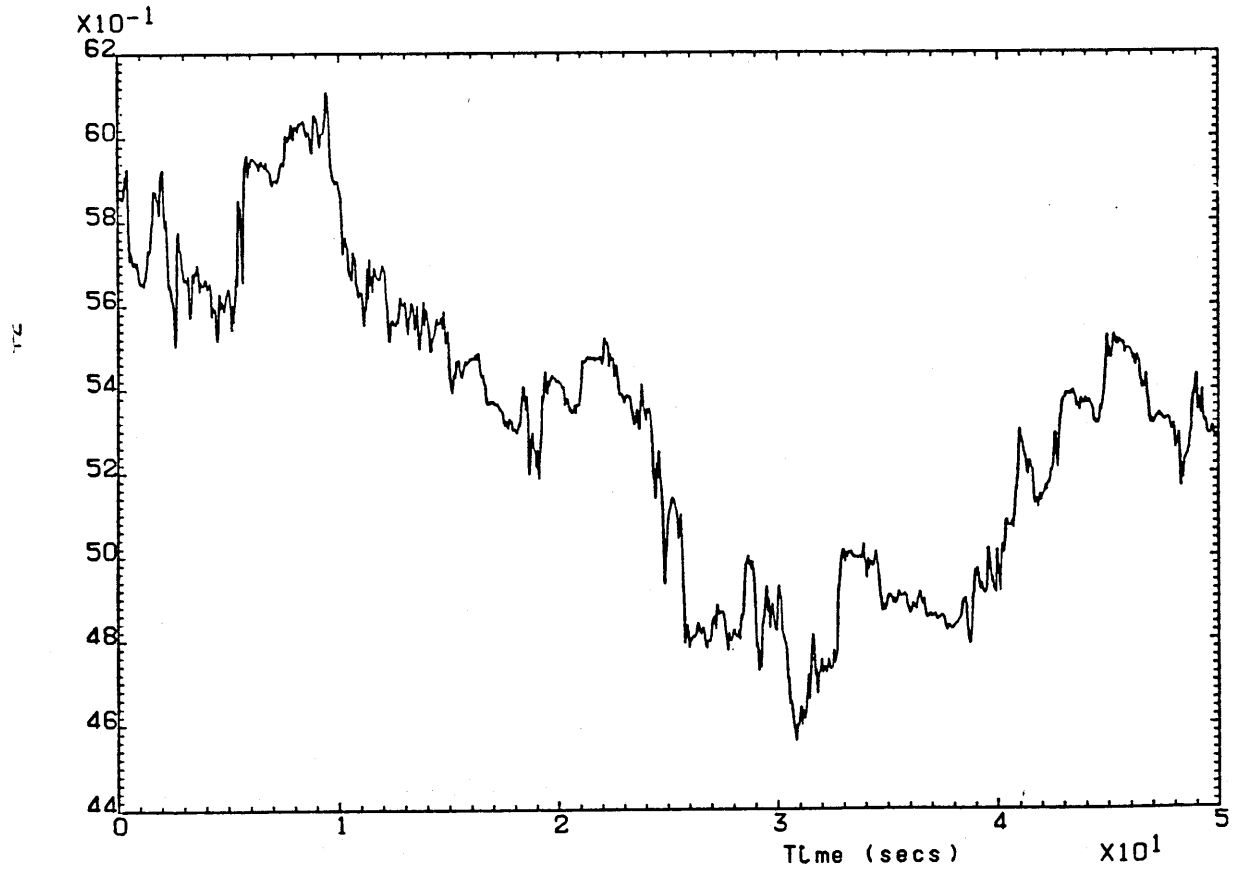


Fig. 4.13 Y_z estimates

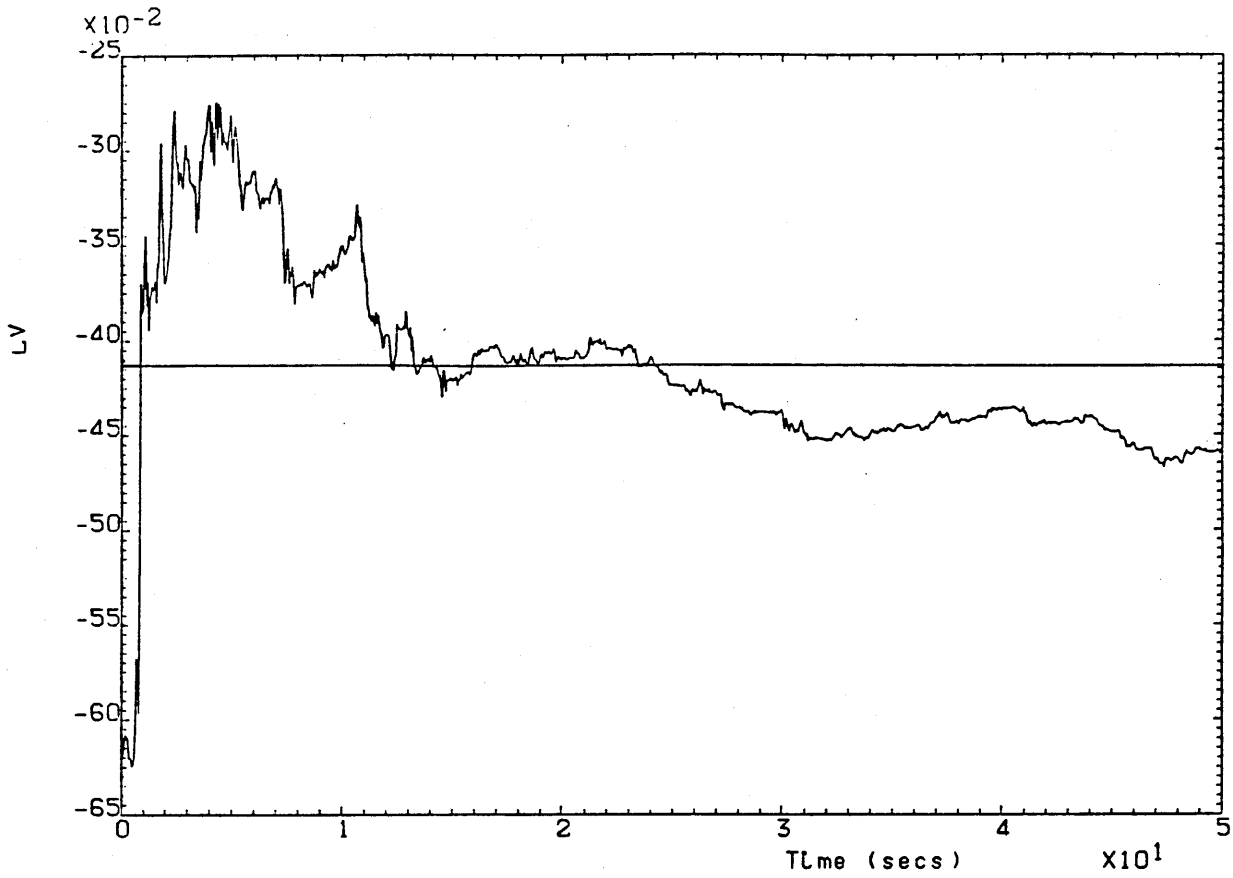


Fig. 4.14 L_v estimates

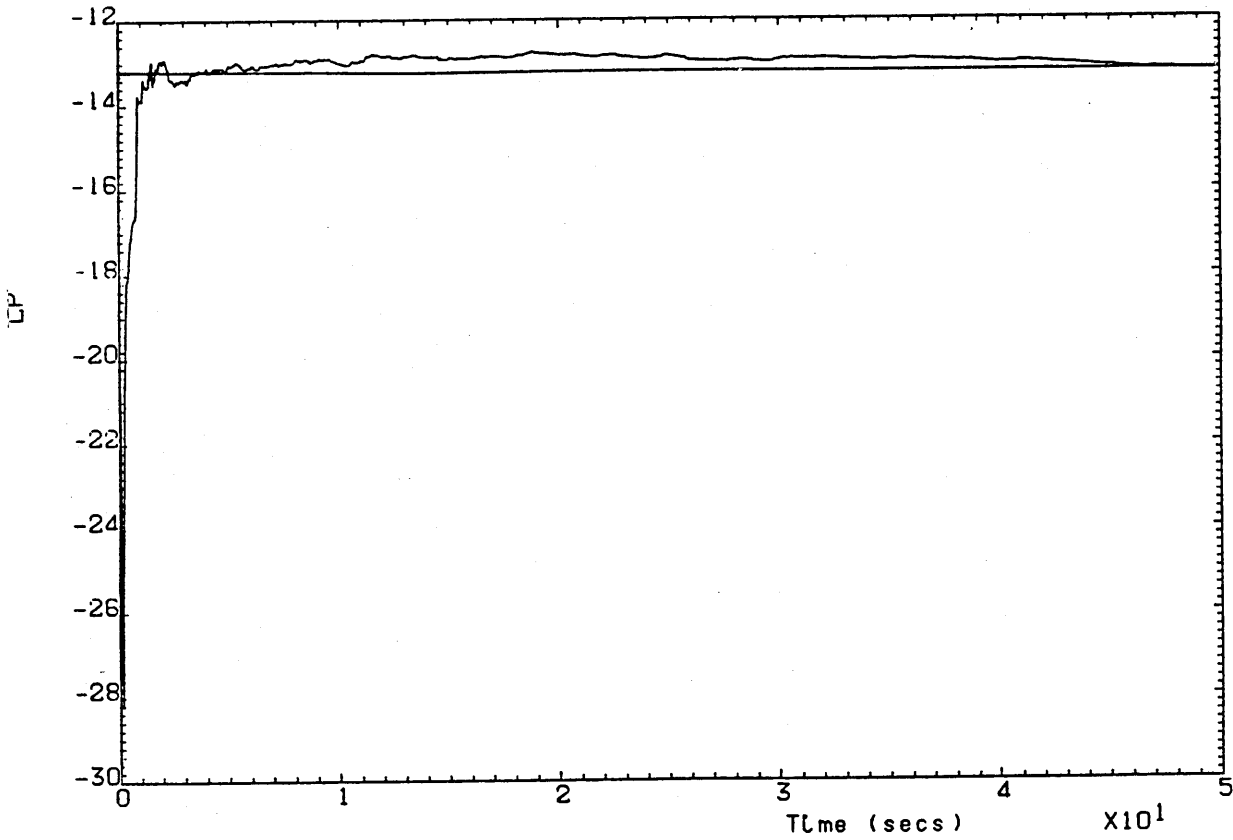


Fig. 4.15 L_p estimates

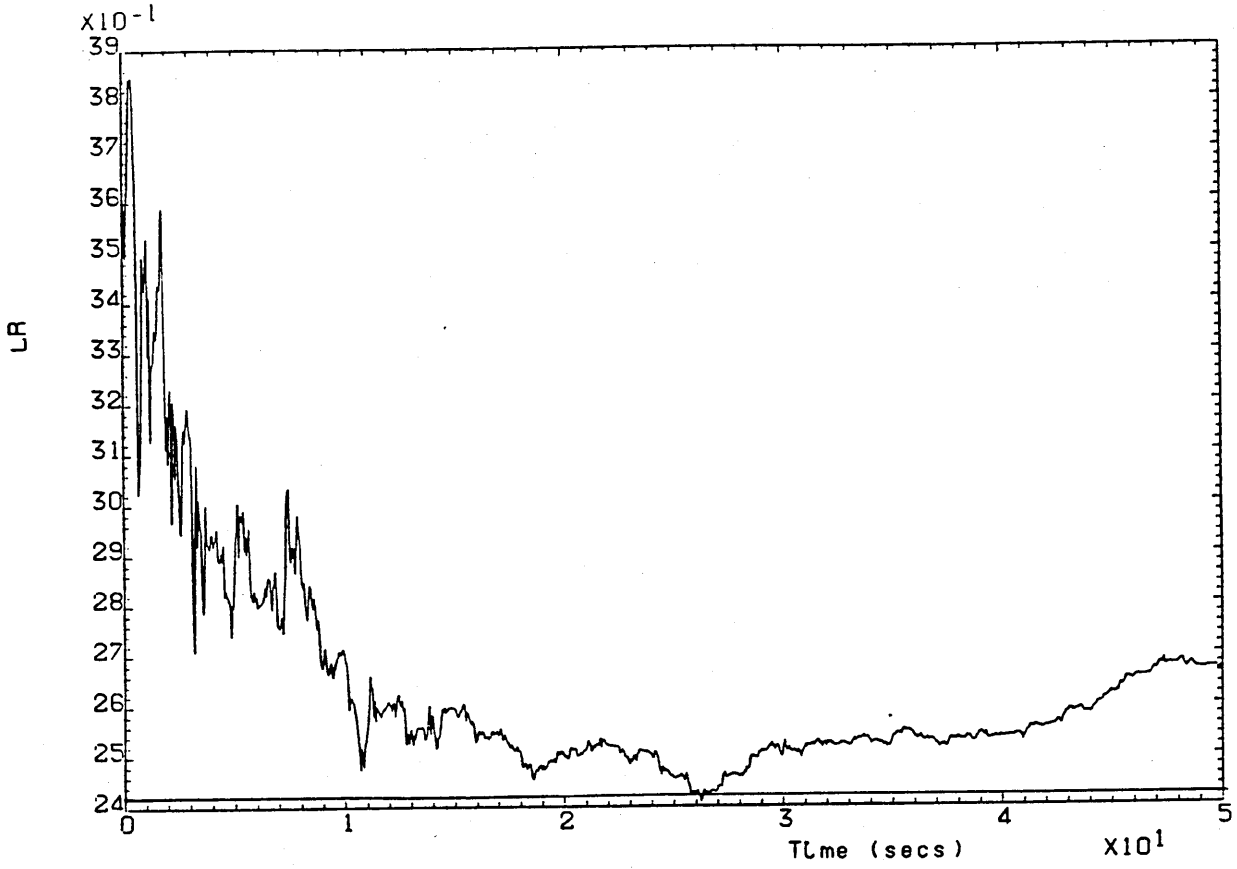


Fig. 4.16 L_r estimates

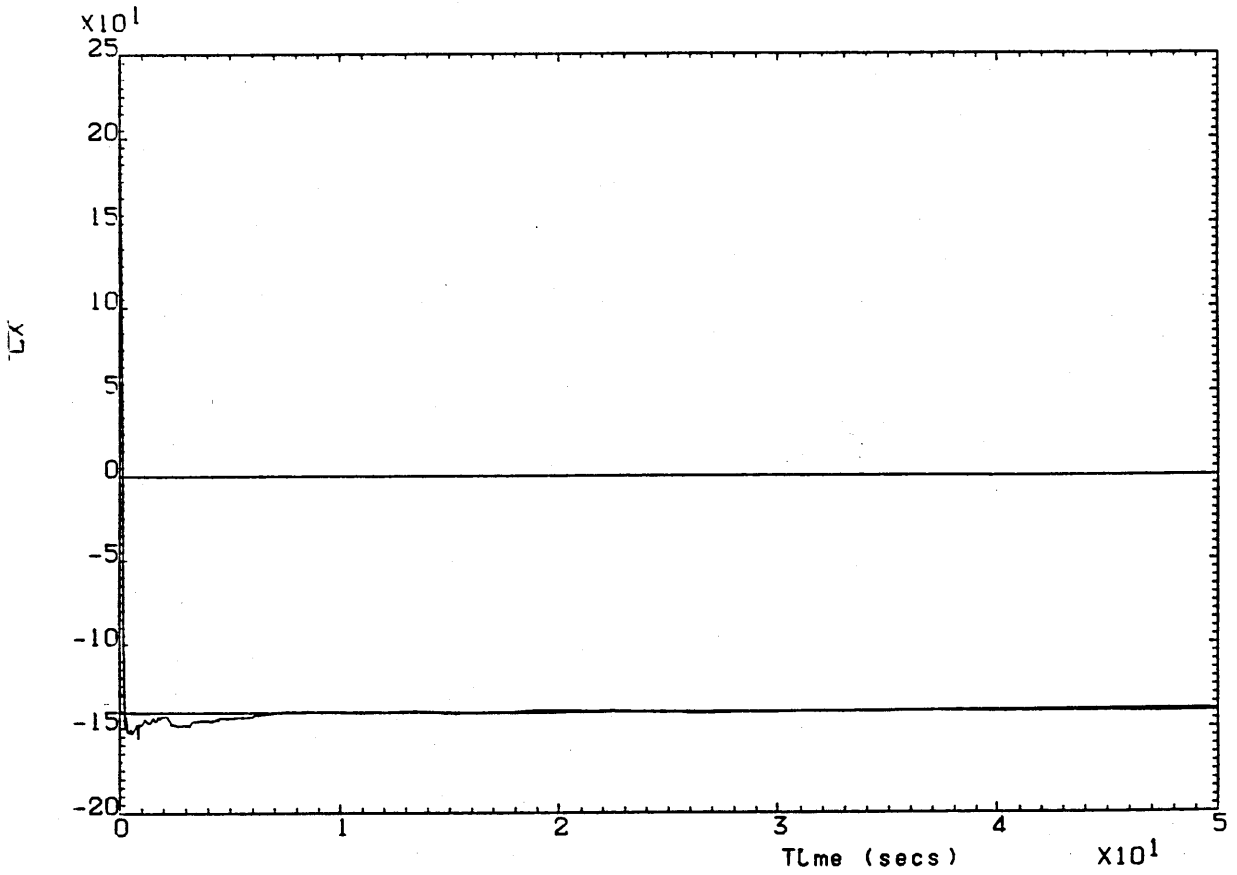


Fig. 4.17 L_x estimates

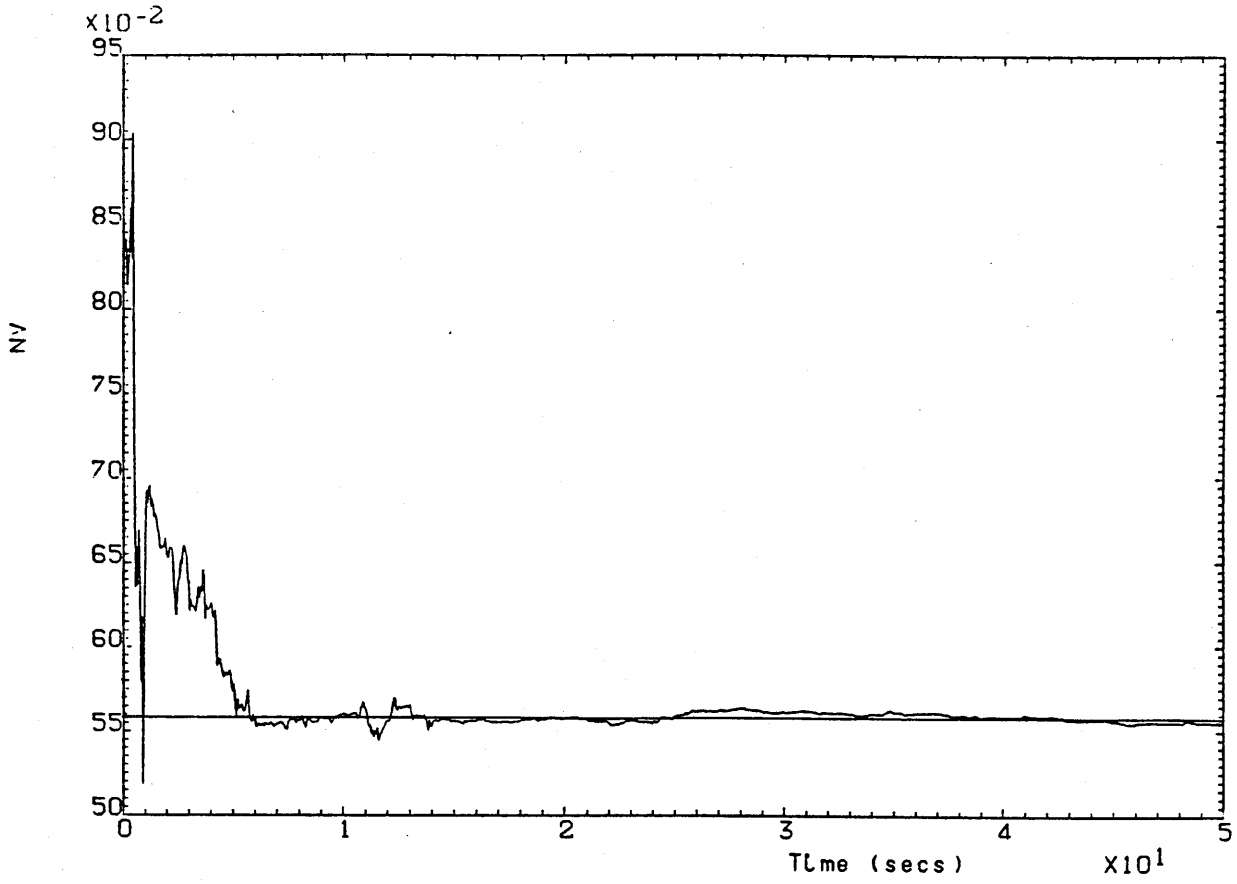


Fig. 4.18 N_V estimates

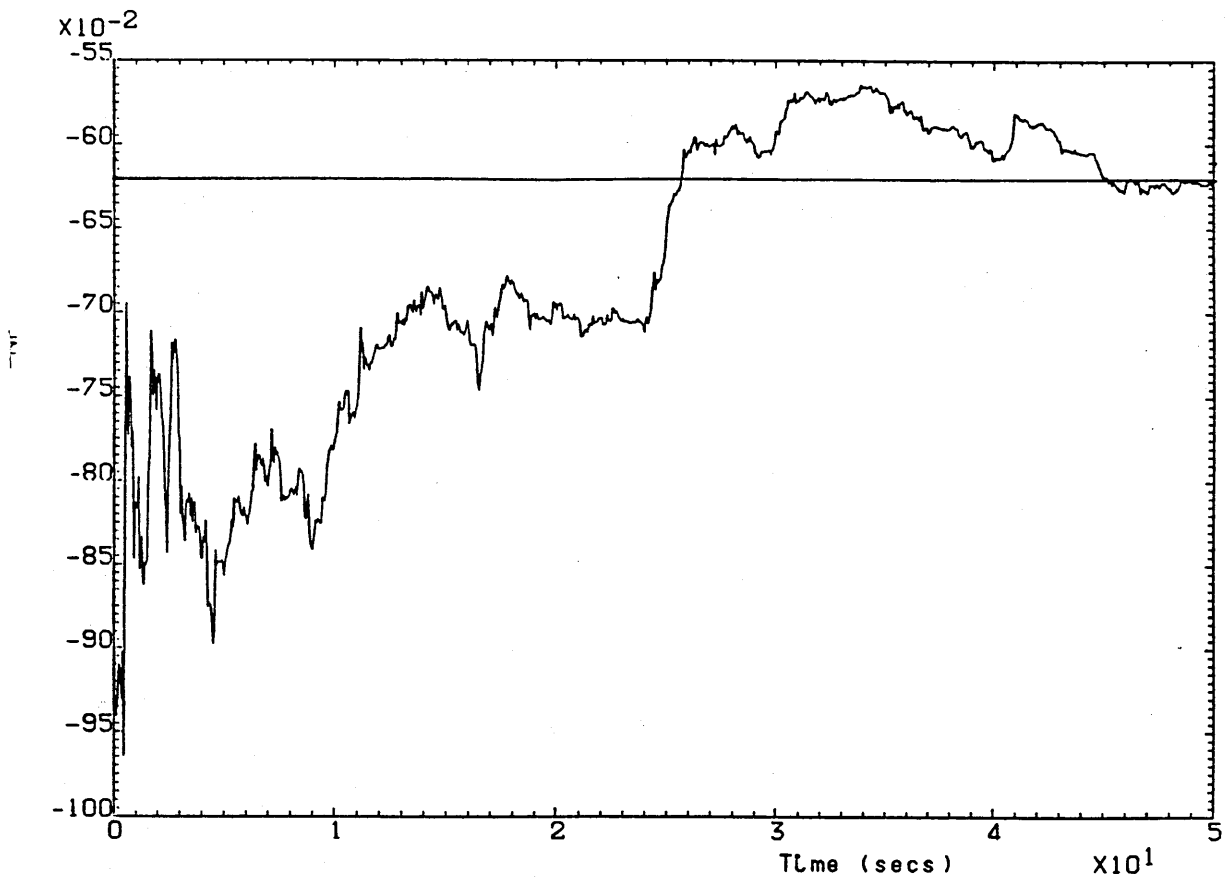


Fig. 4.19 N_p estimates

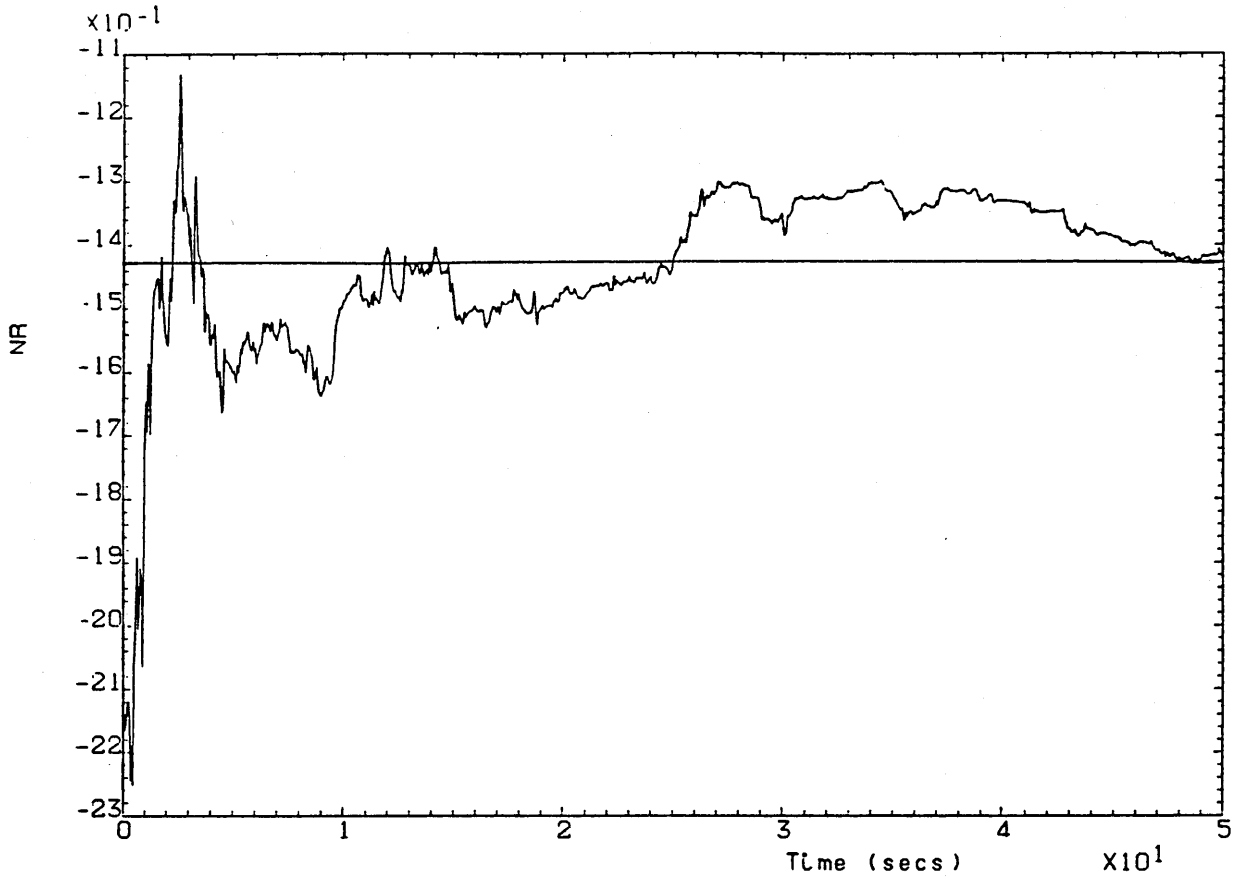


Fig. 4.20 N_r estimates

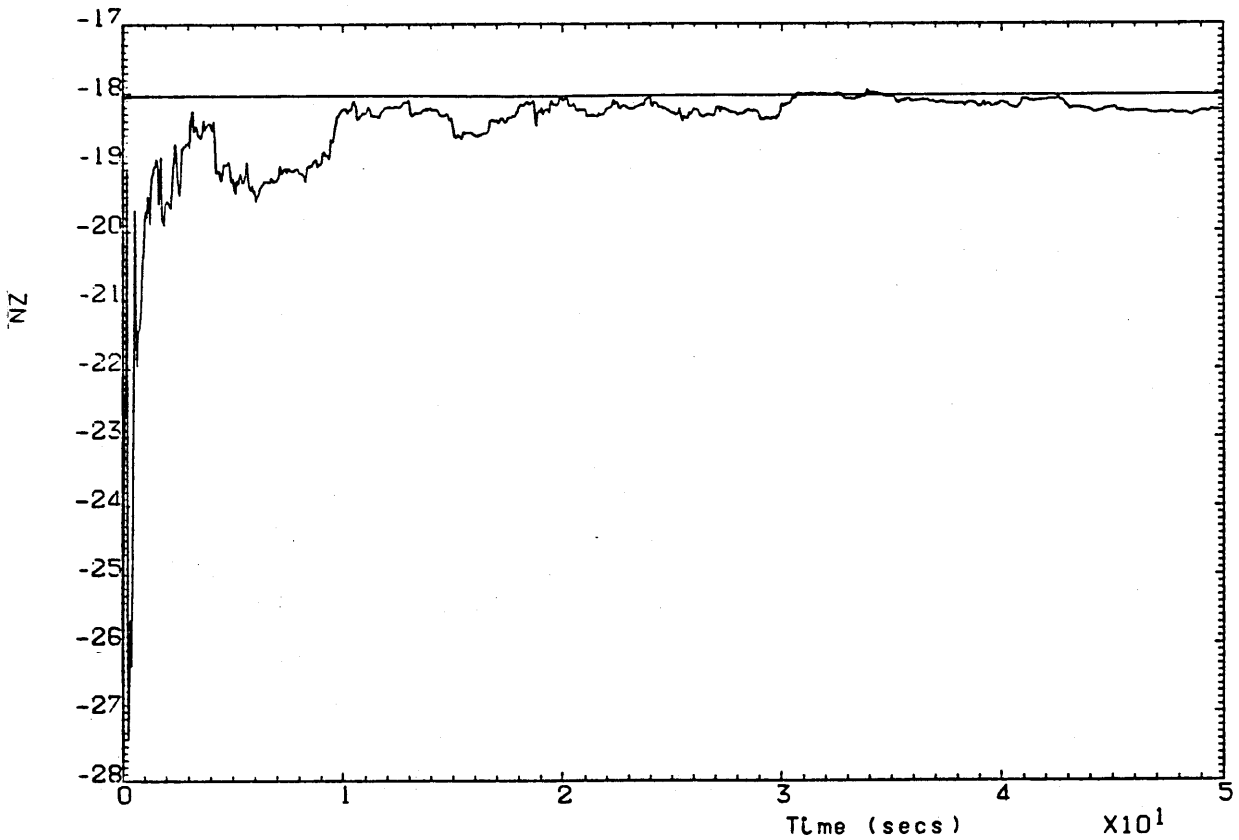


Fig. 4.21 N_z estimates

Chapter 5

THE SOFTWARE

5.1 Introduction

The computer implementation of the equations of motion of X-RAE1 and the identification algorithms is considered in this chapter. The purpose of the software development is twofold:

1. To support the mathematical modelling of X-RAE1, ie:
 - a) Derive the aerodynamic stability and control derivatives for a range of flight velocities.
 - b) Compute the trim conditions for straight, level, horizontal flights of different velocities.
 - c) Develop simulation programmes for the complete 6-DOF non-linear model of X-RAE1 and for the linear longitudinal and lateral models.
2. To implement the parameter identification algorithms (EKF) for the estimation of the aerodynamic stability and control derivatives of X-RAE1.

5.2 Software for the Mathematical Modelling of X-RAE1

5.2.1 Aerodynamic Derivatives

Programme RPVDER.FOR has been developed for the computation of the aerodynamic derivatives of X-RAE1. It is a FORTRAN programme and it can be easily used for any subsonic aircraft when similar data are available.

The inputs to the programme are:

1. Geometrical mass and inertia characteristics of the RPV.
2. Longitudinal stability and control derivatives in the form of curve slopes ($C_{l_{\alpha}}$, $C_{l_{\dot{\alpha}}}$, ..., $C_{m_{\eta}}$).
3. Parameters derived from ESDU data sheets.
4. Velocity of the RPV.

The output is given in the file RPVDER.DAT and consists of:

1. The normalised longitudinal derivatives in body-axes.
2. The system and input matrices of the linear longitudinal model.
3. The normalised lateral derivatives in body-axes.
4. The system and input matrices of the linear lateral model.

A flowchart of the programme RPVDER.FOR is given in Fig. 5.1.

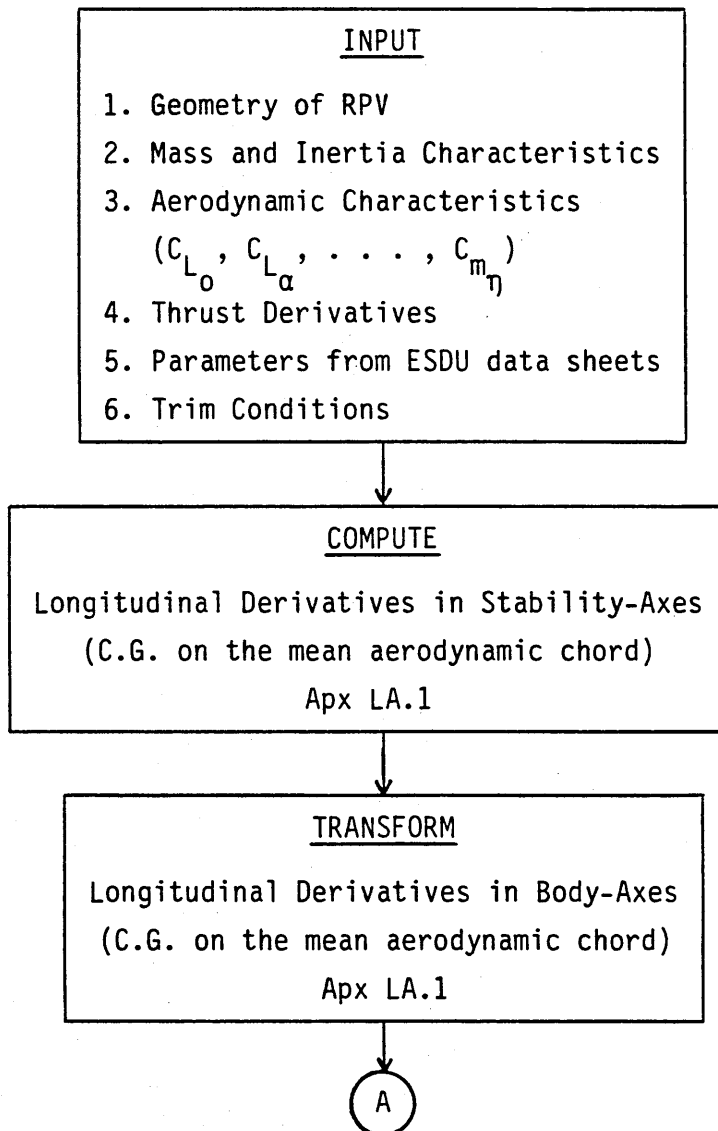


Fig. 5.1 Flowchart of the programme RPVDER.FOR

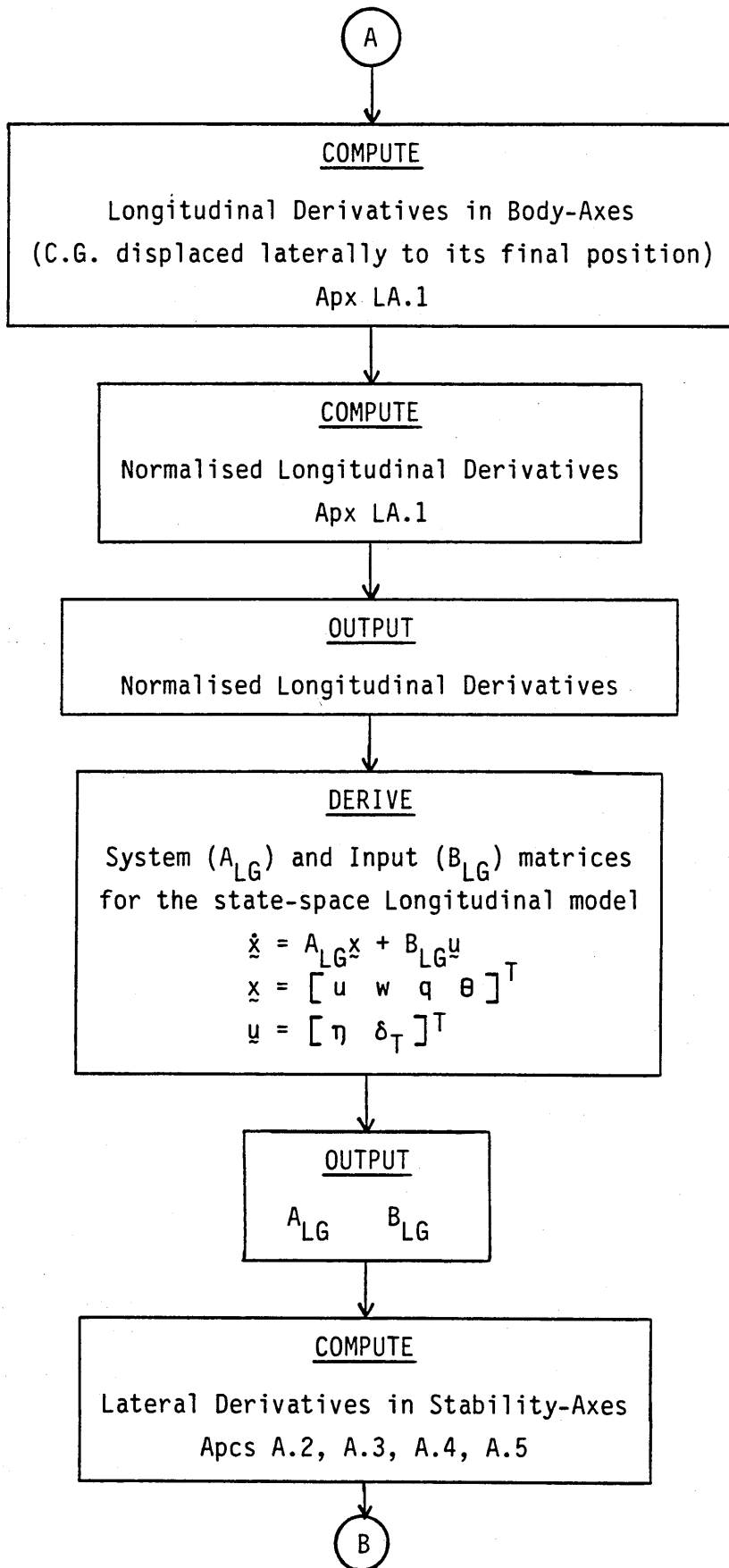


Fig. 5.1 contd. Programme RPVDER.FOR

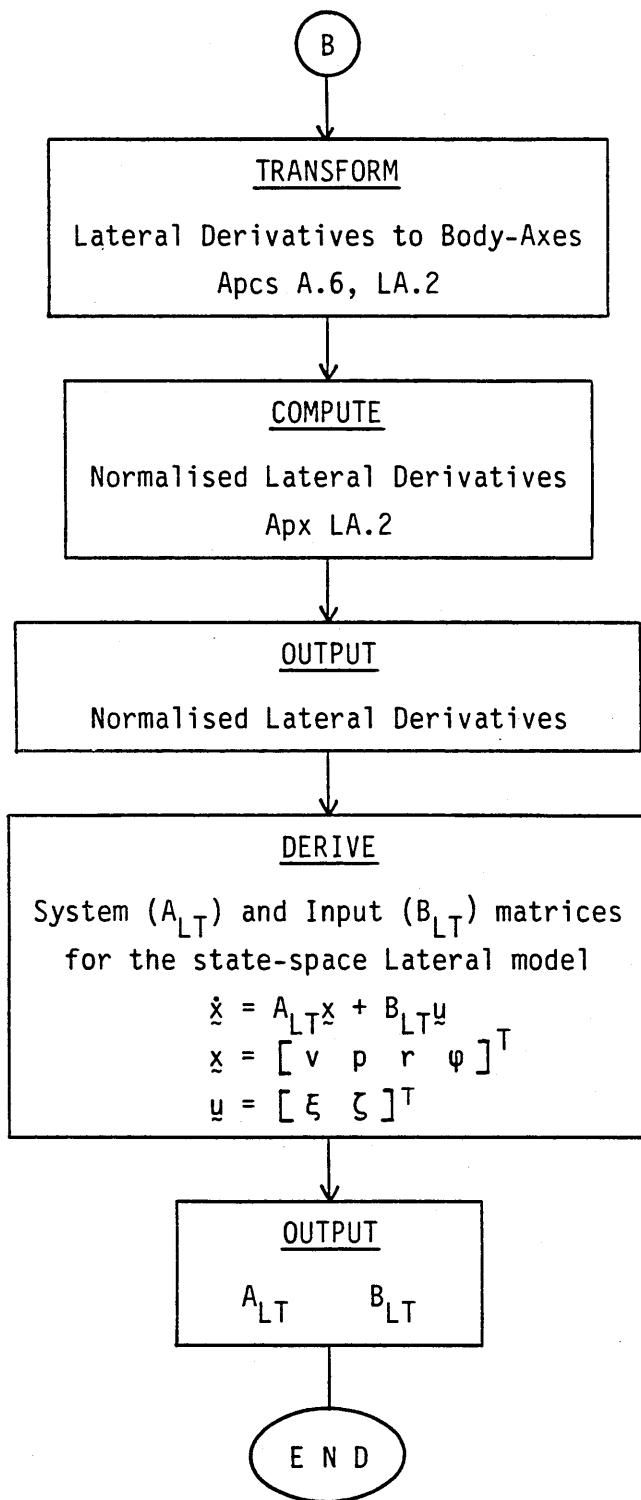


Fig. 5.1 contd. Programme RPVDER.FOR

5.2.2 Trim_Conditions

The FORTRAN programme TRIM.FOR has been implemented for the computation of the trim conditions of X-RAE1 for straight, horizontal flights of a range of flight velocities.

Inputs:

1. Geometry and aerodynamic characteristics of X-RAE1.
2. Required flight velocity.

Outputs (File TRIM.DAT):

1. Angle of attack.
2. Elevator setting.
3. Throttle setting.
4. Lift.
5. Drag.
6. Pitching moment.
7. Thrust.

A flowchart of the programme TRIM.FOR is shown in Fig. 5.2.

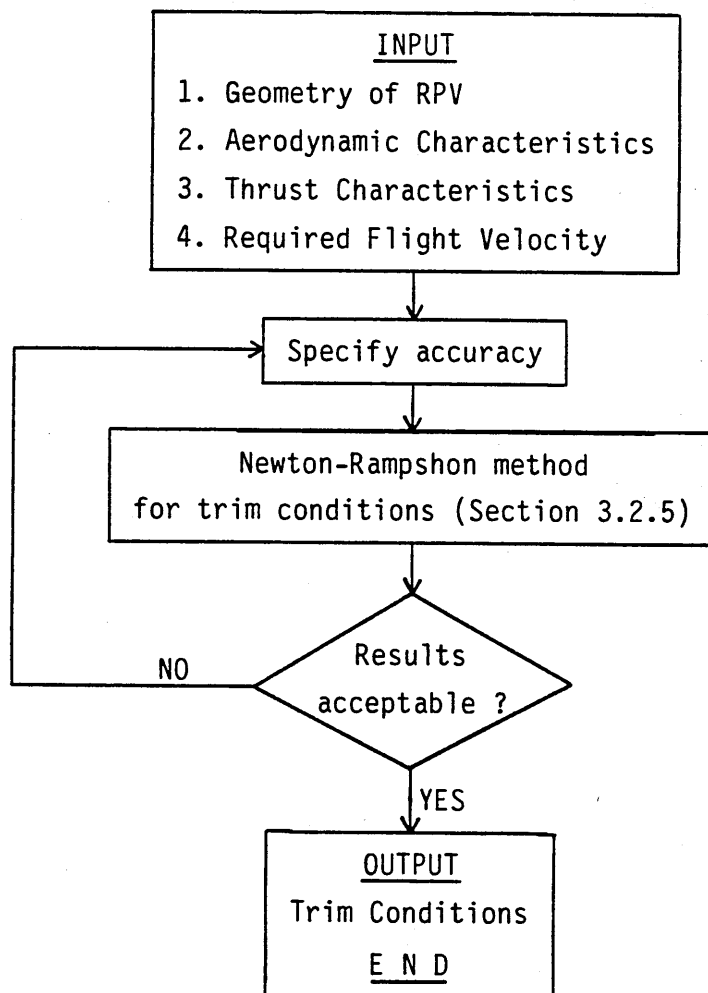


Fig. 5.2 Flowchart of the programme TRIM.FOR

5.2.3 Simulation Programmes

5.2.3a Nonlinear 6-DOF Simulation

The complete 6-DOF equations of motion of X-RAE1 as they are described in Chapter 3 have been used for a simulation study. A simulation programme - RPVPI.CSL - has been developed to accommodate these equations. The simulation language used is the Advanced Continuous Simulation Language (ACSL).

The general structure of the programme is shown in Fig. 5.3 and the main features of it are given below:

Inputs:

Time histories of elevator, aileron and rudder deflections and throttle settings.

Outputs:

1. Rectilinear velocities and accelerations, angular rates and angular accelerations in body axes.
2. Velocity and X-RAE1 position w.r.t. earth.
3. Orientation of X-RAE1 in form of Euler angles.
4. Lateral derivatives in stability and body axes as functions of the angle of attack.

5.2.3b Simulation of the Linear Longitudinal Model

Programme RPNLG.CSL has been developed in ACSL language to simulate the linear longitudinal model of X-RAE1. It uses the longitudinal derivatives as they are computed by the programme RPVDER.FOR.

The inputs to the programme are elevator deflections and variations in throttle settings, and

the outputs are the perturbed longitudinal motion quantities.

The structure of the programme RPVLG.CSL is shown in Fig. 5.4.

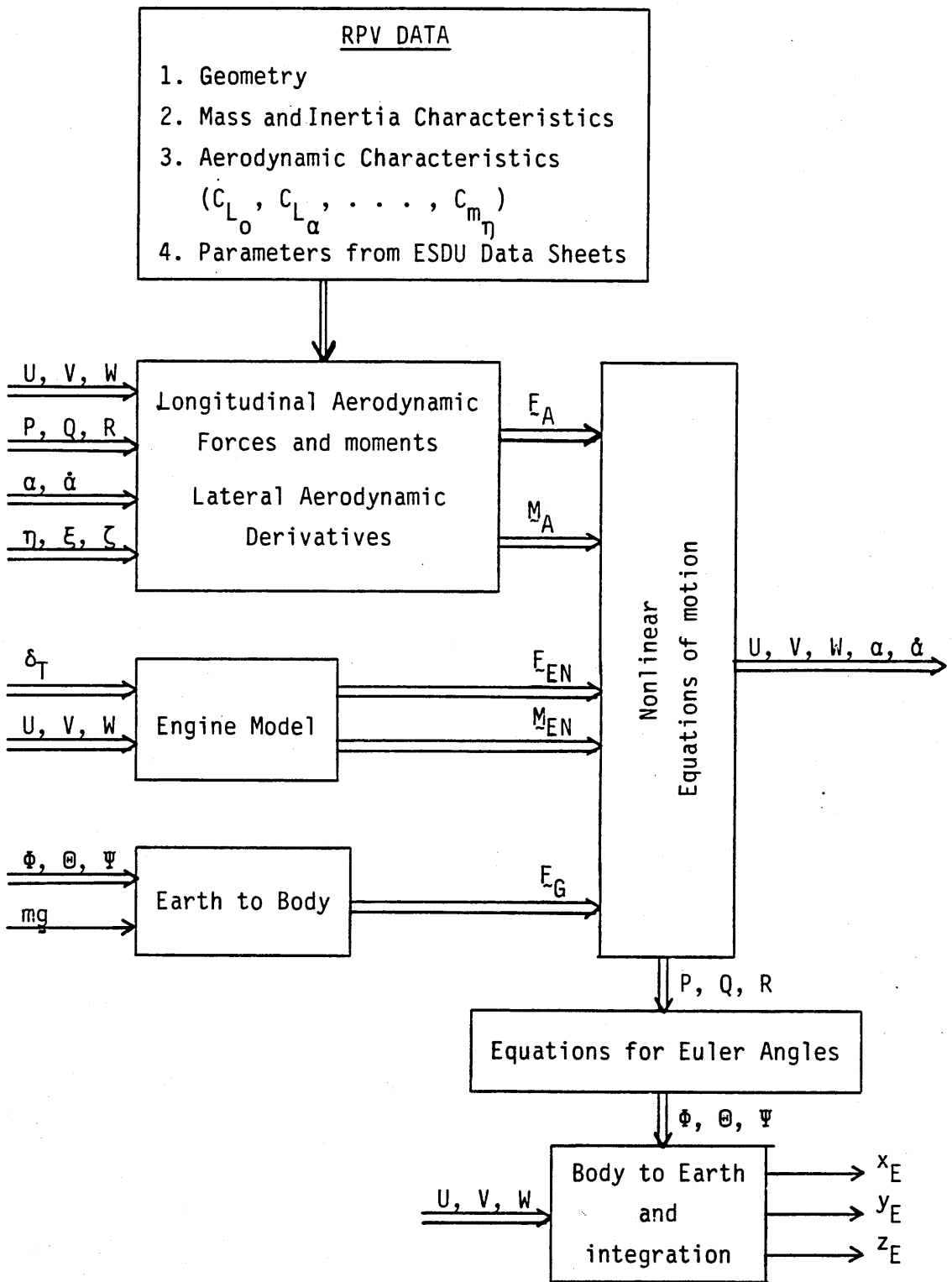


Fig. 5.3 Simulation programme RPVPI.CSL

Non-Linear

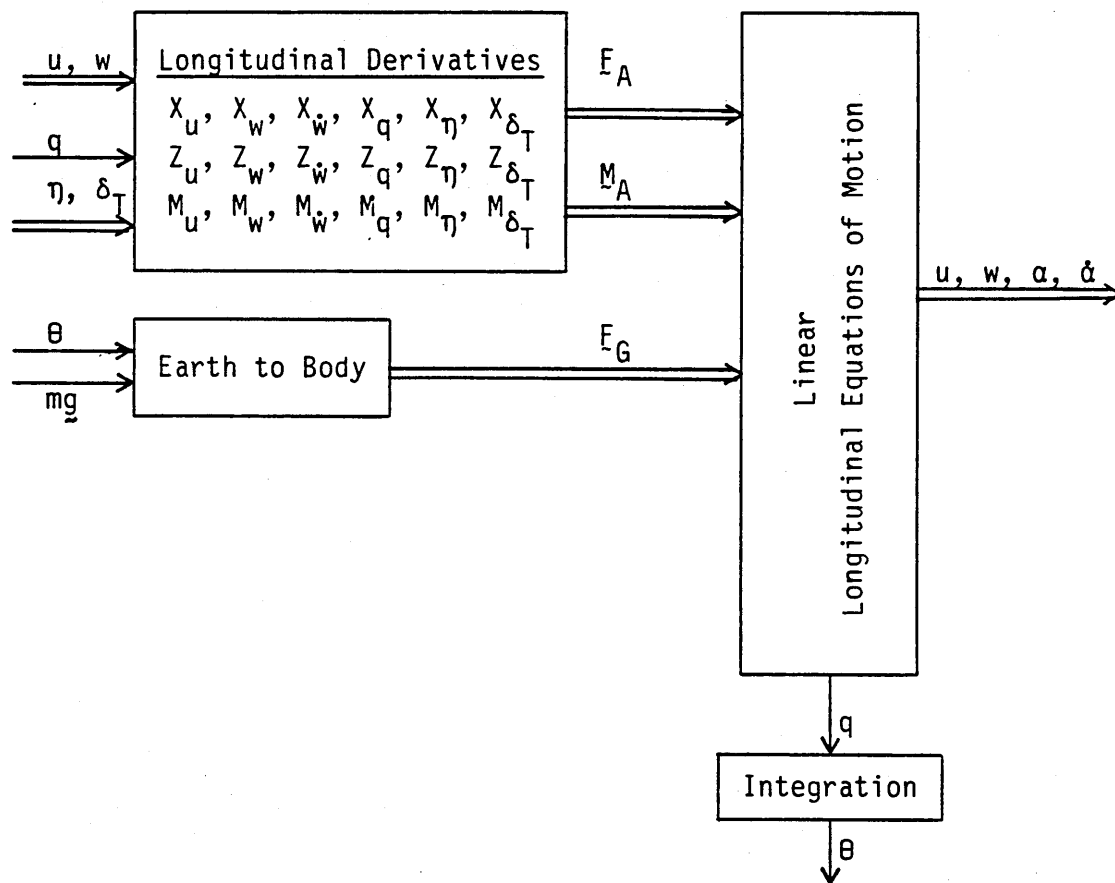


Fig. 5.4 Simulation programme RPVLG.CSL

5.2.3c Simulation of the Linear Lateral Model

The linear lateral equations of motion of X-RAE1 have been implemented by the ACSL programme RVPLT.CSL. The lateral derivatives computed by the programme RPVDER.FOR are used as input data.

The inputs to the programme are aileron and rudder deflections about their trim positions, and

the outputs are the perturbed lateral motion quantities.

The structure of the programme is shown in Fig. 5.5.

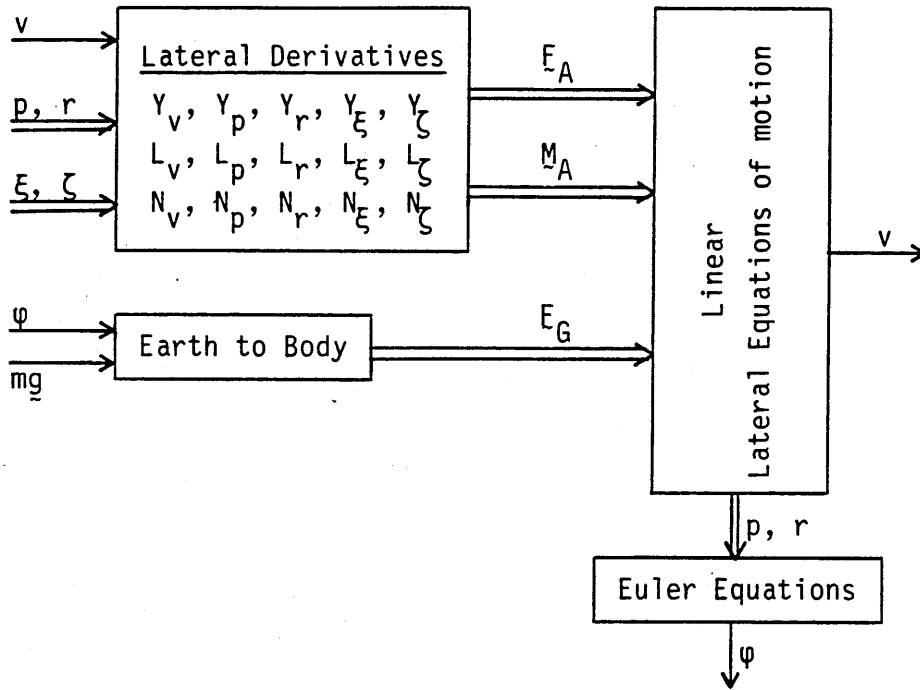


Fig. 5.5 Simulation programme RPVLT.CSL

5.3 Software for the Parameter Identification of X-RAE1

The computer implementation of the EKF algorithms for the identification of the longitudinal and lateral aerodynamic stability and control derivatives of X-RAE1 is presented in this section.

5.3.1 The EKF Algorithm

Programme EXKAL.FOR has been developed for the identification of the aerodynamic derivatives of X-RAE1.

Certain types of inputs (pseudorandom noise, square waves and multisteps) are selected and the outputs of the longitudinal or lateral models of the equivalent discrete systems are simulated.

An EKF is then implemented to identify the parameters of the models. The estimates of the aerodynamic derivatives and the Kalman filter gains as well as the diagonal of the error covariance matrix

are given in the output file EXKAL.DAT. Plots of the time histories of the estimates can also be provided.

The user has to supply the subroutines for the creation of the A, B and C matrices of the equivalent discrete system, the system function f of the augmented system and the matrix F for the EKF.

A flowchart of the programme EXKAL.FOR is shown in Fig. 5.6

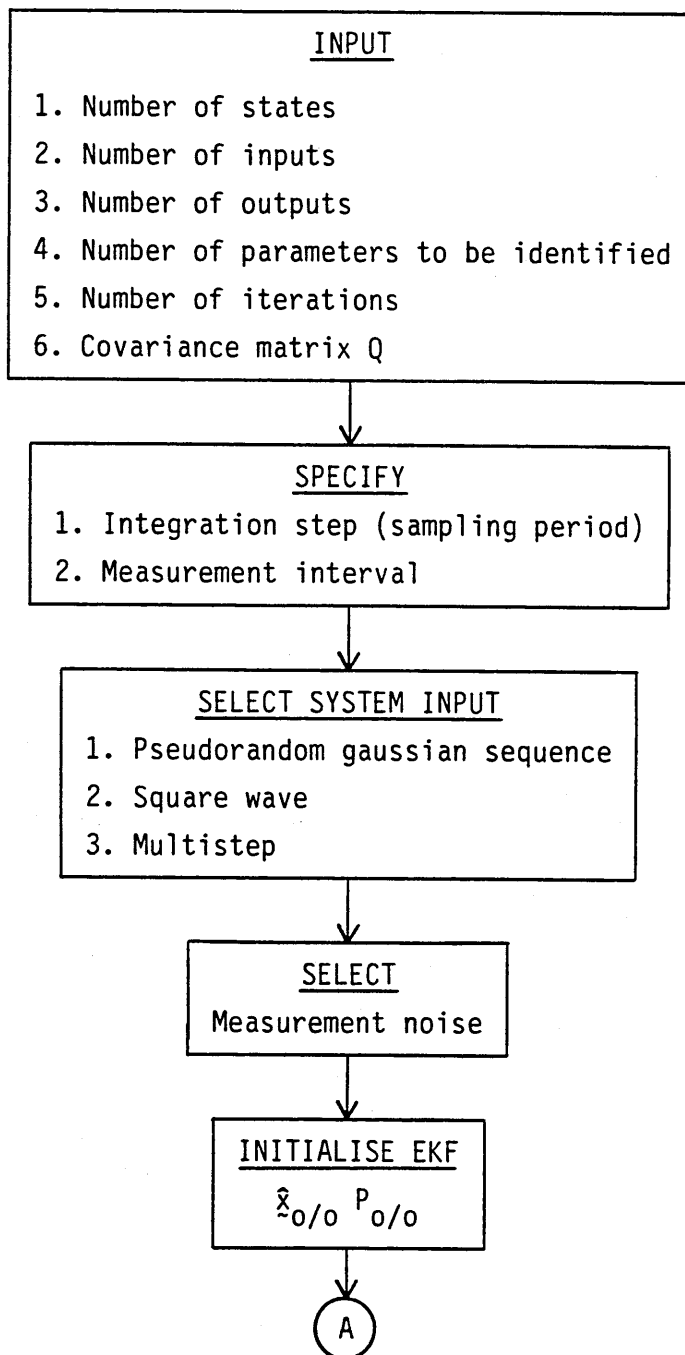


Fig. 5.6 Flowchart of programme EXKAL.FOR

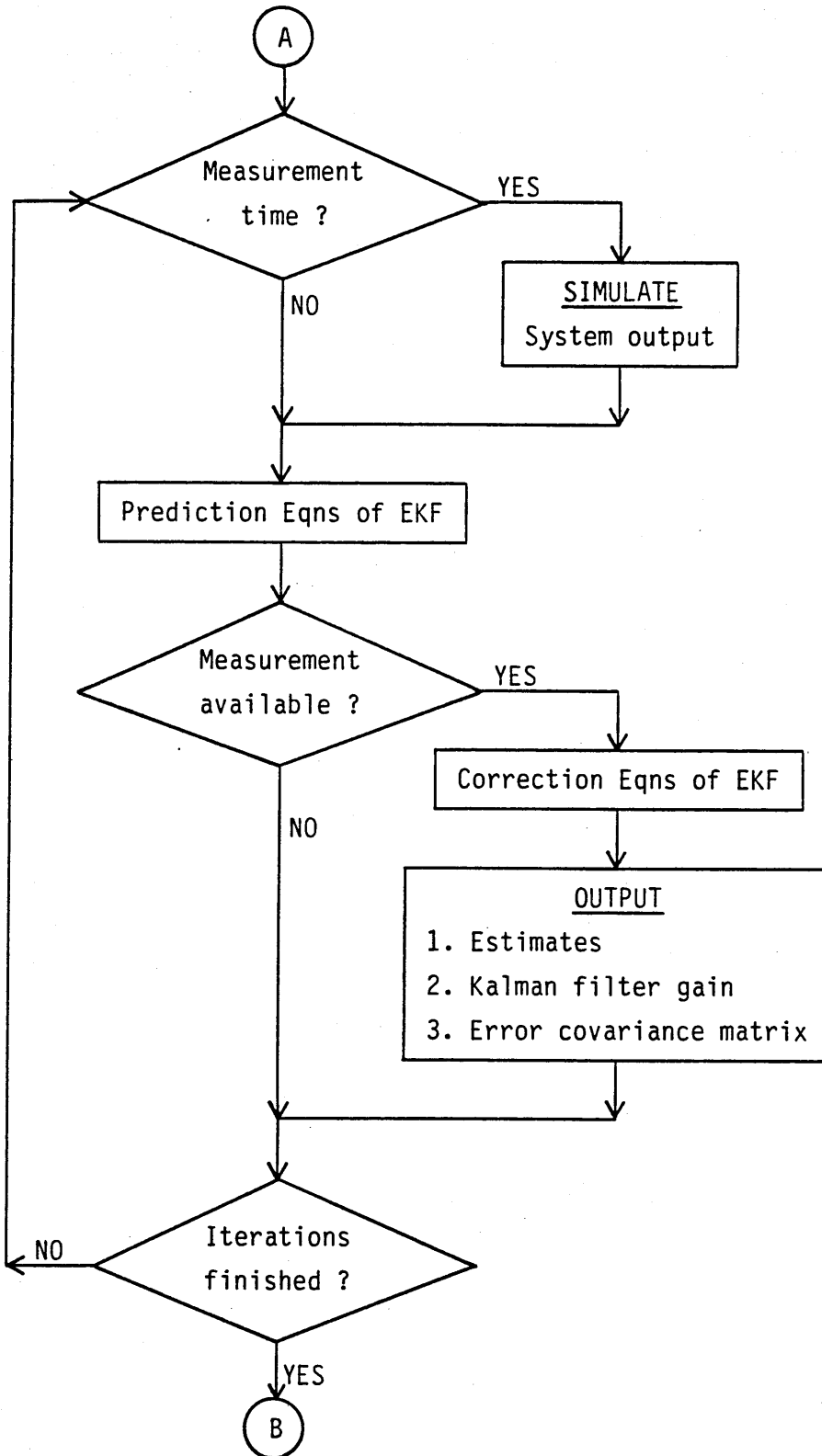


Fig. 5.6 contd. Flowchart of programme EXKAL.FOR

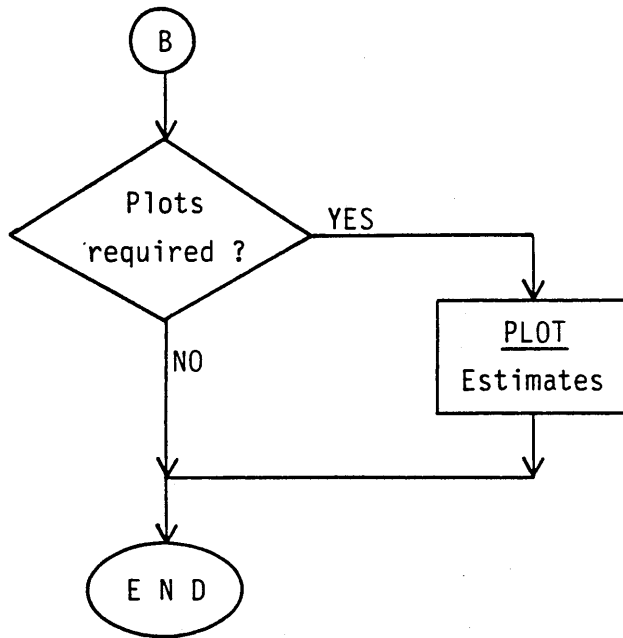


Fig. 5.6 contd. Flowchart of programme EXKAL.FOR

5.3.2 Supporting Subroutines

5.3.2a Subroutine_SMTCS_(A, B, C, H, IS, INP, IO)

Subroutine SMTCS creates the system matrices A, B and C of the equivalent discrete system given the number of states, number of inputs, number of outputs and the sampling period. It has to be supplied by the user.

A(IS,IS)	<u>OUTPUT</u> : System matrix
B(IS,INP)	<u>OUTPUT</u> : Input matrix
C(IO,IS)	<u>OUTPUT</u> : Output matrix
H	<u>INPUT</u> : Sampling period
IS	<u>INPUT</u> : Number of states
INP	<u>INPUT</u> : Number of inputs
IO	<u>INPUT</u> : Number of outputs

5.3.2b Subroutine_SYFN_(F, X, U, H, IAS, INP)

Subroutine SYFN gives as output the system function of the augmented system and it has to be supplied by the user.

F(IAS)	<u>OUTPUT</u> : System function
X(IAS)	<u>INPUT</u> : Augmented state vector
U(INP)	<u>INPUT</u> : System input vector
H	<u>INPUT</u> : Sampling period (integration step)
IAS	<u>INPUT</u> : Number of states of the augmented system
INP	<u>INPUT</u> : Number of inputs

5.3.2c Subroutine_MTXPHI (PHI, X, U, H, IAS, INP)

The matrix F for the EKF algorithm is generated by this subroutine which has to be supplied by the user.

PHI(IAS,IAS)	<u>OUTPUT</u> : Matrix F
X(IAS)	<u>INPUT</u> : Augmented state vector
U(INP)	<u>INPUT</u> : System input vector
H	<u>INPUT</u> : Integration step
IAS	<u>INPUT</u> : Number of states of the augmented system
INP	<u>INPUT</u> : Number of system inputs

5.3.2d Other Subroutines

1. Subroutine SQW (INP,H)
It generates a set of square waves.
2. Subroutine MLSTP (INP,H)
It creates a set of multisteps
3. Subroutine RANDOM (INP)
It generates gaussian random noise

Chapter 5

CONCLUSIONS - RECOMMENDATIONS

A six-degrees of freedom dynamically nonlinear mathematical model of an experimental RPV has been developed. Non-linear aerodynamic effects and cross-coupling terms have been ignored while Euler angles have been employed for the attitude definition of the RPV. (Sensor and actuator characteristics have not been included in the modelling).

From the model developed, simulated data can be provided for flight regimes below stall ($\alpha < 10^\circ$) and pitch angles of less than sixty degrees.

The linearised longitudinal and lateral models for straight, level, horizontal flight at 30 m/sec have also been derived. Phugoid and dutch roll modes have been computed and found to exhibit low damping ratios. A flight control system has to be designed to control these modes. An unstable spiral mode was found but it would not appear to present any obvious difficulties as it is characterised by a large time constant.

The identification of the aerodynamic stability and control derivatives has been undertaken. Pitch, roll and yaw rate measurements corrupted by small amounts of measurement noise have been used while an EKF has been implemented for the estimation of the aerodynamic derivatives.

Small amplitude pseudorandom deflections of the elevator have been applied for the identification of the longitudinal derivatives. It was not possible to identify the z_η derivative from pitch rate measurements as it has negligible effect on the pitch rate. However, good estimates have been obtained for the majority of the longitudinal derivatives.

Small amplitude pseudorandom sequences were used as aileron and rudder inputs. Accurate estimates of the lateral derivatives with the exception of Y_ζ and Y_v have been obtained from roll and yaw rate measurements.

It was difficult to identify Y_ζ since it is not a dominant term in the transfer function between yaw rate and rudder deflection. Y_v could have been identified more accurately through use of low frequency

rudder inputs. It is felt that estimation of the Y_v derivative may be obtained more accurately by using latex measurements.

With a view to improving the mathematical model of the RPV, the following recommendations are suggested:

1. As flight test data is acquired non-linear aerodynamics and cross-coupling terms may be included in the model.
2. Quaternions should be used instead of Euler angles to enable a greater range of manoeuvres to be represented.
3. An atmospheric model could be developed to model gusts. Its inclusion in the overall model would make the latter more realistic.
4. The sensor and actuator characteristics could also be modeled.

REFERENCES

1. Babister A. W. "Aircraft Dynamic Stability and Response". Pergamon Press Ltd., U.K., 1980.
2. Blakelock J. H. "Automatic Control of Aircraft and Missiles". John Wiley & Sons, Inc., 1965.
3. Ellison Don E. "Stability Derivative Estimation at Subsonic Speeds".
Hoak D. E. Annuals New York Academy of Science Inter. Congress on Subsonic Aeronautics, 1980.
4. Etkin B. "Dynamics of Flight Stability and Response". John Wiley & Sons, Inc., 1959.
5. Gill P. E. "Practical Optimization".
Murray W. Academic Press, 1981.
Wright M. H.
6. Hamel P. G. "Aircraft Parameter Identification Methods and Their Applications - Survey and Future Aspects".
paper in AGARD-LS-104, 1979.
7. Jazwinski A. H. "Stochastic Processes and Filtering Theory". Academic Press, 1970.
8. Klein V. "Identification Evaluation Methods".
paper in AGARD-LS-104, 1979.
9. Klein V. "Compatibility Check of Measured Aircraft Responses Using Kinematic Equations and Extended Kalman Filter".
Schuess J. R. NASA TN D-8514, 1977.
10. McRuer D. "Aircraft Dynamics and Automatic Control".
Ashkenas I. Princeton University Press, 1973.
Graham D.

11. Meirovitch L. "Introduction to Dynamics and Control".
John Wiley & Sons, Inc., 1985.
12. Stepner D. E.
Mehra R. K. "Maximum Likelihood Identification and
Optimal Input Design for Identifying
Aircraft Stability and Control Derivatives".
NASA CR-2200, 1973.
13. Theocharis P. "Rigid Body Mechanics".
Lecture Notes (in Greek).
National Technical University of Athens.
14. Thomas H. H. B. M. "State of the Art of Estimation of Derivatives".
NATO Report 339, 1961.
15. Tobak M.
Lessing H. C. "Estimation of Rotary Stability Derivatives
at Subsonic and Transonic Speeds".
NATO Report 343, 1961.
16. Tobak M.
Schiff L. B. "On the Formulation of the Aerodynamic
Characteristics in Aircraft Dynamics".
NASA TR R-456, 1976.
17. Tsympkin Y. Z. "Adaptation and Learning in Automatic Systems".
Academic Press, 1971.
18. Mises Von R. "Theory of flight".
Dover Publications, Inc., New York, 1945, 1959.
19. Young P. "Recursive Estimation and Time-Series Analysis".
Springer-Verlag, 1984.

APPENDIX A.1

1. Longitudinal Aerodynamic Derivatives
2. Engine Model

1. Longitudinal Aerodynamic Derivatives

The longitudinal aerodynamic derivatives of X-RAE1 are estimated in this section. Most of the estimation is based on static wind-tunnel tests of a model fitted with a wing with rounded tips. Measurements from a model with a wing with skid tips are used when other data are not available.

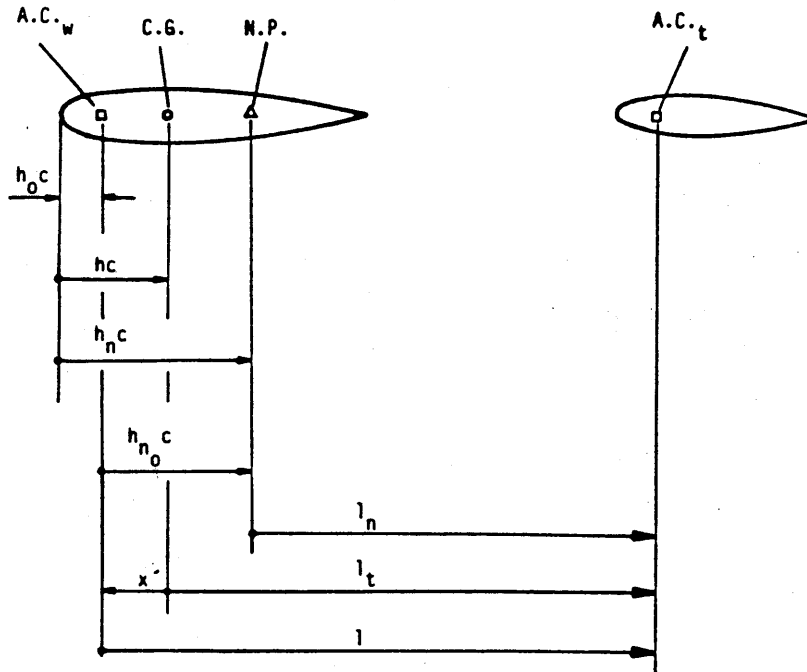


Fig. A.1-1 X-RAE1 longitudinal geometry (Ref. 3)

S	$= 0.9307 \text{ m}^2$
c	$= 0.353 \text{ m}$
S_t	$= 0.2576 \text{ m}^2$
l_t	$= 1.182 \text{ m}$
h_0	$= 0.24$ (skid tips)
h	$= 0.34$
h_n	$= 0.55$ (skid tips)
h_{n0}	$= 0.31$
x'	$= -0.036 \text{ m}$

Table A.1-1 X-RAE1 longitudinal geometry (Ref. 3)

From Table A.1-1 the following Table A.1-2 is constructed to be used for the estimation of the longitudinal derivatives (Ref. 1).

$\bar{V} = \frac{S_t l}{S c} = 0.955$
$F = \frac{c h_{n0}}{l_n} = 0.099$
$V'_T = \frac{\bar{V}}{1 + F} = 0.869$
$k_n = - \frac{\theta C_m}{\theta C_L} = 0.21 \text{ (skid tips)}$
$H_n = h_n - h = 0.21$

Table A.1-2 X-RAE1 parameters for the estimation of the longitudinal derivatives.

1.1 Lift Derivatives

1.1.1 Lift Derivative w.r.t. Angle of Attack

$$C_{L_\alpha} \cong \frac{\theta C_L}{\theta \alpha} = a + \frac{S_t}{S} a_1 \left(1 - \frac{\theta \epsilon}{\theta \alpha}\right) \quad (\text{Ref. 1})$$

where:

$$\frac{\theta \epsilon}{\theta \alpha} = 0.47 \quad (\text{Ref. 3, skid tips}) \quad (1)$$

$$a \cong \frac{\theta C_{L_w}}{\theta \alpha} = 4.53 \text{ /rad} \quad (\text{Ref. 3}) \quad (2)$$

$$a_1 \cong \frac{\theta C_{L_t}}{\theta \alpha_t} = a F \frac{S}{S_t (1 - \theta \epsilon / \theta \alpha)} = 3.10 \text{ /rad} \quad (\text{Ref. 1}) \quad (3)$$

Then:

$C_{L_\alpha} \cong \frac{\theta C_L}{\theta \alpha} = 4.98 \text{ /rad}$	(4)
---	-----

1.1.2 Lift Derivative w.r.t. Rate of the Angle of Attack

$$C_{L\dot{\alpha}} = C_{L\dot{\alpha}|tail} = 2a_1 \frac{S_t l}{S c} \frac{\theta \epsilon}{\theta \alpha} \quad (\text{Ref. 2})$$

Therefore (Eqns 1, 3 and Table A.1-1):

$$C_{L\dot{\alpha}} \cong \frac{\theta C_L}{\theta \left(\frac{\dot{\alpha} c}{2V_T} \right)} = 2.78 \text{ /rad} \quad (5)$$

1.1.3 Lift Derivative w.r.t. Pitch Rate

$$C_{Lq} = C_{Lq|wing} + C_{Lq|tail}$$

where:

$$C_{Lq|wing} = 2a_1 \frac{l_t S_t}{l S} = -0.92 \text{ /rad} \quad (\text{Ref. 2}) \quad (6)$$

$$C_{Lq|tail} = 2 \frac{x}{c} C_{L\dot{\alpha}} = 5.75 \text{ /rad} \quad (\text{Ref. 2}) \quad (7)$$

Then according to Eqns 3 and 4 and to Table A.1-1, C_{Lq} becomes:

$$C_{Lq} \cong \frac{\theta C_L}{\theta \left(\frac{qc}{2V_T} \right)} = 4.83 \text{ /rad} \quad (8)$$

1.1.4 Lift Derivative w.r.t Elevator Deflection

$$C_{L\eta} = \frac{c}{l_t} \frac{V_T a_2}{(1 - H_{nc}/l_t)} \quad (\text{Ref. 1}) \quad (9)$$

where :

$$a_2 \cong \frac{\theta C_{L_t}}{\theta \eta} \quad \text{and is estimated by the following two expressions:}$$

$$\left. \frac{d\eta}{dC_L} \right|_{C_m=0} = \frac{-k_n}{V_T a_2} \quad (\text{Ref. 1})$$

$$\left. \frac{d\eta}{dC_L} \right|_{C_m=0} = \frac{\Delta\eta}{\Delta C_L} = -8.1^\circ \quad (\text{Ref. 3})$$

Therefore $a_2 = 1.76$ /rad and Eqn 9 gives:

$$C_{L_\eta} \cong \frac{\theta C_L}{\theta \eta} = 0.49/\text{rad} \quad (10)$$

1.2 Pitching Moment Derivatives

1.2.1 Pitching Moment Derivative w.r.t. Angle of Attack

$C_{m_\alpha} = -C_{L_\alpha} H_n$ (Ref. 1), so according to Table A.1-2 and Eqn 4 C_{m_α} becomes:

$$C_{m_\alpha} \cong \frac{\theta C_m}{\theta \alpha} = -1.05 / \text{rad} \quad (11)$$

1.2.2 Pitching Moment Derivative w.r.t. Rate of the Angle of Attack

$$C_{m_{\dot{\alpha}}} \cong C_{m_{\dot{\alpha}}|_{\text{tail}}} = -\frac{l_t}{c} C_{L_{\dot{\alpha}}|_{\text{tail}}} \quad (\text{Ref. 2})$$

Therefore (Eqn 5 and Table A.1-1):

$$C_{m_{\dot{\alpha}}} \cong \frac{\theta C_m}{\theta \left(\frac{\dot{\alpha} c}{2V_T} \right)} = -9.32 / \text{rad} \quad (12)$$

1.2.3 Pitching Moment Derivative w.r.t. Pitch Rate

$$C_{m_q} = C_{m_q|wing} + C_{m_q|tail}$$

where:

$$C_{m_q|wing} = -\frac{l_x}{c} C_{L_q|wing} \quad (\text{Ref. 2})$$

$$C_{m_q|tail} = -\frac{l_t}{c} C_{L_q|tail} \quad (\text{Ref. 2})$$

Then from Table A.1-1 and Eqns 6 and 7, C_{m_q} becomes:

$$C_{m_q} \cong \frac{\theta C_m}{\theta \left(\frac{qc}{2V_T} \right)} = -19.15 \text{ /rad} \quad (13)$$

1.2.4 Pitching Moment Derivative w.r.t. Elevator Deflection

$$C_{m_\eta} = -\frac{l_t}{c} C_{L_\eta} \quad (\text{Ref. 1})$$

So (Table A.1-1, Eqn 10):

$$C_{m_\eta} \cong \frac{\theta C_m}{\theta \eta} = -1.63 \text{ /rad} \quad (14)$$

1.3 Drag Derivatives

Drag is estimated from the formula

$$C_D = C_{D_0} + k C_{L_w}^2$$

for the drag coefficient, where C_D is computed by applying regression analysis to wind-tunnel data (Ref. 3).

Then:

$$C_{D_0} = 0.0227 \quad \text{and}$$

$$k = 0.0514$$

Therefore:

$$C_D = 0.0227 + 0.0514 C_{L_w}^2 \quad (15)$$

According to Eqn 15 the derivative of the drag coefficient with respect to angle of attack is:

$$C_{D_\alpha} \cong \frac{\partial C_D}{\partial \alpha} = 2k C_{L_w} C_{L_{\alpha w}} = 0.466 C_{L_w} / \text{rad} \quad (16)$$

If the viscous drag coefficient is defined as

$$C'_D = C_D - \frac{C_L^2}{\pi A} \quad \text{then}$$

$$C'_{D_\alpha} \cong \frac{\partial C'_D}{\partial \alpha} = 0.0801 C_{L_w} / \text{rad} \quad (17)$$

2. Engine Model

2.1 Thrust Components

An analytical method for the computation of the thrust characteristics of X-RAE1 is used. A graphical method, as opposed to the analytical one, is impossible to be used due to lack of sufficient data.

The available power P_{av} for a fixed pitch propeller is given by the formula (Ref. 4):

$$P_{av} = \frac{M_{br}}{r \tan \beta'} V_T - \frac{\alpha_p S_p}{S \sin^3 \beta'} \frac{W}{V_1^2} V_T^3 \quad (18)$$

where:

- M_{br} : Brake torque moment.
- r : Distance of a representative blade element of the propeller from the axis of rotation.
- β' : Representative blade setting angle w.r.t. the zero lift direction of the blade profile.
- α_p : Zero lift drag coefficient of the propeller profile.
- S_p : Blade area.
- S : Wing area.
- W : Weight of the RPV - assumed constant.
- V_1 : $V_1^2 = 2W/\rho S$

If the altitude effects are ignored, P_{av} becomes:

$$P_{av} = k_1 \delta_T V_T - k_2 V_T^3 \quad (19)$$

where:

- $k_1 = [M_{br}(\text{full throttle})]/r \tan \beta'$
- δ_T : throttle setting (from 0 to 1).
- k_2 constant to be computed.
- $r \tan \beta' = p/2$ and p is the propeller pitch.

Computation of k_1

Assume that $P_{br}(\text{full throttle})$ is 50% of 1.9 Kw at 14000RPM (losses not modelled in the P_{av} equation and bad engine performance, Table 3.1)

Then:

$$M_{br}(\text{full throttle}) = P_{br}(\text{full throttle})/2\pi n$$

where

$$P_{br}(\text{full throttle}) = 950 \text{ Watts} \quad \text{and} \\ n = 14000\text{RPM} = 14000/60 \text{ sec}^{-1} \quad (\text{Table 3.1})$$

k_1 then becomes: $k_1 = P_{br}(\text{f. t.})/pn$ ($p=6\text{inches}$), ie:

$$k_1 = 26.7154 \text{ Wsec/m} \quad (20)$$

Computation of k_2

If a maximum speed of 35 m/sec is assumed, the required power P_{re} for an RPV mass of 16 Kgr is:

$$P_{re} = \frac{1}{2} \rho V_T^2 S C_D V_T = 618.24 \text{ Watts.}$$

where:

$$C_D = C_{D_0} + k C_L^2$$

$$C_L = \frac{2W}{\rho V_T^2 S}$$

$$W = mg = 16g$$

Allow a throttle margin and an all-up weight greater than 16 Kgr. So, assume:

$$P_{av} = 700 \text{ Watts at 35 m/sec, full throttle.} \quad (21)$$

Then Eqns 19, 20 and 21 give:

$$k_2 = 0.0055 W(m/sec)^{-3} \quad (22)$$

If T is the thrust produced by the propeller, $T = P_{av}/V_T$ and according to Eqns 19, 20 and 21 the thrust model is

$$T = 26.7154 \delta_T - 0.0055 V_T^2 \quad (23)$$

2.2 Derivatives Due to Thrust

2.2.1 Trust Derivative w.r.t. the Velocity

According to Eqn 23:

$$\frac{\partial T}{\partial V_T} = -0.011 V_T \quad (24)$$

2.2.2 Trust Derivative w.r.t. Throttle Setting

$$\frac{\partial T}{\partial \delta_T} = 26.7154 \quad (25)$$

REFERENCES

1. Klein V. "Determination of Longitudinal Aerodynamic Derivatives from Steady-state Measurement of an Aircraft"
paper, AIAA 77-1123
Atmospheric Flight Mechanics Conference, 1979.
2. Smetana F. O. "Computer Assisted Analysis of Aircraft Performance Stability and Control"
McGraw-Hill Book Company, 1984.
3. Trebble W. J. G. "Low-Speed Wind-Tunnel Tests on a Full-Scale Unmanned Aircraft (X-RAE1)"
Tech. Memo, AERO 2043, RAE, Aug. 1985.
4. Mises Von R. "Theory of Flight"
Dover Publications, Inc., New York, 1945, 1959.

APPENDIX A.2

DERIVATIVES DUE TO SIDESLIP

1. Side Force Due to Sideslip
2. Rolling Moment Due to Sideslip
3. Yawing Moment Due to Sideslip

Appendix A.2

DERIVATIVES DUE TO SIDESLIP

ESDU Data Sheets are used for the estimation of the lateral derivatives due to sideslip. All the derivatives are assumed to be given in stability axes unless it is stated otherwise.

1. Side Force Derivatives Due to Sideslip (Y_v)

$$Y_v = \frac{\partial Y}{\partial v} / \frac{1}{2} \rho V_T S$$

1.1 Wing-Body Side Force Derivative
Due to Sideslip (Item 79006)

$$\left. \begin{aligned} \frac{|z|}{h} = \frac{|h_o|}{H} = 0.139 \quad (\text{Apx A.7}) \\ \frac{2b}{H+W} = 11.04 \quad (\text{Apx A.7}) \end{aligned} \right\} \text{Then } F = 0.012 \quad (\text{Item 79006})$$

$$\left. \begin{aligned} A = 7.48 \quad (\text{Apx A.7}) \\ \lambda = 0.87 \quad (\text{Apx A.7}) \end{aligned} \right\} \text{Then } F_w = 0.820 \quad (\text{Item 79006})$$

$$\begin{aligned} -Y_{vWB} &= \left[0.0714 + 0.674 \frac{h^2}{S_{bs}} + \frac{hbFF_w}{S_{bs}} \left(\frac{4.95|z|}{h} - 0.12 \right) \right] \frac{S_{bs}}{S} \quad (\text{Item 79006}) \\ &= \left[0.0714 + 0.674 \frac{H^2}{S_{bs}} + \frac{HbFF_w}{S_{bs}} \left(4.95 \frac{|h_o|}{H} - 0.12 \right) \right] \frac{S_{bs}}{S} = \\ &= 0.1085 \quad (\text{Apx A.7}) \end{aligned}$$

Therefore:

$Y_{vWB} = -0.1085$

1.2 Contribution of Fin to Side Force Derivative Due to Sideslip
in the Presence of Body Wing and Tailplane (Item 82010)

From Apx A.8:

$$J_B = 0.7513 \quad J_T = 1.304 \quad J_W = 0.91$$

$$C_{L_{\alpha F}} = 1.88 \text{ /rad} \quad S_F = 0.1093 \text{ m}^2$$

Then:

$$Y_{vF} = - J_B J_T J_W C_{L_{\alpha F}} \frac{S_F}{S} = -0.1969$$

$Y_{vF} = -0.1969$

1.3 Side Force Derivative Due to Sideslip
for Complete Aircraft (Item 82011)

$$Y_v = Y_{vWB} + Y_{vF} \text{ therefore:}$$

$Y_v = -0.3054$

2. Rolling Moment Derivatives Due to Sideslip (L_v)

$$L_v = \frac{\partial L}{\partial v} / \frac{1}{2} \rho V_T S b$$

2.1 Effects of Isolated Body (L_{vb}) and Wing-Body Interference (L_{vh}) on Rolling Moment Due to Sideslip (Item 73006)

Isolated Body

$$L_{vb} = -0.014 \frac{l_b}{b} \frac{S_{bm}}{S} \alpha_b = -0.0005 \alpha_b \quad (\text{Apx A.7})$$

where:

α_b : body incidence measured from its zero-lift value (in degrees)

$L_{vb} = -0.0005 \alpha_b$

Wing-body interference

$$\frac{h_o}{H} = -0.139 \quad (\text{Apx A.7})$$

$$\frac{H}{b} = 0.125 \quad (\text{Apx A.7})$$

$$\frac{W}{H} = 0.449 \quad (\text{Apx A.7})$$

$$l = \frac{L_{vh}}{(1 + W/H)f(A)} = -0.0076 \quad (\text{Item 73006})$$

A = 7.48 then (Item 73006), f(A) = 1.08

Therefore:

$L_{vh} = -0.0119$

2.2 Contribution of Wing Planform to
Rolling Moment Derivative Due to Sideslip (L_{vW}) (Item 80033)

$$L_{vW} = [L_{vW}]_0 + [L_{vW}]_{\Lambda_{\frac{1}{2}}} \quad \left| \quad \text{Then } L_{vW} = [L_{vW}]_0 \quad (\text{Item 80033}) \right.$$

$$\Lambda_{\frac{1}{2}} = 0$$

$$-\frac{[L_{vW}]_0}{C_L} = \frac{f_1(\lambda)}{A} - f_2(\lambda) \quad \left| \quad -\frac{L_{vW}}{C_L} = 0.0016 \quad (\text{Item 80033}) \right.$$

$$A = 7.48$$

$$\lambda = 0.87$$

Therefore:

$$L_{vW} = -0.0016C_L$$

where C_L is the wing lift coefficient.

2.3 Contribution of Fin to
Rolling Moment Derivative Due to Sideslip (L_{vF}) (Item 82010)

$$L_{vF} = Y_{vF}(\bar{z}_F \cos \alpha - \bar{l}_F \sin \alpha) / b$$

where:

α : angle between stability x-axis and longitudinal body axis (ie. angle of attack).

Then (Apx A.8), the rolling moment derivative due to sideslip becomes:

$$L_{vF} = \frac{-0.1969(8.87 \cos \alpha - 109.51 \sin \alpha)}{263.8}$$

2.4 Estimation of Rolling Moment Derivative Due to Sideslip
for Complete Aircraft at Subsonic Speeds (Item 81032)

$$L_v = L_{vb} + L_{vh} + L_{vW} + L_{vF} \quad \text{so,}$$

$$L_v = -0.0005\alpha_b - 0.0119 - 0.0016C_L - 0.1969(8.87 \cos \alpha - 109.51 \sin \alpha) / 263.8$$

3. Yawing Moment Derivatives Due to Sideslip (N_V)

$$N_V = \frac{\partial N}{\partial v} / \frac{1}{2} \rho V_T S b$$

3.1 Wing-Body Yawing Moment Derivative Due to Sideslip (N_{VWB}) (Item 79006)

$$-N_{V_{mid}} = \left[0.2575 + \frac{l_b^2}{S_{bs}} (0.0008 \frac{l_b^2}{S_{bs}} - 0.024) \right] \left[1.39 \frac{h_1^{\frac{1}{2}}}{h_2^{\frac{1}{2}}} - 0.39 \right] \frac{S_{bs} l_b}{S b}$$

$$= 0.0515 \quad (\text{Apx A.7})$$

$$N_{VWB} = N_{V_{mid}} + \frac{1 - 0.5l_b}{b} Y_{VWB} \quad (\text{Item 79006})$$

where

l : distance of C.G. from the nose of fuselage ($l=0.681$ m)

Then

$N_{VWB} = -0.0363$

3.2 Contribution of Fin to Yawing Moment Derivative Due to Sideslip (N_{VF}) (Item 82010)

$$N_{VF} = -Y_{VF} (\bar{l}_F \cos \alpha + \bar{z}_F \sin \alpha) / b$$

where:

α : angle between stability x-axis and longitudinal body axis (ie. angle of attack).

Then according to Apx A.8, N_{VF} is:

$N_{VF} = 0.1969(109.51 \cos \alpha + 8.87 \sin \alpha) / 263.8$
--

3.3 Estimation of Yawing Moment Derivative Due to Sideslip for Complete Aircraft at Subsonic Speeds (Item 82011)

$$N_V = N_{VWB} + N_{VF} \quad \text{so,}$$

$N_V = -0.0363 + 0.1969(109.51 \cos \alpha + 8.87 \sin \alpha) / 263.8$

APPENDIX A.3

DERIVATIVES DUE TO RATE OF ROLL

1. Side Force Due to Rate of Roll
2. Rolling Moment Due to Rate of Roll
3. Yawing Moment Due to Rate of Roll

Appendix A.3

DERIVATIVES DUE TO RATE OF ROLL

The lateral derivatives due to rate of roll are estimated in this appendix using ESDU Data Sheets. All the derivatives are assumed to be given in stability axes unless it is stated otherwise.

1. Side Force Derivatives Due to Rate of Roll (Y_p)

$$Y_p = \frac{\partial Y}{\partial p} / \frac{1}{2} \rho V_T S b$$

1.1 Contribution of Wing Planform to Side Force Derivative Due to Rate of Roll (Y_{pW}) (Item 81014)

$$\frac{x_{ac}}{b} = \frac{x_r}{b} = -0.0136 \quad (\text{Apx A.1})$$

Then:

$$\left[\frac{Y_{pW}}{C_L} \right]_0 = 0.078 \quad (\text{Item 81014}), \text{ therefore}$$

$$Y_{pW} = 0.078 C_L$$

1.2 Contribution of Fin to Side Force Derivative Due to Rate of Roll (Y_{pF}) (Item 83006)

$$\frac{b_t}{h_F} = 1.36 \quad (\text{Apx A.8})$$

$$\frac{z_T}{z_F} = 1 \quad (\text{Apx A.8})$$

$$\text{Then, } k_2 = 0.975 \quad k_3 = 1 \quad (\text{Item 83006})$$

$$\text{Also } k_1 = 0.625 \quad (\text{Item 83006})$$

Then (Item 83006) :

$$Y_{pF} = -(k_1 + k_2 k_3) \frac{S_F h_F}{S_b} \left[\frac{(\bar{z}_F^* \cos \alpha - \bar{l}_F^* \sin \alpha) / b - \theta \bar{\sigma}_w / \theta (pb/V_T) - \theta \bar{\sigma}_\alpha / \theta (pb/V_T)}{(\bar{z}_F^* - z_{crF}) / b} \right]$$

where:

α : angle between stability x-axis and longitudinal body axis (ie. angle of attack).

$\theta \bar{\sigma}_w / \theta (pb/V_T) = 0.18$ sidewash term due to wing (independent from angle of attack variations).

$\theta \bar{\sigma}_\alpha / \theta (pb/V_T)$ sidewash term due to body (function of angle of attack). It is given w.r.t.

$$k = [\bar{z}_F^* - (\bar{z}_F^* \cos \alpha - \bar{l}_F^* \sin \alpha)] / b \text{ (Item 83006).}$$

According to Apx A.8, Y_{pF} becomes:

$$Y_{pF} = -0.3133[(11.32 \cos \alpha - 110.19 \sin \alpha) / 263.8 - 0.18 - \theta \bar{\sigma}_\alpha / \theta (pb/V_T)]$$

1.3 Estimation of Side Force Derivative

Due to Rate of Roll for Complete Aircraft (Item 85010)

$$Y_p = Y_{pW} + Y_{pF} \quad \text{ie:}$$

$$Y_p = 0.078 C_L - 0.3133[(11.32 \cos \alpha - 110.19 \sin \alpha) / 263.8 - 0.18 - \theta \bar{\sigma}_\alpha / \theta (pb/V_T)]$$

2. Rolling Moment Derivatives Due to Rate of Roll (L_p)

$$L_p = \frac{\partial L}{\partial p} / \frac{1}{2} \rho V_T S b^2$$

2.1 Rolling Moment Derivative Due to Rate of Roll for Swept and Tapered Wings (L_{pW}) (Item A.06.01.01)

$$\beta = (1-M^2)^{\frac{1}{2}} = 1$$

$$k = \frac{\beta(\alpha_{10})_M}{2\pi} = 1$$

$(\alpha_{10})_M$: two dimensional lift-curve slope ($\approx 2\pi$)

$$\frac{\beta A}{k} = A = 7.48 \quad (\text{Apx A.7})$$

$$\Lambda_E = \tan^{-1}(\tan \Lambda_{\frac{1}{4}}) = 1.66^\circ \quad (\text{Apx A.7})$$

$$\lambda = 0.87 \quad (\text{Apx A.7})$$

Then (Item A.06.01.01):

$$L_{pW} = -0.2438$$

2.2 Contribution of Fin to Rolling Moment Derivative Due to Rate of Roll (L_{pF}), in the Presence of Body, Wing and Tailplane (Item 83006)

$$L_{pF} = Y_{pF}(\bar{z}_F^* \cos \alpha - \bar{y}_F^* \sin \alpha) / b \quad \text{therefore (Apx A.8):}$$

$$L_{pF} = Y_{pF}(11.32 \cos \alpha - 110.19 \sin \alpha) / 263.8$$

2.3 Contribution of Tailplane to Rolling Moment Derivative
Due to Rate of Roll (L_{pT}) (Items 83006, A.06.01.01)

From Item A.06.01.01, $L_{pT} = -0.127$ based on S_t and b_t .

Then:

$$L_{pT} = -0.127 * 0.5 S_t b_t^2 / S b^2 \quad \text{Hence (Apx A.7):}$$

$$L_{pT} = -0.0019$$

2.4 Estimation of the Rolling Moment Derivative (Item 85010)
Due to Rate of Roll for Complete Aircraft

$$L_p = L_{pW} + L_{pF} + L_{pT} \quad \text{so,}$$

$$L_p = -0.2457 + Y_{pF} (11.32 \cos \alpha - 110.19 \sin \alpha) / 263.8$$

3. Yawing Moment Derivatives Due to Rate of Roll (N_p)

$$N_p = \frac{\partial N}{\partial p} / \frac{1}{2} \rho V_T S b^2$$

3.1 Contribution of Wing Planform to Yawing Moment Derivative Due to Rate of Roll (N_{pW}) (Item 81014)

Linear contribution to N_{pW}

$$\left[\frac{N_{pW}}{C_L} \right]_0 = -0.034 \quad (\text{Item 81014, Fig. 1})$$

Nonlinear contribution to N_{pW}

$$\frac{N_{pW}}{\frac{\partial C_D}{\partial \alpha}} = 1.23 \quad (\text{Item 81014, Fig. 3})$$

where $\frac{\partial C_D}{\partial \alpha}$: viscous drag-curve slope (per degrees).

Then

$$N_{pW} = -0.034 C_L + 1.23 \frac{\partial C_D}{\partial \alpha}$$

C_L : wing lift coefficient.

3.2 Contribution of Fin to Yawing Moment Derivative Due to Rate of Roll (N_{pF}) in the Presence of Body, Wing and Tailplane (Item 85010)

$$N_{pF} = -Y_{pF} (\bar{1}_F^* \cos \alpha + \bar{z}_F^* \sin \alpha) / b$$

hence :

$$N_{pF} = -Y_{pF} (110.19 \cos \alpha + 11.32 \sin \alpha) / 263.8$$

3.3 Estimation of Yawing Moment Derivative Due to Rate of Roll
for Complete Aircraft (Item 85010)

$$N_p = N_{pW} + N_{pF} \quad \text{so,}$$

$$N_p = -0.034C_L + 1.23 \frac{\theta C_D'}{\theta \alpha} - Y_{pF}(110.19 \cos \alpha + 11.32 \sin \alpha) / 263.8$$

APPENDIX A.4

DERIVATIVES DUE TO RATE OF YAW

1. Side Force Due to Rate of Yaw
2. Rolling Moment Due to Rate of Yaw
3. Yawing Moment Due to Rate of Yaw

Appendix A.4

DERIVATIVES DUE TO RATE OF YAW

The derivatives due to rate of yaw are estimated in this appendix. Their derivation is based on ESDU Data Sheets. All the derivatives are expressed in stability axes.

1. Side Force Derivatives Due to Rate of Yaw (Y_r)

$$Y_r = \frac{\partial Y}{\partial r} / \frac{1}{2} \rho V_T^2 S_b$$

1.1 Contribution of Body to Side Force Derivative Due to Rate of Yaw (Y_{rB}) (Item 83026)

$$Y_{rB} = -0.04 \frac{S_{bs} l_b}{S_b} \quad \text{therefore (Apcs A.7 and A.8):}$$

$Y_{rB} = -0.0109$

1.2 Contribution of Fin to Side Force Derivative Due to Rate of Yaw (Y_{rF}) (Item 82017)

$$Y_{rF} = -[Y_{vF}]_{J_W=1} (\bar{l}_F \cos \alpha + \bar{z}_F \sin \alpha) / b$$

From Apx A.2 (Section 1.2), $[Y_{vF}]_{J_W=1} = -0.2164$. Then, Y_{rF} becomes (Apcs A.7 and A.8):

$Y_{rF} = 0.2164(109.51 \cos \alpha + 8.87 \sin \alpha) / 263.8$
--

1.3 Estimation of Side Force Derivative Due to Rate of Yaw for Complete Aircraft (Item 84002)

$$Y_r = Y_{rB} + Y_{rF}$$

$Y_r = -0.0109 + 0.2164(109.51 \cos \alpha + 8.87 \sin \alpha) / 263.8$

2. Rolling Moment Derivatives Due to Rate of Yaw (L_r)

$$L_r = \frac{\partial L}{\partial r} / \frac{1}{2} \rho V_T^2 S b^2$$

2.1 Effect of Wing on Rolling Moment Derivative
Due to Rate of Yaw (L_{rW}) (Item 72021)

$$L_{rW} = L_{rp} + L_{r\Gamma} + L_{r\epsilon} + L_{rf}$$

where:

L_{rp} : due to wing planform

$L_{r\Gamma}$: due to dihedral ($L_{r\Gamma} = 0$)

$L_{r\epsilon}$: due to wing twist

L_{rf} : due to flaps ($L_{rf} = 0$, flaps not deflected)

$$\frac{L_{rp}}{C_L} = \frac{1}{g(\Lambda_{\frac{1}{4}})} \frac{L_{rp}}{C_L} * g(\Lambda_{\frac{1}{4}})$$

$$\frac{1}{g(\Lambda_{\frac{1}{4}})} \frac{L_{rp}}{C_L} = 0.1219 \quad (\text{Item 72021 Fig. 1a})$$

$$g(\Lambda_{\frac{1}{4}}) = 1.02 \quad (\text{Item 72021 Fig. 1b})$$

$$\text{Hence } L_{rp} = 0.1243 C_L$$

$$\frac{L_{r\epsilon}}{\epsilon} = -0.00185 \text{ /degree}$$

Then, for $g(\Lambda_{\frac{1}{4}}) = 1.02$ and $\epsilon = 1^\circ$ washout, $L_{r\epsilon} = -0.00189$

So

$$L_{rW} = 0.1243 C_L - 0.00189$$

where C_L is the wing lift coefficient

2.2 Contribution of Fin to Rolling Moment Derivative
Due to Rate of Yaw (L_{rF}) (Item 82017)

$$L_{rF} = Y_{rF}(\bar{z}_F \cos\alpha - \bar{I}_F \sin\alpha)/b$$

So, from Apx A.8

$$L_{rF} = Y_{rF}(8.87\cos\alpha - 109.51\sin\alpha)/263.8$$

2.3 Estimation of Rolling Moment Derivative Due to Rate of Yaw
for Complete Aircraft (Item 84002)

$$L_r = L_{rW} + L_{rF} \quad \text{so:}$$

$$L_r = -0.00189 + 0.1243C_L + Y_{rF}(8.87\cos\alpha - 109.51\sin\alpha)/263.8$$

3. Yawing Moment Derivatives Due to Rate of Yaw (N_r)

$$N_r = \frac{\partial N}{\partial r} / \frac{1}{2} \rho V_T S b^2$$

3.1 Contribution of Body to Yawing Moment Derivative Due to Rate of Yaw (N_{rB}) (Item 83026)

$$N_{rB} = -0.01 \frac{l_{bs}^2}{b^2 S} \quad \text{therefore (ApX A.7):}$$

$$N_{rB} = -0.0022$$

3.2 Effect of Wing on Yawing Moment Derivative Due to Rate of Yaw (N_{rW}) (Item 71017)

$$N_{rW} = \frac{N_{r_o}}{C_{D_o}} C_{D_o} + \frac{N_{r_v}}{C_L^2} C_L^2$$

$$A = 7.48, \quad \lambda = 0.87, \quad \Lambda_{\frac{1}{4}} = 1.66^\circ$$

$$\left(\frac{N_{r_o}}{C_{D_o}} \right)_{\lambda=1} = -0.168 \quad (\text{Item 71017 Fig. 1a})$$

$$\frac{\left(\frac{N_{r_o}}{C_{D_o}} \right)_{\lambda=0.87}}{\left(\frac{N_{r_o}}{C_{D_o}} \right)_{\lambda=1}} = 0.9675 \quad (\text{Item 71017 Fig. 1b})$$

$$\frac{N_{r_o}}{C_{D_o}} = -0.1621$$

$$\left(\frac{N_{r_v}}{C_L^2} \right)_{\lambda=0.5} = -0.008 \quad (\text{Item 71017 Fig. 2c})$$

$$\left(\frac{N_{r_v}}{C_L^2} \right)_{\lambda=1} = -0.01 \quad (\text{Item 71017 Fig. 2c})$$

$$\frac{N_{r_v}}{C_L^2} = -0.009$$

Hence

$$N_{rW} = -0.1621 C_{D_o} - 0.009 C_L^2$$

and C_L : wing lift coefficient

C_{D_o} : wing drag coefficient at zero lift

3.3 Contribution of Fin to Yawing Moment Derivative
Due to Rate of Yaw (N_{rF}) (Item 82017)

$$N_{rF} = -Y_{rF}(\bar{I}_F \cos\alpha + \bar{z}_F \sin\alpha)/b$$

So, from Apx A.8:

$$N_{rF} = -Y_{rF}(109.51\cos\alpha + 8.87\sin\alpha)/263.8$$

3.4 Estimation of Yawing Moment Derivative Due to Yaw Rate
for Complete Aircraft (Item 84002)

$$N_r = N_{rB} + N_{rW} + N_{rF}$$

$$N_r = -0.0022 - 0.1621C_{D_0} - 0.009C_L^2 - Y_{rF}(109.51\cos\alpha + 8.87\sin\alpha)/263.8$$

APPENDIX A.5

DERIVATIVES DUE TO AILERON DEFLECTION

1. Rolling Moment Due to Aileron
2. Yawing Moment Due to Aileron

Appendix A.5

DERIVATIVES DUE TO AILERON DEFLECTION

The rolling moment and yawing moment derivatives of X-RAE1 due to aileron deflection are given in this appendix. The side force due to aileron deflection is assumed negligible. All the derivatives are expressed in stability axes.

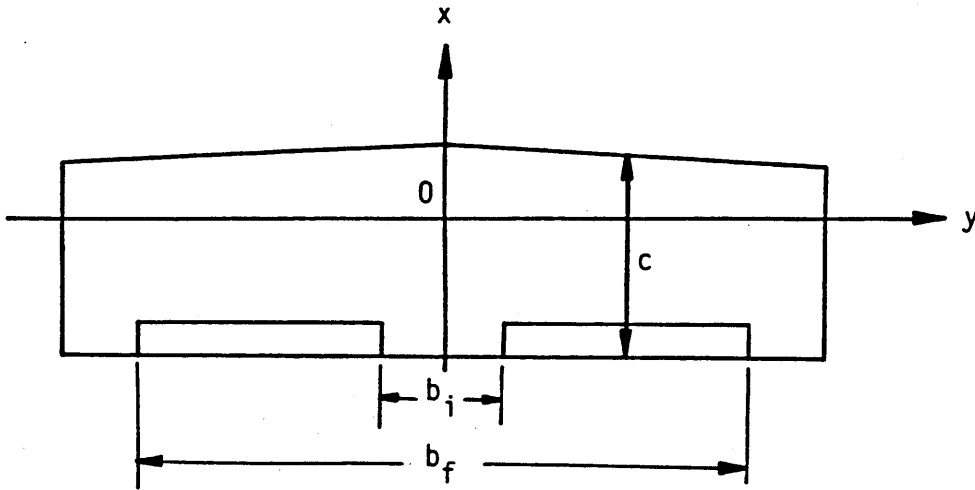


Fig. A.5-1 Aileron geometry of X-RAE1

$b_i = 0.4588 \text{ m} \quad b_f = 1.932 \text{ m} \quad c = 0.357 \text{ m}$

1. Rolling Moment Derivative Due to Aileron Deflection (L_ξ)

$$\frac{\partial L}{\partial \xi} = -\rho V_T^2 \frac{\partial C_L}{\partial \xi} c \int_{b_i/2}^{b_f/2} y dy$$

$\frac{\partial C_L}{\partial \xi} = 1.79 \text{ /rad} \quad (\text{Apx A.9})$

Then, $\frac{\partial L}{\partial \xi} = -\frac{1}{2} \rho V_T^2 0.5626$

$$L_\xi \cong \frac{\partial L}{\partial \xi} / \frac{1}{2} \rho V_T^2 S b = -0.2291 \text{ /rad}$$

2. Yawing Moment Derivative Due to Aileron Deflection (N_{ξ})

The yawing moment due to aileron deflection is caused by the difference on drag between up and down aileron (only vortex drag is assumed). Then, the components that produce the yawing moment are:

$$\underline{\text{Starboard}} : C_{L0} \Delta C_L / \pi A$$

$$\underline{\text{Portboard}} : -C_{L0} \Delta C_L / \pi A$$

where:

$$\Delta C_L \cong \Delta L / \frac{1}{2} \rho V_T^2 S = \frac{c(b_f - b_i) \theta C_L}{S \theta \xi} \xi \quad (\text{Fig. A.5-1})$$

Then:

$$\frac{\theta N_{\xi}}{\theta \xi} = \frac{1}{2} \rho V_T^2 S \frac{C_{L0} \Delta C_L}{\pi A} 2l_n \quad (\text{Fig. A.5-1})$$

$$l_n = (b_f + b_i) / 4 \quad (\text{Fig. A.5-1})$$

Therefore

$$N_{\xi} \cong \frac{\theta N}{\theta \xi} / \frac{1}{2} \rho V_T^2 S b = 0.0195 C_{L0} / \text{rad}$$

where C_{L0} , lift coefficient about which the variation in lift coefficient due to aileron deflection takes place.

APPENDIX A.6

DERIVATIVES DUE TO RUDDER DEFLECTION

1. Side Force Due to Rudder
2. Rolling Moment Due to Rudder
3. Yawing Moment Due to Rudder

Appendix A.6

DERIVATIVES DUE TO RUDDER DEFLECTION

The aerodynamic derivatives of X-RAE1 due to rudder deflection are estimated in this appendix. All the derivatives are given in body axes.

1. Side Force Due to Rudder (Y_{ζ})

If wing, body and tailplane interference is assumed, the side force derivative due to rudder deflection can be expressed as:

$$\frac{\partial Y}{\partial \zeta} = J_B J_T J_W \frac{\partial C_{L_F}}{\partial \zeta} \frac{1}{2} \rho V_T^2 S_F$$

where

$$\frac{\partial C_{L_F}}{\partial \zeta} : \text{lift-curve slope of fin due to rudder deflection.}$$

Then, according to Apcs A.8 and A.9, Y_{ζ} becomes:

$$Y_{\zeta} \cong \frac{\partial Y}{\partial \zeta} / \frac{1}{2} \rho V_T^2 S = 0.1184 \text{ /rad}$$

2. Rolling Moment Derivative Due to Rudder (L_{ζ})

$$\frac{\partial L}{\partial \zeta} = \frac{\partial Y}{\partial \zeta} \bar{z}_F \quad \text{so, according to Apx A.8}$$

$$L_{\zeta} \cong \frac{\partial L}{\partial \zeta} / \frac{1}{2} \rho V_T^2 S b = 0.00398 \text{ /rad}$$

3. Yawing Moment Derivative Due to Rudder (N_{ζ})

$$\frac{\partial N}{\partial \zeta} = - \frac{\partial Y}{\partial \zeta} \bar{y}_F$$

$$\text{so: } N_{\zeta} \cong \frac{\partial N}{\partial \zeta} / \frac{1}{2} \rho V_T^2 S b = -0.0492 \text{ /rad}$$

APPENDIX A.7

XRAE-1 USEFUL DETAILS

1. X-RAE1 Geometry

WING WITH ROUNDED TIPS	
Area (S)	0.9307 m ²
Span (b)	2.638 m
Mean Chord (c)	0.353 m
Aspect Ratio (A)	7.48
Sweepback of Quarter chord ($\Lambda_{\frac{1}{4}}$)	1.66°
Taper Ratio (λ)	0.87
Distance of the Centre of Gravity from leading edge of mean chord	0.34c = 0.121 m
AILERON	
Span	0.7366 m
Chord	0.055 m
TAILPLANE	
Area (S _t)	0.2576 m ²
Span (b _t)	0.2575 m ²
Mean Chord (c _t)	0.2995 m
Tail Arm (l _t)	
(Distance of C.G. to tailplane mean quarter-chord)	1.182 m
Tail Volume (S _t l _t /Sc)	0.932
ELEVATOR	
Span	0.860 m
Chord	0.063 m

Table A.7-1 X-RAE1 geometry (Ref. 1)

2. Centre of Gravity Nominal Position, Cross-Sectional Areas and Side Elevation Area

2.1 C.G. Position and Useful Cross-Sectional Areas (Item 73006)

The centre of gravity is assumed to be the centroid of the cross-section through the longitudinal position of it (0.34c aft of leading edge of mean chord).

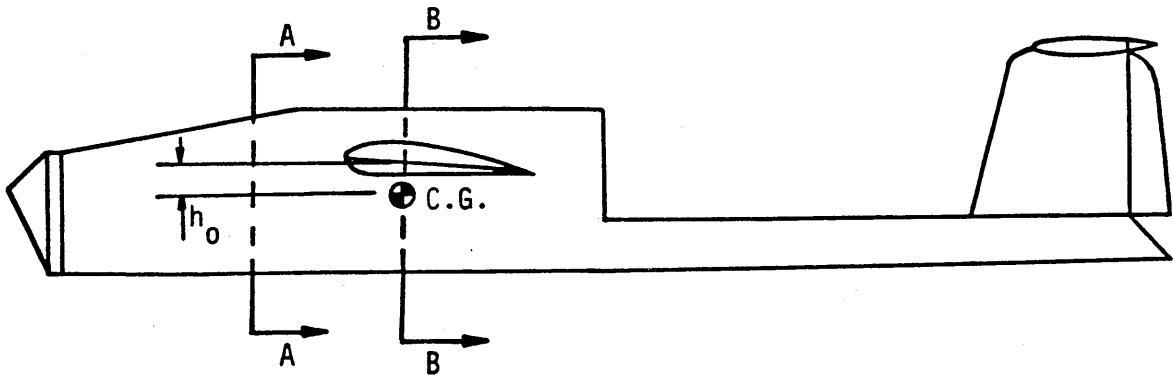


Fig. A.7-1 C.G. nominal position

h_o : lateral distance of C.G. from mean quarter-chord (negative for C.G. below mean quarter chord).

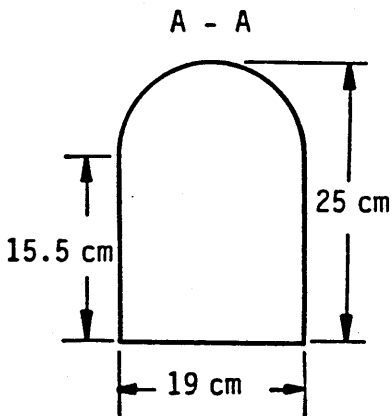


Fig. A.7-2 Maximum cross-sectional area (S_{bm})

$$S_{bm} = 436.26 \text{ cm}^2$$

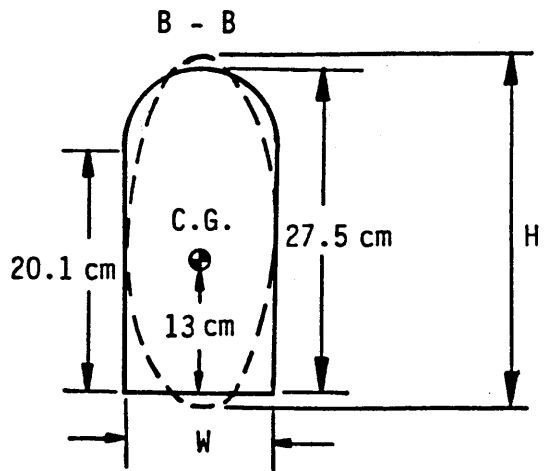


Fig. A.7-3 Equivalent elliptical area (S_{BB})

$$S_{BB} = 383.5 \text{ cm}^2$$

$$H = \frac{4}{\pi W} S_{BB} = 32.99 \text{ cm}$$

2.2 Side Elevation Area (Item 79006)

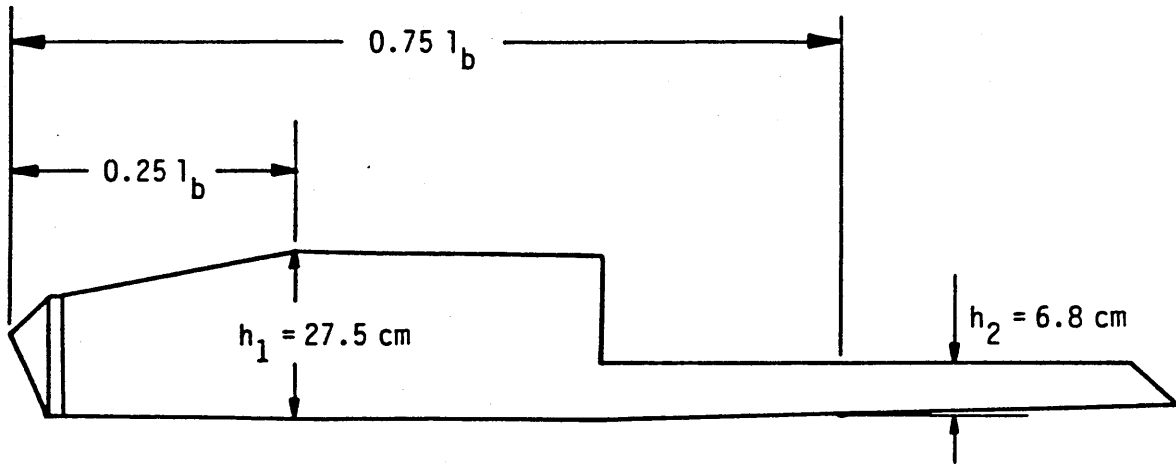


Fig. A.7-4 Side elevation area (S_{bs})

$$S_{bs} = 3187.65 \text{ cm}^2$$

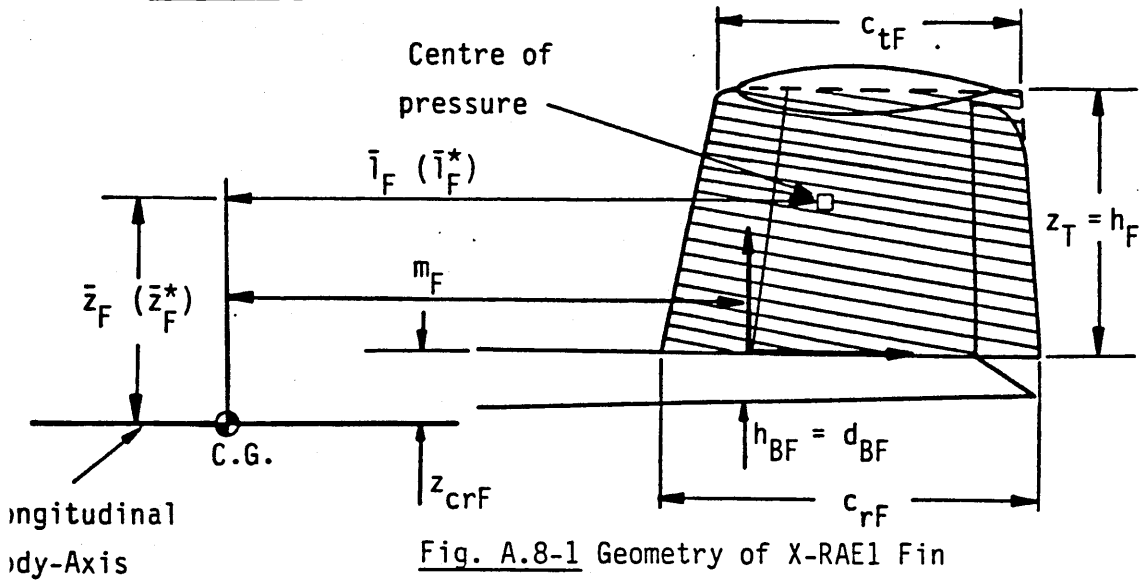
2.3 Summary

Body length (l_b)	210 cm
Maximum cross-sectional area (S_{bm})	436.26 cm ²
Equivalent height (H)	23.99 cm
Width (W)	14.8 cm
Lateral distance of C.G. from mean quarter-chord (h_o)	-4.6 cm
Side elevation area (S_{bs})	3187.65 cm ²

REFERENCES

1. Trebble W. J. G. "Low-Speed Wind-Tunnel Tests on a Full-Scale Unmanned Aircraft (X-RAE1)"
Tech. Memo, AERO 2043, RAE, Aug. 1985.

1. Lift-Curve Slope of Fin (Items 82010, 70011)



c_{rF}	40.0 cm
c_{tF}	36.4 cm
$h_F = z_T$	27.2 cm
$h_{BF} = d_{BF}$	6.0 cm
z_{crF}	5.0 cm
$\Lambda_{\frac{1}{4}F}$	8.0°
m_F	107.9 cm

Table A.8-1 Fin Characteristics

Then (Item 82010, Table A.8-1):

$$S_F = h_F(c_{rF} + c_{tF})/2 = 1093.44 \text{ cm}^2$$

$$A_F = 2h_F^2/S_F = 1.35$$

$$\lambda_F = c_{tF}/c_{rF} = 0.83$$

$$A_F \tan \Lambda_{\frac{1}{2}F} = A_F \tan \Lambda_{\frac{1}{4}F} - (1-\lambda_F)/(1+\lambda_F) = 0.0968$$

$$(1-M^2)^{\frac{1}{2}} A_F = 1.35$$

Hence (Item 70011):

$$C_{L_{\alpha F}} \cong \frac{\theta C_L}{\theta \alpha} \Big|_{\text{Fin}} = 1.88 \text{ /rad}$$

APPENDIX A.8

1. Lift-Curve Slope of Fin
2. Calculation of J_B , J_T and J_W
3. Centre of Pressure of Fin
(for derivatives due to sideslip)
4. Centre of Pressure of Fin
(for derivatives due to rate of roll)

2. Calculation of J_B , J_T and J_W (Item 82010)

$$\left. \begin{aligned} A_F &= 1.35 \\ h_{BF}/(h_{BF} + h_F) &= 0.181 \end{aligned} \right| J_B = 0.7513$$

$$\left. \begin{aligned} \frac{b_t}{h_F} &= 3.16 \quad (\text{Table A.7-1}) \\ \frac{z_F}{h_F} &= 1 \end{aligned} \right| J_T = 1.304$$

$$\frac{z_W}{h_{BW}} = \frac{h_o}{H} = -0.139 \quad \text{then} \quad J_W = 0.91$$

3. Centre of Pressure of Fin

(derivatives due to sideslip) (Item 82010)

$$\bar{z}_{F1} = 0.6h_F = 16.32 \text{ cm} \quad (\text{Item 82010})$$

Then

$$\bar{i}_F = m_F + 0.7\bar{z}_{F1} \tan \Lambda_{\frac{1}{4}F} = 109.51 \text{ cm} \quad (\text{Item 82010})$$

$$\bar{z}_F = z_{crF} + 0.85\bar{z}_{F1} = 8.87 \text{ cm} \quad (\text{Item 82010})$$

$\bar{i}_F = 109.51 \text{ cm}$ $\bar{z}_F = 8.87 \text{ cm}$

4. Centre of Pressure of Fin

(derivatives due to rate of roll) (Item 83006)

$$\bar{i}_F^* = m_F + 0.6h_F \tan \Lambda_{\frac{1}{4}F} = 110.19 \text{ cm} \quad (\text{Item 83006})$$

$$\bar{z}_F^* = z_{crF} + 0.6h_F = 11.32 \text{ cm} \quad (\text{Item 83006})$$

$\bar{i}_F^* = 110.19 \text{ cm}$ $\bar{z}_F^* = 11.32 \text{ cm}$
--

APPENDIX A.9

1. Lift-Curve Slope of Wing
Due to Aileron Deflection.
2. Lift-Curve Slope of Fin
Due to Rudder Deflection

1. Lift-Curve Slope of Wing Due to Aileron Deflection
 (Items W.01.01.05, C.01.01.03, C.01.01.04)

From Item W.01.01.05 ($\log_{10} R = 5.87$, out of range) and for trailing edge transition :

$$\frac{(\alpha_1)_0}{(\alpha_1)_{OT}} = 0.814 \quad (1)$$

Where $(\alpha_1)_{OT} = \theta C_L / \theta \alpha$ for two-dimensional theoretical flow.

Also:

$$\frac{c_f}{c_l} = \frac{0.055}{0.357}$$

c_f : aileron chord

c_l : wing local chord

$$t/c = 0.141$$

$$(\alpha_2)_{OT} = 3.225 \text{ (Item C.01.01.03)} \quad (2)$$

where $(\alpha_2)_{OT} = \theta C_L / \theta \xi$ for two-dimensional theoretical flow.

Then from (1), (2) and Item C.01.01.03

$$\frac{(\alpha_2)_0}{(\alpha_2)_{OT}} = 0.67 \quad \text{so, } (\alpha_2)_0 = 2.16 \text{ /rad}$$

$$\alpha_2 = \frac{\theta C_L}{\theta \xi} = (\alpha_2)_0 f \quad \text{(Item C.01.01.04)}$$

$$f = 0.83 \quad \text{(Item C.01.01.04 no balance)}$$

Therefore

$$\alpha_2 \cong \frac{\theta C_L}{\theta \xi} = 1.79 \text{ /rad}$$

2. Lift-Curve Slope of Fin Due to Rudder Deflection (Item 74011)

$$\left(\frac{\theta C_L}{\theta \alpha} \right)_{FT} = 1.88 \text{ /rad (Apx A.8)}$$

$$\frac{c_f}{c} = 0.22$$

$$c_f = .092 \text{ m : rudder chord}$$

$$c = .42 \text{ m : local fin chord}$$

$$\frac{\theta C_L}{\theta \zeta} = 0.71 \left(\frac{\theta C_L}{\theta \alpha} \right)_{FT} \text{ (Item 74011)}$$

Subscript T means theoretical value. Then:

$$\frac{\theta C_L}{\theta \zeta} = 1.13 \text{ /rad}$$

APPENDIX MI

MOMENTS OF INERTIA OF X-RAE1
(rough estimation)

Appendix MI

MOMENTS OF INERTIA OF X-RAE1

A rough estimation of the moments of inertia of X-RAE1 is given in this appendix. The RPV is assumed to consist of four parts (wing, tail, fin and body) with their masses uniformly distributed (Fig. MI.1). The mass and geometrical characteristics of each part are given in Table MI.1 and the positions of their centres of gravities w.r.t. body axes are shown in Table MI.2.

	Mass (Kgr)	Mean Chord (cm)	Span (cm)	Thickness (cm)
Wing	3.55	35.3	263.8	2.5
Tail	0.39	29.95	86.0	1.4
Fin	0.166	40.0	27.2	1.4
Body	11.434	Length (cm)	Radius (cm)	
		82.0	9.5	

Table MI.1 Assumed mass and geometry of wing, tail, fin and body of X-RAE1.

$x_W = -5.25$	$x_T = -122.225$	$x_F = -120.9$	$x_B = 7.709$
$z_W = -4.25$	$z_T = -22.2$	$z_F = -8.6$	$z_B = 2.202$

Table MI.2 C.G. positions of wing, tail, fin and body w.r.t. body axes.

Then the moments of inertia of X-RAE1 become:

$I_x = 2.1678 \text{ Kgr m}^2$
$I_y = 1.6469 \text{ Kgr m}^2$
$I_z = 3.6962 \text{ Kgr m}^2$

Table MI.3 Moments of inertia of X-RAE1

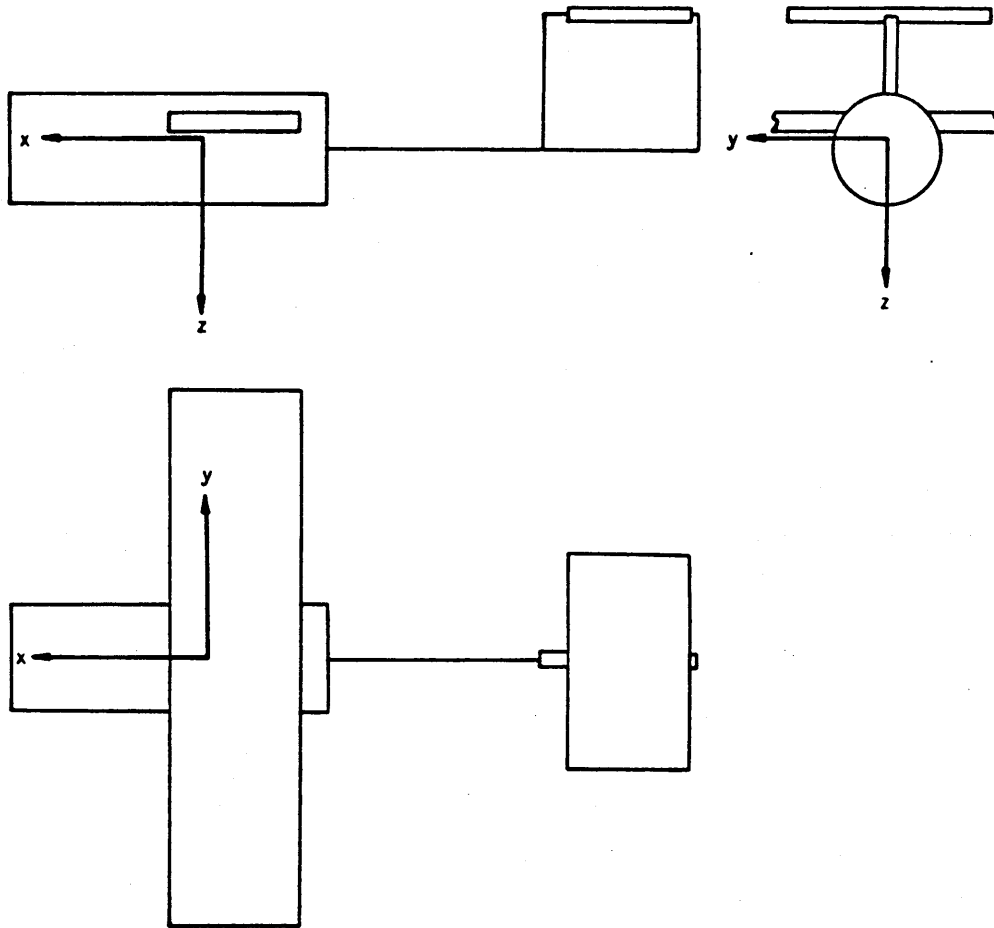


Fig. MI.1 Assumed geometry for the estimation of the moments of inertia of X-RAE1

APPENDIX LA.1

STABILITY and CONTROL DERIVATIVES at 30 m/sec
Longitudinal Model

Appendix LA.1

STABILITY and CONTROL DERIVATIVES at 30 m/sec

Longitudinal Model

1. Introduction

The procedure for the estimation of the longitudinal stability and control derivatives at 30 m/sec is given in this appendix.

C_L , C_D and C_m are referred to, from wind-tunnel measurements, a nominal C.G. on the mean aerodynamic chord $0.34c$ aft of the leading edge. Therefore, the aerodynamic derivatives and the derivatives due to thrust are first evaluated in body axes through the forementioned nominal C.G. and they are transformed afterwards to body axes through the final C.G. (displaced downwards by 4.5 cm, Fig. LA.1-1)

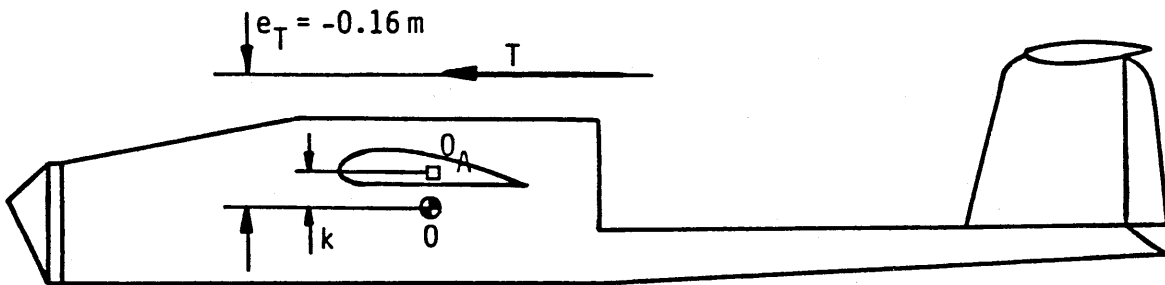


Fig. LA.1-1 Nominal and final C.G.

O_A : nominal C.G.

O : final C.G.

Due to the eccentricity of the thrust axis a thrust moment exists which has to be balanced by an opposite and equal aerodynamic moment for steady-state flight. Therefore, $C_m \neq 0$ at trim.

The trim values of the aerodynamic coefficients as they are derived from programme TRIM.FOR are given in Table LA.1-1.

$\rho = 1.225 \text{ Kgr/m}^3$	$\alpha = -0.025 \text{ rad}$
$g = 9.80665 \text{ m/sec}^2$	$C_L = 0.298$
$V_T = 30.0 \text{ m/sec}$	$C_D = 0.026$
$m = 15.54 \text{ Kgr}$	$C_m = 0.008$
$I_y = 1.6469 \text{ Kgr m}^2$	$C_{D_\alpha} = 0.139 \text{ /rad}$

Table LA.1-1 Trim values for the
Linear Longitudinal model

2. Aerodynamic Derivatives at 30 m/sec
(Derivatives due to thrust are not included)

The aerodynamic derivatives of X-RAE1 at 30 m/sec are presented in this section. The derivatives due to thrust are excluded.

2.1 Aerodynamic Derivatives - Stability Axes
(C.G. on the mean aerodynamic chord)

$$\begin{aligned} \dot{X}_{Au}^1 &= \rho V_T S (-C_D) \\ \dot{X}_{Aw}^1 &= \frac{1}{2} \rho V_T S (C_L - C_{D_\alpha}) \\ \dot{X}_{Aq}^1 &= 0 \\ \dot{X}_{A\dot{w}}^1 &= 0 \\ \dot{Z}_{Au}^1 &= -\rho V_T S C_L \\ \dot{Z}_{Aw}^1 &= -\frac{1}{2} \rho V_T S (C_{L_\alpha} - C_D) \\ \dot{Z}_{Aq}^1 &= -\frac{1}{4} \rho V_T S C_{L_q} \\ \dot{Z}_{A\dot{w}}^1 &= -\frac{1}{4} \rho S c C_{L_{\dot{\alpha}}} \\ \dot{M}_{Au}^1 &= \rho V_T S c C_m \\ \dot{M}_{Aw}^1 &= \frac{1}{2} \rho V_T S c C_{m_\alpha} \\ \dot{M}_{Aq}^1 &= \frac{1}{4} \rho V_T S c^2 C_{m_q} \\ \dot{M}_{A\dot{w}}^1 &= \frac{1}{4} \rho S c^2 C_{m_{\dot{\alpha}}} \end{aligned}$$

$$\dot{\chi}_{A\eta}^1 = 0$$

$$\dot{z}_{A\eta}^1 = -\frac{1}{2} V_T^2 S C_L$$

$$\dot{M}_{A\eta}^1 = \frac{1}{2} V_T^2 S c C_m$$

2.2 Aerodynamic Derivatives - Body Axes (Item 67004)
(C.G. on the mean aerodynamic chord)

$$\dot{\chi}_{Au}^2 = \dot{\chi}_{Au}^1 \cos^2 \alpha - (\dot{\chi}_{Aw}^1 + \dot{z}_{Au}^1) \sin \alpha \cos \alpha + \dot{z}_{Aw}^1 \sin^2 \alpha$$

$$\dot{\chi}_{Aw}^2 = \dot{\chi}_{Aw}^1 \cos^2 \alpha + (\dot{\chi}_{Au}^1 - \dot{z}_{Aw}^1) \sin \alpha \cos \alpha - \dot{z}_{Au}^1 \sin^2 \alpha$$

$$\dot{\chi}_{Aq}^2 = \dot{\chi}_{Aq}^1 \cos \alpha - \dot{z}_{Aq}^1 \sin \alpha$$

$$\dot{\chi}_{Aw}^2 = \dot{\chi}_{Aw}^1 \cos^2 \alpha + (\dot{\chi}_{Au}^1 - \dot{z}_{Aw}^1) \sin \alpha \cos \alpha - \dot{z}_{Au}^1 \sin^2 \alpha$$

$$\dot{z}_{Au}^2 = \dot{z}_{Au}^1 \cos^2 \alpha - (\dot{z}_{Aw}^1 - \dot{\chi}_{Au}^1) \sin \alpha \cos \alpha - \dot{\chi}_{Aw}^1 \sin^2 \alpha$$

$$\dot{z}_{Aw}^2 = \dot{z}_{Aw}^1 \cos^2 \alpha + (\dot{z}_{Au}^1 + \dot{\chi}_{Aw}^1) \sin \alpha \cos \alpha + \dot{\chi}_{Au}^1 \sin^2 \alpha$$

$$\dot{z}_{Aq}^2 = \dot{z}_{Aq}^1 \cos \alpha + \dot{\chi}_{Aq}^1 \sin \alpha$$

$$\dot{z}_{Aw}^2 = \dot{z}_{Aw}^1 \cos^2 \alpha + (\dot{z}_{Au}^1 + \dot{\chi}_{Aw}^1) \cos \alpha \sin \alpha + \dot{\chi}_{Au}^1 \sin^2 \alpha$$

$$\dot{M}_{Au}^2 = \dot{M}_{Au}^1 \cos \alpha - \dot{M}_{Aw}^1 \sin \alpha$$

$$\dot{M}_{Aw}^2 = \dot{M}_{Aw}^1 \cos \alpha + \dot{M}_{Au}^1 \sin \alpha$$

$$\dot{M}_{Aq}^2 = \dot{M}_{Aq}^1$$

$$\dot{M}_{Aw}^2 = \dot{M}_{Aw}^1 \cos \alpha + \dot{M}_{Au}^1 \sin \alpha$$

$$\dot{\chi}_{A\eta}^2 = \dot{\chi}_{A\eta}^1 \cos \alpha - \dot{z}_{A\eta}^1 \sin \alpha$$

$$\dot{z}_{A\eta}^2 = \dot{z}_{A\eta}^1 \cos \alpha + \dot{\chi}_{A\eta}^1 \sin \alpha$$

$$\dot{M}_{A\eta}^2 = \dot{M}_{A\eta}^1$$

3. Derivatives Due to Thrust - Body Axes
(C.G. on the mean aerodynamic chord)

$$\frac{\partial T}{\partial V} = -0.011V_T \quad (\text{Apx A.1})$$

$$\frac{\partial T}{\partial \delta_T} = 26.7154 \quad (\text{Apx A.1})$$

Then:

$$\dot{x}_{Tu}^2 = \frac{\partial T}{\partial V} \cos \alpha = -0.011V_T \cos \alpha$$

$$\dot{x}_{Tw}^2 = \frac{\partial T}{\partial V} \sin \alpha = -0.011V_T \sin \alpha$$

$$\dot{M}_{Tu}^2 = x_{Tu}^2 (e_T + k) = -0.011V_T (-0.115) \cos \alpha \quad (\text{Fig. LA.1-1})$$

$$\dot{M}_{Tw}^2 = x_{Tw}^2 (e_T + k) = -0.011V_T (-0.115) \sin \alpha \quad (\text{Fig. LA.1-1})$$

$$\dot{x}_{\delta_T}^2 = \frac{\partial T}{\partial \delta_T} = 26.7154$$

$$\dot{M}_{\delta_T}^2 = \frac{\partial T}{\partial \delta_T} (e_T + k) = 26.7154 (-0.115)$$

4. Stability and Control Derivatives - Body Axes
(C.G. on the mean aerodynamic chord)

$$\dot{x}_u^- = \dot{x}_{Au}^2 + \dot{x}_{Tu}^2$$

$$\dot{x}_w^- = \dot{x}_{Aw}^2 + \dot{x}_{Tw}^2$$

$$\dot{x}_q^- = \dot{x}_{Aq}^2$$

$$\dot{x}_{\dot{w}}^- = \dot{x}_{A\dot{w}}^2$$

$$\dot{z}_u^- = \dot{z}_{Au}^2$$

$$\dot{z}_w^- = \dot{z}_{Aw}^2$$

$$\dot{z}_q^- = \dot{z}_{Aq}^2$$

$$\dot{z}_{\dot{w}}^- = \dot{z}_{A\dot{w}}^2$$

$$\dot{M}_u^- = \dot{M}_{Au}^2 + \dot{M}_{Tu}^2$$

$$\dot{M}_w^- = \dot{M}_{Aw}^2 + \dot{M}_{Tw}^2$$

$$\dot{M}_q^- = \dot{M}_{Aq}^2$$

$$\dot{M}_{\dot{w}}^- = \dot{M}_{A\dot{w}}^2$$

$$\dot{\chi}'_{\eta} = \dot{\chi}'_{A\eta}{}^2$$

$$\dot{z}'_{\eta} = \dot{z}'_{A\eta}{}^2$$

$$\dot{M}'_{\eta} = \dot{M}'_{A\eta}{}^2$$

$$\dot{\chi}'_{\delta_T} = \dot{\chi}'_{\delta_T}{}^2$$

$$\dot{z}'_{\delta_T} = 0$$

$$\dot{M}'_{\delta_T} = \dot{M}'_{\delta_T}{}^2$$

5. Stability and Control Derivatives - Body Axes (Item 67004)
(C.G. displaced laterally by $k = 0.045$ m)

$$\dot{\chi}'_u = \dot{\chi}'_u$$

$$\dot{\chi}'_w = \dot{\chi}'_w$$

$$\dot{\chi}'_q = \dot{\chi}'_q - k\dot{\chi}'_u$$

$$\dot{\chi}'_{\dot{w}} = \dot{\chi}'_{\dot{w}}$$

$$\dot{z}'_u = \dot{z}'_u$$

$$\dot{z}'_w = \dot{z}'_w$$

$$\dot{z}'_q = \dot{z}'_q - k\dot{z}'_u$$

$$\dot{z}'_{\dot{w}} = \dot{z}'_{\dot{w}}$$

$$\dot{M}'_u = \dot{M}'_u - k\dot{\chi}'_u$$

$$\dot{M}'_w = \dot{M}'_w - k\dot{\chi}'_w$$

$$\dot{M}'_q = \dot{M}'_q - k(\dot{\chi}'_q + \dot{M}'_u) + k^2\dot{\chi}'_u$$

$$\dot{M}'_{\dot{w}} = \dot{M}'_{\dot{w}} - k\dot{\chi}'_{\dot{w}}$$

$$\dot{\chi}'_{\eta} = \dot{\chi}'_{\eta}$$

$$\dot{z}'_{\eta} = \dot{z}'_{\eta}$$

$$\dot{M}'_{\eta} = \dot{M}'_{\eta} - k\dot{\chi}'_{\eta}$$

$$\dot{\chi}'_{\delta_T} = \dot{\chi}'_{\delta_T}$$

$$\dot{M}'_{\delta_T} = \dot{M}'_{\delta_T} - k\dot{\chi}'_{\delta_T}$$

6. Normalised Longitudinal Derivatives at 30 m/sec - Body Axes

$$\begin{aligned} X_u &= \dot{X}_u/m = -0.097 \\ X_w &= \dot{X}_w/m = 0.037 \\ X_q &= \dot{X}_q/m = -0.019 \\ X_{\dot{w}} &= \dot{X}_{\dot{w}}/m = -0.00044 \\ Z_u &= \dot{Z}_u/m = -0.789 \\ Z_w &= \dot{Z}_w/m = -5.496 \\ Z_q &= \dot{Z}_q/m = -0.902 \\ Z_{\dot{w}} &= \dot{Z}_{\dot{w}}/m = -0.018 \\ M_u &= \dot{M}_u/I_y = 0.029 \\ M_w &= \dot{M}_w/I_y = -3.865 \\ M_q &= \dot{M}_q/I_y = -12.381 \\ M_{\dot{w}} &= \dot{M}_{\dot{w}}/I_y = -0.201 \\ X_\eta &= \dot{X}_\eta/m = -0.397 \\ Z_\eta &= \dot{Z}_\eta/m = -16.172 \\ M_\eta &= \dot{M}_\eta/I_y = -179.079 \\ X_{\delta_T} &= \dot{X}_{\delta_T}/m = 1.719 \\ M_{\delta_T} &= \dot{M}_{\delta_T}/I_y = -2.595 \end{aligned}$$

All values are outputs from programme RPVDER.FOR

APPENDIX LA.2

STABILITY and CONTROL DERIVATIVES at 30 m/sec
Lateral Model

Appendix LA.2

STABILITY and CONTROL DERIVATIVES at 30 m/sec

Lateral Model

1. Introduction

The aerodynamic stability and control derivatives of the lateral model of X-RAE1 at 30 m/sec are given in this appendix. They are first estimated in stability axes (Apcs A.2 to A.5) and transformed afterwards in body axes.

2. Stability and Control Derivatives - Stability Axes

$$\left. \begin{aligned} \dot{Y}_v &= \frac{1}{2} \rho V_T S Y_v \\ \dot{L}_v &= \frac{1}{2} \rho V_T S b L_v \\ \dot{N}_v &= \frac{1}{2} \rho V_T S b N_v \end{aligned} \right| \text{Apx A.2}$$

$$\left. \begin{aligned} \dot{Y}_p &= \frac{1}{2} \rho V_T S b Y_p \\ \dot{L}_p &= \frac{1}{2} \rho V_T S b^2 L_p \\ \dot{N}_p &= \frac{1}{2} \rho V_T S b^2 N_p \end{aligned} \right| \text{Apx A.3}$$

$$\left. \begin{aligned} \dot{Y}_r &= \frac{1}{2} \rho V_T S b Y_r \\ \dot{L}_r &= \frac{1}{2} \rho V_T S b^2 L_r \\ \dot{N}_r &= \frac{1}{2} \rho V_T S b^2 N_r \end{aligned} \right| \text{Apx A.4}$$

$$\left. \begin{aligned} \dot{L}_\xi &= \frac{1}{2} \rho V_T^2 S b L_\xi \\ \dot{N}_\xi &= \frac{1}{2} \rho V_T^2 S b N_\xi \end{aligned} \right| \text{Apx A.5}$$

3. Stability and Control Derivatives - Body Axes (Item 67004)

$$\dot{Y}_v = \dot{Y}_v'$$

$$\dot{Y}_p = \dot{Y}_p' \cos \alpha - \dot{Y}_r' \sin \alpha$$

$$\dot{Y}_r = \dot{Y}_r' \cos \alpha + \dot{Y}_p' \sin \alpha$$

$$\dot{L}_v = \dot{L}_v' \cos \alpha - \dot{N}_v' \sin \alpha$$

$$\dot{L}_p = \dot{L}_p' \cos^2 \alpha + \dot{N}_r' \sin^2 \alpha - (\dot{L}_r' + \dot{N}_p') \sin \alpha \cos \alpha$$

$$\dot{L}_r = \dot{L}_r' \cos^2 \alpha - \dot{N}_p' \sin^2 \alpha + (\dot{L}_p' + \dot{N}_r') \sin \alpha \cos \alpha$$

$$\dot{N}_v = \dot{N}_v' \cos \alpha + \dot{L}_v' \sin \alpha$$

$$\dot{N}_p = \dot{N}_p' \cos^2 \alpha - \dot{L}_r' \sin^2 \alpha + (\dot{L}_p' - \dot{N}_r') \sin \alpha \cos \alpha$$

$$\dot{N}_r = \dot{N}_r' \cos^2 \alpha + \dot{L}_p' \sin^2 \alpha + (\dot{L}_r' + \dot{N}_p') \sin \alpha \cos \alpha$$

$$\dot{L}_\xi = \dot{L}_\xi' \cos \alpha - \dot{N}_\xi' \sin \alpha$$

$$\dot{N}_\xi = \dot{N}_\xi' \cos \alpha + \dot{L}_\xi' \sin \alpha$$

$$\dot{Y}_\zeta = \frac{1}{2} \rho V_T^2 S Y_\zeta$$

$$\dot{L}_\zeta = \frac{1}{2} \rho V_T^2 S b L_\zeta$$

$$\dot{N}_\zeta = \frac{1}{2} \rho V_T^2 S b N_\zeta$$

Apx A.6

4. Normalised Lateral Derivatives at 30 m/sec

$$Y_v = \dot{Y}_v / m = -0.336$$

$$Y_p = \dot{Y}_p / m = 0.175$$

$$Y_r = \dot{Y}_r / m = 0.224$$

$$L_v = \dot{L}_v / I_x = -0.414$$

$$L_p = \dot{L}_p / I_x = -13.360$$

$$L_r = \dot{L}_r / I_x = 2.412$$

$$N_v = \dot{N}_v / I_z = 0.558$$

$$N_p = \dot{N}_p / I_z = -0.622$$

$$N_r = \dot{N}_r / I_z = -1.426$$

$$L_\xi = \dot{L}_\xi / I_x = -142.902$$

$$N_\xi = \dot{N}_\xi / I_z = 4.182$$

$$Y_\zeta = \dot{Y}_\zeta / m = 3.909$$

$$L_\zeta = \dot{L}_\zeta / I_x = 2.485$$

$$N_\zeta = \dot{N}_\zeta / I_z = -18.015$$

All values are outputs from the programme RPVDER.FOR

APPENDIX DE

DISCRETISATION OF A
CONTINUOUS TIME SYSTEM

Appendix DE

DISCRETISATION OF A CONTINUOUS TIME SYSTEM

The discrete equivalent of a continuous time system is presented in this appendix. If the continuous time system is expressed in the state space form, ie:

$$\begin{aligned}\dot{\underline{x}}(t) &= A\underline{x}(t) + B\underline{u}(t) \\ \underline{y}(t) &= C\underline{x}(t) + D\underline{u}(t)\end{aligned}$$

and samples are taken every T secs, the equivalent discrete system is:

$$\begin{aligned}\underline{x}(n+1) &= A_d\underline{x}(n) + B_d\underline{u}(n) \\ \underline{y}(n) &= C_d\underline{x}(n) + D_d\underline{u}(n)\end{aligned}$$

where: $\underline{x}(n) = \underline{x}(nT)$, $\underline{u}(n) = \underline{u}(nT)$, $\underline{y}(n) = \underline{y}(nT)$ and

$$A_d = \exp(AT) \approx I + AT \quad (\text{if } T \text{ reasonably small})$$

$$B_d = \left[\int_0^T \exp(A\tau) d\tau \right] B \approx BT \quad (\text{if } T \text{ reasonably small})$$

$$C_d = C$$

$$D_d = D$$

APPENDIX PI.1

PARAMETER IDENTIFICATION
Longitudinal Model

Appendix PI.1

PARAMETER IDENTIFICATION

Longitudinal Model

1. Introduction

The matrices F , H and Q of the EKF algorithm for the identification of the longitudinal model of X-RAE1 are given in this appendix. The system to be identified is of the form (Ch. 4 page 58):

$$\begin{aligned} \underline{x}^*(n+1) &= \underline{f}(\underline{x}^*(n), \eta(n)) + \Gamma(\underline{x}^*(n))\underline{w}(n) \\ \underline{y}(n) &= \underline{h}(\underline{x}^*(n), \eta(n)) + \underline{v}(n) \end{aligned}$$

The EKF algorithm that is used is the one presented in Ch. 4. The only difference is the way in which the error covariance matrix is updated. The expression for P_n is:

$$P_n = [I - J_n H_n] P_{n/n-1} [I - J_n H_n]^T + J_n R J_n^T \quad (1)$$

This formula is equivalent to that appearing in Eqns 4.5 but it is preferable for the following two reasons (Ref. 1):

1. The right hand-side of Eqn 1. is the sum of two positive definite matrices. As a consequence, is better conditioned for numerical computation and will tend to retain more faithfully the positive definiteness and symmetry of P_n .
2. To first order, is insensitive to errors in the filter gain and is to be preferred in numerical computations.

2. The F and H Matrices

The F matrix is computed by the form:

$$F = \frac{\partial \underline{f}}{\partial \underline{x}^*}$$

Then, according to the \underline{f} expression of the longitudinal model (Ch. 4 page 59), the matrix F becomes:

$$\begin{aligned}
 F_{1,1} &= 1 + T_s x_5 & F_{3,1} &= T_s x_{10} \\
 F_{1,2} &= T_s x_6 & F_{3,2} &= T_s x_{11} \\
 F_{1,3} &= 0.704 T_s & F_{3,3} &= 1 + T_s x_{12} \\
 F_{1,4} &= -9.804 T_s & F_{3,4} &= -0.047 T_s \\
 F_{1,5} &= T_s x_1 & F_{3,10} &= T_s x_1 \\
 F_{1,6} &= T_s x_2 & F_{3,11} &= T_s x_2 \\
 & & F_{3,12} &= T_s x_3 \\
 & & F_{3,13} &= T_s \eta \\
 F_{2,1} &= T_s x_7 & & \\
 F_{2,2} &= 1 + T_s x_8 & & \\
 F_{2,3} &= 28.575 T_s & F_{4,3} &= T_s \\
 F_{2,4} &= 0.236 T_s & F_{4,4} &= 1 \\
 F_{2,7} &= T_s x_1 & & \\
 F_{2,8} &= T_s x_2 & & \\
 F_{2,9} &= T_s \eta & &
 \end{aligned}$$

All the other elements of matrix F are zero.

The matrix H is given by the form:

$$H = \frac{\partial h}{\partial x^*}$$

Therefore, $H = \begin{bmatrix} 0 & 0 & 1 & 0 & 0 & \dots & 0 \end{bmatrix}$ (Ch. 4 page)

3. The Covariance Matrix Q

An estimate of the covariance matrix Q of the variation of the aerodynamic derivatives is given in this section. The Q matrix is used only when the system is free of measurement noise to move the estimates to their correct values.

The following procedure is applied for the estimation of the diagonal elements of the Q matrix:

$$u_{\min} = 20 \text{ m/sec}$$

$$u_{\max} = 35 \text{ m/sec}$$

$$\alpha_{\max} = 10^{\circ} = 0.175 \text{ rad}$$

$$w_{\max} = u_{\max} \tan \alpha_{\max} = 6.188 \text{ m/sec}$$

$$\eta_{\max} = 30^{\circ} = 0.524 \text{ rad}$$

$$\dot{w}_{\max} = 3g$$

$$q_{\max} = \dot{w}_{\max} / u_{\min} = 1.471 \text{ rad/sec}$$

Then, using the nominal values of the derivatives (Table 4.1), we have:

X-equation of motion

$$(u\text{-force})_{\max} = X_u u_{\max} = 3.395$$

$$(w\text{-force})_{\max} = X_w w_{\max} = 0.241$$

Z-equation of motion

$$(u\text{-force})_{\max} = Z_u u_{\max} = 27.125$$

$$(w\text{-force})_{\max} = Z_w w_{\max} = 33.409$$

$$(\eta\text{-force})_{\max} = Z_{\eta} \eta_{\max} = 8.325$$

M-equation of motion

$$(u\text{-moment})_{\max} = M_u u_{\max} = 6.475$$

$$(w\text{-moment})_{\max} = M_w w_{\max} = 17.215$$

$$(q\text{-moment})_{\max} = M_q q_{\max} = 26.650$$

$$(\eta\text{-moment})_{\max} = M_{\eta} \eta_{\max} = 92.166$$

Each diagonal element q_k of the covariance matrix is then given by the form:

$$q_k = E [w_k^2]$$

where:

w_k is the kth output of the filter shown in Fig. PI.1-1 and w_{c_k} is noise with covariance

$$E^{\frac{1}{2}}[w_{c_k}^2] = 10\% \text{ of the corresponding force or moment, ie:}$$

$$E^{\frac{1}{2}}[w_{c_1}^2] = 10\% X_u u_{\max} = 0.340$$

$$E^{\frac{1}{2}}[w_{c_2}^2] = 10\% X_w w_{\max} = 0.024$$

$$E^{\frac{1}{2}}[w_{c_3}^2] = 10\% Z_u u_{\max} = 2.713$$

$$E^{\frac{1}{2}}[w_{c_4}^2] = 10\% Z_w w_{\max} = 3.341$$

$$E^{\frac{1}{2}}[w_{c_5}^2] = 10\% Z_{\eta} \eta_{\max} = 0.833$$

$$E^{\frac{1}{2}}[w_{c_6}^2] = 10\% M_u u_{\max} = 0.648$$

$$E^{\frac{1}{2}}[w_{c_7}^2] = 10\% M_w w_{\max} = 1.722$$

$$E^{\frac{1}{2}}[w_{c_8}^2] = 10\% M_q q_{\max} = 2.665$$

$$E^{\frac{1}{2}}[w_{c_9}^2] = 10\% M_{\eta} \eta_{\max} = 9.217$$

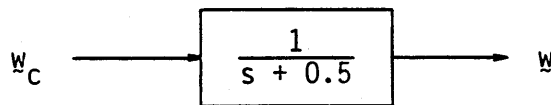


Fig. PI.1-1 Arrangement for the estimation of the diagonal elements of Q

Then, (Ref. 2):

- $q_1 = 0.5$
- $q_2 = 0.002$
- $q_3 = 30.0$
- $q_4 = 45.0$
- $q_5 = 3.0$
- $q_6 = 2.0$
- $q_7 = 12.0$
- $q_8 = 29.0$
- $q_9 = 340.0$

All the other elements of the covariance matrix Q are zero.

4. Derivative Estimates

The estimates of the longitudinal derivatives are given in this section.

Figs PI.1-2 to PI.1-9 are the estimates for a square wave as elevator input (period 0.1 sec and amplitude 0.005rad).

Figs PI.1-10 to PI.1-17 are the estimates for a multistep as elevator input (period 0.35 sec and amplitude 0.005 rad).

REFERENCES

1. Jazwinski A. H. "Stochastic Processes and Filtering Theory" Academic Press, 1970.
2. Papoulis A. "Probability, Random Variables and Stochastic Processes" McGraw-Hill Kogakusha, Ltd., 1965.

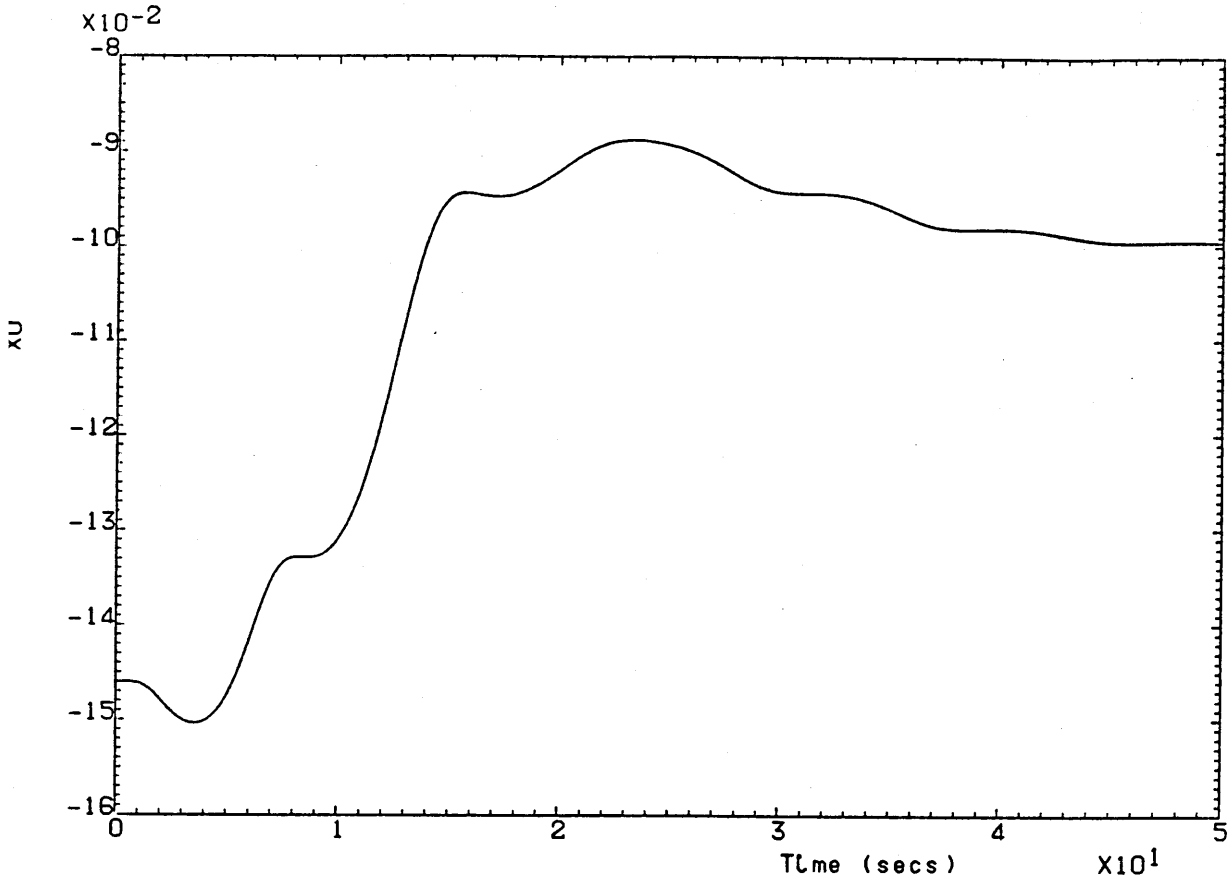


Fig. PI.1-2 x_u estimate (square wave input)

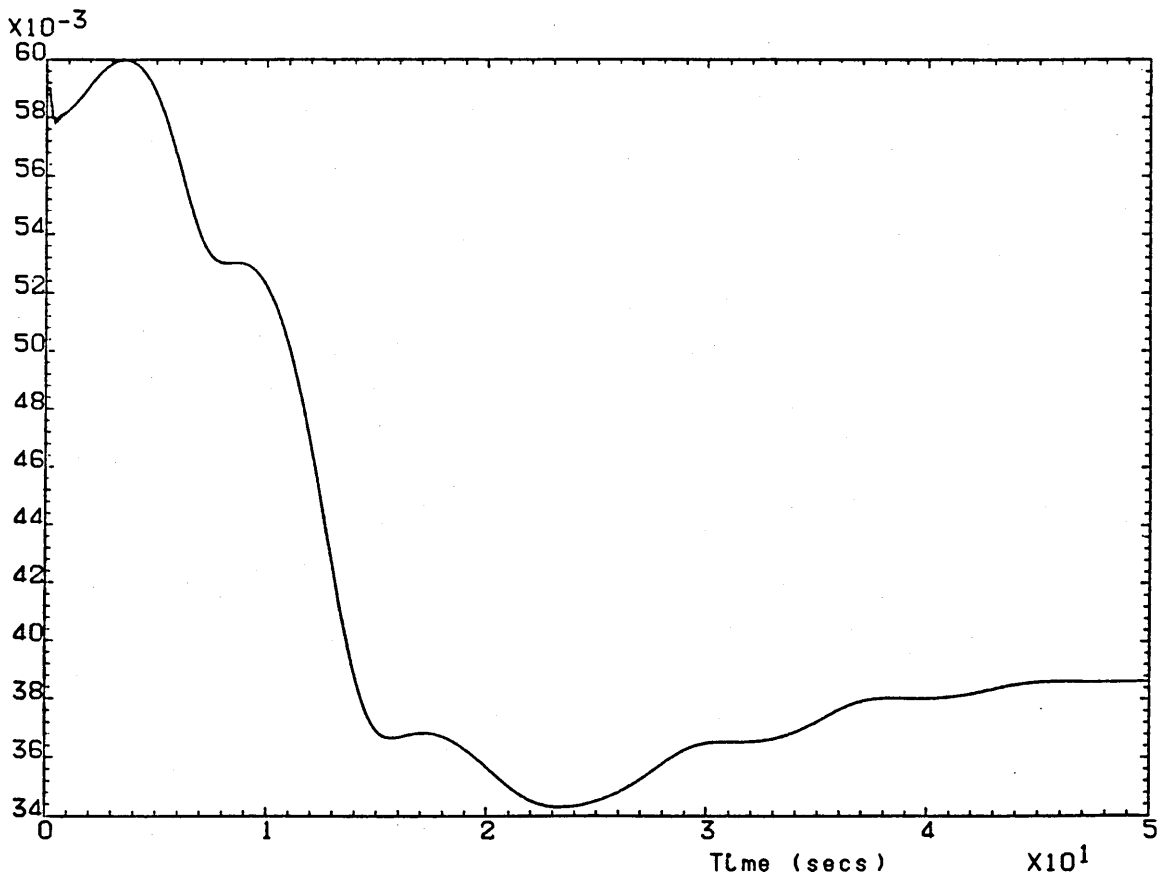


Fig. PI.1-3 x_w estimate (square wave input)

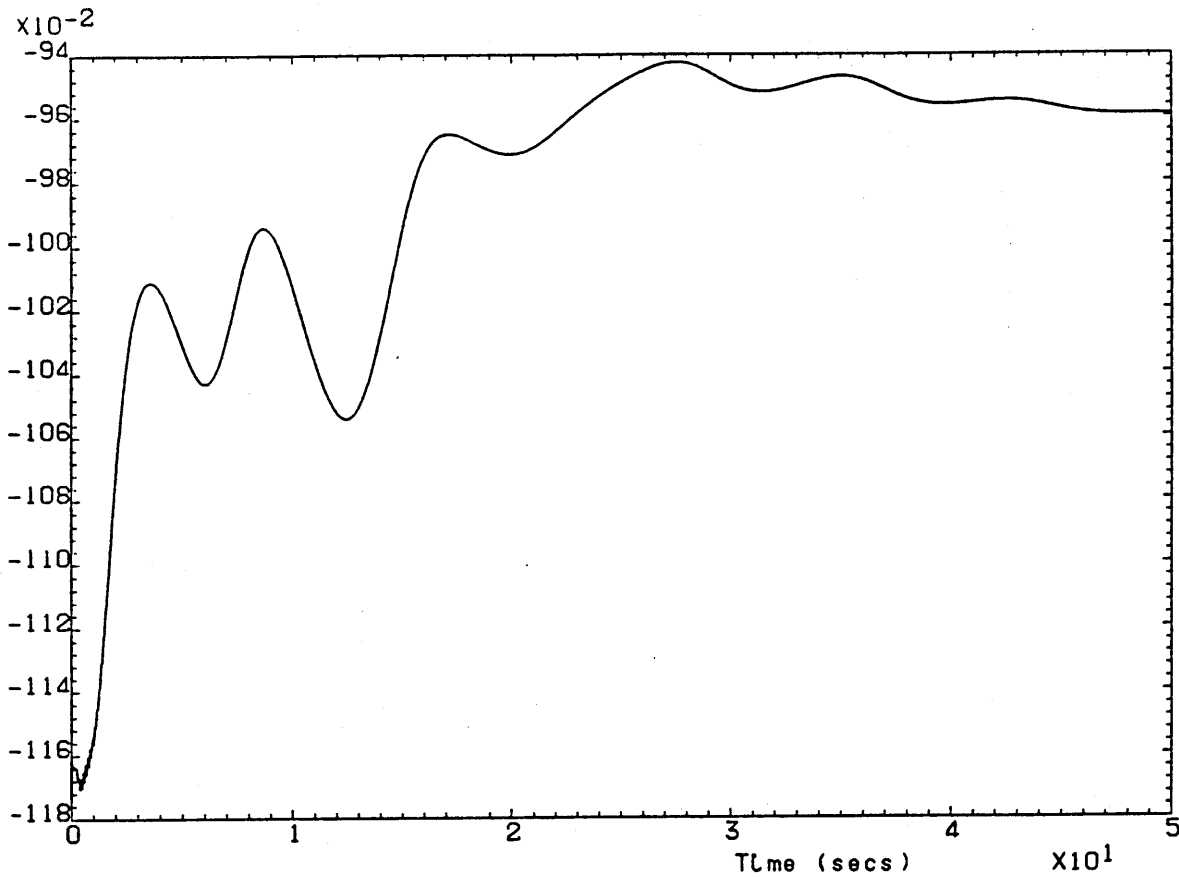


Fig. PI.1-4 z_u estimate (square wave input)

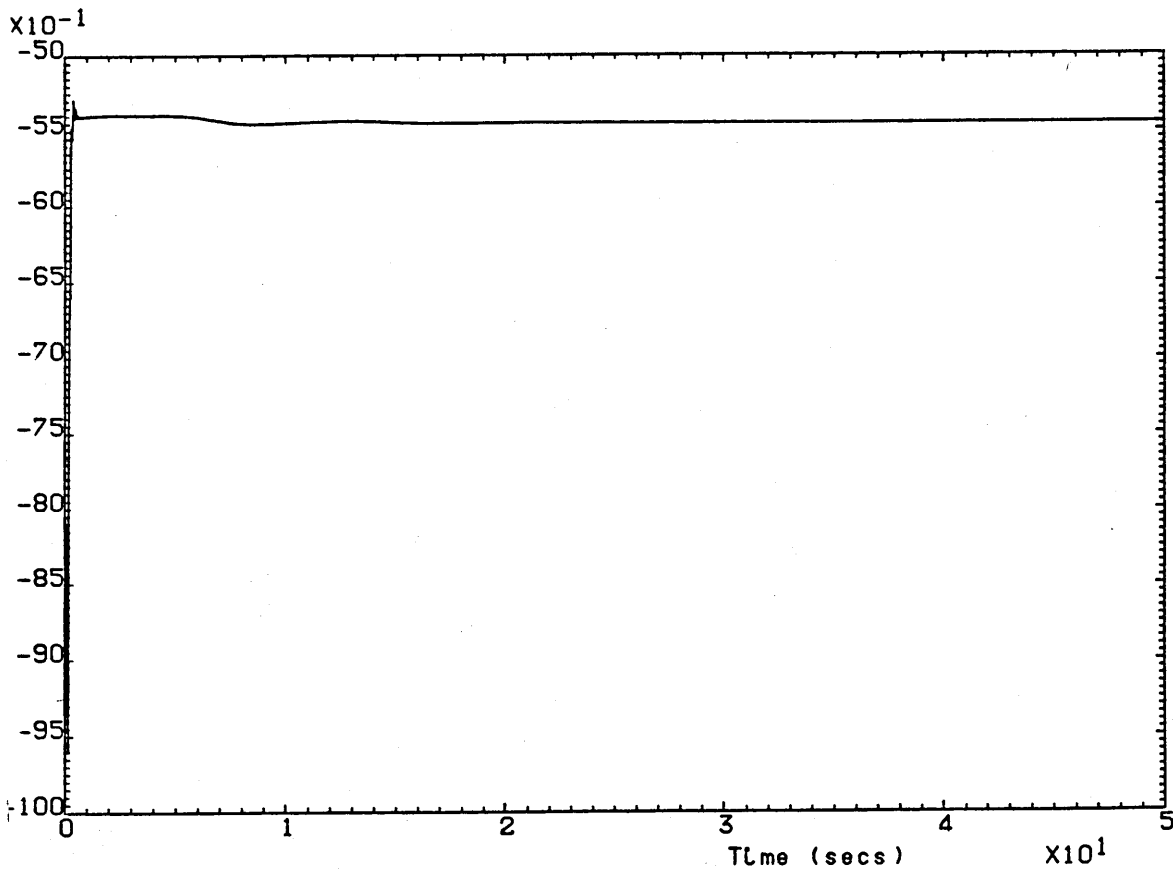


Fig. PI.1-5 z_w estimate (square wave input)

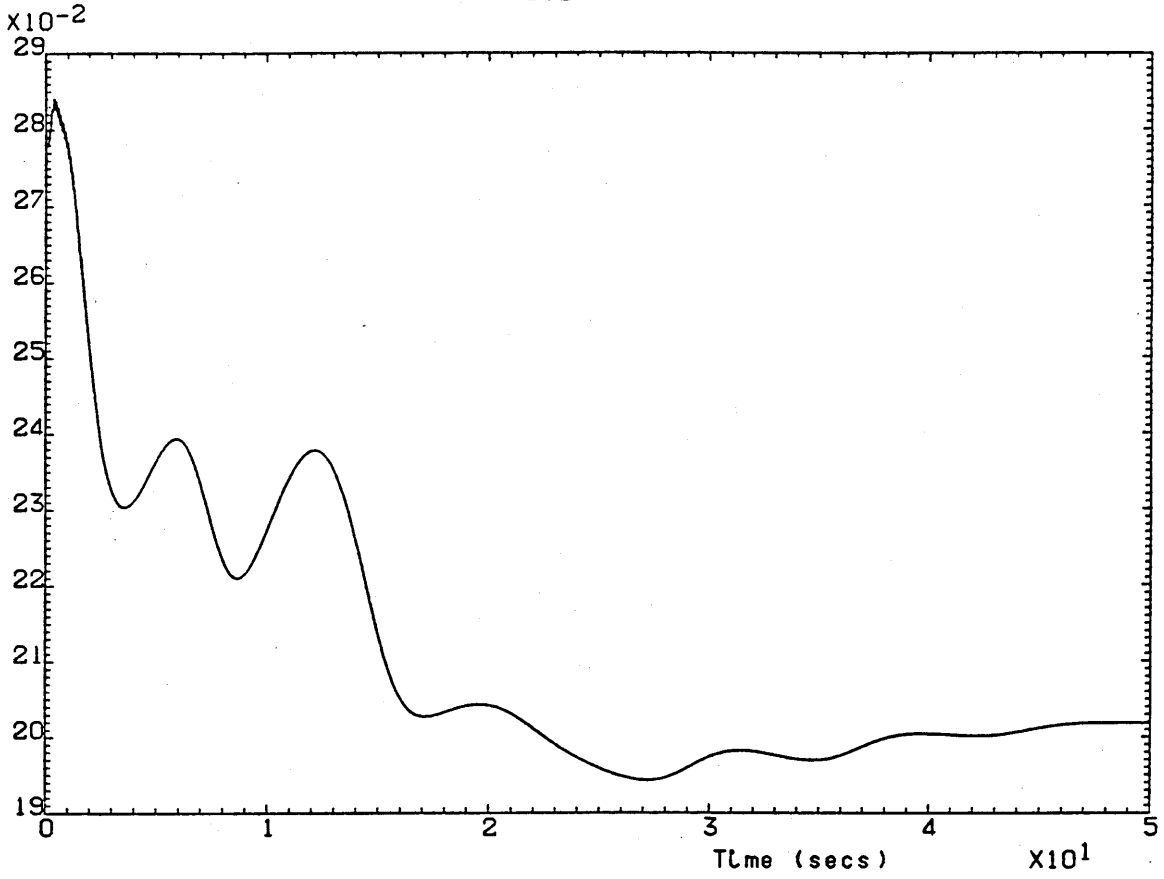


Fig PI.1-6 m_u estimate (square wave input)

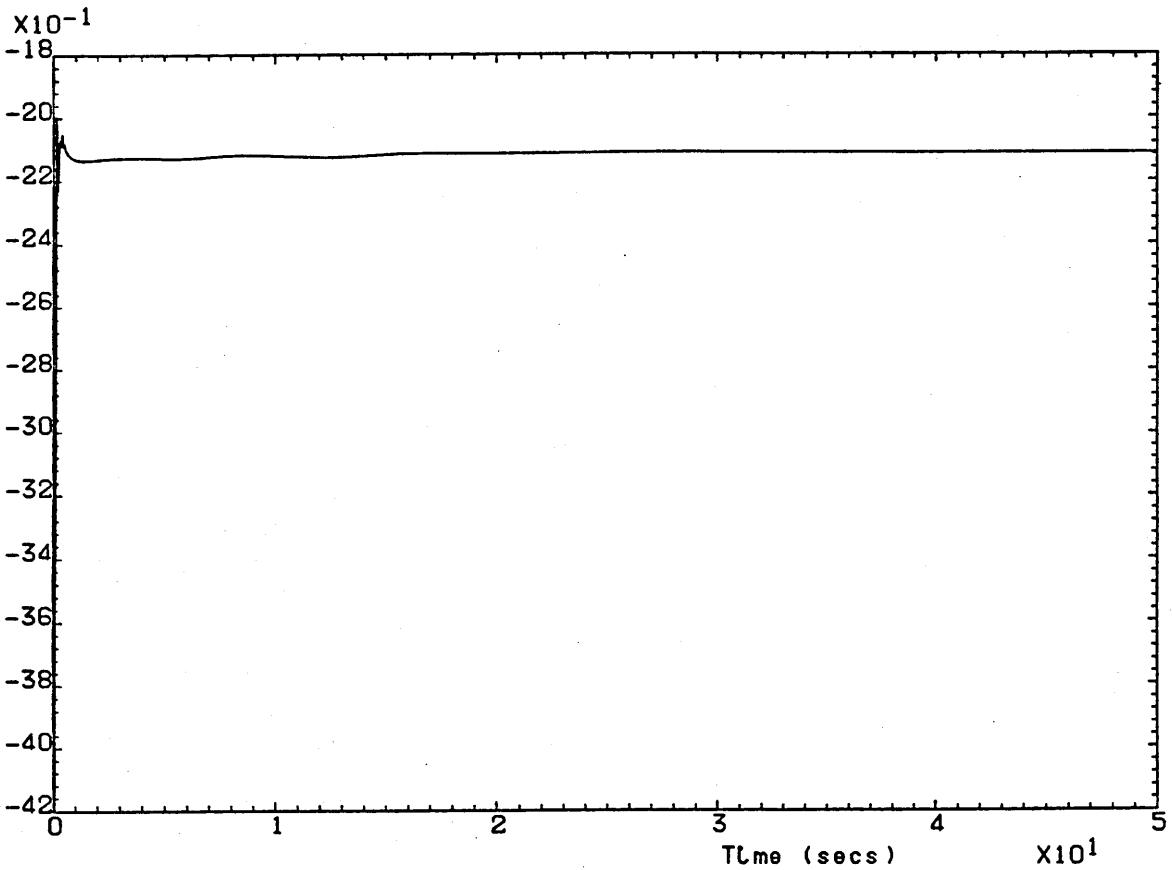


Fig. PI.1-7 m_w estimate (square wave input)

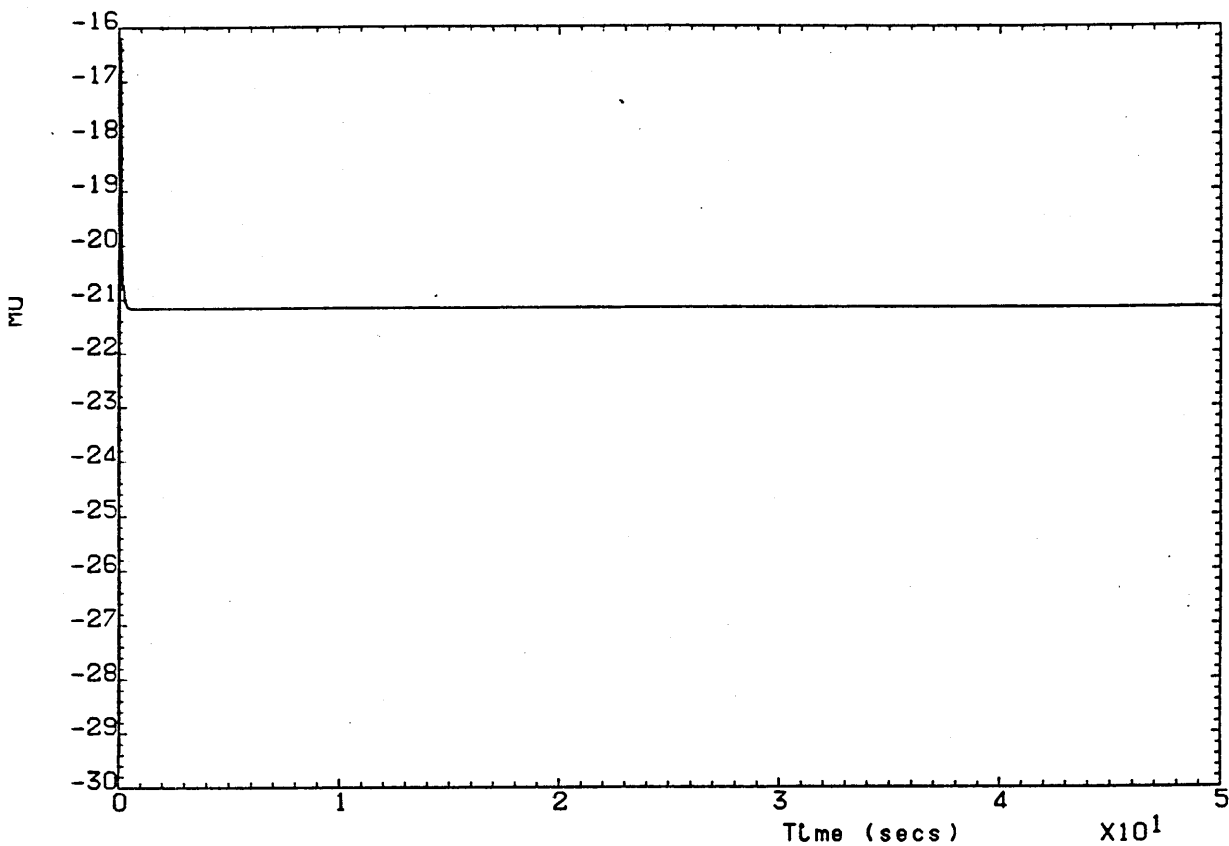


Fig. PI.1-8 m_q estimate (square wave input)

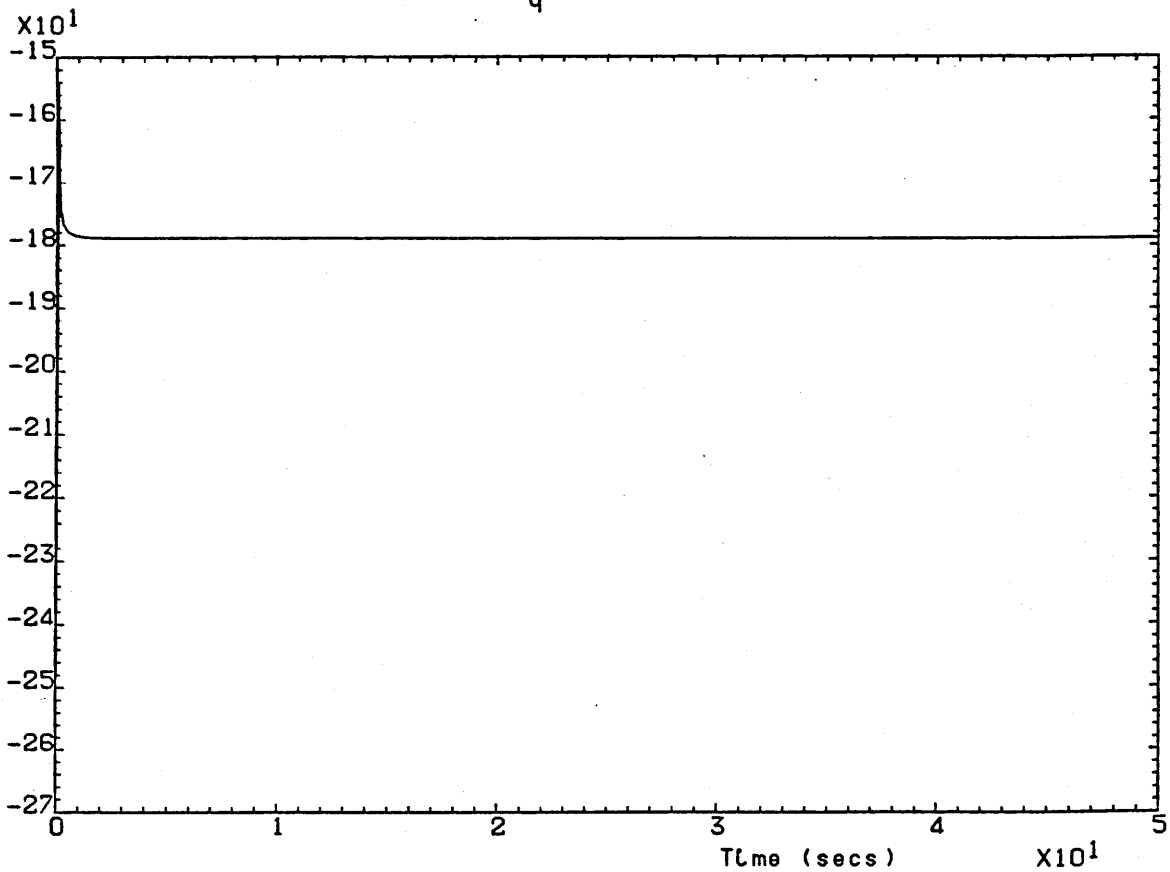


Fig. PI.1-9 m_η estimate (square wave input)

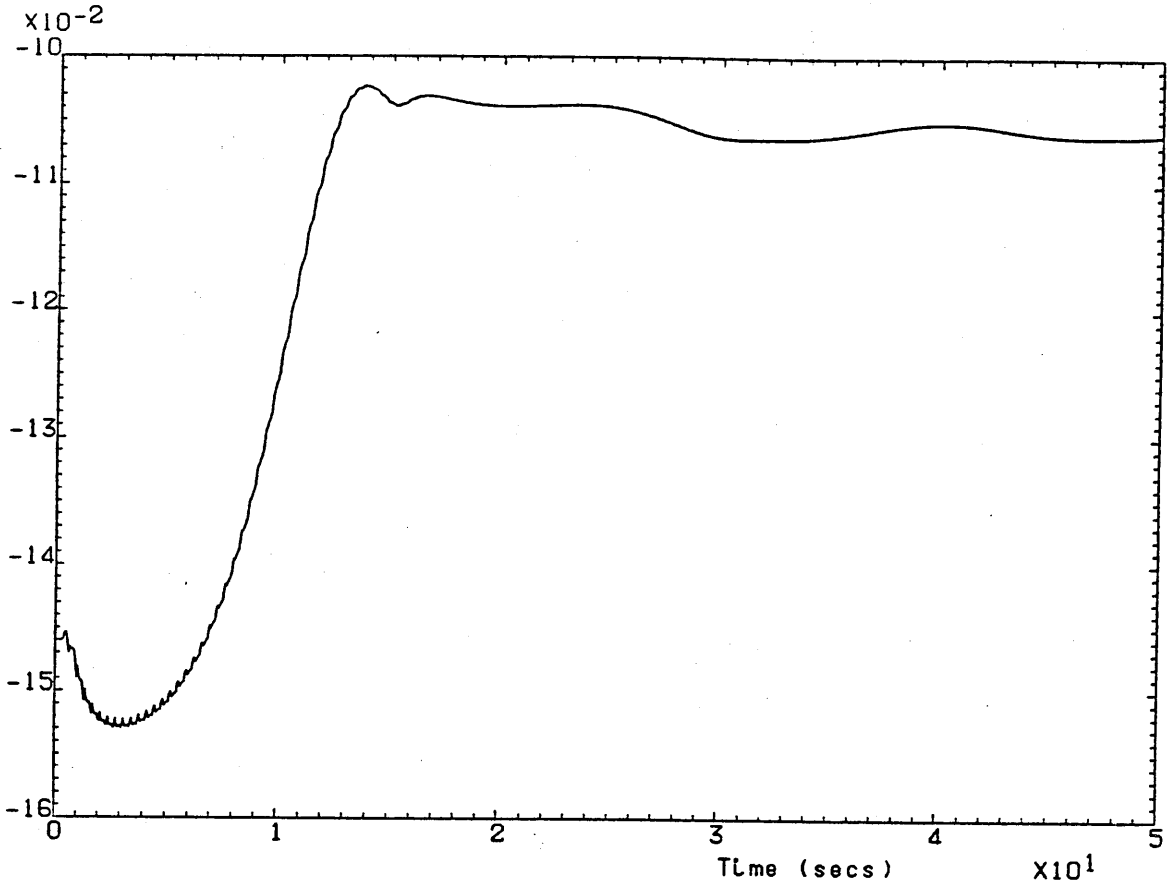


Fig. PI.1-10 x_u estimate (multistep input)

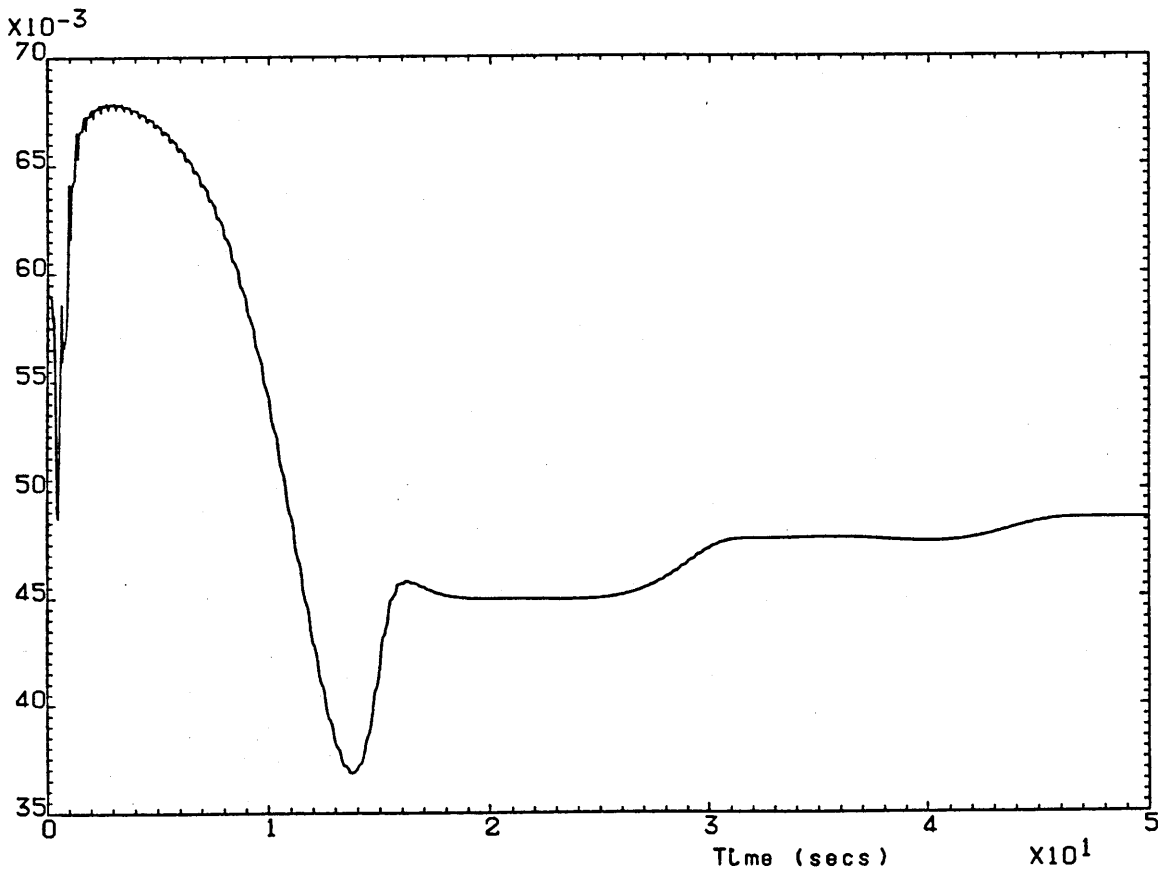


Fig. PI.1-11 x_w estimate (multistep input)

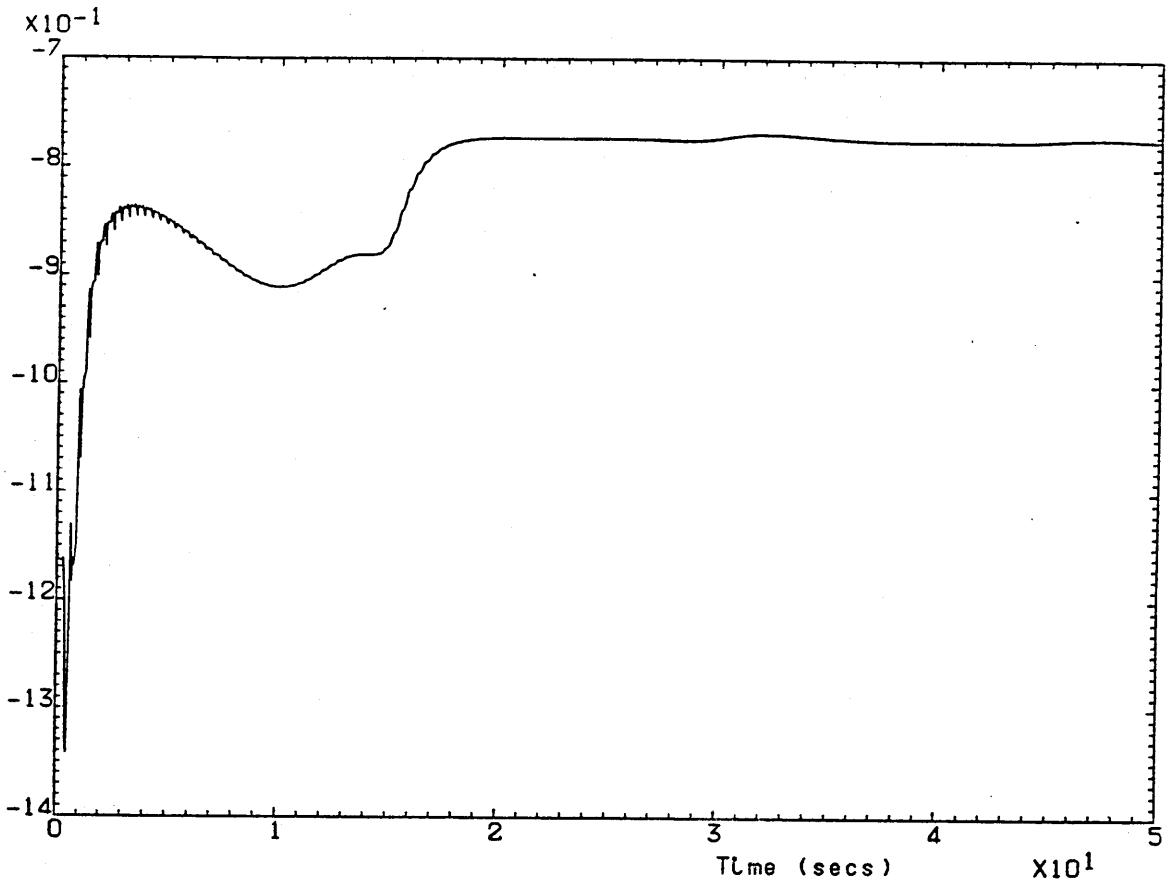


Fig. PI.1-12 z_u estimate (multistep input)

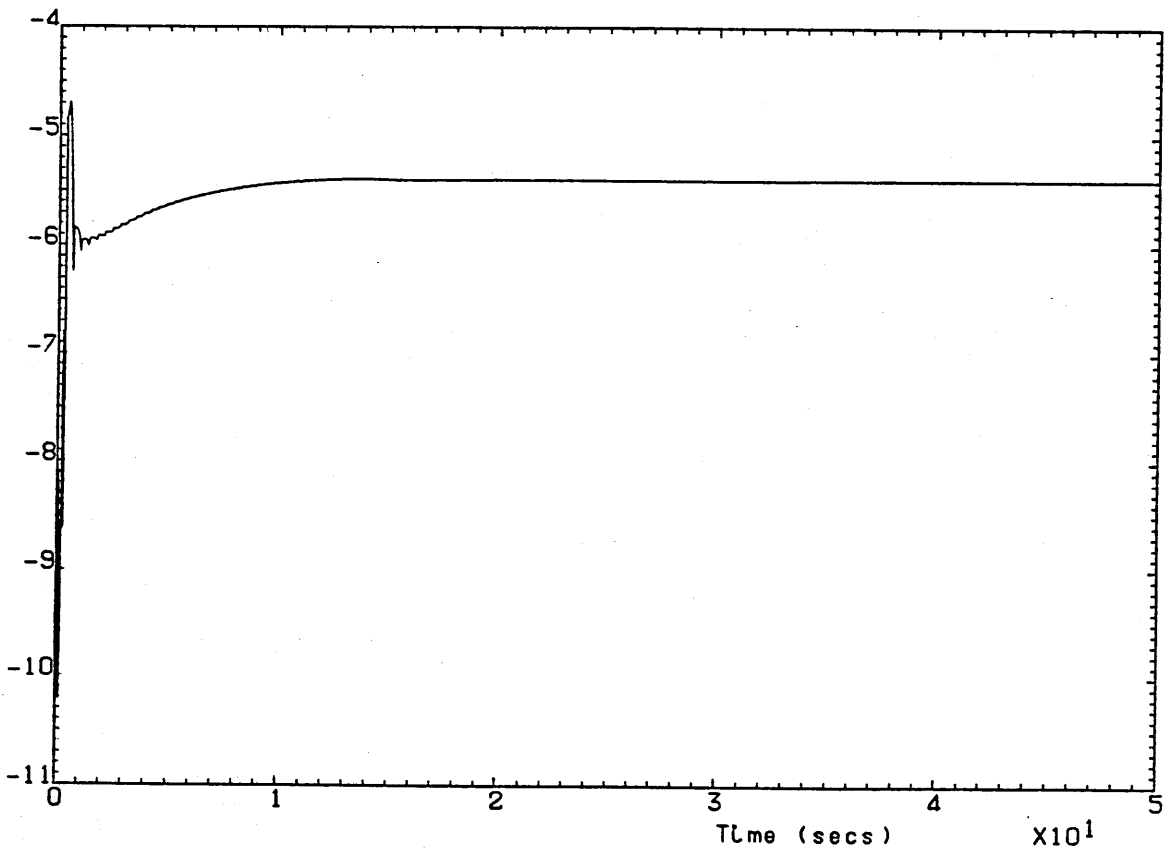


Fig. PI.1-13 z_w estimate (multistep input)

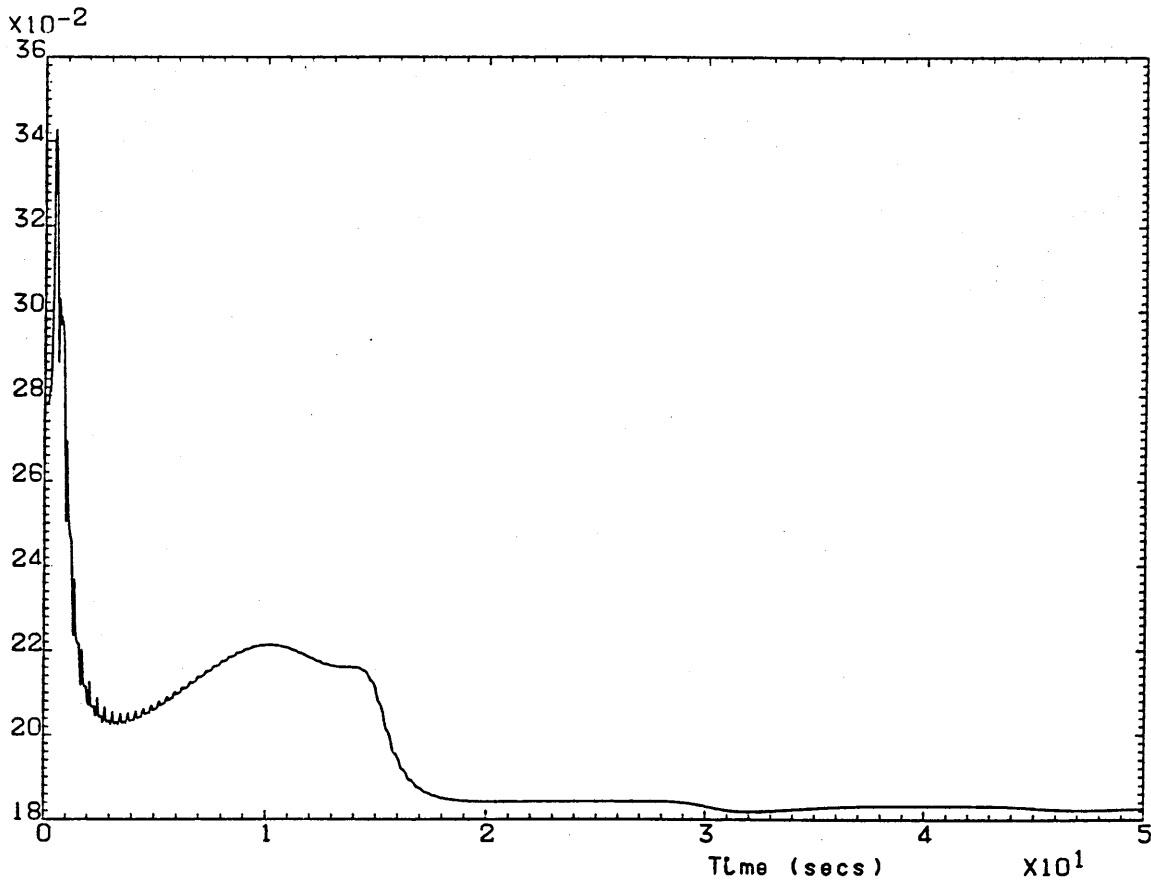


Fig. PI.1-14 m_u estimate (multistep input)

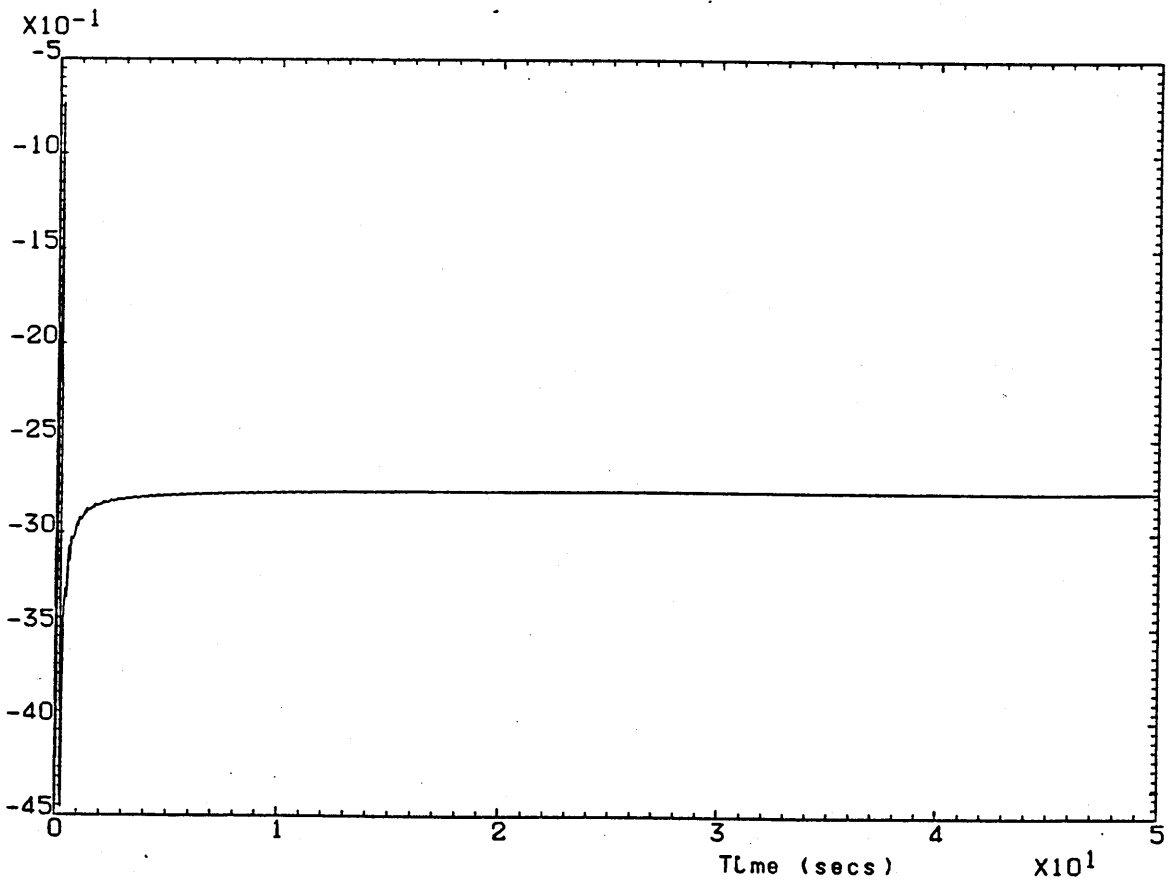


Fig. PI.1-15 m_w estimate (multistep input)

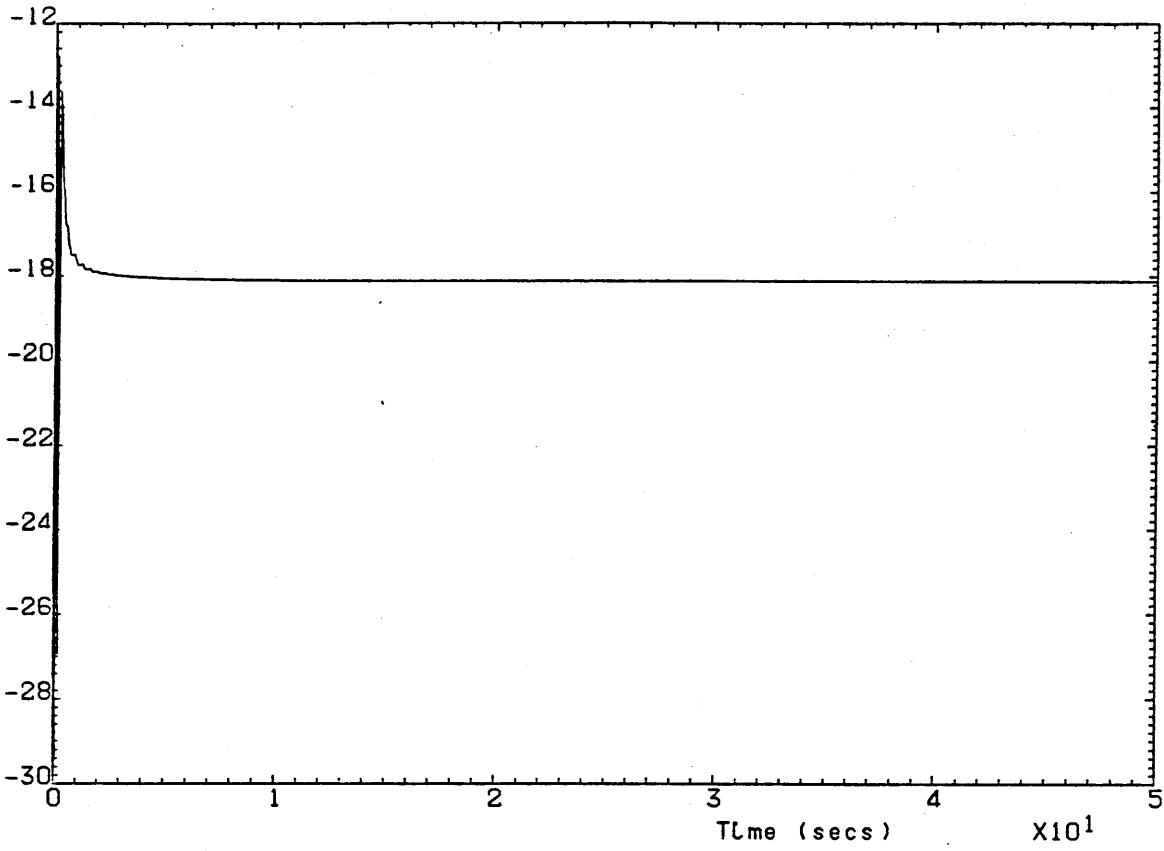


Fig. PI.1-16 m_q estimate (multistep input)

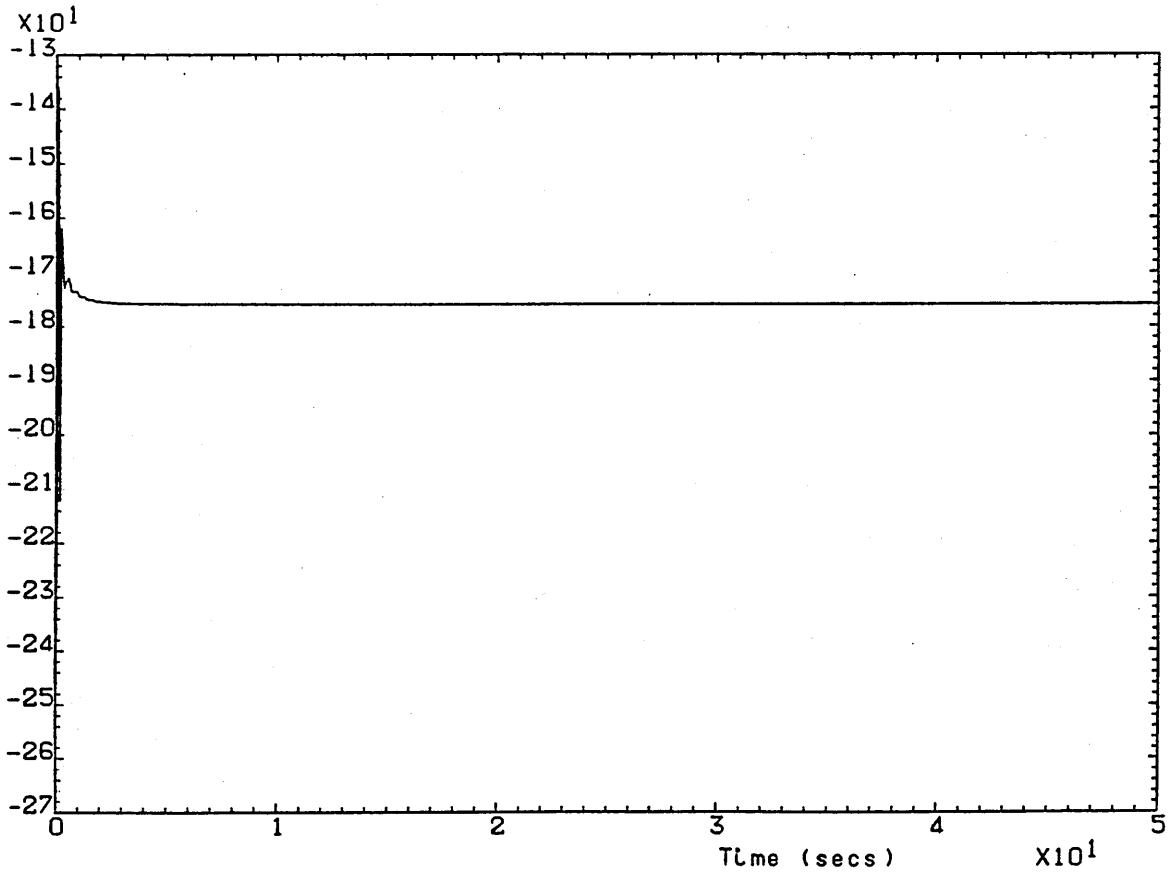


Fig.PI.1-17 m_η estimate (multistep input)

APPENDIX PI.2

PARAMETER IDENTIFICATION

Lateral Model

Appendix PI.2

PARAMETER IDENTIFICATION

Lateral Model

1. F and H Matrices of the Lateral Model

The F and H matrices of the lateral model of X-RAE1 (Ch.4 page 63) are presented in this appendix. They are derived in a similar way to the F and H matrices of the longitudinal model.

The non-zero elements of the F matrix are:

$$\begin{aligned} F_{1,1} &= 1 + T_s x_5 & F_{3,1} &= T_s x_{11} \\ F_{1,2} &= -0.561 T_s & F_{3,2} &= T_s x_{12} \\ F_{1,3} &= -29.767 T_s & F_{3,3} &= 1 + T_s x_{13} \\ F_{1,4} &= 9.804 T_s & F_{3,11} &= T_s x_1 \\ F_{1,5} &= T_s x_1 & F_{3,12} &= T_s x_2 \\ F_{1,6} &= T_s u_2 & F_{3,13} &= T_s x_3 \\ & & F_{3,14} &= T_s u_2 \\ \\ F_{2,1} &= T_s x_7 & & \\ F_{2,2} &= 1 + T_s x_8 & F_{4,2} &= T_s \\ F_{2,3} &= T_s x_9 & F_{4,3} &= -0.025 T_s \\ F_{2,7} &= T_s x_1 & & \\ F_{2,8} &= T_s x_2 & & \\ F_{2,9} &= T_s x_3 & & \\ F_{2,10} &= T_s u_1 & & \end{aligned}$$

The H matrix is:

$$H = \begin{bmatrix} 0 & 1 & 0 & 0 & 0 & \dots & 0 \\ 0 & 0 & 1 & 0 & 0 & \dots & 0 \end{bmatrix}$$

APPENDIX S

SOFTWARE

Programme listings

PROGRAM RPYDER

DIMENSION X(11),Y(11),AS(4,4),BS(4,2)

REAL LF1,LF2,MASS,IX,IY,IZ,K
REAL MUS,MWS,MQS,MWDS,MNS,MUB,MWB,MQB,MWDB,MNB,MTHB
REAL MU,MW,MQ,MWD,MN,MTH
REAL LVS,NVS,LPS,NPS,LRS,NRS,LXS,NXS
REAL LV,NV,LP,NP,LR,NR,LX,NX,LZ,NZ

DATA (X(I),I=1,11)/0.,0.025,0.05,0.075,0.1,0.125,0.15,
* 0.175,0.2,0.225,0.25/
DATA (Y(I),I=1,11)/0.,0.036,0.075,0.114,0.156,0.2,0.25,
* 0.295,0.345,0.4,0.45/

OPEN(FILE='RPYDER',STATUS='NEW',UNIT=7)

C
C RPY GEOMETRY
C

S=.9307
B=2.638
C=.353
AR=7.48
ET=.16
HA=.045
ZF1=.0887
LF1=1.0951
ZF2=.1132
LF2=1.1019

RPY MASS & INERTIA CHARACTERISTICS

MASS=15.54
IX=2.1678
IY=1.6469
IZ=3.6962

RPY STABILITY & CONTROL DERIVATIVES

CLOW=.42
CLAW=4.53
CLO=.398

CLA=4.98
CLAD=2.78
CLQ=4.83
CLN=.49

CDO=.0227
K=.0514

CMO=.055
CMA=-1.05
CMAD=-9.32
CMQ=-19.15
CMN=-1.63

CONSTANTS

RO=1.225
B=9.80665
PI=3.1415926

WRITE(6,110)

10 FORMAT(1X,/,5X,'ENTER VT,ALPHA,EN'/)

READ(6,*) VT,A,EN

WRITE(7,120) VT

20 FORMAT(1X,/,5X,'STEADY STATE VELOCITY',F5.1,//)

DERIVATIVES DUE TO THRUST

TV=-2.*.0055*VT
TTH=26.7154

AERODYNAMIC COEFFICIENTS

CLW=CLOW+CLAW*A

CL=CLO+CLA*A+CLN*EN

CM=CMO+CMA*A+CMN*EN

CD=CDO+K*CLW*CLW

CDA=2.*K*CLW*CLAW

CDVD=2.*CLW*(K-1./(PI*AR))*CLAW*PI/180.

```
*****  
:   
: LONGITUDINAL AERODYNAMIC DERIVATIVES-STABILITY AXES  
: (C.G. on the Mean Aerodynamic Chord)  
:   
*****
```

```
XUS=-RO*VT*S*CD  
XWS=.5*RO*VT*S*(CL-CDA)  
XQS=0.0  
XWDS=0.0  
ZUS=-RO*VT*S*CL  
ZWS=-.5*RO*VT*S*(CLA+CD)  
ZQS=-.25*RO*VT*S*C*CLQ  
ZWDS=-.25*RO*S*C*CLAD  
MUS=RO*VT*S*C*CM  
MWS=.5*RO*VT*S*C*CMA  
MQS=.25*RO*VT*S*C*C*CMQ  
MWDS=.25*RO*S*C*C*CMAD  
XNS=0.0  
ZNS=-.5*RO*VT*VT*S*CLN  
MNS=.5*RO*VT*VT*S*C*CMN
```

```
*****  
:   
: LONGITUDINAL DERIVATIVES-BODY AXES  
: (C.G. on the Mean Aerodynamic Chord)  
:   
*****
```

```
XUB=XUS*(COS(A))**2-(XWS+ZUS)*SIN(A)*COS(A)+ZWS*(SIN(A))**2  
*  
* +TV*COS(A)  
XWB=XWS*(COS(A))**2+(XUS-ZUS)*SIN(A)*COS(A)-ZUS*(SIN(A))**2  
*  
* +TV*SIN(A)  
XQB=XQS*COS(A)-ZQS*SIN(A)  
XWDB=XWDS*(COS(A))**2-ZWDS*SIN(A)*COS(A)  
ZUB=ZUS*(COS(A))**2-(ZWS-XUS)*SIN(A)*COS(A)-XWS*(SIN(A))**2  
ZWB=ZWS*(COS(A))**2+(ZUS+XWS)*SIN(A)*COS(A)+XUS*(SIN(A))**2  
ZQB=ZQS*COS(A)+XQS*SIN(A)  
ZWDB=ZWDS*(COS(A))**2+XWDS*SIN(A)*COS(A)  
MUB=MUS*COS(A)-MWS*SIN(A)+TV*COS(A)*(HA-ET)  
MWB=MWS*COS(A)+MUS*SIN(A)+TV*SIN(A)*(HA-ET)  
MQB=MQS  
MWDB=MWDS*COS(A)  
XNB=XNS*COS(A)-ZNS*SIN(A)  
ZNB=ZNS*COS(A)+XNS*SIN(A)  
MNB=MNS  
XTHB=TTH  
MTHB=TTH*(HA-ET)
```

```
*****  
:   
: LONGITUDINAL DERIVATIVES-BODY AXES  
: (C.G. in Final Position)  
:   
*****
```

```

XU=XUB
XW=XWB
XQ=XQB-HA*XUB
XWD=XWDB
ZU=ZUB
ZW=ZWB
ZQ=ZQB-HA*ZUB
ZWD=ZWDB
MU=MUB-HA*XUB
MW=MWB-HA*XWB
MQ=MQB-HA*(XQB+MUB)+HA*HA*XUB
MWD=MWDB-HA*XWDB
XN=XNB
ZN=ZNB
MN=MNB-HA*XNB
XTH=XTHB
MTH=MTHB-HA*XTHB

```

NORMALISED LONGITUDINAL DERIVATIVES-BODY AXES
(C.G in Final Position)

```

XU=XU/MASS
XW=XW/MASS
XQ=XQ/MASS
XWD=XWD/MASS
XN=XN/MASS
XTH=XTH/MASS

```

```

ZU=ZU/MASS
ZW=ZW/MASS
ZQ=ZQ/MASS
ZWD=ZWD/MASS
ZN=ZN/MASS

```

```

MU=MU/IY
MW=MW/IY
MQ=MQ/IY
MWD=MWD/IY
MN=MN/IY
MTH=MTH/IY

```

```

WRITE(7,10) XU,XW,XQ,XWD,XN,XTH
FORMAT(1X,/,5X,'NORMALISED LONGITUDINAL DERIVATIVES-BODY AXES'
* ,2(1X/),5X,
* 'XU=',FB.3,2X,'XW=',FB.3,2X,'XQ=',FB.3,2X,'XWD=',FB.5,2X,
* 'XN=',FB.3,2X,'XTH=',FB.3)
WRITE(7,20) ZU,ZW,ZQ,ZWD,ZN
FORMAT(5X,'ZU=',FB.3,2X,'ZW=',FB.3,2X,'ZQ=',FB.3,2X,
* 'ZWD=',FB.3,2X,'ZN=',FB.3)
WRITE(7,30) MU,MW,MQ,MWD,MN,MTH
FORMAT(5X,'MU=',FB.3,2X,'MW=',FB.3,2X,'MQ=',FB.3,2X,

```


* 'MWD=' ,F8.3,2X, 'MN=' ,F8.3,2X, 'MTH=' ,F8.3//)

LONGITUDINAL SYSTEM MATRIX

UO=VT*COS(A)
WO=VT*SIN(A)

AS(1,1)=XU+ZU*XWD/(1-ZWD)
AS(1,2)=XW+ZW*XWD/(1-ZWD)
AS(1,3)=XQ-WO+(ZQ+UO)*XWD/(1-ZWD)
AS(1,4)=-G*COS(A)-G*SIN(A)*XWD/(1-ZWD)

AS(2,1)=ZU/(1-ZWD)
AS(2,2)=ZW/(1-ZWD)
AS(2,3)=(ZQ+UO)/(1-ZWD)
AS(2,4)=-G*SIN(A)/(1-ZWD)

AS(3,1)=MU+ZU*MWD/(1-ZWD)
AS(3,2)=MW+ZW*MWD/(1-ZWD)
AS(3,3)=MQ+(ZQ+UO)*MWD/(1-ZWD)
AS(3,4)=-G*SIN(A)*MWD/(1-ZWD)

AS(4,1)=0.0
AS(4,2)=0.0
AS(4,3)=1.0
AS(4,4)=0.0

LONGITUDINAL INPUT MATRIX

BS(1,1)=XN+ZN*XWD/(1-ZWD)
BS(1,2)=XTH

BS(2,1)=ZN/(1-ZWD)
BS(2,2)=0.0

BS(3,1)=MN+ZN*MWD/(1-ZWD)
BS(3,2)=MTH

BS(4,1)=0.0
BS(4,2)=0.0

WRITE(7,101)

1 FORMAT(5X,'LONGITUDINAL SYSTEM MATRIX')

WRITE(7,102) ((AS(I,J),J=1,4),I=1,4)

2 FORMAT(4(F9.3,2X))

WRITE(7,103)

3 FORMAT(1X//5X,'LONGITUDINAL INPUT MATRIX')

```
WRITE(7,104) ((BS(I,J),J=1,2),I=1,4)
104 FORMAT(2(F9.3,2X))
```

```
*****
:
: LATERAL DERIVATIVES-STABILITY AXES
:
*****
```

```
YVS=-.3054*.5*RO*VT*S
LVS=.5*RO*VT*S*B*(-.0119-.0016*CL
* -.1969*(ZF1*COB(A)-LF1*SIN(A))/B)
NVS=.5*RO*VT*S*B*(-.0363+.1969*(LF1*COB(A)+ZF1*SIN(A))/B)
```

```
XC=(ZF2-(ZF2*COB(A)-LF2*SIN(A)))/B
XCA=ABS(XC)
I=1
```

```
11 IF(XCA.EQ.X(I)) THEN
    YPSD=Y(I)*XC/XCA
    ELSE IF(XCA.LT.X(I)) THEN
        YPSD=Y(I-1)+(XCA-X(I-1))*(Y(I)-Y(I-1))/(X(I)-X(I-1))
        YPSD=YPSD*XC/XCA
        GO TO 121
    ELSE
        I=I+1
        GO TO 111
```

ENDIF

```
21 CONTINUE
YPF=-.3133*((ZF2*COB(A)-LF2*SIN(A))/B-.1B-YPSD)
YPS=.5*RO*VT*S*B*(.07B*CL+YPF)
LPB=.5*RO*VT*S*B*B*(-.2457+YPF*(ZF2*COB(A)-LF2*SIN(A))/B)
NPS=.5*RO*VT*S*B*B*(-.034*CL+1.23*CDVD
* -YPF*(LF2*COB(A)+ZF2*SIN(A))/B)
```

```
YRF=.2164*(LF1*COB(A)+ZF1*SIN(A))/B
YRS=.5*RO*VT*S*B*(-.0109+YRF)
LRS=.5*RO*VT*S*B*B*(-.00189+.1243*CL
* +YRF*(ZF1*COB(A)-LF1*SIN(A))/B)
NRS=.5*RO*VT*S*B*B*(-.0022-.1621*CD0-.009*CL*CL
* -YRF*(LF1*COB(A)+ZF1*SIN(A))/B)
```

```
LXS=.5*RO*VT*VT*S*B*(-.2291)
NXS=.5*RO*VT*VT*S*B*.0195*CL
```

```
*****
```

LATERAL DERIVATIVES-BODY AXES

```
*****
```

```
YV=YVS
YP=YPS*COB(A)-YRS*SIN(A)
YR=YRS*COB(A)+YPS*SIN(A)
YZ=.5*RO*VT*VT*S*.1184
```

LV=LVB* $\cos(A)$ -NVB* $\sin(A)$
LP=LPS*($\cos(A)$)**2+NRS*($\sin(A)$)**2-(LRS+NPS)* $\sin(A)$ * $\cos(A)$
LR=LRS*($\cos(A)$)**2-NPS*($\sin(A)$)**2+(LPS-NRS)* $\sin(A)$ * $\cos(A)$
LX=LXS* $\cos(A)$ -NXS* $\sin(A)$
LZ=.5*RO*VT*VT*S*B*.00398

NV=NVB* $\cos(A)$ +LVB* $\sin(A)$
NP=NPS*($\cos(A)$)**2-LRS*($\sin(A)$)**2+(LPS-NRS)* $\sin(A)$ * $\cos(A)$
NR=NRS*($\cos(A)$)**2+LPS*($\sin(A)$)**2+(LRS+NPS)* $\sin(A)$ * $\cos(A)$
NX=NXS* $\cos(A)$ +LXS* $\sin(A)$
NZ=.5*RO*VT*VT*S*B*(-.0492)

NORMALISED LATERAL DERIVATIVES-BODY AXES

YV=YV/MASS
YP=YP/MASS
YR=YR/MASS
YZ=YZ/MASS

LV=LV/IX
LP=LP/IX
LR=LR/IX
LX=LX/IX
LZ=LZ/IX

NV=NV/IZ
NP=NP/IZ
NR=NR/IZ
NX=NX/IZ
NZ=NZ/IZ

WRITE(7,40) YV,YP,YR,YZ
FORMAT(1X//5X,'NORMALISED LATERAL DERIVATIVES-BODY AXES'
* ,2(1X/),5X,
* 'YV=',FB.3,2X,'YP=',FB.3,2X,'YR=',FB.3,2X,'YZ='FB.3)
WRITE(7,50) LV,LP,LR,LX,LZ
FORMAT(5X,'LV=',FB.3,2X,'LP=',FB.3,2X,'LR=',FB.3,2X,
* 'LX=',FB.3,2X,'LZ=',FB.3)
WRITE(7,60) NV,NP,NR,NX,NZ
FORMAT(5X,'NV=',FB.3,2X,'NP=',FB.3,2X,'NR=',FB.3,2X,
* 'NX=',FB.3,2X,'NZ='FB.3///)

LATERAL SYSTEM MATRIX

AS(1,1)=YV
AS(1,2)=YP+W0
AS(1,3)=YR-U0

AS(1,4)=G*COB(A)

AS(2,1)=LV
AS(2,2)=LP
AS(2,3)=LR
AS(2,4)=0.0

AS(3,1)=NV
AS(3,2)=NP
AS(3,3)=NR
AS(3,4)=0.0

AS(4,1)=0.0
AS(4,2)=1.0
AS(4,3)=TAN(A)
AS(4,4)=0.0

LATERAL INPUT MATRIX

BS(1,1)=0.0
BS(1,2)=YZ

BS(2,1)=LX
BS(2,2)=LZ

BS(3,1)=NX
BS(3,2)=NZ

BS(4,1)=0.0
BS(4,2)=0.0

WRITE(7,201)

1 FORMAT(5X,'LATERAL SYSTEM MATRIX'/)

WRITE(7,102) ((AS(I,J),J=1,4),I=1,4)

WRITE(7,202)

2 FORMAT(1X//5X,'LATERAL INPUT MATRIX'/)

WRITE(7,104) ((BS(I,J),J=1,2),I=1,4)

CLOSE(UNIT=7)

STOP

END

PROGRAM TRIM

OPEN(FILE='TRIM',STATUS='NEW',UNIT=7)

S=.9307
C=.353
EM=15.54
G=9.80665

WRITE(6,1)
FORMAT(1X,/,5X,'ENTER STEADY STATE VELOCITY',/)
READ(6,*) VT

Q=.5*1.225*VT*VT

HA=.045
ET=.16

CLO=.398
CLA=4.98
CLN=.49
CLOW=.420
CLAW=4.53

CDO=.0227
DK=.0514

CMO=.055
CMA=-1.05
CMN=-1.63

WRITE(6,2)
FORMAT(1X,/,5X,'ENTER ERROR COEFFICIENT',/)
READ(6,*) ER

I=0
CL=(EM*G)/(Q*S)
A=(CL-CLOW)/CLAW
EN=0.0
I=I+1
EL=Q*S*(CLO+CLA*A+CLN*EN)
CLW=CLOW+CLAW*A
D=Q*S*(CDO+DK*CLW*CLW)
CDA=2.*DK*CLW*CLAW
CM=CMO+CMA*A+CMN*EN

FX=(1.-(HA/ET))*(EL*SIN(A)-D*COS(A))-EM*G*SIN(A)
* +Q*S*C*CM/ET
FZ=(EM*G-EL)*COS(A)-D*SIN(A)
WRITE(6,11) FX,FZ
FORMAT(5X,F12.9,2X,F12.9)
IF((ABS(FX)+ABS(FZ)).LE.ER) GO TO 20

FXA=(1.-(HA/ET))*((Q*S*CLA+D)*SIN(A)+(EL-Q*S*CDA)*COS(A))
* -EM*G*COS(A)+Q*S*C*CMA/ET

```
FXN=(1.-(HA/ET))*Q*S*CLN*SIN(A)+Q*S*C*CMN/ET
FZA=(EL-EM*G-Q*S*CDA)*SIN(A)-(Q*S*CLA+D)*COS(A)
FZN=-Q*S*CLN*COS(A)
```

```
DET=FXA*FZN-FZA*FXN
```

```
A=A-(FZN*FX-FXN*FZ)/DET
EN=EN-(FXA*FZ-FZA*FX)/DET
GO TO 10
```

```
0 T=(EM*G-EL)*SIN(A)+D*COS(A)
  THS=(T+.0055*VT*VT)/26.7154
```

```
WRITE(7,90) I
```

```
0 FORMAT(1X,/,5X,'NUMBER OF ITERATIONS : ',I4,//)
```

```
WRITE(7,100) VT
```

```
00 FORMAT(5X,'STEADY STATE VELOCITY : ',F5.1,//)
```

```
WRITE(7,110) A,EN,THS
```

```
10 FORMAT(5X,'ANGLE OF ATTACK',F16.9,/,5X,
```

```
  * 'ELEVATOR SETTING',F15.9,/,5X,
```

```
  * 'THROTTLE SETTING',F15.9,//)
```

```
AM=Q*B*C*CM
```

```
WRITE(7,120) EL,D,AM,T
```

```
20 FORMAT(5X,'LIFT',F27.9,/,5X,
```

```
  * 'DRAG',F27.9,/,5X,
```

```
  * 'PITCHING MOMENT',F16.9,/,5X,
```

```
  * 'THRUST',F25.9//)
```

```
WRITE(7,130) FX,FZ
```

```
30 FORMAT(5X,'FX=',F12.9,/,5X,'FZ=',F12.9,//)
```

```
WRITE(7,140) ER
```

```
10 FORMAT(5X,'ERROR : ',F10.7)
```

```
CLOSE(UNIT=7)
```

```
STOP
```

```
END
```


RO=1.225
G =9.80665
PI=3.1415926

CINTERVAL CINT=0.005
NSTEPS NSTP=1
VARIABLE TIME=0.0
CONSTANT TMX =39.99

INITIAL

"-----RPV INITIAL CONDITIONS-----"

CONSTANT VTZ=30 , VZ=0.0
,PZ=0.0 , QZ=0.0 , RZ=0.0
,PHZ=0.0, THZ=-0.024524845 , PSZ=0.0
,DNZ=0.044591375 , DZZ=0.0 , DXZ=0.0
,THRZ=0.715571165
,XZ=0.0 , YZ=0.0 , HZ=1000.0

UZ=VTZ*COS(THZ)
WZ=VTZ*SIN(THZ)

END \$ "OF INITIAL"

DYNAMIC

DERIVATIVE

"-----ANGLE OF ATTACK-----"
A=ATAN(W/U)

"-----TOTAL VELOCITY-----"
VT=SQRT(U**2+V**2+W**2)

"-----DYNAMIC PRESSURE-----"
QP=0.5*RO*VT**2

"-----ELEVATOR DEFLECTION-----"
DN=KN1*STEP(TN1)+KN2*STEP(TN2)+DNZ

"-----AILERON DEFLECTION-----"
DX=KX1*STEP(TX1)+KX2*STEP(TX2)+DXZ

"-----RUDDER DEFLECTION-----"
DZ=KZ1*STEP(TZ1)+KZ2*STEP(TZ2)+DZZ

"-----THROTTLE SETTING-----"
THR=KT1*STEP(TT1)+KT2*STEP(TT2)+THRZ

"-----PART OF TOTAL LIFT COEFFICIENT-----"
"-----LIFT DUE TO ANGLE-OF-ATTACK RATE IS EXCLUDED-----"
CL1=CL0+CLA*A+CLQ*Q*C/(2*VT)+CLN*DN

"-----WING-BODY LIFT COEFFICIENT-----"

CLW=CLOW+CLAW*A

"-----TOTAL DRAG COEFFICIENT-----"

CD=CDDW+CDDT+K*CLW**2

"-----THRUST-----"

T =26.7154*THR-0.0055*VT**2

"-----COEFFICIENTS NEEDED FOR LONGITUDINAL EQS-----"

B1=R*V-Q*W-G*SIN(TH)+QP*S*(CL1*SIN(A)-CD*COS(A))/MASS...
+T/MASS

B2=Q*U-P*V+G*COS(TH)*COS(PH) ...
-QP*S*(CL1*COS(A)+CD*SIN(A))/MASS

D =QP*S*CLAD*C/(2*MASS*VT*(U**2+W**2))

D1=1+D*(U*COS(A)+W*SIN(A))

D2=D*(B1*COS(A)+B2*SIN(A))

"-----VELOCITY RATE ALONG XB AXIS-----"

UD=(B1+U*D2)/D1

"-----VELOCITY RATE ALONG ZB AXIS-----"

WD=(B2+W*D2)/D1

"-----ANGLE OF ATTACK RATE-----"

AD=(WD*U-UD*W)/(U**2+W**2)

"-----PITCHING MOMENT COEFFICIENT-----"

CM=CMO+CMA*A+CMAD*AD*C/(2*VT)+CMQ*Q*C/(2*VT)+CMN*DN

"-----LIFT COEFFICIENT-----"

CL=CL1+CLAD*AD*C/(2*VT)

"-----PITCHING ANGULAR ACCELERATION ABOUT YB AXIS-----"

QD=((IZ-IX)*P*R+QP*S*C*CM-T*ET)/IY ...
-HA*QP*S*(CL*SIN(A)-CD*COS(A))/IY

"-----LATERAL STABILITY DERIVATIVES-----"

"-----STABILITY AXES-----"

NV =-0.0363+0.1969*(LF1*COS(A)+ZF1*SIN(A))/B

LV =-0.0119-0.0016*CLW-0.1969*(ZF1*COS(A)-LF1*SIN(A))/B

X1 =(ZF2-(ZF2*COS(A)-LF2*SIN(A)))/B

Y1 =ABS(X1)

YPS =X1*YSD(Y1)/Y1

YPF =-0.3133*((ZF2*COS(A)-LF2*SIN(A))/B-0.18-YPS)

YP =0.078*CL+YPF

CDVD=2*CLW*(K-1/(PI*AR))*CLAW*PI/180.0

NP =-0.034*CL+1.23*CDVD-YPF*(LF2*COS(A)+ZF2*SIN(A))/B

LP =-0.2457+YPF*(ZF2*COS(A)-LF2*SIN(A))/B

YRF =0.2164*(LF1*COS(A)+ZF1*SIN(A))/B

YR =-0.0109+YRF

NR =-0.0022-0.1621*CDDW-0.009*CLW**2 ...

-YRF*(LF1*COS(A)+ZF1*SIN(A))/B

LR =-0.00189+0.1243*CLW+YRF*(ZF1*COS(A)-LF1*SIN(A))/B

NX =0.0195*CLW

"-----TRANSFORMATION TO BODY REFERENCE AXES-----"

YPB=YP*COS(A)-YR*SIN(A)
YRB=YR*COS(A)+YP*SIN(A)
LVB=LV*COS(A)-NV*SIN(A)
LPB=LP*(COS(A))**2-(LR+NP)*SIN(A)*COS(A)+NR*(SIN(A))**2
LRB=LR*(COS(A))**2-(NR-LP)*SIN(A)*COS(A)-NP*(SIN(A))**2
NVB=NV*COS(A)+LV*SIN(A)
NPB=NP*(COS(A))**2-(NR-LP)*SIN(A)*COS(A)-LR*(SIN(A))**2
NRB=NR*(COS(A))**2+(LR+NP)*SIN(A)*COS(A)+LP*(SIN(A))**2
LXB=LX*COS(A)-NX*SIN(A)
NXB=NX*COS(A)+LX*SIN(A)

"-----AERODYNAMIC FORCE ALONG YB AXIS-----"
Y=QP*S*(YVB*V+B*YPB*P+B*YRB*R)/VT+QP*S*YBZ*DZ

"-----AERODYNAMIC MOMENT ABOUT XB AXIS-----"
L=QP*S*B*(LVB*V+B*LPB*P+B*LRB*R)/VT+QP*S*B*(LZB*DZ+LXB*DX)

"-----AERODYNAMIC MOMENT ABOUT ZB AXIS-----"
N=QP*S*B*(NVB*V+B*NPB*P+B*NRB*R)/VT+QP*S*B*(NZB*DZ+NXB*DX)

"-----VELOCITY RATE ALONG YB AXIS-----"
VD=P*W-R*U+G*COS(TH)*SIN(PH)+Y/MASS

"-----ROLLING ANGULAR ACCELERATION ABOUT XB AXIS-----"
PD=((IY-IZ)*Q*R+L)/IX

"-----YAWING ANGULAR ACCELERATION ABOUT ZB AXIS-----"
RD=((IX-IY)*P*Q+N)/IZ

"-----VELOCITY RESOLVED ON EARTH AXES-----"
UE=COS(TH)*COS(PS)*U
+ (SIN(PH)*SIN(TH)*COS(PS)-COS(PH)*SIN(PS))*V ...
+ (COS(PH)*SIN(TH)*COS(PS)+SIN(PH)*SIN(PS))*W

VE=COS(TH)*SIN(PS)*U
+ (SIN(PH)*SIN(TH)*SIN(PS)+COS(PH)*COS(PS))*V ...
+ (COS(PH)*SIN(TH)*SIN(PS)-SIN(PH)*COS(PS))*W

WE=-SIN(TH)*U+SIN(PH)*COS(TH)*V+COS(PH)*COS(TH)*W

HD=-WE

"-----EULER ANGLE RATES-----"
PHD=P+Q*TAN(TH)*SIN(PH)+R*TAN(TH)*COS(PH)
THD=Q*COS(PH)-R*SIN(PH)
PSD=(R*COS(PH)+Q*SIN(PH))/COS(TH)

U =INTEG(UD, UZ)
V =INTEG(VD, VZ)
W =INTEG(WD, WZ)
P =INTEG(PD, PZ)
Q =INTEG(QD, QZ)

```
R =INTEG(RD, RZ)
XE=INTEG(UE, XZ)
YE=INTEG(VE, YZ)
H =INTEG(HD, HZ)
PH=INTEG(PHD,PHZ)
TH=INTEG(THD,THZ)
PS=INTEG(PSD,PSZ)
```

END \$ "OF DERIVATIVE"

```
UPR=U-UZ
WPR=W-WZ
THPR=TH-THZ
ALPHA=A-THZ
HPR=H-HZ
TERMT(TIME.GE.TMX .OR. H.LE.O.O)
```

END \$ "OF DYNAMIC"

END \$ "OF PROGRAM"

PROGRAM XRAE1 LINEAR LONGITUDINAL MODEL

INITIAL

CONSTANT "----AERODYNAMIC DERIVATIVES----"
XU=-0.097 ,XW= 0.037,XQ=-0.019 ,XWD=-0.00044...
,ZU=-0.789 ,ZW=-5.496,ZQ=-0.902 ,ZWD=-0.018 ...
,MU= 0.029 ,MW=-3.865,MQ=-12.381,MWD=-0.201

CONSTANT "-----CONTROL DERIVATIVES-----"
XN=-0.397 ,ZN=-16.172,MN=-179.079 ...
,XTHR=1.719,MTHR=-2.595

CONSTANT "-----ELEVATOR INPUT-----"
TN1=0.0,TN2=0.0,KN1=0.0,KN2=0.0

CONSTANT "-----THROTTLE INPUT-----"
TT1=0.0,TT2=0.0,KT1=0.0,KT2=0.0

TH0=-0.024524845
G=9.80665
VTO=30.0

CINTERVAL CINT=0.05
NSTEPS NSTP=1
VARIABLE TIME=0.0
CONSTANT TMX=40.0

CONSTANT "----INITIAL CONDITIONS----"
UZ=0.0,WZ=0.0,QZ=0.0,THZ=0.0,HZ=0.0

U0=VTO*COS(TH0)
W0=VTO*SIN(TH0)

END \$ "OF INITIAL"

DYNAMIC
DERIVATIVE

"----ELEVATOR DEFLECTION----"
DN=KN1*STEP(TN1)-KN2*STEP(TN2)

"----THROTTLE INPUT----"
THR=KT1*STEP(TT1)-KT2*STEP(TT2)

"----EQUATIONS OF MOTION & GEOMETRY----"
UD=XU*U+XW*W+(XQ-W0)*Q-G*COS(TH0)*TH+XN*DN+XTHR*THR ...
+(ZU*U+ZW*W+(ZQ+U0)*Q-G*SIN(TH0)*TH+ZN*DN)*XWD/(1-ZWD) ...

WD=(ZU*U+ZW*W+(ZQ+U0)*Q-G*SIN(TH0)*TH+ZN*DN)/(1-ZWD) ...

QD=MU*U+MW*W+MQ*Q+MN*DN+MTHR*THR ...
+(ZU*U+ZW*W+(ZQ+U0)*Q-G*SIN(TH0)*TH+ZN*DN)*MWD/(1-ZWD) ...

THD=Q

HD=SIN(THO)*U-COS(THO)*W+VTO*TH

U=INTEG(UD,UZ)

W=INTEG(WD,WZ)

Q=INTEG(QD,QZ)

TH=INTEG(THD,THZ)

H=INTEG(HD,HZ)

END \$ "OF DERIVATIVE"

ALPHA=(UO*W-WO*U)/(VTO**2)

TERMT(TIME.GE.TMX)

END \$ "OF DYNAMIC"

END \$ "OF PROGRAM"

PROGRAM XRAE1 LINEAR LATERAL MODEL
INITIAL

"---AERODYNAMIC DERIVATIVES---"
CONSTANT YV=-0.336 ,YP=0.175 ,YR=0.224...
 ,LV=-0.414 ,LP=-13.360,LR=2.412...
 ,NV=0.558 ,NP=-0.622 ,NR=-1.426
"-----CONTROL DERIVATIVES-----"
CONSTANT YZ=3.909 ,LZ=2.485 ,NZ=-18.015...
 ,LX=-142.902,NX=4.182

"-----AILERON INPUT-----"
CONSTANT TX1=0.0,TX2=0.0,KX1=0.0,KX2=0.0
"-----RUDDER INPUT-----"
CONSTANT TZ1=0.0,TZ2=0.0,KZ1=0.0,KZ2=0.0

TH0=-0.024524845
B=9.80665
VTO=30.0

CINTERVAL CINT=0.005
NSTEPS NSTP=1
VARIABLE TIME=0.0
CONSTANT TMX=40.0

"---INITIAL CONTITIONS---"
CONSTANT VZ=0.0,PZ=0.0,RZ=0.0,PHZ=0.0

U0=VTO*COS(TH0)
W0=VTO*SIN(TH0)
END \$ "OF INITIAL"

DYNAMIC
DERIVATIVE

"---AILERON DEFLECTION---"
DX=KX1*STEP(TX1)-KX2*STEP(TX2)
"---RUDDER DEFLECTION---"
DZ=KZ1*STEP(TZ1)-KZ2*STEP(TZ2)

VD=YV*V+(YP+W0)*P+(YR-U0)*R+B*COS(TH0)*PH+YZ*DZ
PD=LV*V+LP*P+LR*R+LX*DX+LZ*DZ
RD=NV*V+NP*P+NR*R+NX*DX+NZ*DZ
PHD=P+TAN(TH0)*R

V=INTEG(VD,VZ)
P=INTEG(PD,PZ)
R=INTEG(RD,RZ)
PH=INTEG(PHD,PHZ)

END \$ "OF DERIVATIVE"
 TERMT(TIME.GE.TMX)
END \$ "OF DYNAMIC"
END \$ "OF PROGRAM"

PROGRAM KALMAN

DOUBLE PRECISION T(15),W1(4),EPS,HM,HI
REAL XG(1001),YG(10010)
INTEGER IA1(2)

PARAMETER(ISZ=4)
PARAMETER(INPZ=2)
PARAMETER(IOZ=2)
PARAMETER(IPZ=10)
PARAMETER(IASZ=14)
PARAMETER(ITZ=1001)

DOUBLE PRECISION AS(ISZ,ISZ),BS(ISZ,INPZ),CS(IOZ,ISZ),
* X8(ISZ),X18(ISZ),X28(ISZ),U(INPZ),US(INPZ),Y(IOZ),Y8(IOZ),
* Q(IPZ,IPZ),R(IOZ,IOZ),RI(IOZ,IOZ),
* C(IOZ,IASZ),CT(IASZ,IOZ),E(IASZ,IPZ),ET(IPZ,IASZ),
* PHI(IASZ,IASZ),PHIT(IASZ,IASZ),GM(IASZ,IASZ),GP(IASZ,IASZ),
* JK(IASZ,IOZ),JKT(IOZ,IASZ),XM(IASZ),XP(IASZ),UNI(IASZ,IASZ),
* UG(INPZ,ITZ),VG(IOZ,ITZ),V(IOZ),EM(IOZ),ZH(IOZ),
* A1(IASZ,IOZ),A2(IOZ,IOZ),A3(IASZ,IASZ),A4(IASZ,IPZ),
* A5(IASZ,IASZ),A6(IASZ,IASZ),A7(IASZ,IASZ)

COMMON UG

DATA IS,INP,IO,IP/4,2,2,10/
DATA R(1,1),R(1,2),R(2,1),R(2,2)/2.014D-7,0.0,0.0,2.014D-7/

OPEN(FILE='EXKAL',STATUS='NEW',UNIT=17)

ENTER PROCESS MATRIX Q(IP,IP)

WRITE(6,998)
7B FORMAT(2(1X/),5X,'ENTER Q(I,I),I=1,IP')
READ(5,*) (Q(I,I),I=1,IP)
DO 10 I=1,IP
DO 10 J=1,IP
IF(I.NE.J) Q(I,J)=0.0
CONTINUE

ENTER MEASUREMENT AND INTEGRATION STEPS

WRITE(6,999)
7B FORMAT(1X/5X,'ENTER HM,HI')
READ(5,*) HM,HI
WRITE(17,1000) HM,HI
DO 1000
1000 FORMAT(2(1X/),1X,'MEASUREMENT INTERVAL :',F8.4,' secs'/
1 1X,'INTEGRATION STEP :',F8.4,' secs')

IS : NUMBER OF STATES
INP : NUMBER OF INPUTS
IO : NUMBER OF OUTPUTS
IP : NUMBER OF PARAMETERS TO BE IDENTIFIED
IAS : NUMBER OF AUGMENTED STATES

IAS=IS+IP

CREATE SYSTEM MATRICES

CALL SMTCS(AS,BS,CS,HI,IS,INP,IO)

SELECT SYSTEM INPUT

WRITE(6,1010)

010 FORMAT(2(1X/),1X,' SELECT SYSTEM INPUT'//
 1 1X,' TYPE 1 : For SQUARE WAVE'/
 2 1X,' TYPE 2 : For MULTISTEP'/
 3 1X,' TYPE 3 : For RANDOM NOISE'//)

READ(5,*) INPUT

IF(INPUT.EQ.1) CALL SQW(INP,HM)
IF(INPUT.EQ.2) CALL MLSTP(INP,HM)
IF(INPUT.EQ.3) CALL RANDOM(INP)

SELECT MEASUREMENT NOISE

WRITE(6,1020)

020 FORMAT(2(1X/),1X,' SELECT MEASUREMENT NOISE'//
 1 1X,' TYPE 1 : IF YOU WANT NOISE'/
 2 1X,' TYPE 2 : IF YOU DO NOT WANT NOISE'//)

READ(5,*) NOISE

IF(NOISE.NE.1) GO TO 50

DO 20 I=1,IO
EM(I)=0.0
CONTINUE

WRITE(6,1030)


```
030      FORMAT(2(1X/),1X,'      ENTER COVARIANCE R OF
1 MEASUREMENT NOISE'//)
READ(5,*) ((R(I,J),I=1,IO),J=1,IO)
WRITE(17,1040)
040      FORMAT(2(1X/),1X,'COVARIANCE R OF MEASUREMENT NOISE'//)
DO 30 I=1,IO
WRITE(17,1050) (R(I,J),J=1,IO)
0 CONTINUE
050      FORMAT(1X,4F11.5)
```

```
EPS=0.01/DBLE(IO)
I=1
CALL G05CBF(I)
IFAIL=0
CALL G05EAF(EM,IO,R,IO,EPS,T,15,IFAIL)
IF(IFAIL.NE.0) WRITE(6,1060)
060      FORMAT(2(1X/),1X,'ERROR IN G05EAF'//)
DO 40 I=1,1001
IFAIL=0
CALL G05ZFF(ZH,IO,T,15,IFAIL)
IF(IFAIL.NE.0) WRITE(6,1070)
070      FORMAT(2(1X/),1X,'ERROR IN G05ZFF'//)
DO 40 J=1,IO
VG(J,I)=ZH(J)
0 CONTINUE
0 CONTINUE
```

ENTER INITIAL CONDITIONS

```
WRITE(6,1080)
080      FORMAT(2(1X/),1X,'      ENTER AUGMENTED INITIAL
1 STATE VECTOR'//)
READ(5,*) (XM(I),I=1,IAS)
WRITE(17,1090) (XM(I),I=1,IAS)
090      FORMAT(2(1X/),1X,'AUGMENTED INITIAL STATE VECTOR'//
1 17(1X,F11.4//))
```

```
DO 60 I=1,IS
XS(I)=0.0
CONTINUE
```

```
DO 70 I=1,IAS
DO 70 J=1,IAS
GM(I,J)=0.0
CONTINUE
```

WRITE(6,2000)

```
00      FORMAT(2(1X/),1X,'      ENTER DIAGONAL ELEMENS OF GM'//)
READ(5,*) (GM(I,I),I=1,IAS)
WRITE(17,2010) (GM(I,I),I=1,IAS)
10      FORMAT(2(1X/),1X,'DIAGONAL OF GM'//17(1X,F11.4//))
```

```
WRITE(6,2020)
2020 FORMAT(2(1X/),1X,' ENTER NUMBER OF ITERATIONS'//)
READ(5,*) ITER
NPTS=ITER+1
```

```
*****
:
: THE EXTENDED KALMAN FILTER ALGORITHM
:
*****
```

```
I=INT(HM/HI)
```

```
K=0
J=0
```

```
DO 80 L=1,IAS
DO 80 M=1,IO
C(M,L)=0.0
80 CONTINUE
C(1,2)=1.0
C(2,3)=1.0
```

```
CALL TRANS(C,CT,IO,IAS)
CALL MTXE(E,HI,IAS,IP)
CALL TRANS(E,ET,IAS,IP)
CALL MULT(E,Q,A4,IAS,IP,IP)
CALL MULT(A4,ET,A5,IAS,IP,IAS)
CALL NULL(UNI,IAS)
```

```
80 CONTINUE
DO 100 L=1,INP
U(L)=UB(L,K+1)
US(L)=UB(L,K+1)
90 CONTINUE
CALL MULT1(CS,XS,Y,IO,IS)
IF(NOISE.EQ.1) THEN
DO 110 L=1,IO
V(L)=VB(L,K+1)
10 CONTINUE
CALL ADD1(Y,V,Y,IO)
ENDIF
```

```
CALL MULT(GM,CT,A1,IAS,IAS,IO)
CALL MULT(C,A1,A2,IO,IAS,IO)
CALL ADD(R,A2,A2,IO,IO,IO)
IFAIL=0
CALL F01AAF(A2,IO,IO,RI,IO,W1,IFAIL)
IF(IFAIL.NE.0) GO TO 9999
CALL MULT(A1,RI,JK,IAS,IO,IO)
CALL MULT(JK,C,A3,IAS,IO,IAS)
CALL SUB(UNI,A3,A3,IAS,IAS,IAS)
CALL TRANS(A3,A6,IAS,IAS)
CALL MULT(A3,GM,A7,IAS,IAS,IAS)
CALL MULT(A7,A6,GP,IAS,IAS,IAS)
```

```
CALL MULT(JK,R,A1,IAS,IO,IO)
CALL TRANS(JK,JKT,IAS,IO)
CALL MULT(A1,JKT,A6,IAS,IO,IAS)
CALL ADD(GP,A6,GP,IAS,IAS)
CALL MULT1(C,XM,YS,IO,IAS)
CALL SUB1(Y,YS,Y,IO)
CALL MULT1(JK,Y,XP,IAS,IO)
CALL ADD1(XM,XP,XP,IAS)
XG(K+1)=DBLE(K)*HM
DO 11 L=1,IP
M=(L-1)*NPTS+K+1
N=IS+L
YG(M)=XP(N)
1 CONTINUE
IF(MOD(K,10).EQ.0) THEN
WRITE(6,12) K
WRITE(17,12) K
2 FORMAT(1X/5X,'ITERATIONS',I5)
WRITE(6,13) (XS(M),M=1,IS),(XP(M),M=1,IS)
WRITE(17,13) (XS(M),M=1,IS),(XP(M),M=1,IS)
3 FORMAT(1X,'XS',10X,' : ',4F10.4/1X,'XP',10X,' : ',4F10.4)
WRITE(6,14) (XP(M),M=IS+1,IAS)
WRITE(17,14) (XP(M),M=IS+1,IAS)
4 FORMAT(1X,'PARAMETERS : ',10F10.4)
WRITE(6,15) (JK(M,1),M=1,IAS)
WRITE(17,15) (JK(M,1),M=1,IAS)
5 FORMAT(1X,'KALMAN GAIN : ',4(5F10.4/15X))
WRITE(6,16) (GP(M,M),M=1,IAS)
WRITE(17,16) (GP(M,M),M=1,IAS)
6 FORMAT(1X,'COVARIANCE : ',4(5F10.4/15X))
ENDIF
20 CALL MULT1(AS,XS,X1S,IS,IS)
CALL MULT1(BS,US,X2S,IS,INP)
CALL ADD1(X1S,X2S,XS,IS)
CALL SYFN(XM,XP,U,HI,IAS,INP)
CALL MTXPHI(PHI,XP,U,HI,IAS,INP)
CALL TRANS(PHI,PHIT,IAS,IAS)
CALL MULT(PHI,GP,A6,IAS,IAS,IAS)
CALL MULT(A6,PHIT,A7,IAS,IAS,IAS)
CALL ADD(A5,A7,GM,IAS,IAS,IAS)
J=J+1
IF(K.EQ.ITER) GO TO 140
IF(J.EQ.1) THEN
J=0
K=K+1
GO TO 90
ELSE
DO 130 L=1,IAS
XP(L)=XM(L)
DO 130 M=1,IAS
GP(L,M)=GM(L,M)
CONTINUE
GO TO 120
ENDIF
```

40 CONTINUE

PL0T PARAMETERS

```
WRITE(6,2030)
2030 FORMAT(2(1X/),1X,'          PLOT PARAMETERS ?'//
          1          1X,'          TYPE 1 : For YES'//
          2          1X,'          TYPE 2 : For NO'//)
```

```
READ(5,*) IPLOT
IF(IPLOT.EQ.2) STOP
```

```
CALL SAVDRA
CALL DEVPAP(297.0,210.0,0)
CALL WINDO2(0.0,240.0,0.0,170.0)
DO 160 L=1,IP
DO 150 M=1,NPTS
N=M+(L-1)*NPTS
YG(M)=YG(N)
```

50 CONTINUE

```
CALL PICCLE
CALL CHAHAR(0,0)
CALL MOVTO2(20.0,20.0)
CALL GRAF(XG,YG,NPTS,0)
CALL MOVTO2(150.0,5.0)
CALL CHAHOL('Time (secs)*.')
```

```
CALL CHAHAR(0,1)
CALL MOVTO2(9.0,100.0)
READ(5,17) IA1(1),IA1(2)
```

60 CONTINUE

```
CALL DEVEND
STOP
```

```
999 WRITE(6,2040)
2040 FORMAT(1X,'ERROR IN F01AAF')
```

STOP

END

```
SUBROUTINE SMTCS(AS,BS,CS,H,IS,INP,IO)
DOUBLE PRECISION AS(IS,IS),BS(IS,INP),CS(IO,IS)
DOUBLE PRECISION YV,YZ,LV,LP,LR,LX,NV,NP,NR,NZ,H
```

```
DATA YV,YZ/-0.336,3.909/
DATA LV,LP,LR,LX/-0.414,-13.360,2.412,-142.902/
DATA NV,NP,NR,NZ/0.558,-0.622,-1.426,-18.015/
```

```
AS(1,1)=1.+YV*H
AS(1,2)=-0.561*H
AS(1,3)=-29.767*H
AS(1,4)=9.804*H
AS(2,1)=LV*H
AS(2,2)=1.+LP*H
AS(2,3)=LR*H
AS(2,4)=0.0
AS(3,1)=NV*H
AS(3,2)=NP*H
AS(3,3)=1.+NR*H
AS(3,4)=0.0
AS(4,1)=0.0
AS(4,2)=H
AS(4,3)=-0.025*H
AS(4,4)=1.0
```

```
BS(1,1)=0.0
BS(2,1)=LX*H
BS(3,1)=4.182*H
BS(4,1)=0.0
BS(1,2)=YZ*H
BS(2,2)=2.485*H
BS(3,2)=NZ*H
BS(4,2)=0.0
```

```
CS(1,1)=0.0
CS(1,2)=1.0
CS(1,3)=0.0
CS(1,4)=0.0
CS(2,1)=0.0
CS(2,2)=0.0
CS(2,3)=1.0
CS(2,4)=0.0
```

```
RETURN
END
```

```
SUBROUTINE SYFN(F,X,U,H,IAS,INP)
DOUBLE PRECISION F(IAS),X(IAS),U(INP),H
```

```
F(1)=(1.+X(5)*H)*X(1)-.561*H*X(2)-29.767*H*X(3)+9.804*H*X(4)
*
*      +X(6)*H*U(2)
F(2)=X(7)*H*X(1)+(1.+X(8)*H)*X(2)+X(9)*H*X(3)+X(10)*H*U(1)
*
*      +2.485*H*U(2)
F(3)=X(11)*H*X(1)+X(12)*H*X(2)+(1.+X(13)*H)*X(3)+4.182*H*U(1)
*
*      +X(14)*H*U(2)
F(4)=H*X(2)-0.025*H*X(3)+X(4)
DO 10 I=5,IAS
F(I)=X(I)
10      CONTINUE
```

```
RETURN
END
```

```
SUBROUTINE MTXE(E,H,IAS,IP)
DOUBLE PRECISION E(IAS,IP),H
```

```
DO 10 I=1,IAS
DO 10 J=1,IP
E(I,J)=0.
10      CONTINUE
DO 20 I=1,IP
J=I+IAS-IP
E(J,I)=H
20      CONTINUE
```

```
RETURN
END
```

```
SUBROUTINE MTXPHI(PHI,X,U,H,IAS,INP)
DOUBLE PRECISION PHI(IAS,IAS),X(IAS),U(INP),H
```

```
DO 10 I=1,IAS
DO 10 J=1,IAS
PHI(I,J)=0.
```

```
10 CONTINUE
```

```
PHI(1,1)=1.+X(5)*H
PHI(1,2)=-.561*H
PHI(1,3)=-29.767*H
PHI(1,4)=9.804*H
PHI(1,5)=X(1)*H
PHI(1,6)=U(2)*H
```

```
PHI(2,1)=X(7)*H
PHI(2,2)=1.+X(8)*H
PHI(2,3)=X(9)*H
PHI(2,7)=X(1)*H
PHI(2,8)=X(2)*H
PHI(2,9)=X(3)*H
PHI(2,10)=U(1)*H
```

```
PHI(3,1)=X(11)*H
PHI(3,2)=X(12)*H
PHI(3,3)=1.+X(13)*H
PHI(3,11)=X(1)*H
PHI(3,12)=X(2)*H
PHI(3,13)=X(3)*H
PHI(3,14)=U(2)*H
```

```
PHI(4,2)=H
PHI(4,3)=-0.025*H
PHI(4,4)=1.
```

```
DO 20 I=5,IAS
PHI(I,I)=1.
```

```
20 CONTINUE
```

```
RETURN
END
```

```
SUBROUTINE SQW(INP,H)
  DOUBLE PRECISION UG(2,1001),SM(2),P,H
```

```
COMMON UG
```

```
WRITE(6,1000)
```

```
000   FORMAT(2(1X/),1X,'      ENTER : Period'//
      1           1X,'      AND'//
      2           1X,'      Amplitude of SQUARE WAVE'//)
```

```
READ(5,*) P,(SM(I),I=1,INP)
```

```
WRITE(17,1010) P,(SM(I),I=1,INP)
```

```
010   FORMAT(2(1X/),1X,'SYSTEM INPUT : SQUARE WAVE'//
      1           1X,'      Period   ',F15.4,' secs'//
      2           1X,'      Amplitude',4F15.4,' rads')
```

```
P=P/H
```

```
N=INT(P/2.)
```

```
DO 10 J=1,N
```

```
DO 10 I=1,INP
```

```
UG(I,J)=SM(I)
```

```
0 CONTINUE
```

```
DO 20 J=N+1,2*N
```

```
DO 20 I=1,INP
```

```
UG(I,J)=-SM(I)
```

```
0 CONTINUE
```

```
DO 30 J=1,1001-2*N
```

```
DO 30 I=1,INP
```

```
UG(I,J+2*N)=UG(I,J)
```

```
0 CONTINUE
```

```
RETURN
```

```
END
```



```
SUBROUTINE MLSTP(INP,H)
DOUBLE PRECISION UG(2,1001),SM(2),P,H
COMMON UG
```

```
WRITE(6,1000)
1000 FORMAT(2(1X/),1X,' ENTER : Period'/
1 1X,' AND'/
2 1X,' Amplitude of MULTISTEP'//)
READ(5,*) P,(SM(I),I=1,INP)
WRITE(17,1010) P,(SM(I),I=1,INP)
1010 FORMAT(2(1X/),1X,'SYSTEM INPUT : MULTISTEP'/
1 1X,' Period ',F15.5,' secs'/
2 1X,' Amplitude',F15.5,' rads')
WRITE(6,1020)
1020 FORMAT(2(1X/),1X,' DO YOU WANT ONE PERIOD ONLY?'/
1 1X,' TYPE 1 : IF YES'/
2 1X,' TYPE 2 : IF NO')
READ(5,*) IPER
```

```
P=P/H
L=INT(P/7.)
DO 10 J=1,3*L
DO 10 I=1,INP
UG(I,J)=SM(I)
10 CONTINUE
DO 20 J=3*L+1,5*L
DO 20 I=1,INP
UG(I,J)=-SM(I)
20 CONTINUE
DO 30 J=5*L+1,6*L
DO 30 I=1,INP
UG(I,J)=SM(I)
30 CONTINUE
DO 40 J=6*L+1,7*L
DO 40 I=1,INP
UG(I,J)=-SM(I)
40 CONTINUE
IF(IPER.EQ.1) THEN
WRITE(17,1030)
1030 FORMAT(16X,'ONE PERIOD ONLY')
DO 50 J=1,1001-7*L
DO 50 I=1,INP
UG(I,J+7*L)=0.0
50 CONTINUE
ELSE
DO 60 J=1,1001-7*L
DO 60 I=1,INP
UG(I,J+7*L)=UG(I,J)
CONTINUE
ENDIF
RETURN
END
```

```
SUBROUTINE RANDOM(INP)
DOUBLE PRECISION UG(2,1001),E(2),SC(2,2),ZH(2),T(15),EPS
COMMON UG

WRITE(6,1000)
1000   FORMAT(2(1X/),1X,'      ENTER MEAN VECTOR'//)
      READ(5,*) (E(I),I=1,INP)
      WRITE(6,1010)
1010   FORMAT(2(1X/),1X,'      ENTER COVARIANCE MATRIX'//)
      READ(5,*) ((SC(I,J),I=1,INP),J=1,INP)
      WRITE(17,1020)
1020   FORMAT(2(1X/),1X,'SYSTEM INPUT : GAUSSIAN NOISE'//
             1      1X,'Mean'//)
      WRITE(17,1030) (E(I),I=1,INP)
1030   FORMAT(1X,4F15.5)
      WRITE(17,1040)
1040   FORMAT(2(1X/),1X,'Covariance'//)
      DO 10 I=1,INP
      WRITE(17,1050) (SC(I,J),J=1,INP)
10 CONTINUE
1050   FORMAT(1X,4F15.5)

EPS=0.01/DBLE(INP)
I=2
CALL G05CBF(I)
IFAIL=0
CALL G05EAF(E,INP,SC,INP,EPS,T,15,IFAIL)
IF(IFAIL.NE.0) WRITE(6,1060)
1060   FORMAT(2(1X/),1X,'ERROR IN G05EAF')
      DO 20 I=1,1001
      IFAIL=0
      CALL G05EZF(ZH,INP,T,15,IFAIL)
      IF(IFAIL.NE.0) WRITE(6,1070)
070    FORMAT(2(1X/),1X,'ERROR IN G05EZF')
      DO 20 J=1,INP
      UG(J,I)=ZH(J)
10 CONTINUE

RETURN
END
```

```
SUBROUTINE MULT(A,B,C,M,N,K)
DOUBLE PRECISION A(M,N),B(N,K),C(M,K)
```

```
DO 10 I=1,M
DO 10 J=1,K
C(I,J)=0.
DO 10 L=1,N
10 C(I,J)=C(I,J)+A(I,L)*B(L,J)
```

```
RETURN
END
```

```
SUBROUTINE ADD(A,B,C,M,N)
DOUBLE PRECISION A(M,N),B(M,N),C(M,N)
```

```
DO 20 I=1,M
DO 20 J=1,N
20 C(I,J)=A(I,J)+B(I,J)
```

```
RETURN
END
```

```
SUBROUTINE SUB(A,B,C,M,N)
DOUBLE PRECISION A(M,N),B(M,N),C(M,N)
```

```
DO 30 I=1,M
DO 30 J=1,N
30 C(I,J)=A(I,J)-B(I,J)
```

```
RETURN
END
```

```
SUBROUTINE MULT1(A,B,C,M,N)
DOUBLE PRECISION A(M,N),B(N),C(M)
```

```
DO 40 I=1,M
C(I)=0.
DO 40 K=1,N
40 C(I)=C(I)+A(I,K)*B(K)
```

```
RETURN
END
```

```
SUBROUTINE ADD1(A,B,C,M)
DOUBLE PRECISION A(M),B(M),C(M)
```

```
DO 50 I=1,M
50   C(I)=A(I)+B(I)
```

```
RETURN
END
```

```
SUBROUTINE SUB1(A,B,C,M)
DOUBLE PRECISION A(M),B(M),C(M)
```

```
DO 60 I=1,M
60   C(I)=A(I)-B(I)
```

```
RETURN
END
```

```
SUBROUTINE TRANS(A,AT,M,N)
DOUBLE PRECISION A(M,N),AT(N,M)
```

```
DO 70 I=1,N
DO 70 J=1,M
70   AT(I,J)=A(J,I)
```

```
RETURN
END
```

```
SUBROUTINE NULL(AI,M)
DOUBLE PRECISION AI(M,M)
```

```
DO 80 I=1,M
DO 80 J=1,M
AI(I,J)=0.
IF(I.EQ.J) AI(I,J)=1.
80   CONTINUE
```

```
RETURN
END
```

```
SUBROUTINE MULTC(A,B,C,M,N)
DOUBLE PRECISION A(M,N),B(M,N),C
```

```
DO 90 I=1,M
DO 90 J=1,N
90   B(I,J)=A(I,J)*C
```

```
RETURN
END
```

```
SUBROUTINE SMTCS(AS,BS,CS,H,IS,INP,IO)
DOUBLE PRECISION AB(IS,IS),BB(IS,INP),CS(IO,IS)
DOUBLE PRECISION XU,XW,ZU,ZW,ZN,MU,MW,MQ,MN,H
```

```
DATA XU,XW/-0.097,0.039/
DATA ZU,ZW,ZN/-0.775,-5.399,-15.887/
DATA MU,MW,MQ,MN/0.185,-2.782,-18.117,-175.890/
```

```
AS(1,1)=1.+XU*H
AS(1,2)=XW*H
AS(1,3)=0.704*H
AS(1,4)=-9.804*H
AS(2,1)=ZU*H
AS(2,2)=1.+ZW*H
AS(2,3)=28.575*H
AS(2,4)=0.236*H
AS(3,1)=MU*H
AS(3,2)=MW*H
AS(3,3)=1.+MQ*H
AS(3,4)=-0.047*H
AS(4,1)=0.0
AS(4,2)=0.0
AS(4,3)=H
AS(4,4)=1.0
```

```
BS(1,1)=-0.39*H
BS(2,1)=ZN*H
BS(3,1)=MN*H
BS(4,1)=0.0
```

```
CS(1,1)=0.0
CS(1,2)=0.0
CS(1,3)=1.0
CS(1,4)=0.0
```

```
RETURN
END
```

```
SUBROUTINE MTXE(E,H,IAS,IP)
DOUBLE PRECISION E(IAS,IP),H
```

```
DO 10 I=1,IAS
DO 10 J=1,IP
E(I,J)=0.
10 CONTINUE
DO 20 I=1,IP
J=I+IAS-IP
E(J,I)=H
20 CONTINUE
```

```
RETURN
END
```

```
SUBROUTINE SYFN(F,X,U,H,IAS,INP)
DOUBLE PRECISION F(IAS),X(IAS),U(INP),H
```

```
F(1)=(1.+X(5)*H)*X(1)+X(6)*H*X(2)+.704*H*X(3)-9.804*H*X(4)
*      -.39*H*U(1)
```

```
F(2)=X(7)*H*X(1)+(1.+X(8)*H)*X(2)+28.575*H*X(3)+.236*H*X(4)
*      +X(9)*H*U(1)
```

```
F(3)=X(10)*H*X(1)+X(11)*H*X(2)+(1.+X(12)*H)*X(3)-.047*H*X(4)
*      +X(13)*H*U(1)
```

```
F(4)=H*X(3)+X(4)
```

```
DO 10 I=5,IAS
```

```
F(I)=X(I)
```

```
10      CONTINUE
```

```
RETURN
```

```
END
```

SUBROUTINE MTXPHI(PHI,X,U,H,IAS,INP)
DOUBLE PRECISION PHI(IAS,IAS),X(IAS),U(INP),H

DO 10 I=1,IAS

DO 10 J=1,IAS

PHI(I,J)=0.

10 CONTINUE

PHI(1,1)=1.+X(5)*H

PHI(1,2)=X(6)*H

PHI(1,3)=-.704*H

PHI(1,4)=-9.804*H

PHI(1,5)=X(1)*H

PHI(1,6)=X(2)*H

PHI(2,1)=X(7)*H

PHI(2,2)=1.+X(8)*H

PHI(2,3)=28.575*H

PHI(2,4)=-.236*H

PHI(2,7)=X(1)*H

PHI(2,8)=X(2)*H

PHI(2,9)=U(1)*H

PHI(3,1)=X(10)*H

PHI(3,2)=X(11)*H

PHI(3,3)=1.+X(12)*H

PHI(3,4)=-.047*H

PHI(3,10)=X(1)*H

PHI(3,11)=X(2)*H

PHI(3,12)=X(3)*H

PHI(3,13)=U(1)*H

PHI(4,3)=H

PHI(4,4)=1.

DO 20 I=5,IAS

PHI(I,I)=1.

20 CONTINUE

RETURN

END